

GEOMETRY OF MÖBIUS TRANSFORMATIONS

Elliptic, Parabolic and
Hyperbolic Actions of $SL_2(\mathbb{R})$

Vladimir V. Kisil



Imperial College Press

GEOMETRY OF MÖBIUS TRANSFORMATIONS

Elliptic, Parabolic and
Hyperbolic Actions of $SL_2(\mathbb{R})$

This page intentionally left blank

GEOMETRY OF MÖBIUS TRANSFORMATIONS

Elliptic, Parabolic and
Hyperbolic Actions of $SL_2(\mathbb{R})$

Vladimir V. Kisil

University of Leeds, UK



Imperial College Press

Published by

Imperial College Press
57 Shelton Street
Covent Garden
London WC2H 9HE

Distributed by

World Scientific Publishing Co. Pte. Ltd.

5 Toh Tuck Link, Singapore 596224

USA office: 27 Warren Street, Suite 401-402, Hackensack, NJ 07601

UK office: 57 Shelton Street, Covent Garden, London WC2H 9HE

British Library Cataloguing-in-Publication Data

A catalogue record for this book is available from the British Library.

GEOMETRY OF MÖBIUS TRANSFORMATIONS

Elliptic, Parabolic and Hyperbolic Actions of $SL_2(\mathbb{R})$

(with DVD-ROM)

Copyright © 2012 by Imperial College Press

All rights reserved. This book, or parts thereof, may not be reproduced in any form or by any means, electronic or mechanical, including photocopying, recording or any information storage and retrieval system now known or to be invented, without written permission from the Publisher.

For photocopying of material in this volume, please pay a copying fee through the Copyright Clearance Center, Inc., 222 Rosewood Drive, Danvers, MA 01923, USA. In this case permission to photocopy is not required from the publisher.

ISBN-13 978-1-84816-858-9

ISBN-10 1-84816-858-6

Printed in Singapore.

Моим родителям посвящается

Dedicated to my parents

This page intentionally left blank

Preface

Everything new is old... understood again.

Yu.M. Polyakov

The idea proposed by Sophus Lie and Felix Klein was that *geometry is the theory of invariants of a transitive transformation group*. It was used as the main topic of F. Klein's inauguration lecture for professorship at Erlangen in 1872 and, thus, become known as the Erlangen programme (EP). As with any great idea, it was born ahead of its time. It was only much later when the theory of groups, especially the theory of group representations, was able to make a serious impact. Therefore, the EP had been marked as 'producing only abstract returns' (©Wikipedia) and laid on one side.

Meanwhile, the 20th century brought significant progress in representation theory, especially linear representations, which was closely connected to achievements in functional analysis. Therefore, a 'study of invariants' becomes possible in the linear spaces of functions and associated algebras of operators, e.g. the main objects of modern analysis. This is echoed in the saying which Yu.I. Manin attributed to I.M. Gelfand:

Mathematics of any kind is a representation theory.


This attitude can be encoded as the *Erlangen programme at large* (EPAL). In this book, we will systematically apply it to construct geometry of two-dimensional spaces. Further development shall extend it to analytic function theories on such spaces and the associated co- and contra-variant functional calculi with relevant spectra [69]. Functional spaces are naturally associated with algebras of coordinates on a geometrical (or commutative) space. An operator (non-commutative) algebra is fashionably treated as a non-commutative space. Therefore, EPAL plays the same rôle for non-commutative geometry as EP for commutative geometry [59, 60].

EPAL provides a systematic tool for discovering hidden features, which previously escaped attention for various psychological reasons. In a

sense [60], EPAL works like the periodic table of chemical elements discovered by D.I. Mendeleev: it allows us to see which cells are still empty and suggest where to look for the corresponding objects [60].

Mathematical theorems once proved, remain true forever. However, this does not mean we should not revise the corresponding theories. Excellent examples are given in *Geometry Revisited* [23] and *Elementary Mathematics from an Advanced Standpoint* [71, 72]. Understanding comes through comparison and there are many excellent books about the Lobachevsky half-plane which made their exposition through a contrast with Euclidean geometry. Our book offers a different perspective: it considers the Lobachevsky half-plane as one of three sister conformal geometries—elliptic, parabolic, and hyperbolic—on the upper half-plane.

Exercises are an integral part of these notes. If a mathematical statement is presented as an exercise, it is not meant to be peripheral, unimportant or without further use. Instead, the label ‘Exercise’ indicates that demonstration of the result is not very difficult and may be useful for understanding. Presentation of mathematical theory through a suitable collection of exercises has a long history, starting from the famous Polya and Szegő book [92], with many other successful examples following, e.g. [31, 55]. Mathematics is among those enjoyable things which are better to practise yourself rather than watch others doing it.

For some exercises, I know only a brute-force solution, which is certainly undesirable. Fortunately, all of them, marked by the symbol  in the margins, can be done through a Computer Algebra System (CAS). The DVD provided contains the full package and Appendix B describes initial instructions. Computer-assisted exercises also form a test case for our CAS, which validates both the mathematical correctness of the library and its practical usefulness.

All figures in the book are printed in black and white to reduce costs. The coloured versions of all pictures are enclosed on the DVD as well—see Appendix B.1 to find them. The reader will be able to produce even more illustrations him/herself with the enclosed software.

There are many classical objects, e.g. pencils of cycles, or power of a point, which often re-occur in this book under different contexts. The detailed index will help to trace most of such places.

Chapter 1 serves as an overview and a gentle introduction, so we do not give a description of the book content here. The reader is now invited to start his/her journey into Möbius-invariant geometries.

Odessa, January 2012

Contents

<i>Preface</i>	vii
<i>List of Figures</i>	xiii
1. Erlangen Programme: Preview	1
1.1 Make a Guess in Three Attempts	2
1.2 Covariance of FSCc	5
1.3 Invariants: Algebraic and Geometric	8
1.4 Joint Invariants: Orthogonality	9
1.5 Higher-order Joint Invariants: Focal Orthogonality	11
1.6 Distance, Length and Perpendicularity	12
1.7 The Erlangen Programme at Large	15
2. Groups and Homogeneous Spaces	17
2.1 Groups and Transformations	17
2.2 Subgroups and Homogeneous Spaces	20
2.3 Differentiation on Lie Groups and Lie Algebras	23
3. Homogeneous Spaces from the Group $SL_2(\mathbb{R})$	29
3.1 The Affine Group and the Real Line	29
3.2 One-dimensional Subgroups of $SL_2(\mathbb{R})$	30
3.3 Two-dimensional Homogeneous Spaces	32
3.4 Elliptic, Parabolic and Hyperbolic Cases	35
3.5 Orbits of the Subgroup Actions	37
3.6 Unifying EPH Cases: The First Attempt	39
3.7 Isotropy Subgroups	40

4.	The Extended Fillmore–Springer–Cnops Construction	43
4.1	Invariance of Cycles	43
4.2	Projective Spaces of Cycles	45
4.3	Covariance of FSCc	47
4.4	Origins of FSCc	50
4.5	Projective Cross-Ratio	53
5.	Indefinite Product Space of Cycles	55
5.1	Cycles: An Appearance and the Essence	55
5.2	Cycles as Vectors	57
5.3	Invariant Cycle Product	61
5.4	Zero-radius Cycles	64
5.5	Cauchy–Schwarz Inequality and Tangent Cycles	67
6.	Joint Invariants of Cycles: Orthogonality	69
6.1	Orthogonality of Cycles	69
6.2	Orthogonality Miscellanea	72
6.3	Ghost Cycles and Orthogonality	76
6.4	Actions of FSCc Matrices	80
6.5	Inversions and Reflections in Cycles	84
6.6	Higher-order Joint Invariants: Focal Orthogonality	87
7.	Metric Invariants in Upper Half-Planes	91
7.1	Distances	91
7.2	Lengths	94
7.3	Conformal Properties of Möbius Maps	96
7.4	Perpendicularity and Orthogonality	97
7.5	Infinitesimal-radius Cycles	100
7.6	Infinitesimal Conformality	103
8.	Global Geometry of Upper Half-Planes	105
8.1	Compactification of the Point Space	105
8.2	(Non)-Invariance of The Upper Half-Plane	108
8.3	Optics and Mechanics	111
8.4	Relativity of Space-Time	114
9.	Invariant Metric and Geodesics	117
9.1	Metrics, Curves’ Lengths and Extrema	117

9.2	Invariant Metric	122
9.3	Geodesics: Additivity of Metric	123
9.4	Geometric Invariants	126
9.5	Invariant Metric and Cross-Ratio	128
10.	Conformal Unit Disk	131
10.1	Elliptic Cayley Transforms	131
10.2	Hyperbolic Cayley Transform	133
10.3	Parabolic Cayley Transforms	134
10.4	Cayley Transforms of Cycles	136
11.	Unitary Rotations	141
11.1	Unitary Rotations—An Algebraic Approach	141
11.2	Unitary Rotations—A Geometrical Viewpoint	143
11.3	Rebuilding Algebraic Structures from Geometry	146
11.4	Invariant Linear Algebra	148
11.5	Linearisation of the Exotic Form	151
11.6	Conformality and Geodesics	153
	<i>Epilogue: About the Cover</i>	155
	Appendix A Supplementary Material	157
A.1	Dual and Double Numbers	157
A.2	Classical Properties of Conic Sections	158
A.3	Comparison with Yaglom's Book	159
A.4	Other Approaches and Results	159
A.5	FSCc with Clifford Algebras	160
	Appendix B How to Use the Software	163
B.1	Viewing Colour Graphics	163
B.2	Installation of CAS	164
B.3	Using the CAS and Computer Exercises	167
B.4	Library for Cycles	170
B.5	Predefined Objects at Initialisation	172
	<i>Bibliography</i>	173
	<i>Index</i>	181

This page intentionally left blank

List of Figures

1.1	Actions of the subgroups A and N by Möbius transformations	3
1.2	Action of the subgroup K	3
1.3	K -orbits as conic sections	4
1.4	Decomposition of an arbitrary Möbius transformation	5
1.5	Cycle implementations, centres and foci	7
1.6	Different σ -implementations of the same $\check{\sigma}$ -zero-radius cycles	9
1.7	Orthogonality of the first kind in the elliptic point space	10
1.8	Focal orthogonality for circles	12
1.9	Radius and distance for parabolas	13
1.10	The perpendicular as the shortest route to a line.	14
3.1	Actions of isotropy subgroups	41
5.1	Linear spans of cycle pairs in EPH cases	59
5.2	Positive and negative cycles	63
6.1	Relation between centres and radii of orthogonal circles.	70
6.2	Orthogonal pencils of cycles	74
6.3	Nine types of cycle orthogonality	77
6.4	Three types of inversions of the rectangular grid	83
6.5	Focal orthogonality of cycles	90
7.1	Zero-radius cycles and the ‘phase’ transition	102
8.1	Compactification and stereographic projections	107
8.2	Continuous transformation from future to the past	108
8.3	Hyperbolic objects in the double cover	109
8.4	Double cover of the hyperbolic space	110

8.5	Some elementary optical systems and their transfer matrices	112
9.1	Lobachevsky geodesics and extrema of curves' lengths	121
9.2	Region where the triangular inequality fails	126
9.3	Geodesics and equidistant orbits in EPH geometries	130
10.1	Action of the isotropy subgroups under the Cayley transform	137
10.2	Cayley transforms in elliptic, parabolic and hyperbolic spaces	138
10.3	EPH unit disks and actions of one-parameter subgroups	140
11.1	Rotations of algebraic wheels	142
11.2	Geodesics as spokes	154
A.1	Classical definitions of conic sections	158
A.2	The correspondence between complex, dual and double numbers	161
A.3	Comparison with the Yaglom book.	162
B.1	Initial screens of software start up	165

Chapter 1

Erlangen Programme: Preview

The simplest objects with non-commutative (but still associative) multiplication may be 2×2 matrices with real entries. The subset of matrices *of determinant one* has the following properties:

- It is a closed set under multiplication since $\det(AB) = \det A \cdot \det B$.
- The identity matrix is the set.
- Any such matrix has an inverse (since $\det A \neq 0$).

In other words, these matrices form a *group*, the $\mathrm{SL}_2(\mathbb{R})$ group [77] – one of the two most important Lie groups in analysis. The other group is the Heisenberg group [43]. By contrast, the $ax+b$ group, which is used to build wavelets, is only a subgroup of $\mathrm{SL}_2(\mathbb{R})$ – see the numerator in (1.1) below.

The simplest non-linear transforms of the real line – *linear-fractional* or *Möbius maps* – may also be associated with 2×2 matrices, cf. [6, Ch. 13]:

$$g : x \mapsto g \cdot x = \frac{ax + b}{cx + d}, \quad \text{where } g = \begin{pmatrix} a & b \\ c & d \end{pmatrix}, \quad x \in \mathbb{R}. \quad (1.1)$$

An enjoyable calculation shows that the composition of two transforms (1.1) with different matrices g_1 and g_2 is again a Möbius transform with a matrix equal the product $g_1 g_2$. In other words, (1.1) is a (left) action of $\mathrm{SL}_2(\mathbb{R})$.

According to F. Klein's *Erlangen programme* (which was influenced by S. Lie), any geometry deals with invariant properties under a certain transitive group action. For example, we may ask: *What kinds of geometry are related to the $\mathrm{SL}_2(\mathbb{R})$ action (1.1)?*

The Erlangen programme has probably the highest rate of $\frac{\text{praised}}{\text{actually used}}$ among mathematical theories, not only due to the large numerator but also due to the undeservedly small denominator. As we shall see below, Klein's approach provides some surprising conclusions even for such over-studied objects as circles.

1.1 Make a Guess in Three Attempts

It is easy to see that the $\mathrm{SL}_2(\mathbb{R})$ action (1.1) also makes sense as a map of complex numbers $z = x + iy$, $i^2 = -1$, assuming the denominator is non-zero. Moreover, if $y > 0$, then $g \cdot z$ has a positive imaginary part as well, i.e. (1.1) defines a map from the upper half-plane to itself.

However, there is no need to be restricted to the traditional route of complex numbers only. Less-known *double* and *dual* numbers, see [108, Suppl. C] and Appendix A.1, also have the form $z = x + \iota y$ but with different assumptions for the imaginary unit ι : $\iota^2 = 0$ or $\iota^2 = 1$, respectively. We will write ε and j instead of ι within dual and double numbers, respectively. Although the arithmetic of dual and double numbers is different from that of complex numbers, e.g. they have divisors of zero, we are still able to define their transforms by (1.1) in most cases.

Three possible values -1 , 0 and 1 of $\sigma := \iota^2$ will be referred to here as *elliptic*, *parabolic* and *hyperbolic* cases, respectively. We repeatedly meet such a division of various mathematical objects into three classes. They are named by the historic first example—the classification of conic sections—however the pattern persistently reproduces itself in many different areas: equations, quadratic forms, metrics, manifolds, operators, etc. We will abbreviate this separation as the *EPH classification*. The common origin of this fundamental division of any family with one parameter can be seen from the simple picture of a coordinate line split by zero into negative and positive half-axes:

$$\begin{array}{c} \text{---} \quad \quad \quad 0 \quad \quad \quad \text{---} \\ \text{hyperbolic} \quad \uparrow \quad \text{elliptic} \\ \text{parabolic} \end{array} \quad (1.2)$$

Connections between different objects admitting EPH classification are not limited to this common source. There are many deep results linking, for example, the ellipticity of quadratic forms, metrics and operators, e.g. the Atiyah–Singer index theorem. On the other hand, there are still many white spots, empty cells, obscure gaps and missing connections between some subjects.

To understand the action (1.1) in all EPH cases we use the Iwasawa decomposition [77, Sec. III.1] of $\mathrm{SL}_2(\mathbb{R}) = ANK$ into three one-dimensional subgroups A , N and K :

$$\begin{pmatrix} a & b \\ c & d \end{pmatrix} = \begin{pmatrix} \alpha & 0 \\ 0 & \alpha^{-1} \end{pmatrix} \begin{pmatrix} 1 & \nu \\ 0 & 1 \end{pmatrix} \begin{pmatrix} \cos \phi & -\sin \phi \\ \sin \phi & \cos \phi \end{pmatrix}. \quad (1.3)$$

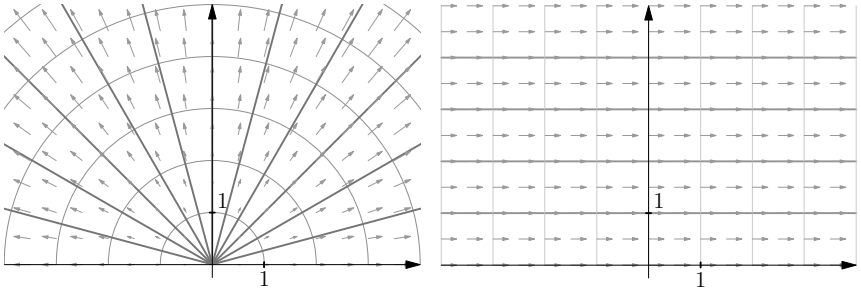


Figure 1.1 Actions of the subgroups A and N by Möbius transformations. Transverse thin lines are images of the vertical axis, grey arrows show the derived action.

Subgroups A and N act in (1.1) irrespective of the value of σ : A makes a dilation by α^2 , i.e. $z \mapsto \alpha^2 z$, and N shifts points to left by ν , i.e. $z \mapsto z + \nu$. This is illustrated by Fig. 1.1.

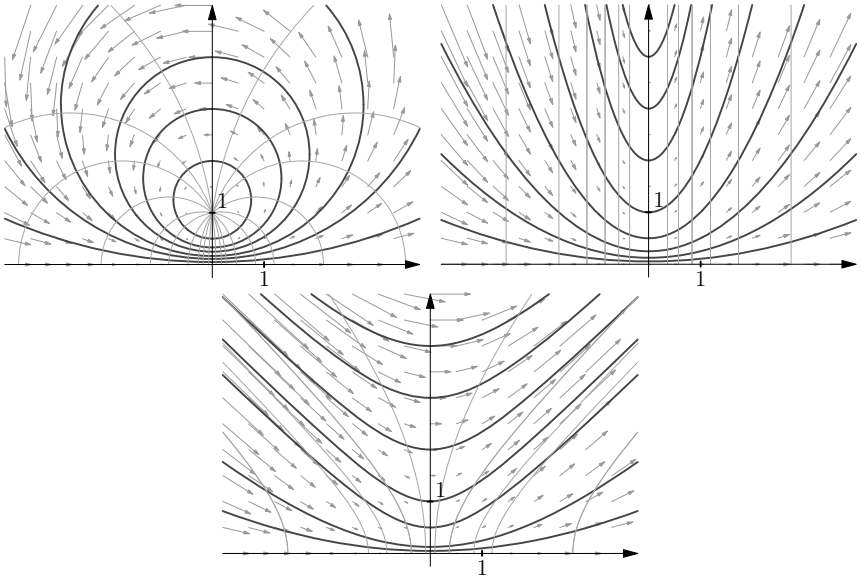


Figure 1.2 Action of the subgroup K . The corresponding orbits are circles, parabolas and hyperbolas shown by thick lines. Transverse thin lines are images of the vertical axis, grey arrows show the derived action.

By contrast, the action of the third matrix from the subgroup K sharply depends on σ —see Fig. 1.2. In elliptic, parabolic and hyperbolic cases,

K -orbits are circles, parabolas and (equilateral) hyperbolas, respectively. Thin traversal lines in Fig. 1.2 join points of orbits for the same values of ϕ and grey arrows represent ‘local velocities’ – vector fields of derived representations.

Definition 1.1. The common name *cycle* [108] is used to denote circles, parabolas and hyperbolas (as well as straight lines as their limits) in the respective EPH case.

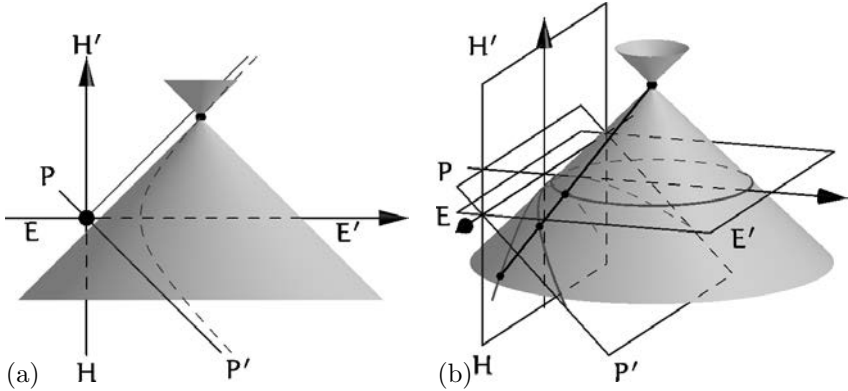


Figure 1.3 K -orbits as conic sections. Circles are sections by the plane EE' , parabolas are sections by PP' and hyperbolas are sections by HH' . Points on the same generator of the cone correspond to the same value of ϕ .

It is well known that any cycle is a *conic section* and an interesting observation is that corresponding K -orbits are, in fact, sections of the same two-sided right-angle cone, see Fig. 1.3. Moreover, each straight line generating the cone, see Fig. 1.3(b), is crossing corresponding EPH K -orbits at points with the same value of parameter ϕ from (1.3). In other words, all three types of orbits are generated by the rotations of this generator along the cone.

K -orbits are K -invariant in a trivial way. Moreover, since actions of both A and N for any σ are extremely ‘shape-preserving’, we find natural invariant objects of the Möbius map:

Theorem 1.2. *The family of all cycles from Definition 1.1 is invariant under the action (1.1).*

Proof. We will show that, for a given $g \in \text{SL}_2(\mathbb{R})$ and a cycle C , its image

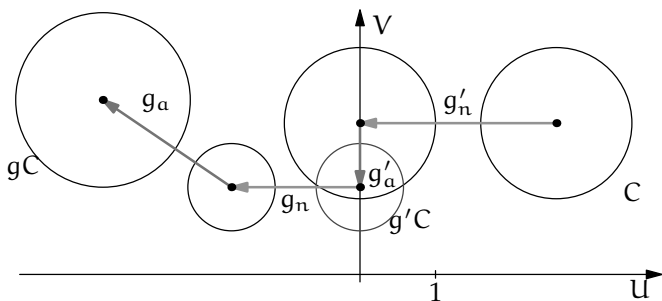


Figure 1.4 Decomposition of an arbitrary Möbius transformation g into a product.

gC is again a cycle. Figure 1.4 provides an illustration with C being a circle, but our reasoning works in all EPH cases.

For a fixed C , there is the unique pair of transformations g'_n from the subgroup N and $g'_a \in A$ that the cycle $g'_a g'_n C$ is exactly a K -orbit. This will be shown later in Exercise 4.7.

We make a decomposition of $g(g'_a g'_n)^{-1}$ into a product similar to (1.3):

$$g(g'_a g'_n)^{-1} = g_a g_n g_k.$$

Since $g'_a g'_n C$ is a K -orbit, we have $g_k(g'_a g'_n C) = g'_a g'_n C$. Then:

$$\begin{aligned} gC &= g(g'_a g'_n)^{-1} g'_a g'_n C = g_a g_n g_k g'_a g'_n C \\ &= g_a g_n g_k(g'_a g'_n C) = g_a g_n g'_a g'_n C. \end{aligned}$$

All transformations from subgroups A and N preserve the shape of any cycles in an obvious way. Therefore, the last expression $g_a g_n g'_a g'_n C$ represents a cycle and our proof is finished. \square

According to Erlangen ideology, we should now study the invariant properties of cycles.

1.2 Covariance of FSCc

Figure 1.3 suggests that we may obtain a unified treatment of cycles in all EPH cases by consideration of higher-dimension spaces. The standard mathematical method is to declare objects under investigation (cycles in our case, functions in functional analysis, etc.) to be simply points of some larger space. This space should be equipped with an appropriate structure to hold information externally which previously described the inner properties of our objects.

A generic cycle is the set of points $(u, v) \in \mathbb{R}^2$ defined for all values of σ by the equation

$$k(u^2 - \sigma v^2) - 2lu - 2nv + m = 0. \quad (1.4)$$

This equation (and the corresponding cycle) is defined by a point (k, l, n, m) from a *projective space* \mathbb{P}^3 , since, for a scaling factor $\lambda \neq 0$, the point $(\lambda k, \lambda l, \lambda n, \lambda m)$ defines an equation equivalent to (1.4). We call \mathbb{P}^3 the *cycle space* and refer to the initial \mathbb{R}^2 as the *point space*.

In order to obtain a connection with the Möbius action (1.1), we arrange numbers (k, l, n, m) into the matrix

$$C_\sigma^s = \begin{pmatrix} l + \check{\imath}sn & -m \\ k & -l + \check{\imath}sn \end{pmatrix}, \quad (1.5)$$

with a new hypercomplex unit $\check{\imath}$ and an additional parameter s , usually equal to ± 1 . The values of $\check{\sigma} := \check{\imath}^2$ are $-1, 0$ or 1 independent of the value of σ . The matrix (1.5) is the cornerstone of an extended *Fillmore–Springer–Cnops construction* (FSCc) [22].

The significance of FSCc in the Erlangen framework is provided by the following result:

Theorem 1.3. *The image \tilde{C}_σ^s of a cycle C_σ^s under transformation (1.1) with $g \in \text{SL}_2(\mathbb{R})$ is given by similarity of the matrix (1.5):*

$$\tilde{C}_\sigma^s = g C_\sigma^s g^{-1}. \quad (1.6)$$

In other words, FSCc (1.5) intertwines Möbius action (1.1) on cycles with linear map (1.6).

There are several ways to prove (1.6). Either by a brute-force calculation (which can, fortunately, be performed by a CAS) in Section 4.3, or through the related orthogonality of cycles [22] – see the end of Section 1.4.

The important observation here is that our extended version of FSCc (1.5) uses an imaginary unit $\check{\imath}$, which is not related to \imath , that defines the appearance of cycles on the plane. In other words, any EPH type of geometry in the cycle space \mathbb{P}^3 admits drawing of cycles in the point space \mathbb{R}^2 as circles, parabolas or hyperbolas. We may think of points of \mathbb{P}^3 as ideal cycles while their depictions on \mathbb{R}^2 are only their shadows on the wall of Plato’s cave.

Figure 1.5(a) shows the same cycles drawn in different EPH styles. We note the first order contact between the circle, parabola and hyperbola in the intersection points with the real line. Informally, we can say that

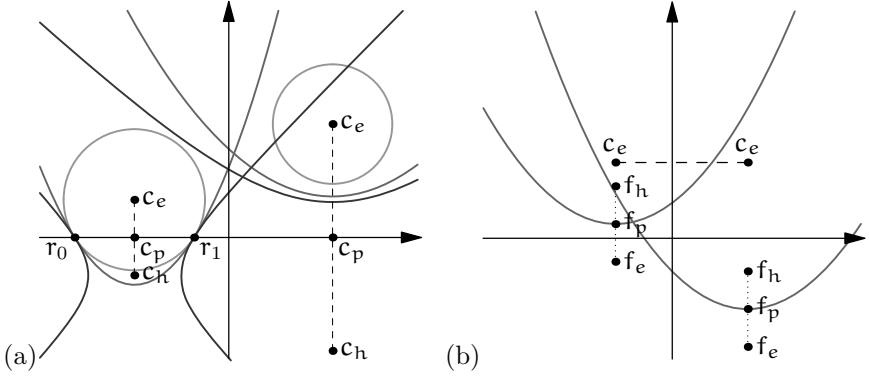


Figure 1.5 Cycle implementations, centres and foci. (a) Different EPH implementations of the same cycles defined by quadruples of numbers. (b) Centres and foci of two parabolas with the same focal length.

EPH realisations of a cycle look the same in a vicinity of the real line. It is not surprising since cycles are invariants of the hypercomplex Möbius transformations, which are extensions of $SL_2(\mathbb{R})$ -action (3.24) on the real line.

Points $c_{e,p,h} = (\frac{l}{k}, -\delta \frac{n}{k})$ on Fig. 1.5(a) are the respective e/p/h-centres of drawn cycles. They are related to each other through several identities:

$$c_e = \bar{c}_h, \quad c_p = \frac{1}{2}(c_e + c_h). \quad (1.7)$$

Figure 1.5(b) presents two cycles drawn as parabolas. They have the same focal length, $\frac{n}{2k}$, and, thus, their e-centres are on the same level. In other words, *concentric* parabolas are obtained by a vertical shift, not by scaling, as an analogy with circles or hyperbolas may suggest.

Figure 1.5(b) also presents points, called e/p/h-foci,

$$f_{e,p,h} = \left(\frac{l}{k}, \frac{\det C_{\sigma}^s}{2nk} \right), \quad (1.8)$$

which are independent of the sign of s . If a cycle is depicted as a parabola, then the h-focus, p-focus and e-focus are, correspondingly, the geometrical focus of the parabola, its vertex, and the point on the directrix nearest to the vertex.

As we will see (cf. Theorems 1.5 and 1.7), all three centres and three foci are useful attributes of a cycle, even if it is drawn as a circle.

1.3 Invariants: Algebraic and Geometric

We use known algebraic invariants of matrices to build appropriate geometric invariants of cycles. It is yet another demonstration that any division of mathematics into subjects is only illusive.

For 2×2 matrices (and, therefore, cycles), there are only two essentially different invariants under similarity (1.6) (and, therefore, under Möbius action (1.1)): the *trace* and the *determinant*. The latter was already used in (1.8) to define a cycle's foci. However, due to the projective nature of the cycle space \mathbb{P}^3 , the absolute values of the trace or determinant are irrelevant, unless they are zero.

Alternatively, we may have a special arrangement for the normalisation of quadruples (k, l, n, m) . For example, if $k \neq 0$, we may normalise the quadruple to $(1, \frac{l}{k}, \frac{n}{k}, \frac{m}{k})$ with the highlighted cycle's centre. Moreover, in this case, $-\det C_{\check{\sigma}}^s$ is equal to the square of cycle's radius, cf. Section 1.6. Another normalisation, $\det C_{\check{\sigma}}^s = \pm 1$, is used in [54] to obtain a good condition for touching circles.

We still have important characterisation even with non-normalised cycles. For example, invariant classes (for different $\check{\sigma}$) of cycles are defined by the condition $\det C_{\check{\sigma}}^s = 0$. Such a class is parameterised only by two real numbers and, as such, is easily attached to a certain point of \mathbb{R}^2 . For example, the cycle $C_{\check{\sigma}}^s$ with $\det C_{\check{\sigma}}^s = 0$, $\check{\sigma} = -1$, drawn elliptically, represents just a point $(\frac{l}{k}, \frac{n}{k})$, i.e. an (elliptic) zero-radius circle. The same condition with $\check{\sigma} = 1$ in hyperbolic drawing produces a null-cone originating at point $(\frac{l}{k}, \frac{n}{k})$:

$$(u - \frac{l}{k})^2 - (v - \frac{n}{k})^2 = 0,$$

i.e. a zero-radius cycle in a hyperbolic metric.

In general, for every concept there are at least nine possibilities: three EPH cases in the cycle space times three EPH realisations in the point space. These nine cases for 'zero-radius' cycles are shown in Fig. 1.6. For example, p-zero-radius cycles in any implementation touch the real axis.

This 'touching' property is a manifestation of the *boundary effect* in the upper-half plane geometry. The famous question about hearing a drum's shape has a counterpart: *Can we see/feel the boundary from inside a domain?*

Both orthogonality relations described below are 'boundary-aware' as well. After all, it is not surprising since $\mathrm{SL}_2(\mathbb{R})$ action on the upper half-plane was obtained as an extension of its action (1.1) on the boundary.

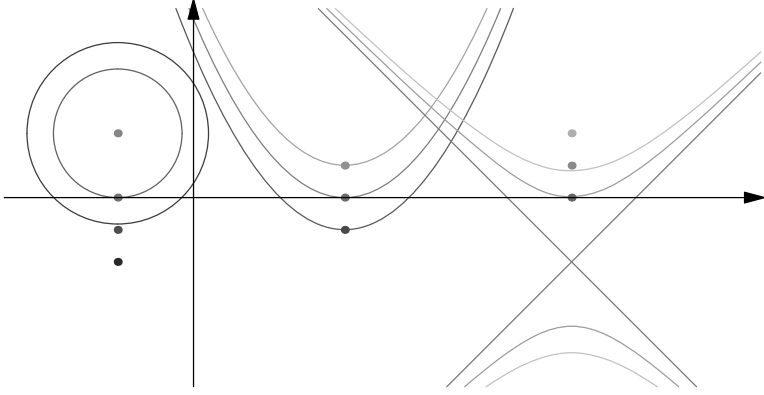


Figure 1.6 Different σ -implementations of the same $\check{\sigma}$ -zero-radius cycles. The corresponding foci belong to the real axis.

According to the categorical viewpoint, internal properties of objects are of minor importance in comparison to their relations with other objects from the same class. As an example, we may give the proof of Theorem 1.3 described at the end of the next section. Thus, from now on, we will look for invariant relations between two or more cycles.

1.4 Joint Invariants: Orthogonality

The most expected relation between cycles is based on the following Möbius-invariant ‘inner product’, built from a trace of the product of two cycles as matrices:

$$\langle C_{\sigma}^s, \tilde{C}_{\sigma}^s \rangle = -\text{tr}(C_{\sigma}^s \overline{\tilde{C}_{\sigma}^s}). \quad (1.9)$$

Here, $\overline{\tilde{C}_{\sigma}^s}$ means the complex conjugation of elements of the matrix \tilde{C}_{σ}^s . Notably, an inner product of this type is used, for example, in GNS construction to make a Hilbert space out of C^* -algebra. The next standard move is given by the following definition:

Definition 1.4. Two cycles are called $\check{\sigma}$ -orthogonal if $\langle C_{\sigma}^s, \tilde{C}_{\sigma}^s \rangle = 0$.

For the case of $\check{\sigma}\sigma = 1$, i.e. when the geometries of the cycle and point spaces are both either elliptic or hyperbolic, such an orthogonality is standard, defined in terms of angles between tangent lines in the intersection points of two cycles. However, in the remaining seven $(9 - 2)$ cases, the innocent-looking Definition 1.4 brings unexpected relations.

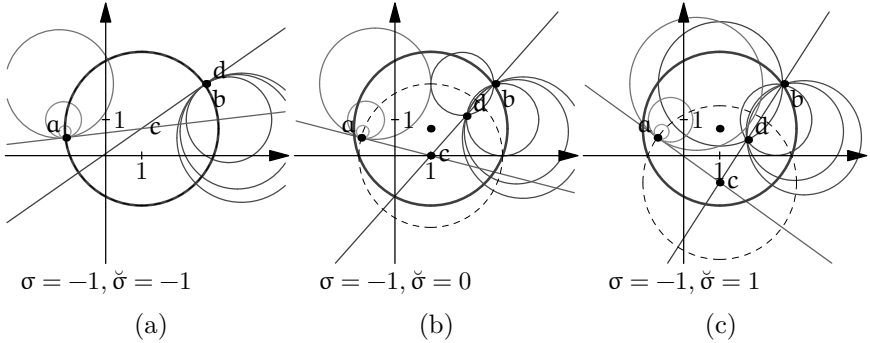


Figure 1.7 Orthogonality of the first kind in the elliptic point space. Each picture presents two groups (green and blue) of cycles which are orthogonal to the red cycle C_σ^s . Point b belongs to C_σ^s and the family of blue cycles passing through b is orthogonal to C_σ^s . They all also intersect at the point d which is the inverse of b in C_σ^s . Any orthogonality is reduced to the usual orthogonality with a new ('ghost') cycle (shown by the dashed line), which may or may not coincide with C_σ^s . For any point a on the 'ghost' cycle, the orthogonality is reduced to the local notion in terms of tangent lines at the intersection point. Consequently, such a point a is always the inverse of itself.

Elliptic (in the point space) realisations of Definition 1.4, i.e. $\sigma = -1$, are shown in Fig. 1.7. Figure 1.7(a) corresponds to the elliptic cycle space, e.g. $\check{\sigma} = -1$. The orthogonality between the red circle and any circle from the blue or green families is given in the usual Euclidean sense. Figure 1.7(b) (parabolic in the cycle space) and Fig. 1.7(c) (hyperbolic) show the non-local nature of the orthogonality. There are analogous pictures in parabolic and hyperbolic point spaces – see Section 6.1.

This orthogonality may still be expressed in the traditional sense if we will associate to the red circle the corresponding 'ghost' circle, which is shown by the dashed lines in Fig. 1.7. To describe the ghost cycle, we need the *Heaviside function* $\chi(\sigma)$:

$$\chi(t) = \begin{cases} 1, & t \geq 0; \\ -1, & t < 0. \end{cases} \quad (1.10)$$

Theorem 1.5. *A cycle is $\check{\sigma}$ -orthogonal to cycle C_σ^s if it is orthogonal in the usual sense to the σ -realisation of 'ghost' cycle \hat{C}_σ^s , which is defined by the following two conditions:*

- i. *The $\chi(\sigma)$ -centre of \hat{C}_σ^s coincides with the $\check{\sigma}$ -centre of C_σ^s .*
- ii. *Cycles \hat{C}_σ^s and C_σ^s have the same roots. Moreover, $\det \hat{C}_\sigma^1 = \det C_\sigma^{\chi(\check{\sigma})}$.*

The above connection between various centres of cycles illustrates their relevance to our approach.

One can easily check the following orthogonality properties of the zero-radius cycles defined in the previous section:

- i. Due to the identity $\langle C_\sigma^s, C_\sigma^s \rangle = 2 \det C_\sigma^s$, zero-radius cycles are self-orthogonal (isotropic).
- ii. A cycle C_σ^s is σ -orthogonal to a zero-radius cycle Z_σ^s if and only if C_σ^s passes through the σ -centre of Z_σ^s .

Sketch of proof of Theorem 1.3. The validity of Theorem 1.3 for a zero-radius cycle

$$Z_\sigma^s = \begin{pmatrix} z & -z\bar{z} \\ 1 & -\bar{z} \end{pmatrix} = \frac{1}{2} \begin{pmatrix} z & z \\ 1 & 1 \end{pmatrix} \begin{pmatrix} 1 & -\bar{z} \\ 1 & -\bar{z} \end{pmatrix}$$

with the centre $z = x + \iota y$ is straightforward. This implies the result for a generic cycle with the help of Möbius invariance of the product (1.9) (and, thus, the orthogonality) and the above relation (Theorem 1.5.ii) between the orthogonality and the incidence. See Exercise 6.7 for details. \square

1.5 Higher-order Joint Invariants: Focal Orthogonality

With our appetite already whet we may wish to build more joint invariants. Indeed, for any polynomial $p(x_1, x_2, \dots, x_n)$ of several non-commuting variables, one may define an invariant joint disposition of n cycles ${}^j C_\sigma^s$ by the condition

$$\text{tr } p({}^1 C_\sigma^s, {}^2 C_\sigma^s, \dots, {}^n C_\sigma^s) = 0.$$

However, it is preferable to keep some geometrical meaning of constructed notions.

An interesting observation is that, in the matrix similarity of cycles (1.6), one may replace element $g \in \text{SL}_2(\mathbb{R})$ by an arbitrary matrix corresponding to another cycle. More precisely, the product $C_\sigma^s \tilde{C}_\sigma^s C_\sigma^s$ is again the matrix of the form (1.5) and, thus, may be associated with a cycle. This cycle may be considered as the reflection of \tilde{C}_σ^s in C_σ^s .

Definition 1.6. A cycle C_σ^s is f-orthogonal to a cycle \tilde{C}_σ^s if the reflection of \tilde{C}_σ^s in C_σ^s is orthogonal (in the sense of Definition 1.4) to the real line. Analytically, this is defined by

$$\text{tr}(C_\sigma^s \tilde{C}_\sigma^s C_\sigma^s R_\sigma^s) = 0. \quad (1.11)$$

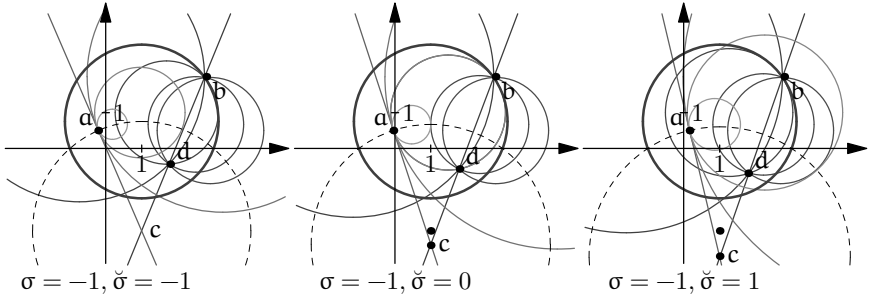


Figure 1.8 Focal orthogonality for circles. To highlight both similarities and distinctions with ordinary orthogonality, we use the same notations as in Fig. 1.7.

Due to invariance of all components in the above definition, f-orthogonality is a Möbius-invariant condition. Clearly, this is not a symmetric relation – if C_σ^s is f-orthogonal to \tilde{C}_σ^s , then \tilde{C}_σ^s is not necessarily f-orthogonal to C_σ^s .

Figure 1.8 illustrates f-orthogonality in the elliptic point space. In contrast to Fig. 1.7, it is not a local notion at the intersection points of cycles for all $\check{\sigma}$. However, it may again be clarified in terms of the appropriate f-ghost cycle, cf. Theorem 1.5.

Theorem 1.7. *A cycle is f-orthogonal to a cycle C_σ^s if it is orthogonal in the traditional sense to its f-ghost cycle $\tilde{C}_\sigma^{\check{\sigma}} = C_\sigma^{\chi(\sigma)} \mathbb{R}_\sigma^{\check{\sigma}} C_\sigma^{\chi(\sigma)}$, which is the reflection of the real line in $C_\sigma^{\chi(\sigma)}$ and χ is the Heaviside function (1.10). Moreover:*

- i. *The $\chi(\sigma)$ -centre of $\tilde{C}_\sigma^{\check{\sigma}}$ coincides with the $\check{\sigma}$ -focus of C_σ^s . Consequently, all lines f-orthogonal to C_σ^s pass the respective focus.*
- ii. *Cycles C_σ^s and $\tilde{C}_\sigma^{\check{\sigma}}$ have the same roots.*

Note the above intriguing interplay between the cycle's centres and foci. Although f-orthogonality may look exotic, it will appear again at the end of next section.

Of course, it is possible to define other interesting higher-order joint invariants of two or even more cycles.

1.6 Distance, Length and Perpendicularity

Geometry in the plain meaning of the word deals with *distances* and *lengths*. Can we obtain them from cycles?

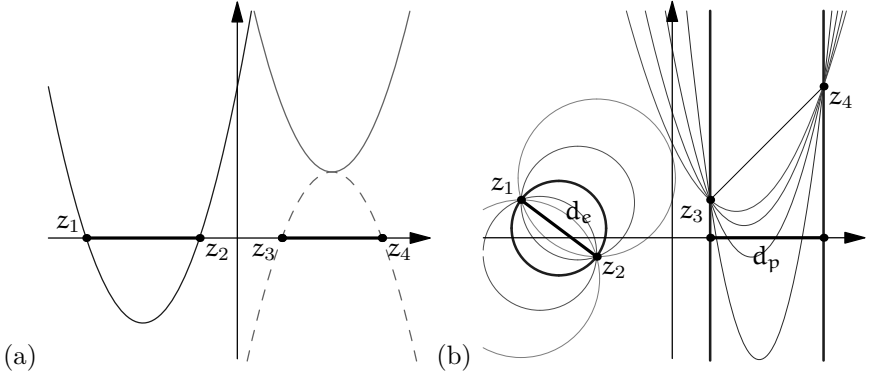


Figure 1.9 Radius and distance for parabolas. (a) The square of the parabolic diameter is the square of the distance between roots if they are real (z_1 and z_2). Otherwise, it is the negative square of the distance between the adjoint roots (z_3 and z_4). (b) Distance is the extremum of diameters in elliptic (z_1 and z_2) and parabolic (z_3 and z_4) cases.

We already mentioned that, for circles normalised by the condition $k = 1$, the value $-\det C_\sigma^s = -\frac{1}{2}\langle C_\sigma^s, C_\sigma^s \rangle$ produces the square of the traditional circle radius. Thus, we may keep it as the definition of the σ -radius for any cycle. However, we then need to accept that, in the parabolic case, the radius is the (Euclidean) distance between (real) roots of the parabola—see Fig. 1.9(a).

Having already defined the radii of circles, we may use them for other measurements in several different ways. For example, the following variational definition may be used:

Definition 1.8. The *distance* between two points is the extremum of diameters of all cycles passing through both points—see Fig. 1.9(b).

If $\sigma = \sigma$, this definition gives, in all EPH cases, the following expression for a distance $d_{e,p,h}(u, v)$ between the endpoints of any vector $w = u + iv$:

$$d_{e,p,h}(u, v)^2 = (u + iv)(u - iv) = u^2 - \sigma v^2. \quad (1.12)$$

The parabolic distance $d_p^2 = u^2$, see Fig. 1.9(b), sits algebraically between d_e and d_h according to the general principle (1.2) and is widely accepted [108]. However, one may be unsatisfied by its degeneracy.

An alternative measurement is motivated by the fact that a circle is the set of equidistant points from its centre. However, there are now several choices for the ‘centre’: it may be either a point from three centres (1.7) or three foci (1.8).

Definition 1.9. The *length* of a directed interval \overrightarrow{AB} is the radius of the cycle with its *centre* (denoted by $l_c(\overrightarrow{AB})$) or *focus* (denoted by $l_f(\overrightarrow{AB})$) at the point A which passes through B .

This definition is less common and has some unusual properties like non-symmetry: $l_f(\overrightarrow{AB}) \neq l_f(\overrightarrow{BA})$. However, it comfortably fits the Erlangen programme due to its $\text{SL}_2(\mathbb{R})$ -conformal invariance:

Theorem 1.10 ([65]). Let l denote either the EPH distances (1.12) or any length from Definition 1.9. Then, for fixed $y, y' \in \mathbb{A}$, the limit

$$\lim_{t \rightarrow 0} \frac{l(g \cdot y, g \cdot (y + ty'))}{l(y, y + ty')}$$

(where $g \in \text{SL}_2(\mathbb{R})$) exists and its value depends only on y and g and is independent of y' .

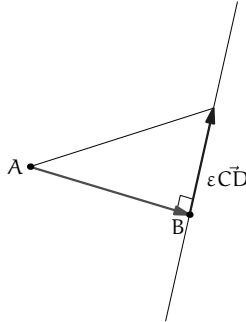


Figure 1.10 The perpendicular as the shortest route to a line.

We may return from lengths to angles noting that, in the Euclidean space, a perpendicular is the shortest route from a point to a line—see Fig. 1.10.

Definition 1.11. Let l be a length or distance. We say that a vector \overrightarrow{AB} is *l -perpendicular* to a vector \overrightarrow{CD} if function $l(\overrightarrow{AB} + \epsilon \overrightarrow{CD})$ of a variable ϵ has a local extremum at $\epsilon = 0$.

A pleasant surprise is that l_f -perpendicularity obtained using the length from focus (Definition 1.9) coincides with f-orthogonality (already defined in Section 1.5), as follows from Theorem 1.7.i.

All these studies are waiting to be generalised to higher-dimensions. Quaternions and Clifford algebras provide a suitable language for this [65, 87].

1.7 The Erlangen Programme at Large

As we already mentioned, the division of mathematics into separate areas is purely imaginary. Therefore, it is unnatural to limit the Erlangen programme only to ‘geometry’. We may continue to look for $\mathrm{SL}_2(\mathbb{R})$ -invariant objects in other related fields. For example, transform (1.1) generates the unitary representation on the space $L_2(\mathbb{R})$:

$$g : f(x) \mapsto \frac{1}{(cx + d)} f\left(\frac{ax + b}{cx + d}\right). \quad (1.13)$$

The above transformations have two invariant subspaces within $L_2(\mathbb{R})$: the Hardy space and its orthogonal complements. These spaces are of enormous importance in *harmonic analysis*. Similar transformations

$$g : f(z) \mapsto \frac{1}{(cz + d)^m} f\left(\frac{az + b}{cz + d}\right), \quad (1.14)$$

for $m = 2, 3, \dots$, can be defined on square-integrable functions in the upper half-plane. The respective invariant subspaces are weighted Bergman spaces of complex-valued analytic and poly-analytic functions.

Transformations (1.14) produce the *discrete series* representations of $\mathrm{SL}_2(\mathbb{R})$, cf. [77, Sec. IX.2]. Consequently, all main objects of *complex analysis* can be obtained in terms of invariants of these representations. For example:

- The Cauchy and Bergman integrals are special cases of *wavelet transform*, cf. [60, Sec. 3]. The corresponding *mother wavelets* are eigenfunctions of operators from the representations of the subgroup K .
- The Cauchy–Riemann and Laplace operators are invariant differential operators. They annihilate the respective mother wavelet which are mentioned above, cf. [66, Sec. 3].
- Taylor series is a decomposition over eigenfunctions of the subgroup K , cf. [58, Sec. 3.4].

It would be an omission to limit this construction only to the discrete series, complex numbers and the subgroup K . Two other series of representations (*principal* and *complimentary* – see [77, Sec. VI.6]) are related to important special functions [106] and differential operators [81]. These series have unitary realisations in dual and double numbers [58, 67]. Their relations with subgroups N' and A' will be shown in Section 3.3.4.

Moving further, we may observe that transform (1.1) is also defined for an element x in any algebra \mathfrak{A} with a unit $\mathbf{1}$ as soon as $(cx + d\mathbf{1}) \in \mathfrak{A}$ has an

inverse. If \mathfrak{A} is equipped with a topology, e.g. is a Banach algebra, then we may study a *functional calculus* for element x [57] in this way. It is defined as an intertwining operator between the representations (1.13) or (1.14) in spaces of analytic functions and similar representations in left \mathfrak{A} -modules.

In the spirit of the Erlangen programme, such functional calculus is still a geometry, since it is dealing with invariant properties under a group action. However, even for the simplest non-normal operator, e.g. a Jordan block of length k , the obtained space is not like a space of points but is, rather, a space of k -th *jets* [61]. Such non-point behaviour is often attributed to *non-commutative geometry* and the Erlangen programme provides an important insight on this popular topic [60].

Of course, there is no reason to limit the Erlangen programme to the group $\mathrm{SL}_2(\mathbb{R})$ only – other groups may be more suitable in different situations. For example, the Heisenberg group and its hypercomplex representations are useful in quantum mechanics [68, 70]. However, $\mathrm{SL}_2(\mathbb{R})$ still possesses large unexplored potential and is a good object to start with.

Chapter 2

Groups and Homogeneous Spaces

Group theory and representation theory are themselves two enormous and interesting subjects. However, they are auxiliary in our consideration and we are forced to restrict our consideration to a brief overview.

2.1 Groups and Transformations

We start from the definition of the central object, which formalises the universal notion of symmetries [52, Sec. 2.1].

Definition 2.1. A *transformation group* G is a non-void set of mappings of a certain set X into itself with the following properties:

- i. The identical map is included in G .
- ii. If $g_1 \in G$ and $g_2 \in G$ then $g_1 g_2 \in G$.
- iii. If $g \in G$ then g^{-1} exists and belongs to G .

Exercise 2.2. List all transformation groups on a set of three elements.

Exercise 2.3. Verify that the following sets are transformation groups:

- i. The group of permutations of n elements.
- ii. The group of rotations of the unit circle \mathbb{T} .
- iii. The groups of shifts of the real line \mathbb{R} and the plane \mathbb{R}^2 .
- iv. The group of one-to-one linear maps of an n -dimensional vector space over a field \mathbb{F} onto itself.
- v. The group of linear-fractional (Möbius) transformations:

$$\begin{pmatrix} a & b \\ c & d \end{pmatrix} : z \mapsto \frac{az + b}{cz + d}, \quad (2.1)$$

of the extended complex plane such that $ad - bc \neq 0$.

It is worth (and often done) to push abstraction one level higher and to keep the group alone without the underlying space:

Definition 2.4. An *abstract group* (or simply *group*) is a non-void set G on which there is a law of *group multiplication* (i.e. mapping $G \times G \rightarrow G$) with the properties:

- i. *Associativity*: $g_1(g_2g_3) = (g_1g_2)g_3$.
- ii. The existence of the *identity*: $e \in G$ such that $eg = ge = g$ for all $g \in G$.
- iii. The existence of the *inverse*: for every $g \in G$ there exists $g^{-1} \in G$ such that $gg^{-1} = g^{-1}g = e$.

Exercise 2.5. Check that any transformation group is an abstract group.

If we forget the nature of the elements of a transformation group G as transformations of a set X then we need to supply a separate ‘multiplication table’ for elements of G . An advantage of a transition to abstract groups is that the same abstract group can act by transformations of apparently different sets.

Exercise 2.6. Check that the following transformation groups (cf. Example 2.3) have the same law of multiplication, i.e. are equivalent as abstract groups:

- i. The group of isometric mapping of an equilateral triangle onto itself.
- ii. The group of all permutations of a set of free elements.
- iii. The group of invertible matrices of order 2 with coefficients in the field of integers modulo 2.
- iv. The group of linear fractional transformations of the extended complex plane generated by the mappings $z \mapsto z^{-1}$ and $z \mapsto 1 - z$.

Exercise 2.7. Expand the list in the above exercise.

It is much simpler to study groups with the following additional property.

Definition 2.8. A group G is *commutative* (or *abelian*) if, for all $g_1, g_2 \in G$, we have $g_1g_2 = g_2g_1$.

However, most of the interesting and important groups are non-commutative.

Exercise 2.9. Which groups among those listed in Exercises 2.2 and 2.3 are commutative?

Groups may have some additional analytical structures, e.g. they can be a topological space with a corresponding notion of limit and respective continuity. We also assume that our topological groups are always *locally compact* [52, Sec. 2.4], that is, there exists a compact neighbourhood of every point. It is common to assume that the topological and group structures are in agreement:

Definition 2.10. If, for a group G , group multiplication and inversion are continuous mappings, then G is a *continuous group*.

Exercise 2.11.

- i. Describe topologies which make groups from Exercises 2.2 and 2.3 continuous.
- ii. Show that a continuous group is locally compact if there exists a compact neighbourhood of its identity.

An even better structure can be found among *Lie groups* [52, Sec. 6], e.g. groups with a differentiable law of multiplication. In the investigation of such groups, we could employ the whole arsenal of analytical tools. Hereafter, most of the groups studied will be Lie groups.

Exercise 2.12. Check that the following are non-commutative Lie (and, thus, continuous) groups:

- i. The $ax + b$ group (or the *affine group*) [101, Ch. 7] of the real line: the set of elements (a, b) , $a \in \mathbb{R}_+$, $b \in \mathbb{R}$ with the group law:

$$(a, b) * (a', b') = (aa', ab' + b).$$

The identity is $(1, 0)$ and $(a, b)^{-1} = (a^{-1}, -b/a)$.

- ii. The *Heisenberg group* \mathbb{H}^1 [43; 101, Ch. 1]: a set of triples of real numbers (s, x, y) with the group multiplication:

$$(s, x, y) * (s', x', y') = (s + s' + \frac{1}{2}(x'y - xy'), x + x', y + y'). \quad (2.2)$$

The identity is $(0, 0, 0)$ and $(s, x, y)^{-1} = (-s, -x, -y)$.

- iii. The $\mathrm{SL}_2(\mathbb{R})$ group [44, 77]: a set of 2×2 matrices $\begin{pmatrix} a & b \\ c & d \end{pmatrix}$ with real entries $a, b, c, d \in \mathbb{R}$ and the determinant $\det = ad - bc$ equal to 1 and the group law coinciding with matrix multiplication:

$$\begin{pmatrix} a & b \\ c & d \end{pmatrix} \begin{pmatrix} a' & b' \\ c' & d' \end{pmatrix} = \begin{pmatrix} aa' + bc' & ab' + bd' \\ ca' + dc' & cb' + dd' \end{pmatrix}.$$

The identity is the unit matrix and

$$\begin{pmatrix} a & b \\ c & d \end{pmatrix}^{-1} = \begin{pmatrix} d & -b \\ -c & a \end{pmatrix}.$$

The above three groups are behind many important results of real and complex analysis [43, 44, 62, 77] and we meet them many times later.

2.2 Subgroups and Homogeneous Spaces

A study of any mathematical object is facilitated by a decomposition into smaller or simpler blocks. In the case of groups, we need the following:

Definition 2.13. A *subgroup* of a group G is subset $H \subset G$ such that the restriction of multiplication from G to H makes H a group itself.

Exercise 2.14. Show that the $ax + b$ group is a subgroup of $\mathrm{SL}_2(\mathbb{R})$.

HINT: Consider matrices $\frac{1}{\sqrt{a}} \begin{pmatrix} a & b \\ 0 & 1 \end{pmatrix}$. \diamond

While abstract groups are a suitable language for investigation of their general properties, we meet groups in applications as transformation groups acting on a set X . We will describe the connections between those two viewpoints. It can be approached either by having a homogeneous space build the class of isotropy subgroups or by having a subgroup define respective homogeneous spaces. The next two subsections explore both directions in detail.

2.2.1 From a Homogeneous Space to the Isotropy Subgroup

Let X be a set and let us define, for a group G , an operation $G : X \rightarrow X$ of G on X . We say that a subset $S \subset X$ is G -invariant if $g \cdot s \in S$ for all $g \in G$ and $s \in S$.

Exercise 2.15. Show that if $S \subset X$ is G -invariant then its complement $X \setminus S$ is G -invariant as well.

Thus, if X has a non-trivial invariant subset, we can split X into disjoint parts. The finest such decomposition is obtained from the following equivalence relation on X , say, $x_1 \sim x_2$, if and only if there exists $g \in G$ such that $gx_1 = x_2$, with respect to which X is a disjoint union of distinct

orbits [76, Sec. I.5], that is subsets of all gx_0 with a fixed $x_0 \in X$ and arbitrary $g \in G$.

Exercise 2.16. Let the group $\mathrm{SL}_2(\mathbb{R})$ act on \mathbb{C} by means of linear-fractional transformations (2.1). Show that there exist three orbits: the real axis \mathbb{R} , the *upper and lower half-planes* \mathbb{R}_\pm^n :

$$\mathbb{R}_\pm^2 = \{x \pm iy \mid x, y \in \mathbb{R}, y > 0\}.$$

Thus, from now on, without loss of generality, we assume that the action of G on X is *transitive*, i.e. for every $x \in X$ we have

$$Gx := \bigcup_{g \in G} gx = X.$$

In this case, X is *G-homogeneous space*.

Exercise 2.17. Show that either of the following conditions define a transitive action of G on X :

- i. For two arbitrary points $x_1, x_2 \in X$, there exists $g \in G$ such that $gx_1 = x_2$.
- ii. Let a fixed point $x_0 \in X$ be given, then, for an arbitrary point $x \in X$, there exists $g \in G$ such that $gx_0 = x$.

Exercise 2.18. Show that, for any group G , we can define its action on $X = G$ as follows:

- i. The *conjugation* $g : x \mapsto gxg^{-1}$.
- ii. The *left shift* $\Lambda(g) : x \mapsto gx$ and the *right shift* $R(g) : x \mapsto xg^{-1}$.

The above actions define group homomorphisms from G to the transformation group of G . However, the conjugation is trivial for all commutative groups.

Exercise 2.19. Show that:

- i. The set of elements $G_x = \{g \in G \mid gx = x\}$ for fixed a point $x \in X$ forms a subgroup of G , which is called the *isotropy (sub)group* of x in G [76, Sec. I.5].
- ii. For any $x_1, x_2 \in X$, isotropy subgroups G_{x_1} and G_{x_2} are *conjugated*, that is, there exists $g \in G$ such that $G_{x_1} = g^{-1}G_{x_2}g$.

This provides a transition from a G -action on a homogeneous space X to a subgroup of G , or even to an equivalence class of such subgroups under conjugation.

Exercise 2.20. Find a subgroup which corresponds to the given action of G on X :

- i. Action of $ax + b$ group on \mathbb{R} by the formula: $(a, b) : x \mapsto ax + b$ for the point $x = 0$.
- ii. Action of $\text{SL}_2(\mathbb{R})$ group on one of three orbit from Exercise 2.16 with respective points $x = 0, i$ and $-i$.

2.2.2 From a Subgroup to the Homogeneous Space

We can also go in the opposite direction – given a subgroup of G , find the corresponding homogeneous space. Let G be a group and H be its subgroup. Let us define the space of *cosets* $X = G/H$ by the equivalence relation: $g_1 \sim g_2$ if there exists $h \in H$ such that $g_1 = g_2 h$.

The space $X = G/H$ is a homogeneous space under the left G -action $g : g_1 \mapsto gg_1$. For practical purposes it is more convenient to have a parametrisation of X and express the above G -action through those parameters, as shown below.

We define a continuous function (section) [52, Sec. 13.2] $s : X \rightarrow G$ such that it is a left inverse to the natural projection $p : G \rightarrow G/H$, i.e. $p(s(x)) = x$ for all $x \in X$.

Exercise 2.21. Check that, for any $g \in G$, we have $s(p(g)) = gh$, for some $h \in H$ depending on g .

Then, any $g \in G$ has a unique decomposition of the form $g = s(x)h$, where $x = p(g) \in X$ and $h \in H$. We define a map r associated to s through the identities:

$$x = p(g), \quad h = r(g) := s(x)^{-1}g.$$

Exercise 2.22. Show that:

- i. X is a left G -homogeneous space with the G -action defined in terms of maps s and p as follows:

$$g : x \mapsto g \cdot x = p(g * s(x)), \quad (2.3)$$

where $*$ is the multiplication on G . This is illustrated by the diagram:

$$\begin{array}{ccc} G & \xrightarrow{g*} & G \\ \uparrow s & & \uparrow s \\ X & \xrightarrow{g*} & X \end{array} \quad (2.4)$$

- ii. The above action of $G : X \rightarrow X$ is transitive on X .
- iii. The choice of a section s is not essential in the following sense. Let s_1 and s_2 be two smooth maps, such that $p(s_i(x)) = x$ for all $x \in X$, $i = 1, 2$. Then, $p(g * s_1(x)) = p(g * s_2(x))$ for all $g \in G$.

Thus, starting from a subgroup H of a group G , we can define a G -homogeneous space $X = G/H$.

2.3 Differentiation on Lie Groups and Lie Algebras

To do some analysis on groups, we need suitably-defined basic operations: differentiation and integration.

Differentiation is naturally defined for Lie groups. If G is a Lie group and G_x is its closed subgroup, then the homogeneous space G/G_x considered above is a smooth manifold (and a *loop* as an algebraic object) for every $x \in X$ [52, Thm. 2 in Sec. 6.1]. Therefore, the one-to-one mapping $G/G_x \rightarrow X : g \mapsto gx$ induces a structure of C^∞ -manifold on X . Thus, the class $C_0^\infty(X)$ of smooth functions with compact supports on x has the natural definition.

For every Lie group G there is an associated *Lie algebra* \mathfrak{g} . This algebra can be realised in many different ways. We will use the following two out of four listed in [52, Sec. 6.3].

2.3.1 One-parameter Subgroups and Lie Algebras

For the first realisation, we consider a *one-dimensional continuous subgroup* $x(t)$ of G as a group homomorphism of $x : (\mathbb{R}, +) \rightarrow G$. For such a homomorphism x , we have $x(s+t) = x(s)x(t)$ and $x(0) = e$.

Exercise 2.23. Check that the following subsets of elements parametrised by $t \in \mathbb{R}$ are one-parameter subgroups:

- i. For the affine group: $a(t) = (e^t, 0)$ and $n(t) = (0, t)$.

ii. For the Heisenberg group \mathbb{H}^1 :

$$s(t) = (t, 0, 0), \quad x(t) = (0, t, 0) \quad \text{and} \quad y(t) = (0, 0, t).$$

iii. For the group $\text{SL}_2(\mathbb{R})$:

$$a(t) = \begin{pmatrix} e^{-t/2} & 0 \\ 0 & e^{t/2} \end{pmatrix}, \quad n(t) = \begin{pmatrix} 1 & t \\ 0 & 1 \end{pmatrix}, \quad (2.5)$$

$$b(t) = \begin{pmatrix} \cosh \frac{t}{2} & \sinh \frac{t}{2} \\ \sinh \frac{t}{2} & \cosh \frac{t}{2} \end{pmatrix}, \quad z(t) = \begin{pmatrix} \cos t & \sin t \\ -\sin t & \cos t \end{pmatrix}. \quad (2.6)$$

The one-parameter subgroup $x(t)$ defines a tangent vector $X = x'(0)$ belonging to the tangent space T_e of G at $e = x(0)$. The Lie algebra \mathfrak{g} can be identified with this *tangent space*. The important *exponential map* $\exp : \mathfrak{g} \rightarrow G$ works in the opposite direction and is defined by $\exp X = x(1)$ in the previous notations. For the case of a matrix group, the exponent map can be explicitly realised through the exponentiation of the matrix representing a tangent vector:

$$\exp(A) = I + A + \frac{A^2}{2} + \frac{A^3}{3!} + \frac{A^4}{4!} + \dots$$

Exercise 2.24. Check that subgroups $a(t)$, $n(t)$, $b(t)$ and $z(t)$ from Exercise 2.23.iii are generated by the exponent map of the following zero-trace matrices:

$$a(t) = \exp \begin{pmatrix} -\frac{t}{2} & 0 \\ 0 & \frac{t}{2} \end{pmatrix}, \quad n(t) = \exp \begin{pmatrix} 0 & t \\ 0 & 0 \end{pmatrix}, \quad (2.7)$$

$$b(t) = \exp \begin{pmatrix} 0 & \frac{t}{2} \\ \frac{t}{2} & 0 \end{pmatrix}, \quad z(t) = \exp \begin{pmatrix} 0 & t \\ -t & 0 \end{pmatrix}. \quad (2.8)$$

2.3.2 Invariant Vector Fields and Lie Algebras

In the second realisation of the Lie algebra, \mathfrak{g} is identified with the left (right) *invariant vector fields* on the group G , that is, first-order differential operators X defined at every point of G and invariant under the left (right) shifts: $X\Lambda = \Lambda X$ ($XR = RX$). This realisation is particularly usable for a Lie group with an appropriate parametrisation. The following examples describe different techniques for finding such invariant fields.

Example 2.25. Let us build left (right) invariant vector fields on G – the $ax+b$ group using the plain definition. Take the basis $\{\partial_a, \partial_b\}$ ($\{-\partial_a, -\partial_b\}$)

of the tangent space T_e to G at its identity. We will propagate these vectors to an arbitrary point through the invariance under shifts. That is, to find the value of the invariant field at the point $g = (a, b)$, we

- i. make the left (right) shift by g ,
- ii. apply a differential operator from the basis of T_e ,
- iii. make the inverse left (right) shift by $g^{-1} = (\frac{1}{a}, -\frac{b}{a})$.

Thus, we will obtain the following invariant vector fields:

$$A^l = a\partial_a, \quad N^l = a\partial_b; \quad \text{and} \quad A^r = -a\partial_a - b\partial_b, \quad N^r = -\partial_b. \quad (2.9)$$

Example 2.26. An alternative calculation for the same Lie algebra can be done as follows. The Jacobians at $g = (a, b)$ of the left and the right shifts

$$\Lambda(u, v) : f(a, b) \mapsto f\left(\frac{a}{u}, \frac{b-v}{u}\right), \quad \text{and} \quad R(u, v) : f(a, b) \mapsto f(ua, va + b)$$

by $h = (u, v)$ are:

$$J_\Lambda(h) = \begin{pmatrix} \frac{1}{u} & 0 \\ 0 & \frac{1}{u} \end{pmatrix}, \quad \text{and} \quad J_R(h) = \begin{pmatrix} u & 0 \\ v & 1 \end{pmatrix}.$$

Then the invariant vector fields are obtained by the transpose of Jacobians:

$$\begin{aligned} \begin{pmatrix} A^l \\ N^l \end{pmatrix} &= J_\Lambda^t(g^{-1}) \begin{pmatrix} \partial_a \\ \partial_b \end{pmatrix} = \begin{pmatrix} a & 0 \\ 0 & a \end{pmatrix} \begin{pmatrix} \partial_a \\ \partial_b \end{pmatrix} = \begin{pmatrix} a\partial_a \\ a\partial_b \end{pmatrix} \\ \begin{pmatrix} A^r \\ N^r \end{pmatrix} &= J_R^t(g) \begin{pmatrix} -\partial_a \\ -\partial_b \end{pmatrix} = \begin{pmatrix} a & b \\ 0 & 1 \end{pmatrix} \begin{pmatrix} -\partial_a \\ -\partial_b \end{pmatrix} = \begin{pmatrix} -a\partial_a - b\partial_b \\ -\partial_b \end{pmatrix} \end{aligned}$$

This rule is a very special case of the general theorem on the change of variables in the calculus of *pseudo-differential operators* (PDO), cf. [42, Thm. 18.1.17; 97, Sec. 4.2].

Example 2.27. Finally, we calculate the invariant vector fields on the $ax + b$ group through a connection to the above one-parameter subgroups. The left-invariant vector field corresponding to the subgroup $a(t)$ from Exercise 2.23.i is obtained through the differentiation of the right action of this subgroup:

$$\begin{aligned} [A^l f](a, b) &= \frac{d}{dt} f((a, b) * (e^t, 0)) \Big|_{t=0} = \frac{d}{dt} f(ae^t, b) \Big|_{t=0} = af'_a(a, b), \\ [N^l f](a, b) &= \frac{d}{dt} f((a, b) * (1, t)) \Big|_{t=0} = \frac{d}{dt} f(a, at + b) \Big|_{t=0} = af'_b(a, b). \end{aligned}$$

Similarly, the right-invariant vector fields are obtained by the derivation of the left action:

$$\begin{aligned}
 [A^r f](a, b) &= \left. \frac{d}{dt} f((e^{-t}, 0) * (a, b)) \right|_{t=0} \\
 &= \left. \frac{d}{dt} f(e^{-t}a, e^{-t}b) \right|_{t=0} = -af'_a(a, b) - bf'_b(a, b), \\
 [N^r f](a, b) &= \left. \frac{d}{dt} f((1, -t) * (a, b)) \right|_{t=0} = \left. \frac{d}{dt} f(a, b-t) \right|_{t=0} = -f'_b(a, b).
 \end{aligned}$$

Exercise 2.28. Use the above techniques to calculate the following left (right) invariant vector fields on the Heisenberg group:

$$S^{l(r)} = \pm \partial_s, \quad X^{l(r)} = \pm \partial_x - \frac{1}{2}y\partial_s, \quad Y^{l(r)} = \pm \partial_y + \frac{1}{2}x\partial_s. \quad (2.10)$$

2.3.3 Commutator in Lie Algebras

The important operation in a Lie algebra is a *commutator*. If the Lie algebra of a matrix group is realised by matrices, e.g. Exercise 2.24, then the commutator is defined by the expression $[A, B] = AB - BA$ in terms of the respective matrix operations. If the Lie algebra is realised through left (right) invariant first-order differential operators, then the commutator $[A, B] = AB - BA$ again defines a left (right) invariant first-order operator – an element of the same Lie algebra.

Among the important properties of the commutator are its anti-commutativity ($[A, B] = -[B, A]$) and the *Jacobi identity*

$$[A, [B, C]] + [B, [C, A]] + [C, [A, B]] = 0. \quad (2.11)$$

Exercise 2.29. Check the following commutation relations:

- i. For the Lie algebra (2.9) of the $ax + b$ group

$$[A^{l(r)}, N^{l(r)}] = N^{l(r)}.$$

- ii. For the Lie algebra (2.10) of Heisenberg group

$$[X^{l(r)}, Y^{l(r)}] = S^{l(r)}, \quad [X^{l(r)}, S^{l(r)}] = [Y^{l(r)}, S^{l(r)}] = 0. \quad (2.12)$$

These are the celebrated *Heisenberg commutation relations*, which are very important in quantum mechanics.

- iii. Denote by A , B and Z the generators of the one-parameter subgroups $a(t)$, $b(t)$ and $z(t)$ in (2.7) and (2.8). The commutation relations in the Lie algebra \mathfrak{sl}_2 are

$$[Z, A] = 2B, \quad [Z, B] = -2A, \quad [A, B] = -\frac{1}{2}Z. \quad (2.13)$$

The procedure from Example 2.27 can also be used to calculate the *derived action* of a G -action on a homogeneous space.

Example 2.30. Consider the action of the $ax + b$ group on the real line associated with the group's name:

$$(a, b) : x \mapsto ax + b, \quad x \in \mathbb{R}.$$

Then, the derived action on the real line is:

$$\begin{aligned} [A^d f](x) &= \left. \frac{d}{dt} f(e^{-t}x) \right|_{t=0} = -x f'(x), \\ [N^d f](a, b) &= \left. \frac{d}{dt} f(x - t) \right|_{t=0} = -f'(x). \end{aligned}$$

This page intentionally left blank

Chapter 3

Homogeneous Spaces from the Group $\mathrm{SL}_2(\mathbb{R})$

Now we adopt the previous theoretical constructions for the particular case of the group $\mathrm{SL}_2(\mathbb{R})$. We are going to describe all homogeneous spaces $\mathrm{SL}_2(\mathbb{R})/H$, where H is a subgroup of $\mathrm{SL}_2(\mathbb{R})$, see Section 2.2.2. To begin with, we start from the two-dimensional subgroup.

3.1 The Affine Group and the Real Line

The affine group of the real line, also known as the $ax + b$ group, can be identified with either subgroup of lower- or upper-triangular matrices:

$$F = \left\{ \frac{1}{\sqrt{a}} \begin{pmatrix} a & 0 \\ c & 1 \end{pmatrix}, a > 0 \right\}, \quad F' = \left\{ \frac{1}{\sqrt{a}} \begin{pmatrix} a & b \\ 0 & 1 \end{pmatrix}, a > 0 \right\}.$$

These subgroups are obviously conjugates of each other and we can consider only the subgroup F here.

The corresponding homogeneous space $X = \mathrm{SL}_2(\mathbb{R})/F$ is one-dimensional and can be parametrised by a real number. Following the construction from Section 2.2.2 and using its notations, we defined the natural projection p as follows:

$$p : \mathrm{SL}_2(\mathbb{R}) \rightarrow \mathbb{R} : \begin{pmatrix} a & b \\ c & d \end{pmatrix} \mapsto \frac{b}{d}. \quad (3.1)$$

Thus, we define the smooth map s to be its left inverse:

$$s : \mathbb{R} \rightarrow \mathrm{SL}_2(\mathbb{R}) : u \mapsto \begin{pmatrix} 1 & u \\ 0 & 1 \end{pmatrix}. \quad (3.2)$$

The corresponding map $r(g) = s(p(g))^{-1}g$ is calculated to be:

$$r : \mathrm{SL}_2(\mathbb{R}) \rightarrow F : \begin{pmatrix} a & b \\ c & d \end{pmatrix} \mapsto \begin{pmatrix} d^{-1} & 0 \\ c & d \end{pmatrix}. \quad (3.3)$$

Consequently, we have a decomposition $g = s(p(g))r(g)$ of the form

$$\begin{pmatrix} a & b \\ c & d \end{pmatrix} = \begin{pmatrix} 1 & \frac{b}{d} \\ 0 & 1 \end{pmatrix} \begin{pmatrix} \frac{1}{d} & 0 \\ c & d \end{pmatrix}.$$

Therefore the action of $\mathrm{SL}_2(\mathbb{R})$ on the real line is

$$g : u \mapsto p(g * s(u)) = \frac{au + b}{cu + d}, \quad \text{where } g = \begin{pmatrix} a & b \\ c & d \end{pmatrix}. \quad (3.4)$$

We obtained Möbius (linear-fractional) transformations of the real line.

Exercise 3.1.

- i. Check that the derived actions, see Exercise 2.30, associated with the one-parameter subgroups $a(t)$, $b(t)$ and $z(t)$ from Exercise 2.24, are, respectively:

$$A_F = x \frac{d}{dx}, \quad B_F = \frac{x^2 - 1}{2} \frac{d}{dx}, \quad Z_F = -(x^2 + 1) \frac{d}{dx}.$$

- ii. Verify that the above operators satisfy the commutator relations for the Lie algebra \mathfrak{sl}_2 , cf. (2.13):

$$[Z_F, A_F] = 2B_F, \quad [Z_F, B_F] = -2A_F, \quad [A_F, B_F] = -\frac{1}{2}Z_F. \quad (3.5)$$

In Section 4.4, we will see the relevance of this action to projective spaces.

3.2 One-dimensional Subgroups of $\mathrm{SL}_2(\mathbb{R})$

Any element of the Lie algebra \mathfrak{sl}_2 defines a one-parameter subgroup of $\mathrm{SL}_2(\mathbb{R})$. We already listed four such subgroups in Exercise 2.23.iii and can provide further examples, e.g. the subgroup of lower-triangular matrices. However, there are only *three* different types of subgroups under the matrix similarity $A \mapsto MAM^{-1}$.

Proposition 3.2. *Any continuous one-parameter subgroup of $\mathrm{SL}_2(\mathbb{R})$ is conjugate to one of the following subgroups:*

$$A = \left\{ \begin{pmatrix} e^{-t/2} & 0 \\ 0 & e^{t/2} \end{pmatrix} = \exp \begin{pmatrix} -t/2 & 0 \\ 0 & t/2 \end{pmatrix}, t \in \mathbb{R} \right\}, \quad (3.6)$$

$$N = \left\{ \begin{pmatrix} 1 & t \\ 0 & 1 \end{pmatrix} = \exp \begin{pmatrix} 0 & t \\ 0 & 0 \end{pmatrix}, t \in \mathbb{R} \right\}, \quad (3.7)$$

$$K = \left\{ \begin{pmatrix} \cos t & \sin t \\ -\sin t & \cos t \end{pmatrix} = \exp \begin{pmatrix} 0 & t \\ -t & 0 \end{pmatrix}, t \in (-\pi, \pi] \right\}. \quad (3.8)$$

Proof. Any one-parameter subgroup is obtained through the exponential map, see Section 2.3,

$$e^{tX} = \sum_{n=0}^{\infty} \frac{t^n}{n!} X^n \quad (3.9)$$

of an element X of the Lie algebra \mathfrak{sl}_2 of $\mathrm{SL}_2(\mathbb{R})$. Such an X is a 2×2 matrix with zero trace. The behaviour of the Taylor expansion (3.9) depends on the properties of the powers X^n . This can be classified by a straightforward calculation:

Lemma 3.3. *The square X^2 of a traceless matrix $X = \begin{pmatrix} a & b \\ c & -a \end{pmatrix}$ is the identity matrix times $a^2 + bc = -\det X$. The factor can be negative, zero or positive, which corresponds to the three different types of the Taylor expansion (3.9) of e^{tX} .*

It is a simple exercise in characteristic polynomials to see that, through the matrix similarity, we can obtain from X a generator

- of the subgroup K if $(-\det X) < 0$,
- of the subgroup N if $(-\det X) = 0$,
- of the subgroup A if $(-\det X) > 0$.

The determinant is invariant under the similarity. Thus, these cases are distinct. \square

Exercise 3.4. Find matrix conjugations of the following two subgroups to A and N respectively:

$$A' = \left\{ \begin{pmatrix} \cosh t & \sinh t \\ \sinh t & \cosh t \end{pmatrix} = \exp \begin{pmatrix} 0 & t \\ t & 0 \end{pmatrix}, t \in \mathbb{R} \right\}, \quad (3.10)$$

$$N' = \left\{ \begin{pmatrix} 1 & 0 \\ t & 1 \end{pmatrix} = \exp \begin{pmatrix} 0 & 0 \\ t & 0 \end{pmatrix}, t \in \mathbb{R} \right\}. \quad (3.11)$$

We will often use subgroups A' and N' as representatives of the corresponding equivalence classes under matrix conjugation.

An interesting property of the subgroups A , N and K is their appearance in the *Iwasawa decomposition* [77, Sec. III.1] of $\mathrm{SL}_2(\mathbb{R}) = ANK$ in the following sense. Any element of $\mathrm{SL}_2(\mathbb{R})$ can be represented as the product:

$$\begin{pmatrix} a & b \\ c & d \end{pmatrix} = \begin{pmatrix} \alpha & 0 \\ 0 & \alpha^{-1} \end{pmatrix} \begin{pmatrix} 1 & \nu \\ 0 & 1 \end{pmatrix} \begin{pmatrix} \cos \phi & -\sin \phi \\ \sin \phi & \cos \phi \end{pmatrix}. \quad (3.12)$$

Exercise 3.5. Check that the values of parameters in the above decomposition are as follows:

$$\alpha = \sqrt{c^2 + d^2}, \quad \nu = ac + bd, \quad \phi = -\arctan \frac{c}{d}.$$

Consequently, $\cos \phi = \frac{d}{\sqrt{c^2 + d^2}}$ and $\sin \phi = \frac{-c}{\sqrt{c^2 + d^2}}$.

The Iwasawa decomposition shows once more that $\mathrm{SL}_2(\mathbb{R})$ is a three-dimensional manifold. A similar decomposition $G = ANK$ is possible for any semisimple Lie group G , where K is the maximal compact group, N is nilpotent and A normalises N . Although the Iwasawa decomposition will be used here on several occasions, it does not play a crucial role in the present consideration. Instead, Proposition 3.2 will be the cornerstone of our construction.

3.3 Two-dimensional Homogeneous Spaces

Here, we calculate the action of $\mathrm{SL}_2(\mathbb{R})$ (2.3) (see Section 2.2.2) on $X = \mathrm{SL}_2(\mathbb{R})/H$ for all three possible one-dimensional subgroups $H = A'$, N' or K . Counting dimensions ($3 - 1 = 2$) suggests that the corresponding homogeneous spaces are two-dimensional manifolds. In fact, we identify X in each case with a subset of \mathbb{R}^2 as follows. First, for every equivalence class $\mathrm{SL}_2(\mathbb{R})/H$ we chose a representative, which is an upper-triangular matrix.

Exercise 3.6. Show that there is at most one upper-triangular matrix in every equivalence class $\mathrm{SL}_2(\mathbb{R})/H$, where $H = A'$, N' or K , where, in the last case, uniqueness is up to the constant factor ± 1 .

HINT: The identity matrix is the only upper-triangular matrix in these three subgroups, where, again, the uniqueness for the subgroup K is understood up to the scalar factor ± 1 . \diamond

The existence of such a triangular matrix will be demonstrated in each case separately. Now, we define the projection $p : \mathrm{SL}_2(\mathbb{R}) \rightarrow X$, assigning $p(g) = (ab, a^2)$, where $\begin{pmatrix} a & b \\ 0 & a^{-1} \end{pmatrix}$ is the only upper-triangular matrix representing the equivalence class of g . We also choose [58, p. 108] the map $s : X \rightarrow G$ in the form:

$$s : (u, v) \mapsto \frac{1}{\sqrt{v}} \begin{pmatrix} v & u \\ 0 & 1 \end{pmatrix}, \quad (u, v) \in \mathbb{R}^2, \quad v > 0. \quad (3.13)$$

This formula will be used for all three possible subgroups H .


3.3.1 From the Subgroup K

The homogeneous space $\mathrm{SL}_2(\mathbb{R})/K$ is the most traditional case in representation theory. The maps p and s defined above produce the following decomposition $g = s(p(g))r(g)$:

$$\begin{pmatrix} a & b \\ c & d \end{pmatrix} = \frac{1}{d^2 + c^2} \begin{pmatrix} 1 & bd + ac \\ 0 & c^2 + d^2 \end{pmatrix} \begin{pmatrix} d & -c \\ c & d \end{pmatrix}. \quad (3.14)$$

Then, the $\mathrm{SL}_2(\mathbb{R})$ -action defined by the formula $g \cdot x = p(g * s(x))$ (2.3) takes the form:

$$\begin{pmatrix} a & b \\ c & d \end{pmatrix} : (u, v) \mapsto \left(\frac{(au + b)(cu + d) + cav^2}{(cu + d)^2 + (cv)^2}, \frac{v}{(cu + d)^2 + (cv)^2} \right). \quad (3.15)$$

Exercise 3.7. Use CAS to check the above formula, as well as analogous formulae (3.18) and (3.21) below. See Appendix B.3 for CAS usage. 

Obviously, it preserves the upper half-plane $v > 0$. The expression (3.15) is very cumbersome and it can be simplified by the complex imaginary unit $i^2 = -1$, which reduces (3.15) to the Möbius transformation

$$\begin{pmatrix} a & b \\ c & d \end{pmatrix} : w \mapsto \frac{aw + b}{cw + d}, \quad \text{where } w = u + iv. \quad (3.16)$$

We need to assign a meaning to the case $cw + d = 0$ and this can be done by the addition of an infinite point ∞ to the set of complex numbers—see, for example, [6, Definition 13.1.3] for details.

In this case, *complex numbers* appeared naturally.

3.3.2 From the Subgroup N'

We consider the subgroup of lower-triangular matrices N' (3.11). For this subgroup, the representative of cosets among the upper-triangular matrices will be different. Therefore, we receive an apparently different decomposition $g = s(p(g))r(g)$, cf. (3.14)

$$\begin{pmatrix} a & b \\ c & d \end{pmatrix} = \frac{1}{d^2} \begin{pmatrix} 1 & bd \\ 0 & d^2 \end{pmatrix} \begin{pmatrix} d & 0 \\ c & d \end{pmatrix}, \quad \text{where } d \neq 0. \quad (3.17)$$

We postpone the treatment of the exceptional case $d = 0$ until Section 8.1. The $\mathrm{SL}_2(\mathbb{R})$ -action (2.3) now takes the form:

$$\begin{pmatrix} a & b \\ c & d \end{pmatrix} : (u, v) \mapsto \left(\frac{au + b}{cu + d}, \frac{v}{(cu + d)^2} \right). \quad (3.18)$$

This map preserves the upper half-plane $v > 0$ just like the case of the subgroup K . The expression (3.18) is simpler than (3.15), yet we can again rewrite it as a linear-fractional transformation with the help of the dual numbers unit $\varepsilon^2 = 0$:

$$\begin{pmatrix} a & b \\ c & d \end{pmatrix} : w \mapsto \frac{aw + b}{cw + d}, \quad \text{where } w = u + \varepsilon v. \quad (3.19)$$

We briefly review the algebra of dual numbers in Appendix A.1. Since they have zero divisors, the fraction is not properly defined for all $cu + d = 0$. The proper treatment will be considered in Section 8.1 since it is not as simple as in the case of complex numbers.

3.3.3 From the Subgroup A'

In the last case of the subgroup A' , the decomposition $g = s(p(g))r(g)$ becomes

$$\begin{pmatrix} a & b \\ c & d \end{pmatrix} = \frac{1}{d^2 - c^2} \begin{pmatrix} 1 & bd - ac \\ 0 & d^2 - c^2 \end{pmatrix} \begin{pmatrix} d & c \\ c & d \end{pmatrix}, \quad \text{where } d \neq \pm c. \quad (3.20)$$

We will again treat the exceptional situation $d = \pm c$ in Section 8.1. The $\text{SL}_2(\mathbb{R})$ -action (2.3) takes the form

$$\begin{pmatrix} a & b \\ c & d \end{pmatrix} : (u, v) \mapsto \left(\frac{(au + b)(cu + d) - cav^2}{(cu + d)^2 - (cv)^2}, \frac{v}{(cu + d)^2 - (cv)^2} \right). \quad (3.21)$$

Notably, this time the map does *not* preserve the upper half-plane $v > 0$: the sign of $(cu + d)^2 - (cv)^2$ is not determined. To express this map as a Möbius transformation, we require the double numbers (also known as *split-complex numbers*) unit $j^2 = 1$:

$$\begin{pmatrix} a & b \\ c & d \end{pmatrix} : w \mapsto \frac{aw + b}{cw + d}, \quad \text{where } w = u + jv.$$

The algebra of double numbers is briefly introduced in Appendix A.1.

3.3.4 Unifying All Three Cases

There is an obvious similarity in the formulae obtained in each of the above cases. To present them in a unified way, we introduce the parameter σ which is equal to -1 , 0 or 1 for the subgroups K , N' or A' , respectively. Then, decompositions (3.14), (3.17) and (3.20) are

$$\begin{pmatrix} a & b \\ c & d \end{pmatrix} = \frac{1}{d^2 - \sigma c^2} \begin{pmatrix} 1 & bd - \sigma ac \\ 0 & d^2 - \sigma c^2 \end{pmatrix} \begin{pmatrix} d & \sigma c \\ c & d \end{pmatrix}, \quad \text{where } d^2 - \sigma c^2 \neq 0. \quad (3.22)$$

The respective $\mathrm{SL}_2(\mathbb{R})$ -actions on the homogeneous space $\mathrm{SL}_2(\mathbb{R})/H$, where $H = A$, N' or K , are given by

$$\begin{pmatrix} a & b \\ c & d \end{pmatrix} : (u, v) \mapsto \left(\frac{(au + b)(cu + d) - \sigma cav^2}{(cu + d)^2 - \sigma(cv)^2}, \frac{v}{(cu + d)^2 - \sigma(cv)^2} \right). \quad (3.23)$$

Finally, this action becomes the linear-fractional (Möbius) transformation for hypercomplex numbers in two-dimensional commutative associative algebra (see Appendix A.1) spanned by 1 and ι :

$$\begin{pmatrix} a & b \\ c & d \end{pmatrix} : w \mapsto \frac{aw + b}{cw + d}, \quad \text{where } w = u + \iota v, \quad \iota^2 = \sigma. \quad (3.24)$$

Thus, a comprehensive study of $\mathrm{SL}_2(\mathbb{R})$ -homogeneous spaces naturally introduces three number systems. Obviously, only one case (complex numbers) belongs to mainstream mathematics. We start to discover empty cells in our periodic table.

Remark 3.8. As we can now see, the dual and double numbers naturally appear in relation to the group $\mathrm{SL}_2(\mathbb{R})$ and, thus, their introduction in [62, 64] was not ‘a purely generalistic attempt’, cf. the remark on quaternions of [93, p. 4].

Remark 3.9. A different choice of the map $s : G/H \rightarrow G$ will produce different (but isomorphic) geometric models. In this way, we will obtain three types of ‘unit disks’ in Chapter 10.

3.4 Elliptic, Parabolic and Hyperbolic Cases

As we have seen in the previous section, there is no need to be restricted to the traditional route of complex numbers only. The arithmetic of dual and double numbers is different from complex numbers mainly in the following aspects:

- i. They have zero divisors. However, we are still able to define their transforms by (3.24) in most cases. The proper treatment of zero divisors will be done through corresponding compactification—see Section 8.1.
- ii. They are not algebraically closed. However, this property of complex numbers is not used very often in analysis.

We have agreed in Section 1.1 that three possible values -1 , 0 and 1 of $\sigma := \iota^2$ will be referred to here as *elliptic*, *parabolic* and *hyperbolic* cases,

respectively. This separation into three cases will be referred to as the *EPH classification*. Unfortunately, there is a clash here with the already established label for the *Lobachevsky geometry*. It is often called hyperbolic geometry because it can be realised as a Riemann geometry on a two-sheet hyperboloid. However, within our framework, the Lobachevsky geometry should be called elliptic and it will have a true hyperbolic counterpart.

Notation 3.10. We denote the space \mathbb{R}^2 of vectors $u + v\iota$ by \mathbb{C} , \mathbb{D} or \mathbb{O} to highlight which number system (complex, dual or double, respectively) is used. The notation \mathbb{A} is used for a generic case. The use of E, P, H or e, p, h (for example, in labelling the different sections of an exercise) corresponds to the elliptic, parabolic, hyperbolic cases.

Remark 3.11. In introducing the parabolic objects on a common ground with elliptic and hyperbolic ones, we should warn against some common prejudices suggested by the diagram (1.2):

- i. The parabolic case is unimportant (has ‘zero measure’) in comparison to the elliptic and hyperbolic cases. As we shall see (e.g. Remark 10.8 and 7.12.ii), the parabolic case presents some richer geometrical features.
- ii. The parabolic case is a limiting situation or an intermediate position between the elliptic and hyperbolic cases. All properties of the former can be guessed or obtained as a limit or an average from the latter two. In particular, this point of view is implicitly supposed in [78].
Although there are some confirmations of this (e.g. Fig. 10.3(E)–(H)), we shall see (e.g. Remark 7.21) that some properties of the parabolic case cannot be guessed in a straightforward manner from a combination of elliptic and hyperbolic cases.
- iii. All three EPH cases are even less disjoint than is usually thought. For example, there are meaningful notions of the *centre of a parabola* (4.3) or the *focus of a circle* (5.2).
- iv. A (co-)invariant geometry is believed to be ‘coordinate-free’, which sometimes is pushed to an absolute mantra. However, our study within the Erlangen programme framework reveals two useful notions (Definition 4.3 and (5.2)), mentioned above, which are defined by coordinate expressions and look very ‘non-invariant’ at first glance.

3.5 Orbits of the Subgroup Actions

We start our investigation of the Möbius transformations (3.24)

$$\begin{pmatrix} a & b \\ c & d \end{pmatrix} : w \mapsto \frac{aw + b}{cw + d}$$

on the hypercomplex numbers $w = u + \iota v$ from a description of orbits produced by the subgroups A , N and K . Due to the Iwasawa decomposition (3.12), any Möbius transformation can be represented as a superposition of these three actions.

The actions of subgroups A and N for any kind of hypercomplex numbers on the plane are the same as on the real line: A dilates and N shifts – see Fig. 1.1 for illustrations. Thin traversal lines in Fig. 1.1 join points of orbits obtained from the vertical axis by the same values of t and grey arrows represent ‘local velocities’ – vector fields of derived representations.

Exercise 3.12. Check that:

- i. The matrix $\begin{pmatrix} e^{-t} & 0 \\ 0 & e^t \end{pmatrix} = \exp \begin{pmatrix} -t & 0 \\ 0 & t \end{pmatrix}$ from A makes a dilation by e^{-2t} , i.e. $z \mapsto e^{-2t}z$. The respective derived action, see Example 2.30, is twice the *Euler operator* $u\partial_u + v\partial_v$.
- ii. The matrix $\begin{pmatrix} 1 & t \\ 0 & 1 \end{pmatrix} = \exp \begin{pmatrix} 0 & t \\ 0 & 0 \end{pmatrix}$ from N shifts points horizontally by t , i.e. $z \mapsto z + t = (u + t) + \iota v$. The respective derived action is ∂_u .
- iii. The subgroup of $\mathrm{SL}_2(\mathbb{R})$ generated by A and N is isomorphic to the $ax + b$ group, which acts transitively on the upper half-plane.
 HINT: Note that the matrix $\begin{pmatrix} \sqrt{a} & b/\sqrt{a} \\ 0 & 1/\sqrt{a} \end{pmatrix} = \begin{pmatrix} 1 & b \\ 0 & 1 \end{pmatrix} \begin{pmatrix} \sqrt{a} & 0 \\ 0 & 1/\sqrt{a} \end{pmatrix}$ maps ι to $a\iota + b$ and use Exercise 2.17.ii. \diamond

By contrast, the action of the third matrix from the subgroup K sharply depends on $\sigma = \iota^2$, as illustrated by Fig. 1.2. In elliptic, parabolic and hyperbolic cases, K -orbits are circles, parabolas and (equilateral) hyperbolas, respectively. The meaning of traversal lines and vector fields is the same as on the previous figure.

Exercise 3.13. The following properties characterise K -orbits:

- i. The derived action of the subgroup K is given by:

$$K_\sigma^d(u, v) = (1 + u^2 + \sigma v^2)\partial_u + 2uv\partial_v, \quad \sigma = \iota^2. \quad (3.25)$$



HINT: Use the explicit formula for Möbius transformation of the components (3.23). An alternative with CAS is provided as well, see Appendix B.3 for usage. \diamond

- ii. A K -orbit in \mathbb{A} passing the point $(0, s)$ has the following equation:

$$(u^2 - \sigma v^2) - 2v \frac{s^{-1} - \sigma s}{2} + 1 = 0. \quad (3.26)$$

HINT: Note that the equation (3.26) defines *contour lines* of the function $F(u, v) = (u^2 - \sigma v^2 + 1)/v$, that is, solve the equations $F(u, v) = \text{const.}$

Then, apply the operator (3.25) to obtain $K_\sigma^d F = 0$. \diamond

- iii. The curvature of a K -orbit at point $(0, s)$ is equal to

$$\kappa = \frac{2s}{1 + \sigma s^2}. \quad (3.27)$$

- iv. The transverse line obtained from the vertical axis has the equations:

$$(u^2 - \sigma v^2) + 2 \cot(2\phi)u - 1 = 0, \quad \text{for } g = \begin{pmatrix} \cos \phi & \sin \phi \\ -\sin \phi & \cos \phi \end{pmatrix} \in K. \quad (3.28)$$

HINT: A direct calculation for a point $(0, s)$ in the formula (3.23) is possible but demanding. A computer symbolic calculation is provided as well. \diamond

Much more efficient proofs will be given later (see Exercise 4.16.ii), when suitable tools will be at our disposal. It will also explain why K -orbits, which are circles, parabolas and hyperbolas, are defined by the same equation (3.26). Meanwhile, these formulae allow us to produce geometric characterisation of K -orbits in terms of classical notions of conic sections, cf. Appendix A.2.

Exercise 3.14. Check the following properties of K -orbits (3.26):

- e. For the elliptic case, the orbits of K are circles. A circle with centre at $(0, (s + s^{-1})/2)$ passing through two points $(0, s)$ and $(0, s^{-1})$.
- p. For the parabolic case, the orbits of K are parabolas with the vertical axis V . A parabola passing through $(0, s)$ has horizontal directrix passing through $(0, s - 1/(4s))$ and focus at $(0, s + 1/(4s))$.
- h. For the hyperbolic case, the orbits of K are hyperbolas with asymptotes parallel to lines $u = \pm v$. A hyperbola passing the point $(0, s)$ has the second branch passing $(0, -s^{-1})$ and asymptotes crossing at the point $(0, (s - s^{-1})/2)$. Foci of this hyperbola are:

$$f_{1,2} = \left(0, \frac{1}{2} \left((1 \pm \sqrt{2})s - (1 \mp \sqrt{2})s^{-1}\right)\right).$$

The amount of similarities between orbits in the three EPH cases suggests that they should be unified one way or another. We start such attempts in the next section.

3.6 Unifying EPH Cases: The First Attempt

It is well known that any K -orbit above is a *conic section* and an interesting observation is that corresponding K -orbits are, in fact, sections of the same two-sided right-angle cone. More precisely, we define the family of double-sided right-angle cones to be parameterized by $s > 0$:


$$x^2 + (y - \frac{1}{2}(s + s^{-1}))^2 - (z - \frac{1}{2}(s - s^{-1}))^2 = 0. \quad (3.29)$$

Therefore, vertices of cones belong to the hyperbola $\{x = 0, y^2 - z^2 = 1\}$ – see Fig. 1.3.

Exercise 3.15. Derive equations for the K -orbits described in Exercise 3.14 by calculation of intersection of a cone (3.29) with the following planes:

- e. Elliptic K -orbits are sections of cones (3.29) by the plane $z = 0$ (EE' on Fig. 1.3).
- p. Parabolic K -orbits are sections of (3.29) by the plane $y = \pm z$ (PP' on Fig. 1.3).
- h. Hyperbolic K -orbits are sections of (3.29) by the plane $y = 0$ (HH' on Fig. 1.3);

Moreover, each straight line generating the cone, see Fig. 1.3(b), is crossing corresponding EPH K -orbits at points with the same value of parameter ϕ from (3.12). In other words, all three types of orbits are generated by the rotations of this generator along the cone.

Exercise 3.16. Verify that the rotation of a cone's generator corresponds to the Möbius transformations in three planes. 

HINT: I do not know a smart way to check this, so a CAS solution is provided. \diamond

From the above algebraic and geometric descriptions of the orbits we can make several observations.

Remark 3.17.

- i. The values of all three vector fields dK_e , dK_p and dK_h coincide on the ‘real’ U -axis ($v = 0$), i.e. they are three different extensions into the

- domain of the same boundary condition. Another origin of this: the axis U is the intersection of planes EE' , PP' and HH' on Fig. 1.3.
- ii. The hyperbola passing through the point $(0, 1)$ has the shortest focal length $\sqrt{2}$ among all other hyperbolic orbits since it is the section of the cone $x^2 + (y - 1)^2 + z^2 = 0$ closest from the family to the plane HH' .
 - iii. Two hyperbolas passing through $(0, v)$ and $(0, v^{-1})$ have the same focal length since they are sections of two cones with the same distance from HH' . Moreover, two such hyperbolas in the lower and upper half-planes passing the points $(0, v)$ and $(0, -v^{-1})$ are sections of the same double-sided cone. They are related to each other as explained in Remark 8.4.

We make a generalisation to all EPH cases of the following notion, which is well known for circles [23, Sec. 2.3] and parabolas [108, Sec. 10]:

Definition 3.18. A *power* p of a point (u, v) with respect to a conic section given by the equation $x^2 - \sigma y^2 - 2lx - 2ny + c = 0$ is defined by the identity

$$p = u^2 - \sigma v^2 - 2lu - 2nv + c. \quad (3.30)$$

Exercise 3.19. Check the following properties:

- i. A conic section is the collection of points having zero power with respect to the section.
- ii. The collection of points having the same power with respect to two given conic sections of the above type is either empty or the straight line. This line is called *radical axis* of the two sections.
- iii. All K -orbits are *coaxial* [23, Sec. 2.3] with the real line being their joint radical axis, that is, for a given point on the real line, its power with respect to any K -orbit is the same.
- iv. All transverse lines (3.28) are coaxial, with the vertical line $u = 0$ being the respective radial axis.

3.7 Isotropy Subgroups

In Section 2.2 we described the two-sided connection between homogeneous spaces and subgroups. Section 3.3 uses it in one direction: from subgroups to homogeneous spaces. The following exercise does it in the opposite way.

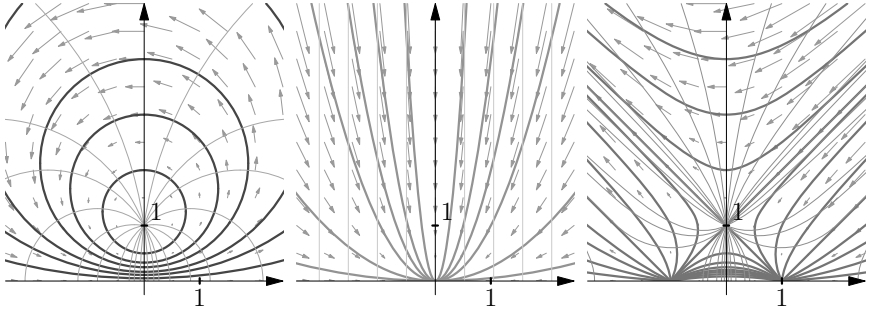


Figure 3.1 Actions of isotropy subgroups K , N' and A' , which fix point ι in three EPH cases.

Exercise 3.20. Let $\mathrm{SL}_2(\mathbb{R})$ act by Möbius transformations (3.24) on the three number systems. Show that the isotropy subgroups of the point ι are:

- e. The subgroup K in the elliptic case. Thus, the elliptic upper half-plane is a model for the homogeneous space $\mathrm{SL}_2(\mathbb{R})/K$.
- p. The subgroup N' (3.11) of matrices

$$\begin{pmatrix} 1 & 0 \\ \nu & 1 \end{pmatrix} = \begin{pmatrix} 0 & -1 \\ 1 & 0 \end{pmatrix} \begin{pmatrix} 1 & \nu \\ 0 & 1 \end{pmatrix} \begin{pmatrix} 0 & 1 \\ -1 & 0 \end{pmatrix} \quad (3.31)$$

in the parabolic case. It also fixes any point εv on the vertical axis, which is the set of zero divisors in dual numbers. The subgroup N' is conjugate to subgroup N , thus the *parabolic upper half-plane* is a model for the homogeneous space $\mathrm{SL}_2(\mathbb{R})/N$.

- h. The subgroup A' (3.10) of matrices

$$\begin{pmatrix} \cosh \tau & \sinh \tau \\ \sinh \tau & \cosh \tau \end{pmatrix} = \frac{1}{2} \begin{pmatrix} 1 & -1 \\ 1 & 1 \end{pmatrix} \begin{pmatrix} e^\tau & 0 \\ 0 & e^{-\tau} \end{pmatrix} \begin{pmatrix} 1 & 1 \\ -1 & 1 \end{pmatrix} \quad (3.32)$$

in the hyperbolic case. These transformations also fix the light cone centred at j , that is, consisting of $j + \text{zero divisors}$. The subgroup A' is conjugate to the subgroup A , thus two copies of the upper half-plane (see Section 8.2) are a model for $\mathrm{SL}_2(\mathbb{R})/A$.

Figure 3.1 shows actions of the above isotropic subgroups on the respective numbers. Note that in parabolic and hyperbolic cases they fix larger sets.

Exercise 3.21. Check further properties of *rotations* around ι , that is, the actions of isotropic subgroups:

- i. Vector fields of the isotropy subgroup actions are

$$(u^2 + \sigma(v^2 - 1))\partial_u + 2uv\partial_v, \quad \text{where } \sigma = \iota^2.$$



- ii. Orbits of the isotropy subgroups A' , N' and K satisfy the equation

$$(u^2 - \sigma v^2) - 2lv - \sigma = 0, \quad \text{where } l \in \mathbb{R}. \quad (3.33)$$

HINT: See method used in Exercise 3.13.ii. An alternative derivation will be available in Exercise 5.24. \diamond

- iii. The isotropy subgroups of ι in all EPH cases are uniformly expressed by matrices of the form

$$\begin{pmatrix} a & \sigma b \\ b & a \end{pmatrix}, \quad \text{where } a^2 - \sigma b^2 = 1.$$

- iv. The isotropy subgroup of a point $u + \iota v$ consists of matrices

$$\begin{pmatrix} \sqrt{1 + \sigma v^2 c^2} + uc & c(\sigma v^2 - u^2) \\ c & \sqrt{1 + \sigma v^2 c^2} - uc \end{pmatrix} \in \text{SL}_2(\mathbb{R})$$

and describe admissible values of the parameter c .

HINT: Use the previous item and the transitive action of the $ax + b$ from Exercise 3.12.iii. \diamond

Definition 3.22. In the hyperbolic case, we extend the subgroup A' to a subgroup A' by the element $\begin{pmatrix} 0 & 1 \\ -1 & 0 \end{pmatrix}$.

This additional element flips the upper and lower half-planes of double numbers—see Section 8.2. Therefore, the subgroup A'_h fixes the set $\{e_1, -e_1\}$.

Lemma 3.23. *Möbius action of $\text{SL}_2(\mathbb{R})$ in each EPH case is generated by action of the corresponding isotropy subgroup (A'_h in the hyperbolic case) and actions of the $ax + b$ group, e.g. subgroups A and N .*

Proof. The $ax + b$ group acts transitively on the upper or lower half-planes. Thus, for any $g \in \text{SL}_2(\mathbb{R})$, there is an h in the $ax + b$ group such that $h^{-1}g$ either fixes e_1 or sends it to $-e_1$. Thus, $h^{-1}g$ is in the corresponding isotropy subgroup. \square

Chapter 4

The Extended Fillmore–Springer–Cnops Construction

Cycles—circles, parabolas and hyperbolas—are invariant families under their respective Möbius transformations. We will now proceed with a study of the invariant properties of cycles according to the Erlangen programme. A very powerful tool used in these notes is the representation of cycles by appropriate 2×2 matrices.

4.1 Invariance of Cycles

K -orbits, shown in Fig. 1.2, are K -invariant in a trivial way. Moreover, since actions of both A and N for any σ are extremely ‘shape-preserving’, see Exercise 3.12, we meet natural invariant objects of the Möbius map:

Definition 4.1. The common name *cycle* [108] is used to denote circles, parabolas with horizontal directrices and equilateral hyperbolas with vertical axes of symmetry (as well as straight lines as the limiting cases of any from above) in the respective EPH case.

It is known, from analytic geometry, that a cycle is defined by the equation

$$k(u^2 - \sigma v^2) - 2lu - 2nv + m = 0, \quad (4.1)$$

where $\sigma = \iota^2$ and k, l, n, m are real parameters, such that *not all of them* are equal to zero. Using hypercomplex numbers, we can write the same equation as, cf. [108, Suppl. C(42a)],

$$Kw\bar{w} - Lw + \bar{L}\bar{w} + M = 0, \quad (4.2)$$

where $w = u + \iota v$, $K = \iota k$, $L = n + \iota l$, $M = \iota m$ and conjugation is defined by $\bar{w} = u - \iota v$.

Exercise 4.2. Check that such cycles result in straight lines for certain k, l, n, m and, depending on the case, one of the following:

- e. In the elliptic case: circles with centre $(\frac{l}{k}, \frac{n}{k})$ and squared radius $m - \frac{l^2 + n^2}{k}$.
- p. In the parabolic case: parabolas with horizontal directrices and focus at $(\frac{l}{k}, \frac{m}{2n} - \frac{l^2}{2nk} + \frac{n}{2k})$.
- h. In the hyperbolic case: rectangular hyperbolas with centre $(\frac{l}{k}, -\frac{n}{k})$ and vertical axes of symmetry.

Hereafter, the words parabola and hyperbola always assume only the above described types. Straight lines are also called *flat cycles*.

All three EPH types of cycles enjoy many common properties, sometimes even beyond those which we normally expect. For example, the following definition is quite intelligible even when extended from the above elliptic and hyperbolic cases to the parabolic one:

Definition 4.3. $\hat{\sigma}$ -Centre of the σ -cycle (4.1) for any EPH case is the point $(\frac{l}{k}, -\hat{\sigma}\frac{n}{k}) \in \mathbb{A}$. Notions of e-centre, p-centre, h-centre are used according the adopted EPH notations.

Centres of straight lines are at infinity, see Subsection 8.1.

Remark 4.4. Here we use a signature $\hat{\sigma} = -1, 0$ or 1 of a number system which does not coincide with the signature σ of the space \mathbb{A} . We will also need a third signature $\check{\sigma}$ to describe the geometry of cycles in Definition 4.11.

Exercise 4.5. Note that some quadruples (k, l, n, m) may correspond through Equation (4.1) to the empty set on a certain point space \mathbb{A} . Give the full description of parameters (k, l, n, m) and σ which leads to the empty set.

HINT: Use the coordinates of the cycle's centre and completion to full squares to show that the empty set may appear only in the elliptic point space. Such circles are usually called *imaginary*. \diamond

The usefulness of this definition, even in the parabolic case, will be justified, for example, by

- the uniformity of the description of relations between the centres of orthogonal cycles, see the next subsection and Fig. 6.3,
- the appearance of *concentric parabolas* in Fig. 10.3($P_e:N$ and $P_h:N$).

Here is one more example of the natural appearance of concentric parabolas:

Exercise 4.6. Show that, in all EPH cases, the locus of points having a fixed *power* with respect to a given cycle C is a cycle concentric with C .

This property is classical for circles [23, Sec. 2.3] and is also known for parabolas [108, Sec. 10]. However, for parabolas, Yaglom used the word ‘concentric’ in quotes, since he did not define the centres of a parabola explicitly.

The family of all cycles from Definition 4.1 is invariant under Möbius transformations (3.24) in all EPH cases, which was already stated in Theorem 1.2. The only gap in its proof was a demonstration that we can always transform a cycle to a K -orbit.

Exercise 4.7. Let C be a cycle in \mathbb{A} with its centre on the vertical axis. Show that there is the unique scaling $w \mapsto a^2w$ which maps C into a K -orbit.

HINT: Check that a cycle in \mathbb{A} with its centre belonging to the vertical axis is completely defined by the point of its intersection with the vertical axis and its curvature at this point. Then find the value of a for a scaling such that the image of C will satisfy the relation (3.27). \diamond

We fully describe how cycles are transformed by Möbius transformations in Theorem 4.13.

4.2 Projective Spaces of Cycles

Figure 1.3 suggests that we may obtain a unified treatment of cycles in all EPH cases by consideration of higher-dimension spaces. The standard mathematical method is to declare objects under investigation to be simply points of some larger space.

Example 4.8. In functional analysis, sequences or functions are considered as points (vectors) of certain linear spaces. Linear operations (addition and multiplication by a scalar) on vectors (that is, functions) are defined point-wise.

If an object is considered as a point (in a new space) all information about its inner structure is lost, of course. Therefore, this space should be equipped with an appropriate structure to hold information externally which previously described the inner properties of our objects. In other words,

the inner structure of an object is now revealed through its relations to its peers¹.

Example 4.9. Take the linear space of continuous real-valued functions on the interval $[0, 1]$ and introduce the *inner product* of two functions by the formula:

$$\langle f, g \rangle = \int_0^1 f(t) g(t) dt.$$

It allows us to define the *norm* of a function and the *orthogonality* of two functions. These are the building blocks of *Hilbert space* theory, which recovers much of Euclidean geometry in terms of the spaces of functions.

We will utilise the above fundamental approach for cycles. A generic cycle from Definition 4.1 is the set of points $(u, v) \in \mathbb{A}$ defined for the respective values of σ by the equation

$$k(u^2 - \sigma v^2) - 2lu - 2nv + m = 0. \quad (4.3)$$

This equation (and the corresponding cycle) is completely determined by a point $(k, l, n, m) \in \mathbb{R}^4$. However, this is not a one-to-one correspondence. For a scaling factor $\lambda \neq 0$, the point $(\lambda k, \lambda l, \lambda n, \lambda m)$ defines an equivalent equation to (4.3). Thus, we prefer to consider the *projective space* \mathbb{P}^3 , that is, \mathbb{R}^4 factorised by the equivalence relation $(k, l, n, m) \sim (\lambda k, \lambda l, \lambda n, \lambda m)$ for any real $\lambda \neq 0$. A good introductory read on projective spaces is [95, Ch. 10].

Definition 4.10. We call \mathbb{P}^3 the *cycle space* and refer to the initial \mathbb{A} as the *point space*. The correspondence which associates a point of the cycle space to a cycle equation (4.3) is called map Q .

We also note that the Equation (4.2) of a cycle can be written as a quadratic form

$$Kw_1\bar{w}_1 - Lw_1\bar{w}_2 + \bar{L}\bar{w}_1w_2 + Mw_2\bar{w}_2 = 0 \quad (4.4)$$

in the homogeneous coordinates (w_1, w_2) , such that $w = \frac{w_1}{w_2}$. Since quadratic forms are related to square matrices, see Section 4.4, we define another map on the cycle space as follows.

Definition 4.11. We arrange numbers (k, l, n, m) into the *cycle matrix*

$$C_\sigma^s = \begin{pmatrix} l + \check{\imath}sn & -m \\ k & -l + \check{\imath}sn \end{pmatrix}, \quad (4.5)$$

¹The same is true for human beings.

with a new hypercomplex unit $\check{\iota}$ and an additional real parameter s , which is usually equal to ± 1 . If we omit it in the cycle notation $C_{\check{\sigma}}$, then the value $s = 1$ is assumed.

The values of $\check{\sigma} := \check{\iota}^2$ are $-1, 0$ or 1 , independent of the value of σ . The parameter $s = \pm 1$ often (but not always) is equal to σ . Matrices which differ by a real non-zero factor are considered to be equivalent.

We denote by M such a map from \mathbb{P}^3 to the projective space of 2×2 matrices.

The matrix (4.5) is the cornerstone of the (extended) *Fillmore–Springer–Cnops construction (FSCc)* [22] and is closely related to the technique recently used by A.A. Kirillov to study the Apollonian gasket [54]. A hint for the composition of this matrix is provided by the following exercise.

Exercise 4.12. Let the space \mathbb{A}^2 be equipped with a product of symplectic type

$$[w, w'] = \bar{w}_1 w'_2 - \bar{w}_2 w'_1,$$

where $w^{(\iota)} = (w_1^{(\iota)}, w_2^{(\iota)}) \in \mathbb{A}^2$. Letting $C = \begin{pmatrix} L & -M \\ K & \bar{L} \end{pmatrix}$, check that the equation of the cycle (4.4) is given by the expression $[w, Cw] = 0$.

Identifications of both Q and M are straightforward. Indeed, a point $(k, l, n, m) \in \mathbb{P}^3$ equally well represents (as soon as $\sigma, \check{\sigma}$ and s are already fixed) both the Equation (4.3) and the line of matrix (4.5). Thus, for fixed $\sigma, \check{\sigma}$ and s , one can introduce the correspondence between quadrics and matrices shown by the horizontal arrow on the following diagram:

$$\begin{array}{ccc} & \mathbb{P}^3 & \\ Q \swarrow & & \nwarrow M \\ \text{Quadrics on } \mathbb{A} & \xleftrightarrow{Q \circ M} & M_2(\mathbb{A}) \end{array} \quad (4.6)$$

which combines Q and M .

4.3 Covariance of FSCc

At first glance, the horizontal arrow in (4.6) seems to be of little practical interest since it depends on too many different parameters ($\sigma, \check{\sigma}$ and s). However, the following result demonstrates that it is compatible with simple calculations of cycles' images under the Möbius transformations.

Theorem 4.13. *The image \tilde{C}_α^s of a cycle C_α^s under transformation (3.24) in \mathbb{A} with $g \in \text{SL}_2(\mathbb{R})$ is given by similarity of the matrix (4.5):* 

$$\tilde{C}_\alpha^s = g C_\alpha^s g^{-1}. \quad (4.7)$$

In other word, FSCc (4.5) intertwines Möbius action (3.24) on cycles with linear map (4.7). Explicitly, it means:

$$\begin{pmatrix} \tilde{l} + \check{l}s\tilde{n} & -\tilde{m} \\ \tilde{k} & -\tilde{l} + \check{l}s\tilde{n} \end{pmatrix} = \begin{pmatrix} a & b \\ c & d \end{pmatrix} \begin{pmatrix} l + \check{l}s n & -m \\ k & -l + \check{l}s n \end{pmatrix} \begin{pmatrix} d & -b \\ -c & a \end{pmatrix}. \quad (4.8)$$

Proof. There are several ways to prove (4.7), but for now we present a brute-force calculation, which can fortunately be performed by a CAS [65]. See Appendix B for information on how to install (Section B.2) and start (Section B.3) the software, which will be sufficient for this proof. Further use of the software would be helped by learning which methods are available from the library (Section B.4) and which predefined objects exist upon initialisation (Section B.5). Assuming the above basics are known we proceed as follows.

First, we build a cycle passing a given point $P=[u, v]$. For this, a generic cycle C with parameters (k, l, n, m) is bounded by the corresponding condition:

```
In [2]: C2=C.subject_to(C.passing(P))
```

Then, we build the conjugated cycle with a generic $g = \begin{pmatrix} a & b \\ c & d \end{pmatrix} \in \text{SL}_2(\mathbb{R})$ and a hypercomplex unit \mathbf{es} and parameter $\mathbf{s} = \pm 1$:

```
In [3]: C3=C2.sl2_similarity(a, b, c, d, es, matrix([[1,0],[0,s]]))
```

We also find the image of P under the Möbius transformation with the same element of $g \in \text{SL}_2(\mathbb{R})$ but a different hypercomplex unit \mathbf{e} :

```
In [4]: P1=clifford_moebius_map(sl2_clifford(a, b, c, d, e), P, e)
```

Finally, we check that the conjugated cycle $C3$ passes the Möbius transform $P1$. A simplification based on the determinant value 1 and $\mathbf{s} = \pm 1$ will be helpful:

```
In [5]: print C3.val(P1).subs([a==(1+b*c)/d,pow(s,2)==1]) \
        .normal().is_zero()
```

```
Out[5]: True
```

Thus, we have confirmation that the theorem is true in the stated generality. One may wish that every mathematical calculation can be done as simply. □

Remark 4.14. There is a bit of cheating in the above proof. In fact, the library does not use the hypercomplex form (4.5) of FSCc matrices. Instead, it operates with non-commuting Clifford algebras, which makes it usable at any dimension – see Section A.5 and [63, 65].

The above proof cannot satisfy everyone’s aesthetic feeling. For this reason, an alternative route based on orthogonality of cycles [22] will be given later – see Exercise 6.7.

It is worth noticing that the image \tilde{C}_α^s under similarity (4.7) is independent of the values of s and $\check{\sigma}$. This, in particular, follows from the following exercise.

Exercise 4.15. Check that the image $(\tilde{k}, \tilde{l}, \tilde{n}, \tilde{m})$ of the cycle (k, l, n, m) under similarity with $g = \begin{pmatrix} a & b \\ c & d \end{pmatrix} \in \mathrm{SL}_2(\mathbb{R})$ is

$$(\tilde{k}, \tilde{l}, \tilde{n}, \tilde{m}) = (kd^2 + 2lcd + mc^2, kbd + l(bc + ad) + mac, n, kb^2 + 2lab + ma^2).$$

This can also be presented through matrix multiplication:

$$\begin{pmatrix} \tilde{k} \\ \tilde{l} \\ \tilde{n} \\ \tilde{m} \end{pmatrix} = \begin{pmatrix} d^2 & 2cd & 0 & c^2 \\ bd & bc + ad & 0 & ac \\ 0 & 0 & 1 & 0 \\ b^2 & 2ab & 0 & a^2 \end{pmatrix} \begin{pmatrix} k \\ l \\ n \\ m \end{pmatrix}.$$

Now we have an efficient tool for investigating the properties of some notable cycles, which have appeared before.

Exercise 4.16. Use the similarity formula (4.7) for the following:

- i. Show that the real axis $v = 0$ is represented by the line passing through $(0, 0, 1, 0)$ and a matrix $\begin{pmatrix} s\check{\iota} & 0 \\ 0 & s\check{\iota} \end{pmatrix}$. For any $\begin{pmatrix} a & b \\ c & d \end{pmatrix} \in \mathrm{SL}_2(\mathbb{R})$, we have

$$\begin{pmatrix} a & b \\ c & d \end{pmatrix} \begin{pmatrix} s\check{\iota} & 0 \\ 0 & s\check{\iota} \end{pmatrix} \begin{pmatrix} d & -b \\ -c & a \end{pmatrix} = \begin{pmatrix} s\check{\iota} & 0 \\ 0 & s\check{\iota} \end{pmatrix},$$
 i.e. the real line is $\mathrm{SL}_2(\mathbb{R})$ -invariant.
- ii. Write matrices which describe cycles represented by A , N and K -orbits shown in Figs. 1.1 and 1.2. Verify that matrices representing these cycles are invariant under the similarity with elements of the respective subgroups A , N and K .
- iii. Show that cycles $(1, 0, n, \sigma)$, which are orbits of isotropy groups as described in Exercise 3.21.ii, are invariant under the respective matrix similarity for the respective values of $\sigma = \iota^2$ and any real n .

- iv. Find the cycles which are transverse to orbits of the isotropy subgroups, i.e. are obtained from the vertical axis by the corresponding actions.

These easy examples also show that the software is working as expected.

4.4 Origins of FSCc

The Fillmore–Springer–Cnops construction, in its generalised form, will play a central rôle in our subsequent investigation. Thus, it is worth looking at its roots and its origins before we begin using it. So far, it has appeared from the thin air, but can we intentionally invent it? Are there further useful generalisations of FSCc? All these are important questions and we will make an attempt to approach them here.

As is implied by its name, FSCc was developed in stages. Moreover, it appeared independently in a different form in the recent work of Kirillov [54]. This indicates the naturalness and objectivity of the construction. We are interested, for now, in the flow of ideas rather than exact history or proper credits. For the latter, the reader may consult the original works [21; 22; 27; 54; 94, Ch. 18] as well as references therein. Here, we treat the simplest two-dimensional case. In higher dimensions, non-commutative Clifford algebras are helpful with some specific adjustments.

4.4.1 Projective Coordinantes and Polynomials

An important old observation is that Möbius maps appear from linear transformations of homogeneous (projective) coordinates, see [84, Ch. 1] for this in a context of invariant theory. This leads to the FSCc in several steps:

- i. Take a real projective space \mathbb{P}^1 as a quotient of \mathbb{R}^2 by the equivalence relation $(x, y) \sim (tx, ty)$ for $t \neq 0$. Then, any line with $y \neq 0$ can be represented by $(x/y, 1)$. Thus, the invertible linear transformation

$$\begin{pmatrix} a & b \\ c & d \end{pmatrix} \begin{pmatrix} x \\ y \end{pmatrix} = \begin{pmatrix} ax + by \\ cx + dy \end{pmatrix}, \quad g = \begin{pmatrix} a & b \\ c & d \end{pmatrix} \in \mathrm{SL}_2(\mathbb{R}), \quad \begin{pmatrix} x \\ y \end{pmatrix} \in \mathbb{R}^2 \quad (4.9)$$

will become the Möbius transformation (3.4) on the representatives $\begin{pmatrix} u \\ 1 \end{pmatrix}$. Similarly, we can consider Möbius actions on complex numbers $w = u + iv$.

- ii. The next observation [21] is that, if we replace the vector $\begin{pmatrix} w \\ 1 \end{pmatrix}$, $w \in \mathbb{C}$

by a 2×2 matrix $\begin{pmatrix} w & w \\ 1 & 1 \end{pmatrix}$, then the matrix multiplication with $g \in \mathrm{SL}_2(\mathbb{R})$ will transform it as two separate copies of the vector in (4.9). The ‘twisted square’ of this matrix is

$$Z = \begin{pmatrix} w & -w\bar{w} \\ 1 & -\bar{w} \end{pmatrix} = \frac{1}{2} \begin{pmatrix} w & w \\ 1 & 1 \end{pmatrix} \begin{pmatrix} 1 & -\bar{w} \\ 1 & -\bar{w} \end{pmatrix}. \quad (4.10)$$

Then, the linear action (4.9) on vectors is equivalent to the similarity gZg^{-1} for the respective matrix Z from (4.10).

- iii. Finally, one can link matrices Z in (4.10) with zero-radius circles, see Exercise 5.17.i, which are also in one-to-one correspondences with their centres. Then, the above similarity $Z \mapsto gZg^{-1}$ can be generalised to the action (4.7).

Another route was used in a later book of Cnops [22]: a predefined geometry of spheres, specifically their orthogonality, was encoded in the respective matrices of the type (4.5). Similar connections between geometry of cycles and matrices lead Kirillov, see [54, Sec. 6.3] and the end of this section. He arrived at an identification of disks with Hermitian matrices (which is similar to FSCc) through the geometry of Minkowski space-time and the intertwining property of the actions of $\mathrm{SL}_2(\mathbb{C})$.

There is one more derivation of FSCc based on projective coordinates. We can observe that the homogeneous form (4.4) of cycle’s equation (4.2) can be written using matrices as follows:

$$Kw_1\bar{w}_1 - Lw_1\bar{w}_2 + \bar{L}\bar{w}_1w_2 + Mw_2\bar{w}_2 = (-\bar{w}_2 \ \bar{w}_1) \begin{pmatrix} L & -M \\ K & \bar{L} \end{pmatrix} \begin{pmatrix} w_1 \\ w_2 \end{pmatrix} = 0. \quad (4.11)$$

Then, the linear action (4.9) on vectors $\begin{pmatrix} w_1 \\ w_2 \end{pmatrix}$ corresponds to conjugated action on 2×2 matrices $\begin{pmatrix} L & -M \\ K & \bar{L} \end{pmatrix}$ by the intertwining identity:

$$(\bar{w}'_1 \ \bar{w}'_2) \begin{pmatrix} L & -M \\ K & \bar{L} \end{pmatrix} \begin{pmatrix} w'_1 \\ w'_2 \end{pmatrix} = (\bar{w}_1 \ \bar{w}_2) \begin{pmatrix} L' & -M' \\ K' & \bar{L}' \end{pmatrix} \begin{pmatrix} w_1 \\ w_2 \end{pmatrix}, \quad (4.12)$$

where the respective actions of $\mathrm{SL}_2(\mathbb{R})$ on vectors and matrices are

$$\begin{pmatrix} w'_1 \\ w'_2 \end{pmatrix} = \begin{pmatrix} a & b \\ c & d \end{pmatrix} \begin{pmatrix} w_1 \\ w_2 \end{pmatrix}, \quad \text{and} \quad \begin{pmatrix} L' & -M' \\ K' & \bar{L}' \end{pmatrix} = \begin{pmatrix} a & b \\ c & d \end{pmatrix}^{-1} \begin{pmatrix} L & -M \\ K & \bar{L} \end{pmatrix} \begin{pmatrix} a & b \\ c & d \end{pmatrix}.$$

In other words, we obtained the usual FSCc with the intertwining property of the type (4.7). However, the generalised form FSCc does not result from this consideration yet.

Alternatively, we can represent the Equation (4.4) as:

$$Kw_1\bar{w}_1 - Lw_1\bar{w}_2 + \bar{L}\bar{w}_1w_2 + Mw_2\bar{w}_2 = (\bar{w}_1 \ \bar{w}_2) \begin{pmatrix} K & \bar{L} \\ -L & M \end{pmatrix} \begin{pmatrix} w_1 \\ w_2 \end{pmatrix} = 0.$$

Then, the intertwining relation similar to (4.12) holds if matrix similarity is replaced by the *matrix congruence*:

$$\begin{pmatrix} K' & \bar{L}' \\ -L' & M' \end{pmatrix} = \begin{pmatrix} a & b \\ c & d \end{pmatrix}^T \begin{pmatrix} K & \bar{L} \\ -L & M \end{pmatrix} \begin{pmatrix} a & b \\ c & d \end{pmatrix}.$$

This identity provides a background to the *Kirillov correspondence* between circles and matrices, see [54, Sec. 6.3]. Clearly, it is essentially equivalent to FSCc and either of them may be depending on a convenience. It does not hint at the generalised form of FSCc either.

We will mainly work with the FSCc, occasionally stating equivalent forms of our results for the Kirillov correspondence.

4.4.2 Co-Adjoint Representation

In the above construction, the identity (4.11) requires the same imaginary unit to be used in the quadratic form (the left-hand side) and the FSCc matrix (the right-hand side). How can we arrive at the generalised FSCc directly without an intermediate step of the standard FSCc with the same type of EPH geometry used in the point cycle spaces? We will consider a route originating from the representation theory.

Any group G acts on itself by the *conjugation* $g : x \mapsto gxg^{-1}$, see 2.18.i. This map obviously fixes the group identity e . For a Lie group G , the tangent space at e can be identified with its Lie algebra \mathfrak{g} , see Subsection 2.3.1. Then, the derived map for the conjugation at e will be a linear map $\mathfrak{g} \rightarrow \mathfrak{g}$. This is an *adjoint representation* of a Lie group G on its Lie algebra. This is the departure point for Kirillov's orbit method, which is closely connected to induced representations, see [52, 53].

Example 4.17. In the case of $G = \mathrm{SL}_2(\mathbb{R})$, the group operation is the multiplication of 2×2 matrices. The Lie algebra \mathfrak{g} can be identified with the set of traceless matrices, which we can write in the form $\begin{pmatrix} l & -m \\ k & -l \end{pmatrix}$ for $k, l, m \in \mathbb{R}$. Then, the co-adjoint action of $\mathrm{SL}_2(\mathbb{R})$ on \mathfrak{sl}_2 is:

$$\begin{pmatrix} a & b \\ c & d \end{pmatrix} : \begin{pmatrix} l & -m \\ k & -l \end{pmatrix} \mapsto \begin{pmatrix} a & b \\ c & d \end{pmatrix}^{-1} \begin{pmatrix} l & -m \\ k & -l \end{pmatrix} \begin{pmatrix} a & b \\ c & d \end{pmatrix}. \quad (4.13)$$

We can also note that the above transformation fixes matrices $\begin{pmatrix} n & 0 \\ 0 & n \end{pmatrix}$ which are scalar multiples of the identity matrix. Thus, we can consider the conjugated action (4.13) of $\mathrm{SL}_2(\mathbb{R})$ on the pairs of matrices, or intervals in the matrix space of the type

$$\left\{ \begin{pmatrix} l & -m \\ k & -l \end{pmatrix}, \begin{pmatrix} n & 0 \\ 0 & n \end{pmatrix} \right\}, \text{ or, using hypercomplex numbers, } \begin{pmatrix} l + \imath n & -m \\ k & -l + \imath n \end{pmatrix}.$$

In other words, we obtained the generalised FSCc, cf. (4.5), and the respective action of $\mathrm{SL}_2(\mathbb{R})$. However, a connection of the above pairs of matrices with the cycles on a plane does not follow from the above consideration and requires some further insights.

Remark 4.18. Note that scalar multiplies of the identity matrix, which are invariant under similarity, correspond in FSCc to the real line, which is also Möbius invariant.

4.5 Projective Cross-Ratio

An important invariant of Möbius transformations in complex numbers is the *cross-ratio* of four distinct points, see [6, Sec. 13.4]:

$$[z_1, z_2, z_3, z_4] = \frac{(z_1 - z_3)(z_2 - z_4)}{(z_1 - z_2)(z_3 - z_4)}. \quad (4.14)$$

Zero divisors make it difficult to handle a similar fraction in dual and double numbers. Projective coordinates are again helpful in this situation – see [15]. Define the *symplectic form*, cf. [2, Sec. 41], of two vectors by

$$\omega(z, z') = xy' - x'y, \quad \text{where } z = (x, y), \ z' = (x', y') \in \mathbb{A}^2. \quad (4.15)$$

The one-dimensional projective space $\mathbb{P}^1(\mathbb{A})$ is the quotient of \mathbb{A}^2 with respect to the equivalence relation: $z \sim z'$ if their symplectic form vanishes. We also say [15] that two points in $\mathbb{P}^1(\mathbb{A})$ are *essentially distinct* if there exist their representatives $z, z' \in \mathbb{A}^2$ such that $\omega(z, z')$ is not a zero divisor.

Definition 4.19. [15] The *projective cross-ratio* of four essentially distinct points $z_i \in \mathbb{P}^1(\mathbb{A})$ represented by $(x_i, y_i) \in \mathbb{A}^2$, $i = 1, \dots, 4$, respectively, is defined by:

$$[z_1, z_2, z_3, z_4] = \frac{(x_1 y_3 - x_3 y_1)(x_2 y_4 - x_4 y_2)}{(x_1 y_2 - x_2 y_1)(x_3 y_4 - x_4 y_3)} \in \mathbb{P}^1(\mathbb{A}). \quad (4.16)$$

Exercise 4.20. Check that:

- i. Let the map $S : \mathbb{A} \rightarrow \mathbb{P}^1(\mathbb{A})$ be defined by $z \mapsto (z, 1)$. Then, it intertwines the Möbius transformations on \mathbb{A} with linear maps (4.9).
- ii. The map S intertwines cross-ratios in the following sense:

$$S([z_1, z_2, z_3, z_4]) = [S(z_1), S(z_2), S(z_3), S(z_4)], \quad (4.17)$$

where $z_i \in \mathbb{C}$, and the left-hand side contains the classic cross-ratio (4.14) while the right-hand side the projective (4.16).

- iii. The symplectic form (4.15) on \mathbb{A}^2 is invariant if vectors are multiplied by a 2×2 real matrix with the unit determinant.
- iv. The projective cross-ratio (4.16) is invariant if points in \mathbb{A}^2 are multiplied by a matrix from $\text{SL}_2(\mathbb{R})$. Then, the classic cross-ratio (4.14) is invariant under the Möbius transformations, cf. (4.17).

Exercise 4.21. [15] Check further properties of the projective cross-ratio.

- i. Find transformations of $[z_1, z_2, z_3, z_4]$ under all permutations of points.
- ii. Demonstrate the *cancellation formula* for cross-ratios:

$$[z_1, z_2, z_3, z_4][z_1, z_3, z_5, z_4] = [z_1, z_2, z_5, z_4], \quad (4.18)$$

where, in the left-hand side, values in \mathbb{A}^2 are multiplied component-wise. Such a multiplication is commutative but not associative on $\mathbb{P}^1(\mathbb{A})$.

We say that a collection of points of $\mathbb{P}^1(\mathbb{A})$ is *concylic* if all their representatives in \mathbb{A}^2 satisfy to Equation (4.11) for some FSCc matrix $\begin{pmatrix} L & -M \\ K & \bar{L} \end{pmatrix}$.

Exercise 4.22. [15] Show that:

- i. Any collection of points in \mathbb{A} belonging to some cycle is mapped by S from Exercise 4.20.i to concyclic points in $\mathbb{P}^1(\mathbb{A})$.
- ii. For any three essentially distinct points z_1, z_2 and $z_3 \in \mathbb{P}^1(\mathbb{A})$ there is a fixed 2×2 matrix A such that $[z_1, z_2, z, z_3] = Az$ for any $z \in \mathbb{P}^1(\mathbb{A})$. Moreover, the matrix A has a determinant which is not a zero divisor.
- iii. Any four essentially distinct points in $\mathbb{P}^1(\mathbb{A})$ are concyclic if and only if their projective cross-ratio is $S(r)$ for some real number r .

HINT: Let $[z_1, z_2, z, z_3]$ correspond through S to a real number. We know that $[z_1, z_2, z, z_3] = Az$ for an invertible A , then $\bar{A}\bar{z} = Az$ or $\bar{z} = \bar{A}^{-1}Az$. Multiply both sides of the last identity by row vector $(-\bar{y}, \bar{x})$, where $z = \begin{pmatrix} x \\ y \end{pmatrix}$. The final step is to verify that $\bar{A}^{-1}A$ has the FSCc structure, cf. [15, Sec. 4]. \diamond

We have seen another way to obtain FSCc—from the projective cross-ratio.

Chapter 5

Indefinite Product Space of Cycles

In the previous chapter, we represented cycles by points of the projective space \mathbb{P}^3 or by lines of 2×2 matrices. The latter is justified so far only by the similarity formula (4.7). Now, we will investigate connections between cycles and vector space structure. Thereafter we will use the special form of FSCc matrices to introduce very important additional structure in the cycle space.

5.1 Cycles: An Appearance and the Essence

Our extension (4.5) of FSCc adds two new elements in comparison with the standard one [22]:

- The hypercomplex unit $\check{\iota}$, which is independent from ι .
- The additional sign-type parameter s .

Such a possibility of an extension exists because elements of $\text{SL}_2(\mathbb{R})$ are matrices with real entries. For generic Möbius transformations with hypercomplex-valued matrices considered in [22], it is impossible.

Indeed, the similarity formula (4.8) does not contain any squares of hypercomplex units, so their type is irrelevant for this purpose. At the moment, the hypercomplex unit $\check{\iota}$ serves only as a placeholder which keeps components l and n separated. However, the rôle of $\check{\iota}$ will be greatly extended thereafter. On the other hand, the hypercomplex unit ι defines the appearance of cycles on the plane, that is, any element (k, l, n, m) in the cycle space \mathbb{P}^3 admits its drawing as circles, parabolas or hyperbolas in the point space \mathbb{A} . We may think on points of \mathbb{P}^3 as ideal cycles while their depictions on \mathbb{A} are only their shadows on the wall of Plato's cave. More prosaically, we can consider cones and their (conic) sections as in Fig. 1.3.

Of course, some elliptic shadows may be imaginary, see Exercise 4.5, but, in most cases, we are able to correctly guess a cycle from its σ -drawing.

Exercise 5.1. Describe all pairs of different cycles C_σ^s and \tilde{C}_σ^s such that their σ -drawing for some σ are exactly the same sets.

HINT: Note that the vertical axis is the p-drawing of two different cycles $(1, 0, 0, 0)$ and $(0, 1, 0, 0)$ and make a proper generalisation of this observation. \diamond

Figure 1.5(a) shows the same cycles drawn in different EPH styles. Points $c_\sigma = (\frac{l}{k}, -\sigma\frac{n}{k})$ are their respective e/p/h-centres from Definition 4.3. They are related to each other through several identities:

$$c_e = \bar{c}_h, \quad c_p = \frac{1}{2}(c_e + c_h). \quad (5.1)$$

From analytic geometry, we know that a parabola with the equation $ku^2 - 2lu - 2nv + m = 0$ has a *focal length*, the distance from its focus to the vertex, equal to $\frac{n}{2k}$. As we can see, it is half of the second coordinate in the e-centre. Figure 1.5(b) presents two cycles drawn as parabolas. They have the same focal length $\frac{n}{2k}$ and, thus, their e-centres are on the same level. In other words, *concentric* parabolas are obtained by a vertical shift, not by scaling, as an analogy with circles or hyperbolas may suggest.

We already extended the definition of centres from circles and hyperbolas to parabolas. It is time for a courtesy payback: parabolas share with other types of cycles their focal attributes.

Definition 5.2. A $\hat{\sigma}$ -*focus*, where $\hat{\sigma}$ is a variable of EPH type, of a cycle $C = (k, j, n, m)$ is the point in \mathbb{A}

$$f_{\hat{\sigma}} = \left(\frac{l}{k}, \frac{\det C_{\hat{\sigma}}^s}{2nk} \right) \quad \text{or, explicitly,} \quad f_{\hat{\sigma}} = \left(\frac{l}{k}, \frac{mk - l^2 + \hat{\sigma}n^2}{2nk} \right). \quad (5.2)$$

We also use the names *e-focus*, *p-focus*, *h-focus* and $\hat{\sigma}$ -*focus*, in line with previous conventions.

The *focal length* of the cycle C is $\frac{n}{2k}$.

Note that values of all centres, foci and the focal length are independent of a choice of a quadruple of real numbers (k, l, n, m) which represents a point in the projective space \mathbb{P}^3 .

Figure 1.5(b) presents e/p/h-foci of two parabolas with the same focal length. If a cycle is depicted as a parabola, then the h-focus, p-focus and e-focus are, correspondingly, the geometrical *focus* of the parabola, the *vertex* of the parabola, and the point on the *directrix* of the parabola nearest to the vertex.

As we will see, cf. Propositions 6.19 and 6.40, all three centres and three foci are useful attributes of a cycle, even if it is drawn as a circle.

Remark 5.3. Such a variety of choices is a consequence of the usage of $\mathrm{SL}_2(\mathbb{R})$ —a smaller group of symmetries in comparison to the all Möbius maps of \mathbb{A} . The $\mathrm{SL}_2(\mathbb{R})$ group fixes the real line and, consequently, a decomposition of vectors into ‘real’ (1) and ‘imaginary’ (ι) parts is obvious. This permits us to assign an arbitrary value to the square of the hypercomplex unit ι .

The exceptional rôle of the real line can be viewed in many places. For example, geometric invariants defined below, e.g. orthogonalities in Sections 6.1 and 6.6, demonstrate ‘awareness’ of the real-line invariance in one way or another. We will call this the *boundary effect* in the upper half-plane geometry. The famous question about hearing a drum’s shape has a counterpart:

Can we see/feel the boundary from inside a domain?

Remarks 5.19, 6.4, 6.20 and 6.35 provide hints for positive answers.

Exercise 5.4. Check that different realisations of the same cycle have these properties in common:

- All implementations have the same vertical axis of symmetry.
- Intersections with the real axis (if they exist) coincide, see points r_0 and r_1 for the left triple of cycles in Fig. 1.5(a). Moreover, all three EPH drawings of a cycle have common tangents at these intersection points.
- Centres of circle c_e and corresponding hyperbolas c_h are mirror reflections of each other in the real axis with the parabolic centre as the middle point.
- The $\check{\sigma}$ -focus of the elliptic K -orbits, see Exercise 3.14.e, is the reflection in the real axis of the midpoint between the $\check{\sigma}$ -centre of this orbit and the inverse of its h -centre.

Exercise 3.14 gives another example of similarities between different implementations of the same cycles defined by the Equation (3.26).

5.2 Cycles as Vectors

Elements of the projective space \mathbb{P}^3 are lines in the linear space \mathbb{R}^4 . Would it be possible to pick a single point on each line as its ‘label’? We may wish to do this for the following reasons:

- i. To avoid ambiguity in representation of the same cycle by different quadruples (k, l, n, m) and $k', l', n', m')$.
- ii. To have explicit connections with relevant objects (see below).

However, the general scheme of projective spaces does not permit such a unique representation serving the whole space. Otherwise the cumbersome construction with lines in vector spaces would not be needed. Nevertheless, there are several partial possibilities which have certain advantages and disadvantages. We will consider two such opportunities, calling them *normalisation of a cycle*.

The first is very obvious: we try to make the coefficient k in front of the squared terms in cycle equation (4.1) equal to 1. The second normalises the value of the determinant of the cycle's matrix. More formally:

Definition 5.5. A FSCc matrix representing a cycle is said to be *k-normalised* if its $(2, 1)$ -element is 1 and it is *det $\check{\sigma}$ -normalised* if its $\check{\sigma}$ -determinant is equal to ± 1 .

Exercise 5.6. Check that:

- i. Element $(1, 1)$ of the k -normalised $C_{\check{\sigma}}^1$ matrix is the $\check{\sigma}$ -centre of the cycle.
- ii. Any cycle (k, l, n, m) with $k \neq 0$ has an equivalent k -normalised cycle. Cycles which do not admit k -normalisation correspond to single straight lines in any point space.
- iii. det-normalisation is preserved by matrix similarity with $\text{SL}_2(\mathbb{R})$ elements, as in Theorem 4.13, while k -normalisation is not.
- iv. Any cycle with a non-zero $\check{\sigma}$ -determinant admits det $\check{\sigma}$ -normalisation. Cycles which cannot be det $\check{\sigma}$ -normalised will be studied in Section 5.4. What are cycles which cannot be det $\check{\sigma}$ -normalised for any value of $\check{\sigma}$?

Thus, each normalisation may be preferred in particular circumstances. The det-normalisation was used, for example, in [54] to obtain a satisfactory condition for *tangent circles*, cf. Exercise 5.26.ii. On the other hand, we will see in Section 7.1 that $\det C_{\check{\sigma}}^s$ of a k -normalised cycle is equal to the square of the *cycle radius*.

Remark 5.7. It is straightforward to check that there is one more cycle normalisation which is invariant under similarity (4.7). It is given by the condition $n = 1$. However, we will not use it at all in this work.

A cycle's normalisation is connected with scaling of vectors. Now we turn to the second linear operation: addition. Any two different lines define

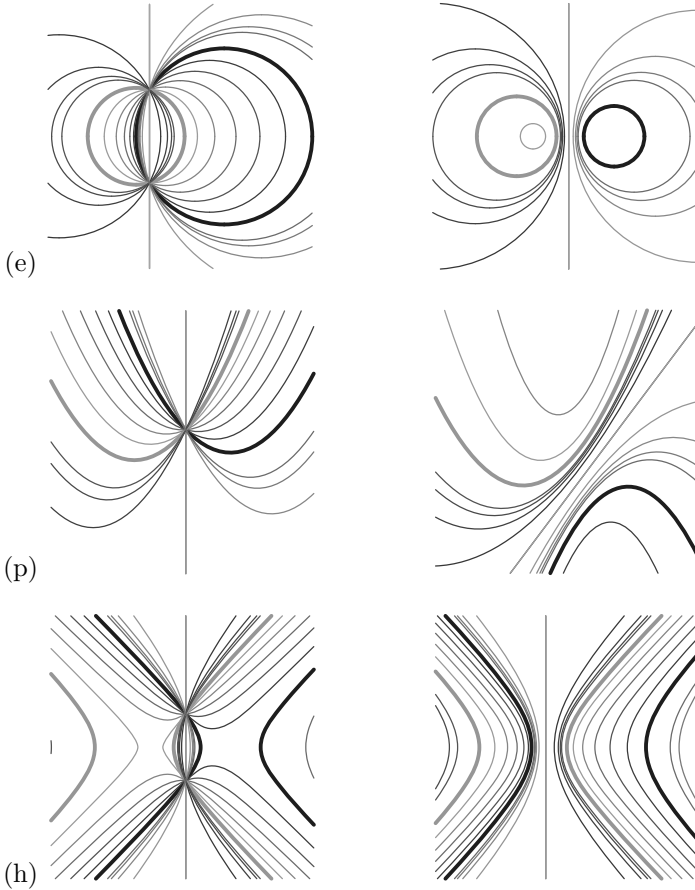


Figure 5.1 Linear spans of cycle pairs in EPH cases. The initial pairs of cycles are drawn in bold (green and blue). The cycles which are between the generators are drawn in the transitional green-blue colours. The red components are used for the outer cycles. The left column shows the appearance of the pencil if the generators intersect and the right if they are disjoint.

a unique two-dimensional plane passing through them. Vectors from the plane are linear combinations of two vectors spanning each line. If we consider circles corresponding to elements of the linear span, we will obtain a pencil of circles, see [12, Sec. 10.10; 23, Sec. 2.3]. As usual, there is no need to be restricted to circles only:

Definition 5.8. A *pencil* of cycles is the linear span (in the sense of \mathbb{R}^4) of two cycles.

Figure 5.1 shows the appearance of such pencils as circles, parabolas and hyperbolas. The elliptic case is very well known in classical literature, see [23, Figs. 2.2(A,B,C); 2.3A], for example. The appearance of pencils is visually different for two cases: spanning cycles are either intersecting or disjoint. These two possibilities are represented by the left and right columns in Fig. 5.1. We shall return to these situations in Corollary 5.27.

Exercise 5.9. Investigate the following:



- i. What happens with an elliptic pencil if one of spanning circles is imaginary? Or if both spanning circles are imaginary?
- ii. How does a pencil look if one spanning cycle is a straight line? If both cycles are straight lines?
- iii. A pair of circles is symmetric about the line joining their centres. Thus, circular pencils look similar regardless of the direction of this line of centres. Our hyperbolas and parabolas have a special orientation: their axes of symmetry are vertical. Thus, a horizontal or vertical line joining the centres of two hyperbolas/parabolas make a special arrangement, and it was used for Fig. 5.1. How do hyperbolic pencils look if the line of centres is not horizontal?

Exercise 5.10. Show the following:

- i. The image of a pencil of cycles under a Möbius transformation is again a pencil of cycles.
- ii. A pencil spanned by two concentric cycles consists of concentric cycles.
- iii. All cycles in a pencil are coaxial, see Exercise 3.19.iii for the definition. The joint radical axis, see Exercise 3.19.ii, is the only straight line in the pencil. This is also visible from Fig. 5.1.
- iv. Let two pencils of cycles have no cycle in common. Then, any cycle from \mathbb{P}^3 belongs to a new pencil spanned by two cycles from two given pencils.

This section demonstrated that there are numerous connections between the linear structure of the cycle space \mathbb{P}^3 and the geometrical property of cycles in the point space \mathbb{A} .

5.3 Invariant Cycle Product

We are looking for a possibility to enrich the geometry of the cycle space through the FSCc matrices. Many important relations between cycles are based on the following Möbius invariant cycle product.



Definition 5.11. The *cycle $\check{\sigma}$ -product* of two cycles is given by

$$\langle C_{\check{\sigma}}^s, \tilde{C}_{\check{\sigma}}^s \rangle = -\operatorname{tr}(C_{\check{\sigma}}^s \overline{\tilde{C}_{\check{\sigma}}^s}), \quad (5.3)$$

that is, the negative trace of the matrix product of $C_{\check{\sigma}}^s$ and hypercomplex conjugation of $\tilde{C}_{\check{\sigma}}^s$.

As we already mentioned, an inner product of type (5.3) is used, for example, in the Gelfand–Naimark–Segal (GNS) construction to make a Hilbert space out of C^* -algebra. This may be more than a simple coincidence since FSCc matrices can be considered as linear operators on a two-dimensional vector space. However, a significant difference with the Hilbert space inner product is that the cycle product is indefinite, see Exercise 5.12.iv for details. Thus, cycles form a Pontryagin or Krein space [33] rather than Euclidean or Hilbert. A geometrical interpretation of the cycle product will be given in Exercise 7.6.iii.

Exercise 5.12. Check that:

- i. The value of cycle product (5.3) will remain the same if both matrices are replaced by their images under similarity (4.7) with the same element $g \in \operatorname{SL}_2(\mathbb{R})$. 
- ii. The $\check{\sigma}$ -cycle product (5.3) of cycles defined by quadruples (k, l, n, m) and $(\tilde{k}, \tilde{l}, \tilde{n}, \tilde{m})$ is given by 

$$-2\tilde{l}l + 2\check{\sigma}s^2\tilde{n}n + \tilde{k}m + \tilde{m}k. \quad (5.4a)$$


More specifically, and also taking into account the value $s = \pm 1$, it is

$$-2\tilde{n}n - 2\tilde{l}l + \tilde{k}m + \tilde{m}k, \quad (5.4e)$$

$$-2\tilde{l}l + \tilde{k}m + \tilde{m}k, \quad (5.4p)$$

$$2\tilde{n}n - 2\tilde{l}l + \tilde{k}m + \tilde{m}k \quad (5.4h)$$

in the elliptic, parabolic and hyperbolic cases, respectively.

- iii. Let $C_{\check{\sigma}}$ and $\tilde{C}_{\check{\sigma}}$ be two cycles defined by e-centres (u, v) and (\tilde{u}, \tilde{v}) with σ -determinants $-r^2$ and $-\tilde{r}^2$, respectively. Then, their $\check{\sigma}$ -cycle product explicitly is 

$$\langle C_{\check{\sigma}}, \tilde{C}_{\check{\sigma}} \rangle = (u - \tilde{u})^2 - \sigma(v - \tilde{v})^2 - 2(\sigma - \check{\sigma})v\tilde{v} - r^2 - \tilde{r}^2. \quad (5.5)$$

- iv. The cycle product is a symmetric bilinear function of two cycles. It is *indefinite* in the sense that there are two cycles $C_{\check{\sigma}}$ and $\tilde{C}_{\check{\sigma}}$ such that

$$\langle C_{\check{\sigma}}, C_{\check{\sigma}} \rangle > 0 \quad \text{and} \quad \langle \tilde{C}_{\check{\sigma}}, \tilde{C}_{\check{\sigma}} \rangle < 0.$$

HINT: It is easy to show symmetry of the cycle product from the explicit value (5.4a). This is not so obvious from the initial definition (5.3) due to the presence of hypercomplex conjugation. \diamond

A simple, but interesting, observation is that, for FSCc matrices representing cycles, we obtain the second classical invariant (determinant) under similarities (4.7) from the first (trace) as follows:

$$\langle C_{\check{\sigma}}^s, C_{\check{\sigma}}^s \rangle = -\text{tr}(C_{\check{\sigma}}^s \overline{C_{\check{\sigma}}^s}) = 2 \det C_{\check{\sigma}}^s = 2(-l^2 + \check{\sigma} s^2 n^2 + mk). \quad (5.6)$$

Therefore it is not surprising that the determinant of a cycle enters Definition 5.2 of the foci and the following definition:

Definition 5.13. We say that a $C_{\check{\sigma}}$ is $\check{\sigma}$ -zero-radius, $\check{\sigma}$ -positive or $\check{\sigma}$ -negative cycle if the value of the cycle product of $C_{\check{\sigma}}$ with itself (5.6) (and thus its determinant) is zero, positive or negative, respectively.

These classes of cycles fit naturally to the Erlangen programme.

Exercise 5.14. Show that the zero-radius, positive and negative cycles form three non-empty disjoint Möbius-invariant families.

HINT: For non-emptiness, see Exercise 5.12.iv or use the explicit formula (5.6). \diamond

The following relations are useful for a description of these three classes of cycles.

Exercise 5.15. Check that:

- i. For any cycle $C_{\check{\sigma}}^s$ there is the following relation between its determinants evaluated with elliptic, parabolic and hyperbolic unit $\check{\gamma}$:

$$\det C_e^s \leq \det C_p^s \leq \det C_h^s.$$

- ii. The negative of the parabolic determinant, $-\det C_p^s$, of a cycle (k, l, n, m) coincides with the discriminant of the quadratic equation

$$ku^2 - 2lu + m = 0, \quad (5.7)$$

which defines intersection of the cycle with the real line (in any EPH presentation).

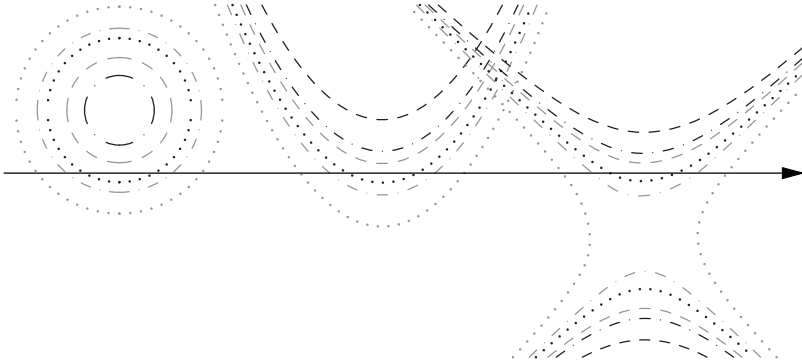


Figure 5.2 Positive and negative cycles. Evaluation of determinants with elliptic value $\sigma = -1$ shown by dotted drawing, with the hyperbolic $\sigma = 1$ by dashed and with intermediate parabolic $\sigma = 0$ by dash-dotted. Blue cycles are positive for respective σ and green cycles are negative. Cycles positive for one value of σ can be negative for another. Compare this figure with zero-radius cycles in Fig. 1.6.

We already illustrated zero-radius cycles in Fig. 1.6. This will be compared with positive and negative cycles for various values of σ in Fig. 5.2. The positive or negative aspect of cycles has a clear geometric manifestation for some combinations of σ and $\check{\sigma}$.

Exercise 5.16. Verify the following statements:

- e. Circles corresponding to e-positive cycles are imaginary. All regular circles are e-negative.
- p. Parabolas drawn from p- and e-negative cycles have two points of intersection with the real axis, and those drawn from p- and h-positive cycles do not intersect the real axis.
- h. Hyperbolas representing h-negative cycles have ‘vertical’ branches and those representing h-positive cycles have ‘horizontal’ ones.

HINT: Write the condition for a hyperbola defined by the Equation (4.1) to intersect the vertical line passing its centres. \diamond

Of course, manifestations of the indefinite nature of the cycle product (5.3) are not limited to the above examples and we will meet more of them on several other occasions.

5.4 Zero-radius Cycles

Due to the projective nature of the cycle space \mathbb{P}^3 , the absolute values of the cycle product (5.3) on non-normalised matrices are irrelevant, unless it is zero. There are many reasons to take a closer look at cycles with a zero-value product – zero-radius cycles, for example:

- They form a Möbius-invariant family.
- They are on the boundary between positive and negative cycles.
- They do not admit det-normalisation.

To highlight that a certain cycle is $\check{\sigma}$ -zero-radius we will denote it by $Z_{\check{\sigma}}^s$. A justification of the chosen name for such cycles is given in Exercise 5.16.e – further connections will be provided in Section 7.1.

As often happens in our study, we again have nine different possibilities – for cycles drawn in three EPH types in the point space (parametrised by σ) there are three independent conditions $\det C_{\check{\sigma}}^s = 0$ in the cycle space (parametrised by $\check{\sigma}$). This is illustrated in Fig. 1.6.

Exercise 5.17. Show that:

- Any $\check{\sigma}$ -zero-radius cycle admitting k -normalisation can be represented by the matrix

$$Z_{\check{\sigma}}^s = \begin{pmatrix} z & -z\bar{z} \\ 1 & -\bar{z} \end{pmatrix} = \frac{1}{2} \begin{pmatrix} z & z \\ 1 & 1 \end{pmatrix} \begin{pmatrix} 1 & -\bar{z} \\ 1 & -\bar{z} \end{pmatrix} = \begin{pmatrix} u_0 + \check{\sigma}sv_0 & u_0^2 - \check{\sigma}v_0^2 \\ 1 & -u_0 + \check{\sigma}sv_0 \end{pmatrix}, \quad (5.8)$$

for some $z = u_0 + \check{\sigma}sv_0$ being its centre and $s = \pm 1$. Compare with (4.10).

- Describe all $\check{\sigma}$ -zero-radius cycles which cannot be k -normalised.
- The $\check{\sigma}$ -focus of the $\check{\sigma}$ -zero-radius cycle belongs to the real axis – see Fig. 1.6.
- Let $Z_{\check{\sigma}}^s$ and $\tilde{Z}_{\check{\sigma}}^s$ be two k -normalised $\check{\sigma}$ -zero-radius cycles of the form (5.8) with e-centres (u_0, v_0) and (u_1, v_1) . Then

$$\langle Z_{\check{\sigma}}^s, \tilde{Z}_{\check{\sigma}}^s \rangle = (u_0 - u_1)^2 - \check{\sigma}(v_0 - v_1)^2. \quad (5.9)$$

As follows from (5.8), the class of $\check{\sigma}$ -zero-radius cycles is parametrised by two real numbers (u, v) only and, as such, is easily attached to the respective point of $z = u + \check{\sigma}v \in \mathbb{A}$, at least in the elliptic and hyperbolic point spaces. In \mathbb{D} , a connection between a $\check{\sigma}$ -zero-radius cycle and its centre is obscure.

Exercise 5.18. Prove the following observations from Fig. 1.6:

- i. The cycle $Z_{\check{\sigma}}^s$ (5.8) with $\det Z_{\check{\sigma}}^s = 0$, $\check{\sigma} = -1$ drawn elliptically is just a single point (u_0, v_0) , i.e. an (elliptic) zero-radius circle.
- ii. The same condition $\det Z_{\check{\sigma}}^s = 0$ with $\check{\sigma} = 1$ in the hyperbolic drawing produces a *light cone* originating at point (u_0, v_0)

$$(u - u_0)^2 - (v - v_0)^2 = 0,$$

- i.e. a zero-radius cycle in hyperbolic metric, see Section 7.1.
- iii. p-zero-radius cycles in any implementation touch the real axis, see Fig. 1.6.
- iv. An h-zero-radius cycle in \mathbb{A} with the e-center (a, b) intersects the real axis at points $(a \pm b, 0)$ with slopes ± 1 , see Fig. 1.6.

HINT: Use implicit derivation. Also, for a parabola, it follows from the Exercise 5.17.iii and the classical reflection property of parabolas, cf. App. A.2. \diamond

- v. The e-centre of the transformation $gZ_{\check{\sigma}}^s g^{-1}$, $g \in \mathrm{SL}_2(\mathbb{R})$ of the $\check{\sigma}$ -zero-radius cycle (5.8) coincides with the Möbius action $g \cdot z$ in $\mathbb{R}^{\check{\sigma}}$, where z is the e-centre of $Z_{\check{\sigma}}^s$.

HINT: The result can be obtained along the lines from Subsection 4.4.1. \diamond

Remark 5.19. The above ‘touching’ property (5.18.iii) and intersection behaviour (5.18.iv) are manifestations of the already-mentioned boundary effect in the upper half-plane geometry, see Remark 5.3.

The previous exercise shows that $\check{\sigma}$ -zero-radius cycles ‘encode’ points into the ‘cycle language’. The following reformulation of Exercise 5.18.v stresses that this encoding is Möbius-invariant as well.

Lemma 5.20. *The conjugate $g^{-1}Z_{\check{\sigma}}^s(y)g$ of a $\check{\sigma}$ -zero-radius cycle $Z_{\check{\sigma}}^s(y)$ with $g \in \mathrm{SL}_2(\mathbb{R})$ is a $\check{\sigma}$ -zero-radius cycle $Z_{\check{\sigma}}^s(g \cdot y)$ with centre at $g \cdot y$ – the Möbius transform of the centre of $Z_{\check{\sigma}}^s(y)$.*

Furthermore, we can extend the relation between a zero-radius cycle $Z_{\check{\sigma}}$ and points through the following connection of $Z_{\check{\sigma}}$ with the power of its centre.

Exercise 5.21. Let Z_{σ} be the zero-radius cycle (5.8) defined by $z = u - \iota \sigma v$, that is, with the σ -centre at the point (u, v) . Show that, in the elliptic and hyperbolic (but not parabolic) cases, a power of a point, see Definition 3.18, $(u, v) \in \mathbb{A}$ with respect to a cycle C_{σ} , is equal to the cycle product $\langle Z_{\sigma}, C_{\sigma} \rangle$, where both cycles are k -normalised.

It is noteworthy that the notion of a point’s power is not Möbius-invariant even despite its definition through the invariant cycle product. This is due

to the presence of non-invariant k -normalisation. This suggests extending the notion of the power from a point (that is, a zero-radius cycle) to arbitrary cycles:

Definition 5.22. A $(\sigma, \check{\sigma})$ -power of a cycle C with respect to another cycle \tilde{C} is equal to their cycle product $\langle C_{\check{\sigma}}, \tilde{C}_{\check{\sigma}} \rangle$, where both matrices are \det_{σ} -normalised.

Since both elements of this definition—the cycle product and det-normalisation—are Möbius-invariant, the resulting value is preserved by Möbius transformations as well. Of course, the (e,e)-variant of this notion is well known in the classical theory.

Exercise 5.23. Show that the (e,e)-power of a circle C with respect to another circle \tilde{C} has an absolute value equal to the *inversive distance* between C and \tilde{C} , see [5, Defn. 3.2.2; 7, Sec. 4; 23, Sec. 5.8 and Thm. 5.91]:

$$d(C, \tilde{C}) = \left| \frac{|c_1 - c_2|^2 - r_1^2 - r_2^2}{2r_1 r_2} \right|. \quad (5.10)$$

Here, $c_{1,2}$ and $r_{1,2}$ are the e-centres and radii of the circles. We will develop this theme in Exercise 7.8.

As another illustration of the technique based on zero-radius cycles, we return to orbits of isotropy subgroups, cf. Exercise 3.21.ii.

Exercise 5.24. Fulfil the following steps:

- i. Write the coefficients of the σ -zero-radius cycle $Z_{\sigma}(\iota)$ in \mathbb{A} with e-centre at the hypercomplex unit $\iota = (0, 1)$.
- ii. According to Exercise 5.18.v, $Z_{\sigma}(\iota)$ is invariant under the similarity $Z_{\sigma}(\iota) \mapsto hZ_{\sigma}(\iota)h^{-1}$ with h in the respective isotropy subgroups K , N' and A' of ι . Check this directly.
- iii. Write the coefficients of a generic cycle in the pencil spanned by $Z_{\sigma}(\iota)$ and the real line. Note that the real line is also invariant under the action of the isotropy subgroups (as any other Möbius transformations) and conclude that any cycle from the pencil will also be invariant under the action of the isotropy subgroups. In other words, those cycles are orbits of the isotropy subgroups. Check that you obtained their equation (3.33).

We halt our study of zero-radius cycles on their own, but they will appear repeatedly in the following text in relation to other objects.

5.5 Cauchy–Schwarz Inequality and Tangent Cycles

We already noted that the invariant cycle product is a special (and remarkable!) example of an indefinite product in a vector space. Continuing this comparison, it will be interesting to look for a role of a Cauchy–Schwarz–type inequality

$$\langle x, y \rangle \langle y, x \rangle \leq \langle x, x \rangle \langle y, y \rangle, \quad (5.11)$$

which is a cornerstone of the theory of inner product spaces, cf. [55, Sec. 5.1].

First of all, the classical form (5.11) of this inequality failed in any indefinite product space. This can be seen from examples or an observation that all classical proofs start from the assumption that $\langle x + ty, x + ty \rangle \geq 0$ in an inner product space. In an indefinite product space, there are always pairs of vectors which realise any of three possible relations:

$$\langle x, y \rangle \langle y, x \rangle \leq \langle x, x \rangle \langle y, y \rangle.$$

Some regularity appears from the fact that the type of inequality is inherited by linear spans.

Exercise 5.25. Let two vectors x and y in an indefinite product space satisfy either of the inequalities:

$$\langle x, y \rangle \langle y, x \rangle < \langle x, x \rangle \langle y, y \rangle \quad \text{or} \quad \langle x, y \rangle \langle y, x \rangle > \langle x, x \rangle \langle y, y \rangle.$$

Then, any two non-collinear vectors z and w from the real linear span of x and y satisfy the corresponding inequality:

$$\langle z, w \rangle \langle w, z \rangle < \langle z, z \rangle \langle w, w \rangle \quad \text{or} \quad \langle z, w \rangle \langle w, z \rangle > \langle z, z \rangle \langle w, w \rangle.$$

The equality $\langle x, y \rangle \langle y, x \rangle = \langle x, x \rangle \langle y, y \rangle$ always implies $\langle z, w \rangle \langle w, z \rangle = \langle z, z \rangle \langle w, w \rangle$.

The above Cauchy–Schwarz relations have a clear geometric meaning.

Exercise 5.26. Check the following:

- i. Let C_σ and \tilde{C}_σ be two cycles defined by e-centres (u, v) and (\tilde{u}, \tilde{v}) with σ -determinants $-r^2$ and $-\tilde{r}^2$. The relations

$$\langle C_\sigma^s, \tilde{C}_\sigma^s \rangle^2 \leq \langle C_\sigma^s, C_\sigma^s \rangle \langle \tilde{C}_\sigma^s, \tilde{C}_\sigma^s \rangle$$

guarantee that σ -implementations of C_σ and \tilde{C}_σ for $\sigma = \pm 1$ are intersecting, tangent or disjoint, respectively. What happens for the parabolic value $\sigma = 0$?

HINT: Determine the sign of the expression $\langle C_\sigma^s, \tilde{C}_\sigma^s \rangle - \sqrt{\langle C_\sigma^s, C_\sigma^s \rangle \langle \tilde{C}_\sigma^s, \tilde{C}_\sigma^s \rangle}$ using the formula (5.5). For the parabolic case, Exercise 7.2.p will be useful. ◊

- ii. Let two cycles C_σ and \tilde{C}_σ be in \det_σ -normalised form. Deduce from the previous item the following Descartes–Kirillov condition [54, Lem. 6.3] for C_σ and \tilde{C}_σ to be externally tangent:

$$\det(C_\sigma + \tilde{C}_\sigma) = 0 \quad \text{and} \quad \langle C_\sigma, \tilde{C}_\sigma \rangle > 0. \quad (5.12)$$

Moreover, $C_\sigma + \tilde{C}_\sigma$ is the σ -zero-radius cycle at the tangent point of C_σ and \tilde{C}_σ .

HINT: The identity in (5.12) follows from the inequality there and the relation $|\langle C_\sigma, \tilde{C}_\sigma \rangle| = \sqrt{\langle C_\sigma^s, C_\sigma^s \rangle \langle \tilde{C}_\sigma^s, \tilde{C}_\sigma^s \rangle} = 1$ for tangent cycles from the first item. For the last statement, use Exercise 5.21. \diamond

The previous two exercises imply (see also Exercise 6.10.iii):

Corollary 5.27. *For a given pencil of cycles, see Definition 5.8, either all cycles are pair-wise disjoint, or every pair of cycles are tangent, or all of them have at least two common points.*

Zero-radius cycles form a two-parameter family (in fact, a manifold) in the three-dimensional projective cycle space \mathbb{P}^3 . It is not flat, as can be seen from its intersection with projective lines – cycle pencils. The Cauchy–Schwarz inequality turns out to be relevant here as well.

Exercise 5.28. A pencil of cycles either contains at most two $\check{\sigma}$ -zero-radius cycles or consists entirely of $\check{\sigma}$ -zero-radius cycles. Moreover:

- i. A pencil spanned by two different cycles cannot consist only of $\check{\sigma}$ -zero-radius cycles. Describe all pencils consisting only of p- and h-zero-radius cycles.

HINT: Formula (5.9) will be useful for describing pencils consisting of (and thus spanned by) $\check{\sigma}$ -zero-radius cycles. Orbits of subgroup N' shown on the central drawing of Fig. 3.1 are an example of pencils of p-zero-radius cycles drawn as parabolas. You can experiment with σ -drawing of certain $\check{\sigma}$ -zero-radius pencils. \diamond

- ii. A pencil spanned by two different cycles C_σ^s and \tilde{C}_σ^s , which does not consist only of $\check{\sigma}$ -zero-radius cycles, has exactly two, one or zero $\check{\sigma}$ -zero-radius cycles depending on which of three possible Cauchy–Schwarz-type relations holds:

$$\langle C_\sigma^s, \tilde{C}_\sigma^s \rangle^2 \leq \langle C_\sigma^s, C_\sigma^s \rangle \langle \tilde{C}_\sigma^s, \tilde{C}_\sigma^s \rangle.$$

HINT: Write the expression for the cycle product of the span $tC_\sigma^s + \tilde{C}_\sigma^s$, $t \in \mathbb{R}$ with itself in terms of products $\langle C_\sigma^s, \tilde{C}_\sigma^s \rangle$, $\langle C_\sigma^s, C_\sigma^s \rangle$ and $\langle \tilde{C}_\sigma^s, \tilde{C}_\sigma^s \rangle$. \diamond



Chapter 6

Joint Invariants of Cycles: Orthogonality

The invariant cycle product, defined in the previous chapter, allows us to define joint invariants of two or more cycles. Being initially defined in an algebraic fashion, they also reveal their rich geometrical content. We will also see that FSCc matrices define reflections and inversions in cycles, which extend Möbius maps.

6.1 Orthogonality of Cycles

According to the categorical viewpoint, the internal properties of objects are of minor importance in comparison with their relations to other objects from the same class. Such a projection of internal properties into external relations was also discussed at the beginning of Section 4.2. As a further illustration, we may give the proof of Theorem 4.13, outlined below. Thus, we will now look for invariant relations between two or more cycles.

After we defined the invariant cycle product (5.3), the next standard move is to use the analogy with Euclidean and Hilbert spaces and give the following definition:

Definition 6.1. Two cycles C_{σ}^s and \tilde{C}_{σ}^s are called $\check{\sigma}$ -orthogonal if their $\check{\sigma}$ -cycle product vanishes:

$$\langle C_{\sigma}^s, \tilde{C}_{\sigma}^s \rangle = 0. \quad (6.1)$$

Here are the most fundamental properties of cycle orthogonality:

Exercise 6.2. Use Exercise 5.12 to check the following:

- i. The $\check{\sigma}$ -orthogonality condition (6.1) is invariant under Möbius transformations.

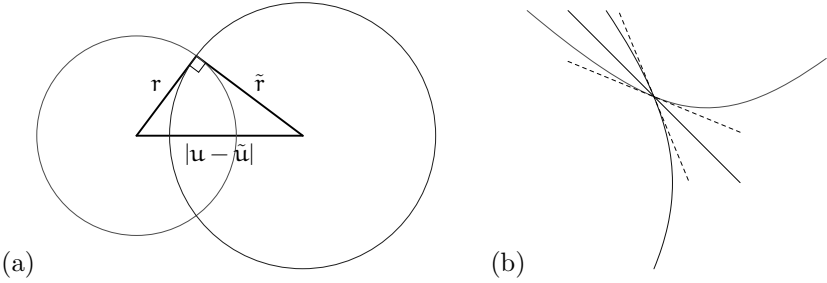


Figure 6.1 Relation between centres and radii of orthogonal circles.

- ii. The explicit expression for $\check{\sigma}$ -orthogonality of cycles in terms of their coefficients is

$$2\check{\sigma}\tilde{n}n - 2\tilde{l}l + \tilde{k}m + \tilde{m}k = 0. \quad (6.2)$$

- iii. The $\check{\sigma}$ -orthogonality of cycles defined by their e-centres (u, v) and (\tilde{u}, \tilde{v}) with σ -determinants $-r^2$ and $-\tilde{r}^2$, respectively, is:

$$(u - \tilde{u})^2 - \sigma(v - \tilde{v})^2 - 2(\sigma - \check{\sigma})v\tilde{v} - r^2 - \tilde{r}^2 = 0. \quad (6.3)$$

- iv. Two circles are e-orthogonal if their tangents at an intersection point form a right angle.

HINT: Use the previous formula (6.3), the inverse of Pythagoras' theorem and Fig. 6.1(a) for this. \diamond

The last item can be reformulated as follows: For circles, their e-orthogonality as vectors in the cycle spaces \mathbb{P}^3 with the cycle product (5.3) coincides with their orthogonality as geometrical sets in the point space \mathbb{C} . This is very strong support for FSCc and the cycle product (5.3) defined from it. Thereafter, it is tempting to find similar interpretations for other types of orthogonality. The next exercise performs the first step for the case of σ -orthogonality in the matching point space \mathbb{A} .

Exercise 6.3. Check the following geometrical meaning for σ -orthogonality of σ -cycles. 

- (e,h) Let $\sigma = \pm$. Then, two cycles in \mathbb{A} (that is, circles or hyperbolas) are σ -orthogonal if slopes S_1 and S_2 of their tangents at the intersection point satisfy the condition

$$S_1 S_2 = \sigma. \quad (6.4)$$

The geometrical meaning of this condition can be given either in terms of angles (A) or centres (C):

- (A) For the case $\sigma = -1$ (circles), equation (6.4) implies orthogonality of the tangents, cf. Exercise 6.2.iv. For $\sigma = 1$, two hyperbolas are h-orthogonal if lines with the slopes ± 1 bisect the angle of intersection of the hyperbolas, see Fig. 6.1(b).

HINT: Define a cycle C_σ by the condition that it passes a point $(u, v) \in \mathbb{A}$. Define a second cycle \tilde{C}_σ by both conditions: it passes the same point (u, v) and is orthogonal to C_σ . Then use the implicit derivative formula to find the slopes of tangents to C_σ and \tilde{C}_σ at (u, v) . A script calculating this in CAS is also provided. \diamond

- (C) In the cases $\sigma = \pm 1$, the tangent to one cycle at the intersection point passes the centre of another cycle.

HINT: This fact is clear for circles from inspection of, say, Fig. 6.1(a). For hyperbolas, it is enough to observe that the slope of the tangent to a hyperbola $y = 1/x$ at a point $(x, 1/x)$ is $-1/x^2$ and the slope of the line from the centre $(0, 0)$ to the point $(x, 1/x)$ is $1/x^2$, so the angle between two lines is bisected by a vertical/horizontal line. All our hyperbolas are obtained from $y = 1/x$ by rotation of $\pm 45^\circ$ and scaling. \diamond

- (p) Let $\sigma = 0$ and a parabola C_p have two real roots u_1 and u_2 . If a parabola \tilde{C}_p is p -orthogonal to C_p , then the tangent to \tilde{C}_p at a point above one of the roots $u_{1,2}$ passes the p -centre $(\frac{u_1+u_2}{2}, 0)$ of C_p .

Remark 6.4. Note that the geometric p -orthogonality condition for parabolas is non-local in the sense that it does not direct behaviour of tangents at the intersection points. Moreover, orthogonal parabolas need not intersect at all. We shall see more examples of such non-locality later. The relation 6.3(p) is also another example of boundary awareness, cf. Remark 5.3 – we are taking a tangent of one parabola above the point of intersection of the other parabola with the boundary of the upper half-plane.

The stated geometrical conditions for orthogonality of cycles are not only necessary but are sufficient as well.

Exercise 6.5.

- i. Prove the converses of the two statements in Exercise 6.3.

HINT: To avoid irrationalities in the parabolic case and to make the calculations accessible for CAS, you may proceed as follows. Define a generic parabola passing (u, v) and use implicit derivation to find its tangent at this point. Define the second parabola passing $(u, 0)$ and its centre at the intersection of the tangent of the first parabola at (u, v) and the horizontal axis. Then, check the



p-orthogonality of the two parabolas. \diamond

- ii. Let a parabola have two tangents touching it at (u_1, v_1) and (u_2, v_2) and these tangents intersect at a point (u, v) . Then, $u = \frac{u_1 + u_2}{2}$.

HINT: Use the geometric description of p-orthogonality and note that the two roots of a parabola are interchangeable in the necessary condition for p-orthogonality. \diamond

We found geometrically necessary and sufficient conditions for σ -orthogonality in the matching point space \mathbb{A} . The remaining six non-matching cases will be reduced to this in Section 6.3 using an auxiliary ghost cycle. However, it will be useful to study some more properties of orthogonality.

6.2 Orthogonality Miscellanea

The explicit formulae (6.2) and (6.3) allow us to obtain several simple and yet useful conclusions.

Exercise 6.6. Show that:

- i. A cycle is $\check{\sigma}$ -self-orthogonal (isotropic) if and only if it is $\check{\sigma}$ -zero-radius cycle (5.8).
- ii. For $\check{\sigma} = \pm 1$, there is no non-trivial cycle orthogonal to all other non-trivial cycles. For $\check{\sigma} = 0$, only the horizontal axis $v = 0$ is orthogonal to all other non-trivial cycles.
- iii. If two real (e-negative) circles are e-orthogonal, then they intersect. Give an example of h-orthogonal hyperbolas which do not intersect in \mathbb{O} .
HINT: Use properties of the Cauchy–Schwarz inequality from Exercise 5.26.i. \diamond
- iv. A cycle C_σ^s is σ -orthogonal to a zero-radius cycle Z_σ^s (5.8) if and only if σ -implementation of C_σ^s passes through the σ -centre of Z_σ^s , or, analytically,

$$k(u^2 - \sigma v^2) - 2\langle (l, n), (u, \check{\sigma} v) \rangle + m = 0. \quad (6.5)$$

- v. For $\check{\sigma} = \pm 1$, any cycle is uniquely defined by the family of cycles orthogonal to it, i.e. $(C_\sigma^{s\perp})^\perp = \{C_\sigma^s\}$.
For $\check{\sigma} = 0$, the set $(C_\sigma^{s\perp})^\perp$ is the pencil spanned by C_σ^s and the real line. In particular, if C_σ^s has real roots, then all cycles in $(C_\sigma^{s\perp})^\perp$ have these roots.

The connection between orthogonality and incidence from Exercise 6.6.iv allows us to combine the techniques of zero-radius cycles and orthogonality in an efficient tool.

Exercise 6.7. Fill all gaps in the following proof:

Sketch of an alternative proof of Theorem 4.13. We already mentioned in Subsection 4.4.1 that the validity of Theorem 4.13 for a zero-radius cycle (5.8)

$$Z_{\sigma}^s = \begin{pmatrix} z & -z\bar{z} \\ 1 & -\bar{z} \end{pmatrix} = \frac{1}{2} \begin{pmatrix} z & z \\ 1 & 1 \end{pmatrix} \begin{pmatrix} 1 & -\bar{z} \\ 1 & -\bar{z} \end{pmatrix}$$

with the centre $z = x + iy$ is a straightforward calculation – see also Exercise 5.18.v. This implies the result for a generic cycle with the help of

- Möbius invariance of the product (5.3) (and thus orthogonality) and
- the above relation 6.6.iv between the orthogonality and the incidence.

The idea of such a proof is borrowed from [22] and details can be found therein. \square

The above demonstration suggests a generic technique for extrapolation of results from zero-radius cycles to the entire cycle space. We will formulate it with the help of a map Q from the cycle space to conics in the point space from Definition 4.10.

Proposition 6.8. *Let $T : \mathbb{P}^3 \rightarrow \mathbb{P}^3$ be an orthogonality-preserving map of the cycle space, i.e. $\langle C_{\sigma}^s, \tilde{C}_{\sigma}^s \rangle = 0 \Leftrightarrow \langle TC_{\sigma}^s, T\tilde{C}_{\sigma}^s \rangle = 0$. Then, for $\sigma \neq 0$, there is a map $T_{\sigma} : \mathbb{A} \rightarrow \mathbb{A}$, such that Q intertwines T and T_{σ} :*

$$QT_{\sigma} = TQ. \quad (6.6)$$

Proof. If T preserves orthogonality (i.e. the cycle product (5.3) and, consequently, the determinant, see (5.6)) then the image $TZ_{\sigma}^s(u, v)$ of a zero-radius cycle $Z_{\sigma}^s(u, v)$ is again a zero-radius cycle $Z_{\sigma}^s(u_1, v_1)$. Thus we can define T_{σ} by the identity $T_{\sigma} : (u, v) \mapsto (u_1, v_1)$.

To prove the intertwining property (6.6) we need to show that, if a cycle C_{σ}^s passes through (u, v) , then the image TC_{σ}^s passes through $T_{\sigma}(u, v)$. However, for $\sigma \neq 0$, this is a consequence of the T -invariance of orthogonality and the expression of the point-to-cycle incidence through orthogonality from Exercise 6.6.iv. \square

Exercise 6.9. Let $T_i : \mathbb{P}^3 \rightarrow \mathbb{P}^3$, $i = 1, 2$ be two orthogonality-preserving maps of the cycle space. Show that, if they coincide on the subspace of $\check{\sigma}$ -zero-radius cycles, $\check{\sigma} \neq 0$, then they are identical in the whole \mathbb{P}^3 .

We defined orthogonality from an inner product, which is linear in each component. Thus, orthogonality also respects linearity.

Exercise 6.10. Check the following relations between orthogonality and pencils:

- i. Let a cycle $C_{\check{\sigma}}$ be $\check{\sigma}$ -orthogonal to two different cycles $\tilde{C}_{\check{\sigma}}$ and $\hat{C}_{\check{\sigma}}$. Then $C_{\check{\sigma}}$ is $\check{\sigma}$ -orthogonal to every cycle in the pencil spanned by $\tilde{C}_{\check{\sigma}}$ and $\hat{C}_{\check{\sigma}}$.
- ii. Check that all cycles $\check{\sigma}$ -orthogonal with $\check{\sigma} = \pm 1$ to two different cycles $\tilde{C}_{\check{\sigma}}$ and $\hat{C}_{\check{\sigma}}$ belong to a single pencil. Describe such a family for $\check{\sigma} = 0$.
HINT: For the case $\check{\sigma} = 0$, the family is spanned by an additional cycle, which was mentioned in Exercise 6.6.ii. \diamond
- iii. If two circles are non-intersecting, then the orthogonal pencil passes through two points, which are the only two e-zero-radius cycles in the pencil. And *vice versa*: a pencil orthogonal to two intersecting circles consists of disjoint circles. Tangent circles have the orthogonal pencils of circles which are all tangent at the same point, cf. Corollary 5.27.

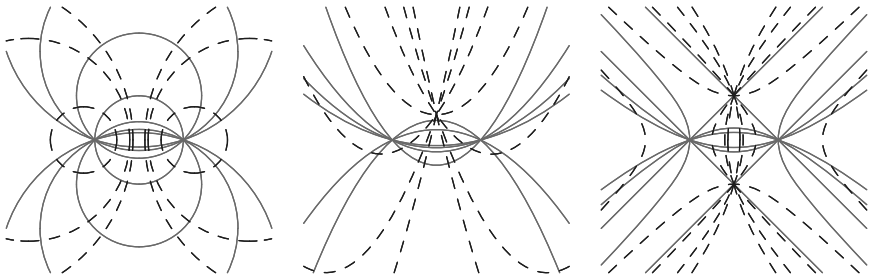


Figure 6.2 σ -orthogonal pencils of σ -cycles. One pencil is drawn in green, the others in blue and dashed styles.

Exercise 6.10.ii describes two *orthogonal pencils* such that each cycle in one pencil is orthogonal to every cycle in the second. In terms of indefinite linear algebra, see [33, Sec. 2.2], we are speaking about the orthogonal complement of a two-dimensional subspace in a four-dimensional space and it turns out to be two-dimensional as well. For circles, this construction is well known, see [12, Sec. 10.10; 23, Sec. 5.7]. An illustration for three cases is provided by Fig. 6.2. The reader may wish to experiment more with orthogonal complements to various parabolic and hyperbolic pencils—see Fig. 5.1 and Exercise 5.9.

Such orthogonal pencils naturally appear in many circumstances and we already met them on several occasions. We know from Exercise 3.19.iii and 3.19.iv that K -orbits and transverse lines make coaxial pencils which turn to be in a relation:

Exercise 6.11. Check that any K -orbit (3.26) in \mathbb{A} is σ -orthogonal to any transverse line (3.28). Figure 1.2 provides an illustration.

HINT: There are several ways to check this. A direct calculation based on the explicit expressions for cycles is not difficult. Alternatively, we can observe that the pencil of transverse lines is generated by K -action from the vertical axis and orthogonality is Möbius-invariant. \diamond

We may describe a finer structure of the cycle space through Möbius-invariant subclasses of cycles. Three such families—zero-radius, positive and negative cycles—were already considered in Sections 5.3 and 5.4. They were defined using the properties of the cycle product with itself. Another important class of cycles is given by the value of its cycle product with the real line.

Definition 6.12. A cycle $C_{\check{\sigma}}^s$ is called *selfadjoint* if it is $\check{\sigma}$ -orthogonal with $\check{\sigma} \neq 0$ to the real line, i.e. it is defined by the condition $\langle C_{\check{\sigma}}^s, R_{\check{\sigma}}^s \rangle = 0$, where $R_{\check{\sigma}}^s = (0, 0, 1, 0)$ corresponds to the horizontal axis $v = 0$.

The following algebraic properties of selfadjoint cycles easily follow from the definition.

Exercise 6.13. Show that:

- i. Selfadjoint cycles make a Möbius-invariant family.
- ii. A selfadjoint cycle $C_{\check{\sigma}}^s$ is defined explicitly by $n = 0$ in (4.1) for both values $\check{\sigma} = \pm 1$.
- iii. Any of the following conditions are necessary and sufficient for a cycle to be selfadjoint:
 - All three centres of the cycle coincide.
 - At least two centres of the cycle belong to the real line.

From these analytic conditions, we can derive a geometric characterisation of selfadjoint cycles.

Exercise 6.14. Show that selfadjoint cycles have the following implementations in the point space \mathbb{A} :

(e,h) Circles or hyperbolas with their geometric centres on the real line.

- (p) Vertical lines, consisting of points (u, v) such that $|u - u_0| = r$ for some $u_0 \in \mathbb{R}$, $r \in \mathbb{R}_+$. The cycles are also given by the $\|x - y\| = r^2$ in the parabolic metric defined below in (7.3).

Notably, selfadjoint cycles in the parabolic point space were labelled as ‘parabolic circles’ by Yaglom – see [108, Sec. 7]. On the other hand, Yaglom used the term ‘parabolic cycle’ for our p-cycle with non-zero k and n .

Exercise 6.15. Show that:

- i. Any cycle $C_\sigma^s = (k, l, n, m)$ belongs to a pencil spanned by a selfadjoint cycle HC_σ^s and the real line

$$C_\sigma^s = HC_\sigma^s + nR_\sigma^s, \quad \text{where } HC_\sigma^s = (k, l, 0, m). \quad (6.7)$$

This identity is a definition of linear orthogonal projection H from the cycle space to its subspace of selfadjoint cycles.

- ii. The decomposition of a cycle into the linear combination of a selfadjoint cycle and the real line is Möbius-invariant:

$$g \cdot C_\sigma^s = g \cdot HC_\sigma^s + nR_\sigma^s.$$

HINT: The first two items are small pieces of linear algebra in an indefinite product space, see [33, Sec. 2.2]. \diamond

- iii. Cycles C_σ^s and HC_σ^s have the same real roots.

We are now equipped to consider the geometrical meaning of all nine types of cycle orthogonality.

6.3 Ghost Cycles and Orthogonality

For the case of $\check{\sigma}\sigma = 1$, i.e. when geometries of the cycle and point spaces are both either elliptic or hyperbolic, $\check{\sigma}$ -orthogonality can be expressed locally through tangents to cycles at the intersection points – see Exercise 6.3(A). A semi-local condition also exists: the tangent to one cycle at the intersection point passes the centre of the second cycle – see Exercise 6.3(C). We may note that, in the pure parabolic case $\sigma = \check{\sigma} = 0$, the geometric orthogonality condition from Exercise 6.3(p) can be restated with help from Exercise 6.15.i as follows:

Corollary 6.16. *Two p-cycles C_p and \tilde{C}_p are p-orthogonal if the tangent to C_p at its intersection point with the projection HC_p^s (6.7) of \tilde{C}_p to selfadjoint cycles passes the p-centre of \tilde{C}_p .*

HINT: In order to reformulate Exercise 6.3(p) to the present form, it is enough to use Exercises 6.14(p) and 6.15.iii. \diamond

The three cases with matching geometries in point and cycle spaces are now quite well unified. Would it be possible to extend such a geometric interpretation of orthogonality to the remaining six ($= 9 - 3$) cases?

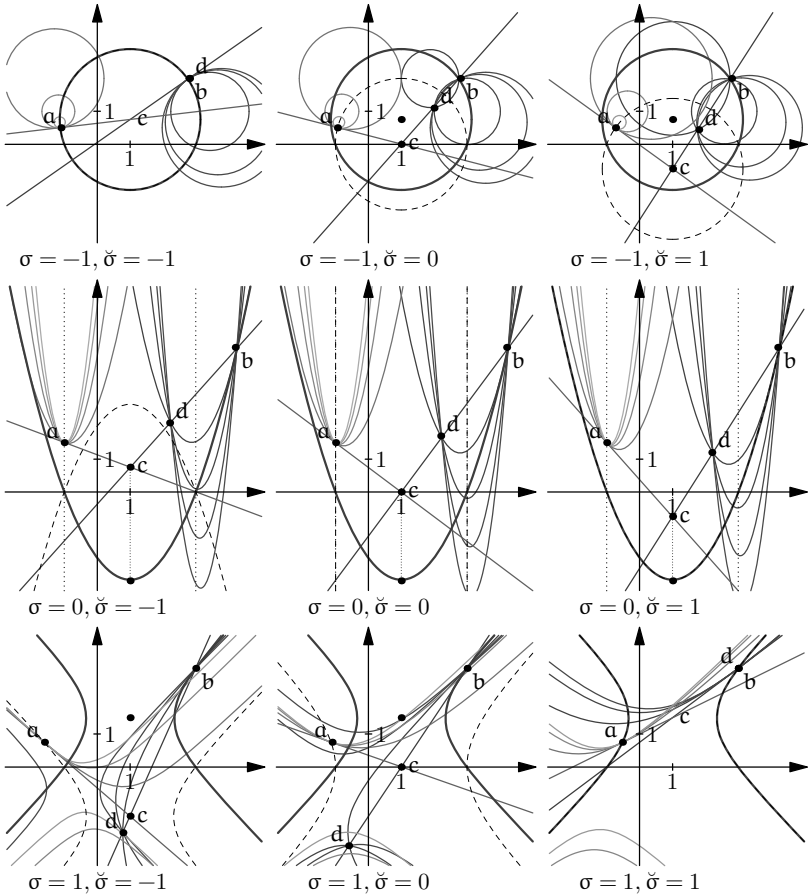


Figure 6.3 Three types of orthogonality in the three types of the point space.

Each picture presents two groups (green and blue) of cycles which are orthogonal to the red cycle C_σ^s . Point b belongs to C_σ^s and the family of blue cycles passing through b also intersects at the point d , which is the inverse of b in C_σ^s . Any orthogonality is reduced to the usual orthogonality with a new ('ghost') cycle (shown by the dashed line), which may or may not coincide with C_σ^s . For any point a on the 'ghost' cycle, the orthogonality is reduced to the semi-local notion in the terms of tangent lines at the intersection point. Consequently, such a point a is always the inverse of itself.

Elliptic realisations (in the point space) of Definition 6.1, i.e. $\sigma = -1$, were shown in Fig. 1.7 and form the first row in Fig. 6.3. The left picture in this row corresponds to the elliptic cycle space, e.g. $\tilde{\sigma} = -1$. The orthogonality between the red circle and any circle from the blue or green families is given in the usual Euclidean sense described in Exercise 6.3(e,h). In other words, we can decide on the orthogonality of circles by observing the angles between their tangents at the arbitrary small neighbourhood of the intersection point. Therefore, all circles from either the green or blue families, which are orthogonal to the red circle, have common tangents at points a and b respectively.

The central (parabolic in the cycle space) and the right (hyperbolic) pictures show the non-local nature of orthogonality if $\sigma \neq \tilde{\sigma}$. The blue family has the intersection point b with the red circle, and tangents to blue circles at b are different. However, we may observe that all of them pass the second point d . This property will be used in Section 6.5 to define the inversion in a cycle. A further investigation of Fig. 6.3 reveals that circles from the green family have a common tangent at point a , however this point does not belong to the red circle. Moreover, in line with the geometric interpretation from Exercise 6.3(C), the common tangent to the green family at a passes the p-centre (on the central parabolic drawing) or h-centre (on the right hyperbolic drawing).

There are analogous pictures in parabolic and hyperbolic point spaces as well and they are presented in the second and third rows of Fig. 6.3. The behaviour of green and blue families of cycles at point a , b and d is similar up to the obvious modification: the EPH case of the point space coincides with EPH case of the cycle spaces in the central drawing of the second row and the right drawing of the third row.

Therefore, we will clarify the nature of orthogonality if the locus of such points a with tangents passing the other cycle's $\tilde{\sigma}$ -centre are described. We are going to demonstrate that this locus is a cycle, which we shall call a 'ghost'. The ghost cycle is shown by the dashed lines in Fig. 6.3. To give an analytic description, we need the Heaviside function $\chi(\sigma)$:

$$\chi(t) = \begin{cases} 1, & t \geq 0; \\ -1, & t < 0. \end{cases} \quad (6.8)$$

More specifically, we note the relations $\chi(\sigma) = \sigma$ if $\sigma = \pm 1$ and $\chi(\sigma) = 1$ if $\sigma = 0$. Thus, the Heaviside function will be used to avoid the degeneracy of the parabolic case.


Definition 6.17. For a cycle $C_{\check{\sigma}}$ in the σ -implementation, we define the associated $(\check{\sigma})$ -ghost cycle $\check{C}_{\check{\sigma}}$ by the following two conditions:

- i. The $\chi(\sigma)$ -centre of $\check{C}_{\check{\sigma}}$ coincides with the $\check{\sigma}$ -centre of $C_{\check{\sigma}}$.
- ii. The determinant of $\check{C}_{\check{\sigma}}^1$ is equal to the determinant of $C_{\check{\sigma}}^{\check{\sigma}}$.

Exercise 6.18. Verify the following properties of a ghost cycle: 

- i. $\check{C}_{\check{\sigma}}$ coincides with C_{σ} if $\sigma\check{\sigma} = 1$.
- ii. $\check{C}_{\check{\sigma}}$ has common roots (real or imaginary) with C_{σ} .
- iii. For a cycle $C_{\check{\sigma}}$, its p-ghost cycle $\check{C}_{\check{\sigma}}$ and the non-selfadjoint part $HC_{\check{\sigma}}$ (6.7) coincide.
- iv. All straight lines $\check{\sigma}$ -orthogonal to a cycle pass its $\check{\sigma}$ -centre.

The significance of the ghost cycle is that the $\check{\sigma}$ -orthogonality between two cycles in \mathbb{A} is reduced to σ -orthogonality to the ghost cycle.

Proposition 6.19. Let cycles $C_{\check{\sigma}}$ and $\check{C}_{\check{\sigma}}$ be $\check{\sigma}$ -orthogonal in \mathbb{A} and let $\check{C}_{\check{\sigma}}$ be the ghost cycle of $C_{\check{\sigma}}$. Then: 

- i. $\check{C}_{\check{\sigma}}$ and $\check{C}_{\check{\sigma}}$ are σ -orthogonal in \mathbb{A} for seven cases except two cases $\sigma = 0$ and $\check{\sigma} = \pm 1$.
- ii. In the σ -implementation, the tangent line to $\check{C}_{\check{\sigma}}$ at its intersection point with
 - (a) the ghost cycle \check{C}_{σ} , if $\sigma = \pm 1$, or
 - (b) the non-selfadjoint part $HC_{\check{\sigma}}$ (6.7) of the cycle $C_{\check{\sigma}}$, if $\sigma = 0$,
 passes the $\check{\sigma}$ -centre of $C_{\check{\sigma}}$, which coincides with the σ -centre of \check{C}_{σ} .

Proof. The statement 6.19.i can be shown by algebraic manipulation, possibly in CAS. Then, the non-parabolic case 6.19.ii(a) follows from the first part 6.19.i, which reduces non-matching orthogonality to a matching one with the ghost cycle, and the geometric description of matching orthogonality from Exercise 6.3. Therefore, we only need to provide a new calculation for the parabolic case 6.19.ii(b). Note that, in the case $\sigma = \check{\sigma} = 0$, there is no disagreement between the first and second parts of the proposition since $HC_{\check{\sigma}} = \check{C}_{\check{\sigma}}$ due to 6.18.iii. □

Consideration of ghost cycles does present orthogonality in geometric term, but it hides the symmetry of this relation. Indeed, it is not obvious that $\check{C}_{\check{\sigma}}^s$ relates to the ghost of $C_{\check{\sigma}}^s$ in the same way as $C_{\check{\sigma}}^s$ relates to the ghost of $\check{C}_{\check{\sigma}}^s$.

Remark 6.20. Elliptic and hyperbolic ghost cycles are symmetric in the real line and the parabolic ghost cycle has its centre on it—see Fig. 6.3. This is an illustration of the boundary effect from Remarks 5.3.

Finally, we note that Proposition 6.19 expresses $\check{\sigma}$ -orthogonality through the $\check{\sigma}$ -centre of cycles. It illustrates the meaningfulness of various centres within our approach which may not be so obvious at the beginning.

6.4 Actions of FSCc Matrices

Definition 4.11 associates a 2×2 -matrix to any cycle. These matrices can be treated analogously to elements of $\mathrm{SL}_2(\mathbb{R})$ in many respects. Similar to the $\mathrm{SL}_2(\mathbb{R})$ action (3.24), we can consider a fraction-linear transformation on the point space \mathbb{A} defined by a cycle and its FSCc matrix

$$C_\sigma^s : w \mapsto C_\sigma^s(w) = \frac{(l + \iota sn)\bar{w} - m}{k\bar{w} + (-l + \iota sn)}, \quad (6.9)$$

where C_σ^s is, as usual (4.5),

$$C_\sigma^s = \begin{pmatrix} l + \iota sn & -m \\ k & -l + \iota sn \end{pmatrix} \quad \text{and} \quad w = u + \iota v, \quad \sigma = \iota^2.$$

Exercise 6.21. Check that $w = u + \iota v \in \mathbb{A}$ is a fixed point of the map $C_\sigma^{-\sigma}$ (6.9) if and only if the σ -implementation of $C_\sigma^{-\sigma}$ passes w . If $\det \tilde{C}_\sigma^s \neq 0$ then the second iteration of the map is the identity.

We can also extend the conjugated action (4.7) on the cycle space from $\mathrm{SL}_2(\mathbb{R})$ to cycles. Indeed, a cycle \tilde{C}_σ^s in the matrix form acts on another cycle C_σ^s by the $\check{\sigma}$ -similarity

$$\tilde{C}_\sigma^{s_1} : C_\sigma^s \mapsto -\tilde{C}_\sigma^{s_1} \overline{C_\sigma^s} \tilde{C}_\sigma^{s_1}. \quad (6.10)$$

The similarity can be considered as a transformation of the cycle space \mathbb{P}^3 to itself due to the following result.

Exercise 6.22. Check that:

- i. The cycle $\check{\sigma}$ -similarity (6.10) with a cycle \tilde{C}_σ^s , where $\det \tilde{C}_\sigma^s \neq 0$, preserves the structure of FSCc matrices and $\tilde{C}_\sigma^{s_1}$ is its fixed point. In a non-singular case, $\det \tilde{C}_\sigma^s \neq 0$, the second iteration of similarity is the identity map.



- ii. The $\check{\sigma}$ -similarity with a $\check{\sigma}$ -zero-radius cycle $Z_{\check{\sigma}}^s$ always produces this cycle.
- iii. The $\check{\sigma}$ -similarity with a cycle (k, l, n, m) is a linear transformation of the cycle space \mathbb{R}^4 with the matrix


$$\begin{pmatrix} km - \det C_{\check{\sigma}} & -2kl & 2\check{\sigma}kn & k^2 \\ lm & -2l^2 - \det C_{\check{\sigma}} & 2\check{\sigma}ln & kl \\ nm & -2nl & 2\check{\sigma}n^2 - \det C_{\check{\sigma}} & kn \\ m^2 & -2ml & 2\check{\sigma}mn & km - \det C_{\check{\sigma}} \end{pmatrix} \\ = \begin{pmatrix} k \\ l \\ n \\ m \end{pmatrix} \cdot \begin{pmatrix} m & -2l & 2\check{\sigma}n & k \end{pmatrix} - \det(C_{\check{\sigma}}) \cdot I_{4 \times 4}.$$

Note the apparent regularity of its entries.

Remark 6.23. Here is another example where usage of complex (dual or double) numbers is different from Clifford algebras. In order to use commutative hypercomplex numbers, we require the complex conjugation for the cycle product (5.3), linear-fractional transformation (6.9) and cycle similarity (6.10). Non-commutativity of Clifford algebras allows us to avoid complex conjugation in all these formulae – see Appendix A.5. For example, the reflection in the real line (complex conjugation) is given by matrix similarity with the corresponding matrix $\begin{pmatrix} e_1 & 0 \\ 0 & -e_1 \end{pmatrix}$.

A comparison of Exercises 6.21 and 6.22 suggests that there is a connection between two actions (6.9) and (6.10) of cycles, which is similar to the relation $\mathrm{SL}_2(\mathbb{R})$ actions on points and cycles from Lemma 5.20.

Exercise 6.24. Letting $\det \tilde{C}_{\check{\sigma}}^s \neq 0$, show that:

- i. The $\check{\sigma}$ -similarity (6.10) $\check{\sigma}$ -preserves the orthogonality relation (6.1). 
- More specifically, if $\dot{C}_{\check{\sigma}}^s$ and $\ddot{C}_{\check{\sigma}}^s$ are matrix similarity (6.10) of cycles $C_{\check{\sigma}}^s$ and $\hat{C}_{\check{\sigma}}^s$, respectively, with the cycle $\tilde{C}_{\check{\sigma}}^{s_1}$, then

$$\langle \dot{C}_{\check{\sigma}}^s, \ddot{C}_{\check{\sigma}}^s \rangle = \langle C_{\check{\sigma}}^s, \hat{C}_{\check{\sigma}}^s \rangle (\det \tilde{C}_{\check{\sigma}}^s)^2.$$

HINT: Note that $\tilde{C}_{\check{\sigma}}^s \overline{\tilde{C}_{\check{\sigma}}^s} = -\det(\tilde{C}_{\check{\sigma}}^s)I$, where I is the identity matrix. This is a particular case of the *Vahlen condition*, see [27, Prop. 2]. Thus, we have

$$\dot{C}_{\check{\sigma}}^s \overline{\ddot{C}_{\check{\sigma}}^s} = -\tilde{C}_{\check{\sigma}}^{s_1} C_{\check{\sigma}}^s \overline{\hat{C}_{\check{\sigma}}^s \tilde{C}_{\check{\sigma}}^{s_1}} \cdot \det \tilde{C}_{\check{\sigma}}^s.$$

The final step uses the invariance of the trace under the matrix similarity. A CAS calculation is also provided. \diamond

- ii. The image $\tilde{Z}_\sigma^s = C_\sigma^{s_2} \overline{Z_\sigma^{s_1}} C_\sigma^{s_2}$ of a σ -zero-radius cycle $\tilde{Z}_\sigma^{s_1}$ under the similarity (6.10) is a σ -zero-radius cycle $\tilde{Z}_\sigma^{s_1}$. The $(s_1 s_2)$ -centre of \tilde{Z}_σ^s is the linear-fractional transformation (6.9) of the (s_2/s_1) -centre of Z_σ^s .
- iii. Both formulae (6.9) and (6.10) define the same transformation of the point space \mathbb{A} , with $\sigma = \tilde{\sigma} \neq 0$. Consequently, the linear-fractional transformation (6.9) maps cycles to cycles in these cases.

HINT: This part follows from the first two items and Proposition 6.8. \diamond

- iv. There is a cycle C_σ^s such that neither map of the parabolic point space \mathbb{D} represents similarity with C_σ^s .

HINT: Consider $\tilde{C}_\sigma^s = (1, 0, \frac{1}{2}, -1)$ and a cycle C_σ^s passing point (u, v) . Then the similarity of C_σ^s with \tilde{C}_σ^s passes the point $T(u, v) = (\frac{1+v}{u}, \frac{v+v^2}{u^2})$ if and only if either

- C_σ^s is a straight line, or
- (u, v) belongs to \tilde{C}_σ^s and is fixed by the above map T .

That is, the map T of the point space \mathbb{D} serves flat cycles and \tilde{C}_σ^s but no others. Thus, there is no map of the point space which is compatible with the cycle similarity for an arbitrary cycle. \diamond

Several demonstrations of inversion are provided in Fig. 6.4. The initial setup is shown in Fig. 6.4(a)—the red unit circle and the grid of horizontal (green) and vertical (blue) straight lines. It is very convenient in this case that the grid is formed by two orthogonal pencils of cycles, which can be considered to be of any EPH type. Figure 6.4(b) shows e-inversion of the grid in the unit circle, which is, of course, the locus of fixed points. Straight lines of the rectangular grid are transformed to circles, but orthogonality between them is preserved—see Exercise 6.24.i.

Similarly, Fig. 6.4(c) presents the result of p-inversion in the degenerated parabolic cycle $u^2 - 1 = 0$. This time the grid is mapped to two orthogonal pencils of parabolas and vertical lines. Incidentally, due to the known optical illusion, we perceive these vertical straight lines as being bent.

Finally, Fig. 6.4(d) demonstrates h-inversion in the unit hyperbola $u^2 - v^2 - 1 = 0$. We again obtained two pencils of orthogonal hyperbolas. The bold blue cycles—the dot at the origin in (b), parabola in (c) and two lines (the light cone) in (d)—will be explained in Section 8.1. Further details are provided by the following exercise.

Exercise 6.25. Check that the rectangular grid in Fig. 6.4(a) is produced by horizontal and vertical lines given by quadruples $(0, 0, 1, m)$ and $(0, 1, 0, m)$, respectively.

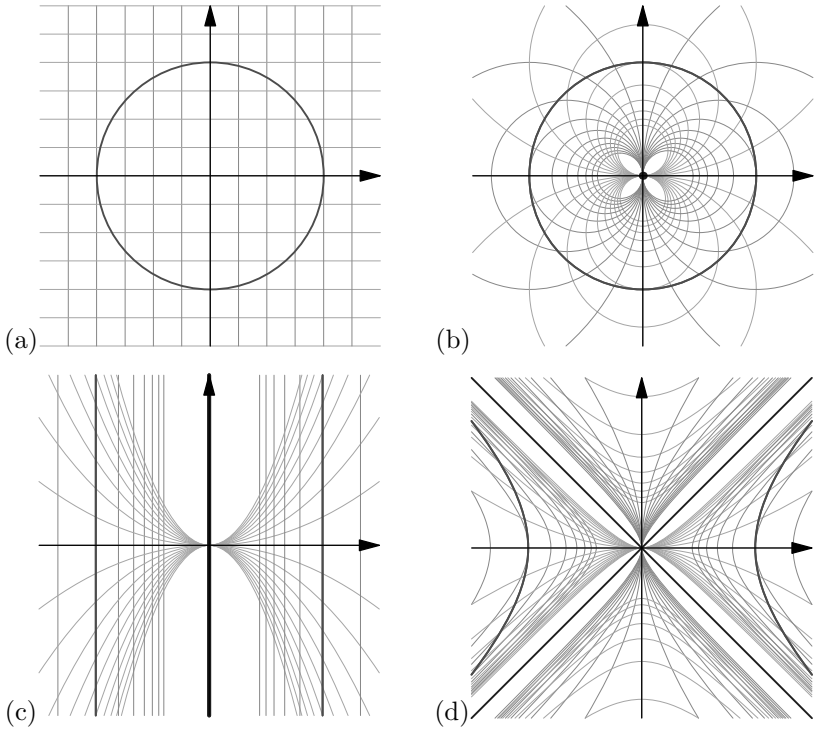


Figure 6.4 Three types of inversions of the rectangular grid. The initial rectangular grid (a) is inverted elliptically in the unit circle (shown in red) in (b), parabolically in (c) and hyperbolically in (d). The blue cycle (collapsed to a point at the origin in (b)) represent the image of the cycle at infinity under inversion.

The similarity with the cycle $(1, 0, 0, -1)$ sends a cycle (k, l, n, m) to (m, l, n, k) . In particular, the image of the grid are cycles $(m, 0, 1, 0)$ and $(m, 1, 0, 0)$.

We conclude this section by an observation that cycle similarity is similar to a mirror reflection, which preserves the directions of vectors parallel to the mirror and reverses vectors which are orthogonal.

Exercise 6.26. Let $\det \tilde{C}_\sigma^s \neq 0$. Then, for similarity (6.10) with \tilde{C}_σ^s :

i. Verify the identities

$$\begin{aligned} -\tilde{C}_\sigma^{s_1} \overline{\tilde{C}_\sigma^s} \tilde{C}_\sigma^{s_1} &= \det_{\tilde{\sigma}}(\tilde{C}_\sigma^{s_1}) \cdot \tilde{C}_\sigma^{s_1} \quad \text{and} \\ -\tilde{C}_\sigma \overline{\tilde{C}_\sigma^s} \tilde{C}_\sigma &= -\det_{\tilde{\sigma}}(\tilde{C}_\sigma) \cdot C_\sigma, \end{aligned}$$



where C_σ^s is a cycle $\check{\sigma}$ -orthogonal to \tilde{C}_σ^s . Note the difference in the signs in the right-hand sides of both identities.

- ii. Describe all cycles which are fixed (as points in the projective space \mathbb{P}^3) by the similarity with the given cycle \tilde{C}_σ^s .

HINT: Use a decomposition of a generic cycle into a sum \tilde{C}_σ^s and a cycle orthogonal to \tilde{C}_σ^s similar to (6.7). \diamond

As we will see in the next section, these orthogonal reflections in the cycle space correspond to ‘bent’ reflections in the point space.

6.5 Inversions and Reflections in Cycles

The maps in point and cycle spaces considered in the previous section were introduced from the action of FSCc matrices of cycles. They can also be approached from the more geometrical viewpoint. There are at least two natural ways to define an inversion in a cycle:

- One possibility uses orthogonality from Section 6.1. As we can observe from Fig. 6.3, all cycles from the blue family passing the point b also meet again at the point d . This defines a correspondence $b \leftrightarrow d$ on the point space.
- Another option defines ‘reflections in cycles’. The mirror reflection $z \rightarrow \bar{z}$ in the horizontal axis is a fundamental operation. If we transform a generic cycle to the real line, then we can extend the notion of reflection to the cycle.

We can formalise the above observations as follows.

Definition 6.27. For a given cycle C_σ^s , we define two maps of the point space \mathbb{A} associated to it:

- A $\check{\sigma}$ -inversion in a σ -cycle C_σ^s sends a point $b \in \mathbb{A}$ to the second point d of the intersection of all σ -cycles $\check{\sigma}$ -orthogonal to C_σ^s and passing through b – see Fig. 6.3.
- A $\check{\sigma}$ -reflection in a σ -cycle C_σ^s is given by $M^{-1}RM$, where M is a $\check{\sigma}$ -similarity (6.10) which sends the σ -cycle C_σ^s into the horizontal axis and R is the mirror reflection of \mathbb{A} in that axis.

We are going to see that inversions are given by (6.9) and reflections are expressed through (6.10), thus they are essentially the same for EH cases in light of Exercise 6.24.i. However, some facts are easier to establish using

the inversion and others in terms of reflection. Thus, it is advantageous to keep both notions. Since we have three different EPH orthogonalities between cycles for every type of point space, there are also three different inversions in each of them.

Exercise 6.28. Prove the following properties of inversion:



- i. Let a cycle \tilde{C}_σ^s be $\check{\sigma}$ -orthogonal to a cycle $C_\sigma^s = (k, l, n, m)$. Then, for any point $u_1 + \iota v_1 \in \mathbb{A}$ ($\iota^2 = \sigma$) belonging to σ -implementation of \tilde{C}_σ^s , this implementation also passes through the image of $u_1 + \iota v_1$ under the Möbius transform (6.9) defined by the matrix $C_\sigma^{\check{\sigma}}$:

$$u_2 + \iota v_2 = C_\sigma^{\check{\sigma}}(u_1 - \iota v_1) = \begin{pmatrix} l + \iota \check{\sigma} n & -m \\ k & -l + \iota \check{\sigma} n \end{pmatrix} (u_1 - \iota v_1). \quad (6.11)$$

Thus, the point $u_2 + \iota v_2$ is the *inversion* of $u_1 + \iota v_1$ in C_σ^s .

- ii. Conversely, if a cycle \tilde{C}_σ^s passes two different points $u_1 + \iota v_1$ and $u_2 + \iota v_2$ related through (6.11), then \tilde{C}_σ^s is $\check{\sigma}$ -orthogonal to C_σ^s .
- iii. If a cycle \tilde{C}_σ^s is $\check{\sigma}$ -orthogonal to a cycle C_σ^s , then the $\check{\sigma}$ -inversion in C_σ^s sends \tilde{C}_σ^s to itself.
- iv. $\check{\sigma}$ -inversion in the σ -implementation of a cycle C_σ^s coincides with σ -inversion in its $\check{\sigma}$ -ghost cycle \tilde{C}_σ^s .

Note the interplay between parameters σ and $\check{\sigma}$ in the above statement 6.28.i. Although we are speaking about $\check{\sigma}$ -orthogonality, we take the Möbius transformation (6.11) with the imaginary unit ι such that $\iota^2 = \sigma$ (as the signature of the point space). On the other hand, the value $\check{\sigma}$ is used there as the s -parameter for the cycle $C_\sigma^{\check{\sigma}}$.

Proposition 6.29. *The reflection 6.27.ii of a zero-radius cycle Z_σ^s in a cycle C_σ^s is given by the similarity $C_\sigma^s \overline{Z_\sigma^s} C_\sigma^s$.*

Proof. Let a cycle \tilde{C}_σ^s have the property $\tilde{C}_\sigma^s \overline{C_\sigma^s} \tilde{C}_\sigma^s = R_\sigma^s$, where R_σ^s is the cycle representing the real line. Then, $\tilde{C}_\sigma^s R_\sigma^s \tilde{C}_\sigma^s = C_\sigma^s$, since $\tilde{C}_\sigma^s \tilde{C}_\sigma^s = \tilde{C}_\sigma^s \overline{C_\sigma^s} = -\det \tilde{C}_\sigma^s I$. The mirror reflection in the real line is given by the similarity with R_σ^s , therefore the transformation described in 6.27.ii is a similarity with the cycle $\tilde{C}_\sigma^s R_\sigma^s \tilde{C}_\sigma^s = C_\sigma^s$ and, thus, coincides with (6.11). \square

Corollary 6.30. *The $\check{\sigma}$ -inversion with a cycle C_σ^s in the point space \mathbb{A} coincides with $\check{\sigma}$ -reflection in C_σ^s .*

The auxiliary cycle \tilde{C}_σ^s from the above proof of Prop. 6.29 is of separate interest and can be characterised in the elliptic and hyperbolic cases as follows.

Exercise 6.31. Let $C_\sigma^s = (k, l, n, m)$ be a cycle such that $\check{\sigma} \det C_\sigma^s > 0$ for $\check{\sigma} \neq 0$. Let us define the cycle \tilde{C}_σ^s by the quadruple $(k, l, n \pm \sqrt{\check{\sigma} \det C_\sigma^s}, m)$. Then:

- i. $\tilde{C}_\sigma^s C_\sigma^s \tilde{C}_\sigma^s = \mathbb{R}$ and $\tilde{C}_\sigma^s \mathbb{R} \tilde{C}_\sigma^s = C_\sigma^s$.
- ii. \tilde{C}_σ^s and C_σ^s have common roots.
- iii. In the $\check{\sigma}$ -implementation, the cycle C_σ^s passes the centre of \tilde{C}_σ^s .

HINT: One can directly observe 6.31.ii for real roots, since they are fixed points of the inversion. Also, the transformation of C_σ^s to a flat cycle implies that C_σ^s passes the centre of inversion, hence 6.31.iii. There is also a CAS calculation for this. \diamond

Inversions are helpful for transforming pencils of cycles to the simplest possible form.

Exercise 6.32. Check the following:

- i. Let the σ -implementation of a cycle C_σ^s pass the σ -centre of a cycle \tilde{C}_σ^s . Then, the σ -reflection of C_σ^s in \tilde{C}_σ^s is a straight line.
- ii. Let two cycles C_σ^s and \tilde{C}_σ^s intersect in two points $P, P' \in \mathbb{A}$ such that $P - P'$ is not a divisor of zero in the respective number system. Then, there is an inversion which maps the pencil of cycles orthogonal to C_σ^s and \tilde{C}_σ^s (see Exercise 6.10.ii) into a pencil of concentric cycles.

HINT: Make an inversion into a cycle with σ -centre P , then C_σ^s and \tilde{C}_σ^s will be transformed into straight lines due to the previous item. These straight lines will intersect in a finite point P' which is the image of P under the inversion. The pencil orthogonal to C_σ^s and \tilde{C}_σ^s will be transformed to a pencil orthogonal to these two straight lines. A CAS calculations shows that all cycles from the pencil have σ -centre at P' . \diamond


A classical source of the above result in inversive geometry [23, Thm. 5.71] tells that an inversion can convert any pair of non-intersecting circles to concentric ones. This is due to the fact that an orthogonal pencil to the pencil generated by two non-intersecting circles always passes two special points – see Exercise 6.10.iii for further development.

Finally, we compare our consideration for the parabolic point space with Yaglom's book. The Möbius transformation (6.9) and the respective

inversion illustrated by Fig. 6.4(c) essentially coincide with the *inversion of the first kind* from [108, Sec. 10]. Yaglom also introduces the *inversion of the second kind*, see [108, Sec. 10]. For a parabola $v = k(u - l)^2 + m$, he defined the map of the parabolic point space to be

$$(u, v) \mapsto (u, 2(k(u - l)^2 + m) - v), \quad (6.12)$$

i.e. the parabola bisects the vertical line joining a point and its image. There are also other geometric characterisations of this map in [108], which make it very similar to the Euclidean inversion in a circle. Here is the resulting expression of this transformation through the usual inversion in parabolas:

Exercise 6.33. The inversion of the second kind (6.12) is a composition of three Möbius transformations (6.9) defined by cycles $(1, l, 2m, l^2 + m/k)$, $(1, l, 0, l^2 + m/k)$ and the real line in the parabolic point space \mathbb{D} . 

Möbius transformations (6.9) and similarity (6.12) with FSCc matrices map cycles to cycles just like matrices from $\text{SL}_2(\mathbb{R})$ do. It is natural to ask for a general type of matrices sharing this property. For this, see works [22, 27, 94] which deal with more general elliptic and hyperbolic (but not parabolic) cases. It is beyond the scope of our consideration since it derails from the geometry of upper half-plane. We only mention the rôle of the Vahlen condition, $C_\sigma^s \overline{C_\sigma^s} = -\det(C_\sigma^s)I$, used in Exercise 6.24.i.

6.6 Higher-order Joint Invariants: Focal Orthogonality

Considering Möbius action (1.1), there is no need to be restricted to joint invariants of two cycles only. Indeed, for any polynomial $p(x_1, x_2, \dots, x_n)$ of several non-commuting variables, one may define an invariant joint disposition of n cycles ${}^j C_\sigma^s$ by the condition

$$\text{tr } p({}^1 C_\sigma^s, {}^2 C_\sigma^s, \dots, {}^n C_\sigma^s) = 0, \quad (6.13)$$

where the polynomial of FSCc matrices is defined through standard matrix algebra. To create a Möbius invariant which is not affected by the projectivity in the cycle space we can either

- use a polynomial p which is homogeneous in every variable x_i , or
- substitute variables x_i with the cycles' det-normalised FSCc matrices.

Let us construct some lower-order realisations of (6.13). In order to be essentially different from the previously considered orthogonality, such

invariants may either contain non-linear powers of the same cycle, or accommodate more than two cycles. In this respect, consideration of higher-order invariants is similar to a transition from Riemannian to Finsler geometry [20, 29]. The latter is based on the replacement of the quadratic line element $g^{ij} dx_i dx_j$ in the tangent space by a more complicated function.

A further observation is that we can simultaneously study several invariants of various orders and link one to another by some operations. There are some standard procedures changing orders of invariants working in both directions:

- i. Higher-order invariants can be built on top of those already defined;
- ii. Lower-order invariants can be derived from higher ones.

Consider both operations as an example. We already know that a similarity of a cycle with another cycle produces a new cycle. The cycle product of the latter with a third cycle creates a joint invariant of these three cycles

$$\langle {}^1C_\sigma^s {}^2C_\sigma^s {}^1C_\sigma^s, {}^3C_\sigma^s \rangle, \quad (6.14)$$

which is built from the second-order invariant $\langle \cdot, \cdot \rangle$. Now we can reduce the order of this invariant by fixing ${}^3C_\sigma^s$ to be the real line, since it is $\text{SL}_2(\mathbb{R})$ -invariant. This invariant deserves special consideration. Its geometrical meaning is connected to the matrix similarity of cycles (6.10) (inversion in cycles) and orthogonality.

Definition 6.34. A cycle \tilde{C}_σ^s is $\tilde{\sigma}$ -focal orthogonal (or $f_{\tilde{\sigma}}$ -orthogonal) to a cycle C_σ^s if the $\tilde{\sigma}$ -reflection of C_σ^s in \tilde{C}_σ^s is $\tilde{\sigma}$ -orthogonal (in the sense of Definition 6.1) to the real line. We denote it by $\tilde{C}_\sigma^s \dashv C_\sigma^s$.

Remark 6.35. This definition is explicitly based on the invariance of the real line and is an illustration to the boundary value effect from Remark 5.3.

Exercise 6.36. f-orthogonality is equivalent to either of the following

- i. The cycle $\tilde{C}_\sigma^s \overline{C_\sigma^s} \tilde{C}_\sigma^s$ is a *selfadjoint cycle*, see Definition 6.12.
- ii. Analytical condition:

$$\langle \tilde{C}_\sigma^s \overline{C_\sigma^s} \tilde{C}_\sigma^s, R_\sigma^s \rangle = \text{tr}(\tilde{C}_\sigma^s \overline{C_\sigma^s} \tilde{C}_\sigma^s R_\sigma^s) = 0. \quad (6.15)$$

Remark 6.37. It is easy to observe the following:

- i. f-orthogonality is not symmetric: $C_\sigma^s \dashv \tilde{C}_\sigma^s$ does not imply $\tilde{C}_\sigma^s \dashv C_\sigma^s$.
- ii. Since the horizontal axis R_σ^s and orthogonality (6.1) are $\text{SL}_2(\mathbb{R})$ -invariant objects, f-orthogonality is also $\text{SL}_2(\mathbb{R})$ -invariant.

However, an invariance of f-orthogonality under inversion of cycles required some study since, in general, the real line is not invariant under such transformations.

Exercise 6.38. The image $\hat{C}_\sigma^{s_1} R_\sigma^s \hat{C}_\sigma^{s_1}$ of the real line under inversion in $\hat{C}_\sigma^{s_1} = (k, l, n, m)$ with $s \neq 0$ is the cycle

$$(2ss_1\check{\sigma}kn, 2ss_1\check{\sigma}ln, -\det(C_\sigma^{s_1}), 2ss_1\check{\sigma}mn).$$

It is the real line again if $\det(C_\sigma^{s_1}) \neq 0$ and either

- i. $s_1n = 0$, in which case it is a composition of $\mathrm{SL}_2(\mathbb{R})$ -action by $\begin{pmatrix} l & -m \\ k & -l \end{pmatrix}$ and the reflection in the real line, or
- ii. $\check{\sigma} = 0$, i.e. the parabolic case of the cycle space.

If either of two conditions is satisfied then f-orthogonality $\tilde{C}_\sigma^s \dashv C_\sigma^s$ is preserved by the $\check{\sigma}$ -similarity with $\hat{C}_\sigma^{s_1}$.

The following explicit expressions of f-orthogonality reveal further connections with cycles' invariants.

Exercise 6.39. f-orthogonality of \tilde{C}_σ^s to C_σ^s is given by either of the equivalent identities

$$\begin{aligned} sn(\tilde{l}^2 + \check{\sigma}s_1^2\tilde{n}^2 - \tilde{m}\tilde{k}) + s_1\tilde{n}(m\tilde{k} - 2\tilde{l}l + k\tilde{m}) &= 0 \quad \text{or} \\ n\det(\tilde{C}_\sigma^1) + \tilde{n}\langle C_\sigma^1, \tilde{C}_\sigma^1 \rangle &= 0, \quad \text{if } s = s_1 = 1. \end{aligned}$$

The f-orthogonality may again be related to the usual orthogonality through an appropriately chosen *f-ghost cycle*, cf. Proposition 6.19:

Proposition 6.40. Let C_σ^s be a cycle. Then, its f-ghost cycle $\check{C}_\sigma^{\check{\sigma}} = C_\sigma^{\chi(\sigma)} \mathbb{R}_\sigma^{\check{\sigma}} C_\sigma^{\chi(\sigma)}$ is the reflection of the real line in $C_\sigma^{\chi(\sigma)}$, where $\chi(\sigma)$ is the Heaviside function (6.8). Then:

- i. Cycles C_σ^1 and $\check{C}_\sigma^{\check{\sigma}}$ have the same roots.
- ii. The $\chi(\sigma)$ -centre of $\check{C}_\sigma^{\check{\sigma}}$ coincides with the $(-\check{\sigma})$ -focus of C_σ^s , consequently all straight lines $\check{\sigma}$ -f-orthogonal to C_σ^s pass its $(-\check{\sigma})$ -focus.
- iii. f-inversion in C_σ^s defined from f-orthogonality (see Definition 6.27.i) coincides with the usual inversion in $\check{C}_\sigma^{\check{\sigma}}$.

Note the above intriguing interplay between the cycle's centres and foci. It also explains our choice of name for focal orthogonality, cf. Definition 6.17.i. f-Orthogonality and the respective f-ghost cycles are presented in Fig. 6.5, which uses the same outline and legend as Fig. 6.3.

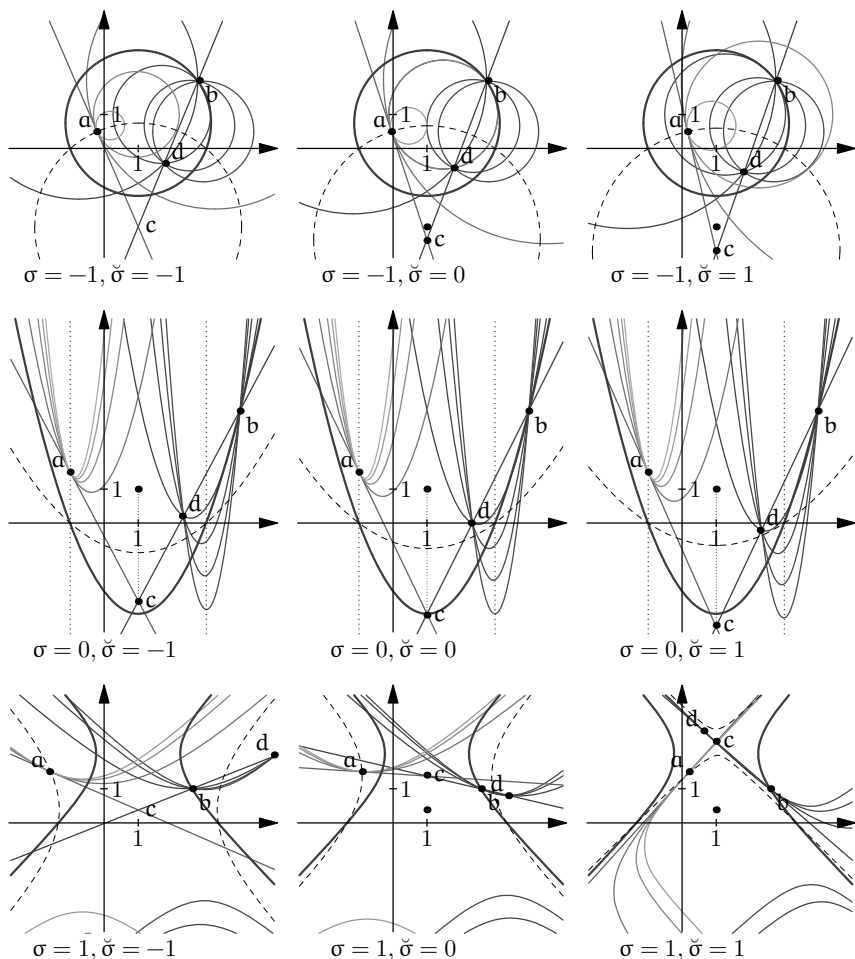


Figure 6.5 Focal orthogonality of cycles. In order to highlight both the similarities and distinctions with the ordinary orthogonality, we use the same notations as in Fig. 6.3.

The definition of f-orthogonality may look rather extravagant at first glance. However, it will find new support when we again consider lengths and distances in the next chapter. It will also be useful for infinitesimal cycles, cf. Section 7.5.

Of course, it is possible and meaningful to define other interesting higher-order joint invariants of two or even more cycles.

Chapter 7

Metric Invariants in Upper Half-Planes

So far, we have discussed only invariants like orthogonality, which are related to angles. However, *geometry*, in the plain meaning of the word, deals with measurements of *distances* and *lengths*. We will derive metrical quantities from cycles in a way which shall be Möbius-invariant.

7.1 Distances

Cycles are covariant objects performing as ‘circles’ in our three EPH geometries. Now we play *the traditional mathematical game*: turn some properties of classical objects into definitions of new ones.

Definition 7.1. The $\check{\sigma}$ -radius $r_{\check{\sigma}}$ of a cycle $C_{\check{\sigma}}^s$, if squared, is equal to the minus $\check{\sigma}$ -determinant of the cycle’s k -normalised (see Definition 5.5) matrix, i.e.

$$r_{\check{\sigma}}^2 = -\frac{\langle C_{\check{\sigma}}^s, C_{\check{\sigma}}^s \rangle}{2k^2} = -\frac{\det C_{\check{\sigma}}^s}{k^2} = \frac{l^2 - \check{\sigma}s^2n^2 - km}{k^2}. \quad (7.1)$$

As usual, the $\check{\sigma}$ -diameter of a cycle is two times its radius.

The expression (7.1) for radius through the invariant cycle product resembles the definition of the norm of a vector in an inner product space [55, Sec. 5.1].

Exercise 7.2. Check the following geometrical content of the formula (7.1):

- (e,h) The value of (7.1) is the usual radius of a circle or hyperbola given by the equation $k(u^2 - \sigma v^2) - 2lu - 2nv + m = 0$.
- (p) The diameter of a parabola is the (Euclidean) distance between its (real) roots, i.e. solutions of $ku^2 - 2lu + m = 0$, or roots of its ‘adjoint’ parabola $-ku^2 + 2lu + m - \frac{2l^2}{k} = 0$ (see Fig. 1.9(a)).

Exercise 7.3. Check the following relations:



- i. The $\check{\sigma}$ -radius of a cycle $C_{\check{\sigma}}^s$ is equal to $1/k$, where k is the $(2, 1)$ -entry of the \det -normalised FSCc matrix (see Definition 5.5) of the cycle.
- ii. Let $u_{\check{\sigma}}$ be the second coordinate of a cycle's $\check{\sigma}$ -focus and f be its focal length. Then, the square of the cycle's $\check{\sigma}$ -radius is

$$r_{\check{\sigma}}^2 = -4fu_{\check{\sigma}}.$$

- iii. Cycles (5.8) have zero $\check{\sigma}$ -radius, thus Definitions 5.13 and 7.1 agree.

An intuitive notion of a distance in both mathematics and everyday life is usually of a variational nature. We naturally perceive a straight line as the route of the shortest distance between two points. Then, we can define the distance along a curved path through an approximation. This variational nature is also echoed in the following definition:

Definition 7.4. The $(\sigma, \check{\sigma})$ -distance $d_{\sigma, \check{\sigma}}(P, P')$ between two points P and P' is the extremum of $\check{\sigma}$ -diameters for all σ -implementations of cycles passing P and P' .

It is easy to see that the distance is a symmetric function of two points.

Lemma 7.5. *The distance between two points $P = u + \iota v$ and $P' = u' + \iota v'$ in the elliptic or hyperbolic spaces is*



$$d_{\sigma, \check{\sigma}}^2(P, P') = \frac{\check{\sigma}((u - u')^2 - \sigma(v - v')^2) + 4(1 - \sigma\check{\sigma})vv'}{(u - u')^2\check{\sigma} - (v - v')^2}((u - u')^2 - \sigma(v - v')^2), \quad (7.2)$$

and, in parabolic space, it is (see Fig. 1.9(b) and also [108, (5), p. 38])

$$d_{p, \check{\sigma}}^2(y, y') = (u - u')^2. \quad (7.3)$$

Proof. Let $C_s^\sigma(l)$ be the family of cycles passing through both points (u, v) and (u', v') (under the assumption $v \neq v'$) and parametrised by its coefficient l , which is the first coordinate of the cycle's centre. By a symbolic calculation in CAS, we found that the only critical point of $\det(C_s^\sigma(l))$ is

$$l_0 = \frac{1}{2} \left((u' + u) + (\check{\sigma}\sigma - 1) \frac{(u' - u)(v^2 - v'^2)}{(u' - u)^2\check{\sigma} - (v - v')^2} \right). \quad (7.4)$$

Note that, for the case $\sigma\check{\sigma} = 1$, i.e. when both point and cycle spaces are simultaneously either elliptic or hyperbolic, this expression reduces to the expected midpoint $l_0 = \frac{1}{2}(u + u')$. Since, in the elliptic or hyperbolic case, the parameter l can take any real value, the extremum of $\det(C_s^\sigma(l))$ is

reached in l_0 and is equal to (7.2), again calculated by CAS. A separate calculation for the case $v = v'$ gives the same answer.

In the parabolic case, possible values of l are either in the ranges $(-\infty, \frac{1}{2}(u + u'))$ or $(\frac{1}{2}(u + u'), \infty)$, or only $l = \frac{1}{2}(u + u')$ since, for that value, a parabola should flip between the upward and downward directions of its branches. In any of these cases, the extreme value corresponds to the boundary point $l = \frac{1}{2}(u + u')$ and is equal to (7.3). \square

To help understand the complicated identity (7.2), we may observe that

$$\begin{aligned} d_{e,e}^2(P, P') &= (u - u')^2 + (v - v')^2, & \text{for elliptic values } \sigma = \check{\sigma} = -1, \\ d_{h,h}^2(P, P') &= (u - u')^2 - (v - v')^2, & \text{for hyperbolic values } \sigma = \check{\sigma} = 1. \end{aligned}$$

These are familiar expressions for distances in the elliptic and hyperbolic spaces. However, for other cases (such that $\sigma\check{\sigma} = -1$ or 0) quite different results are obtained. For example, $d_{\sigma,\check{\sigma}}^2(P, P')$ does not tend to 0 if $P \rightarrow P'$ in the usual sense.

Exercise 7.6. Show that:

- i. In the three cases $\sigma = \check{\sigma} = -1, 0$ or 1 , which were typically studied in the literature, the above distances are conveniently defined through the arithmetic of corresponding numbers:

$$d_{\sigma,\sigma}^2(u + \iota v) = (u + \iota v)(u - \iota v) = w\bar{w}. \quad (7.5)$$

- ii. Unless $\sigma = \check{\sigma}$, the parabolic distance $d_{p,\check{\sigma}}$ (7.3) is not obtained from (7.2) by the substitution $\sigma = 0$.
- iii. If cycles C_σ^s and $\tilde{C}_{\check{\sigma}}^s$ are k -normalised, then

$$\langle C_\sigma^s - \tilde{C}_{\check{\sigma}}^s, C_\sigma^s - \tilde{C}_{\check{\sigma}}^s \rangle = 2 \det(C_\sigma^s - \tilde{C}_{\check{\sigma}}^s) = -2d_{\sigma,\check{\sigma}}^2(P, \tilde{P}),$$

where P and \tilde{P} are e- or h-centres of C_σ^s and $\tilde{C}_{\check{\sigma}}^s$. Therefore, we can rewrite the relation (5.5) for the cycle product


$$\langle C_\sigma^s, \tilde{C}_{\check{\sigma}}^s \rangle = d_{\sigma,\check{\sigma}}^2(P, \tilde{P}) - r_\sigma^2 - \tilde{r}_{\check{\sigma}}^2,$$

using r_σ and $\tilde{r}_{\check{\sigma}}$ —the $\check{\sigma}$ -radii of the respective cycles. In particular, cf. (5.9),


$$\langle Z_\sigma^s, \tilde{Z}_{\check{\sigma}}^s \rangle = d_{\sigma,\check{\sigma}}^2(P, \tilde{P}),$$

for k -normalised $\check{\sigma}$ -zero-radius cycles Z_σ^s and $\tilde{Z}_{\check{\sigma}}^s$ with centres P and \tilde{P} . From Exercise 5.21 we can also derive that $d_{\sigma,\check{\sigma}}^2(P, \tilde{P})$ is equal to the power of the point P (\tilde{P}) with respect to the cycle $\tilde{Z}_{\check{\sigma}}^s$ (Z_σ^s).

The distance allows us to expand the result for all EPH cases, which is well known in the cases of circles [23, Sec. 2.1] and parabolas [108, Sec. 10].

Exercise 7.7. Show that the power of a point W with respect to a cycle (see Definition 3.18) is the product $d_\sigma(W, P) \cdot d_\sigma(W, P')$ of (σ, σ) -distances (7.5), where P and P' are any two points of the cycle which are collinear with W . 

HINT: Take $P = (u, v)$ and $P' = (u', v')$. Then, any collinear W is $(tu + (1 - t)u', tv + (1 - t)v')$ for some $t \in \mathbb{R}$. Furthermore, a simple calculation shows that $d_\sigma(y, z) \cdot d_\sigma(z, y') = t(t - 1)d_\sigma^2(y, y')$. The last expression is equal to the power of W with respect to the cycle—this step can be done by CAS. \diamond

Exercise 7.8. Let two cycles have e-centres P and P' with $\check{\sigma}$ -radii $r_{\check{\sigma}}$ and $r'_{\check{\sigma}}$. Then, the $(\check{\sigma}, \check{\sigma})$ -power of one cycle with respect to another from Definition 5.22 is, cf. the elliptic case in (5.10), 

$$\frac{d_{\check{\sigma}, \check{\sigma}}^2(P, P') - r_{\check{\sigma}}^2 - r_{\check{\sigma}}'^2}{2r_{\check{\sigma}} r_{\check{\sigma}}'}.$$

7.2 Lengths

During geometry classes, we often make measurements with a compass, which is based on the idea that *a circle is a locus of points equidistant from its centre*. We can expand it for all cycles with the following definition:

Definition 7.9. The $(\sigma, \check{\sigma}, \hat{\sigma})$ -length from the $\hat{\sigma}$ -centre (from the $\hat{\sigma}$ -focus) of a directed interval \overrightarrow{AB} is the $\check{\sigma}$ -radius of the σ -cycle with its $\hat{\sigma}$ -centre ($\hat{\sigma}$ -focus) at the point A which passes through B . These lengths are denoted by $l_c(\overrightarrow{AB})$ and $l_f(\overrightarrow{AB})$, respectively.

It is easy to be confused by the triple of parameters σ , $\check{\sigma}$ and $\hat{\sigma}$ in this definition. However, we will rarely operate in such a generality, and some special relations between the different sigmas will often be assumed. We also do not attach the triple $(\sigma, \check{\sigma}, \hat{\sigma})$ to $l_c(\overrightarrow{AB})$ and $l_f(\overrightarrow{AB})$ in formulae, since their values will be clear from the surrounding text.

Exercise 7.10. Check the following properties of the lengths:

- i. The length is *not* a symmetric function of two points (unlike the distance).

- ii. A cycle is uniquely defined by its elliptic or hyperbolic centre and a point which it passes. However, the parabolic centre is not as useful. Consequently, lengths from the parabolic centre are not properly defined, therefore we always assume $\hat{\sigma} = \pm 1$ for lengths from a centre.
- iii. A cycle is uniquely defined by any focus and a point which it passes.

We now turn to calculations of the lengths.

Lemma 7.11. *For two points $P = u + \iota v$, $P' = u' + \iota v' \in \mathbb{A}$:*

- i. *The $\check{\sigma}$ -length from the $\hat{\sigma}$ -centre for $\hat{\sigma} = \pm 1$ between P and P' is*

$$l_{c_{\hat{\sigma}}}^2(\overrightarrow{PP'}) = (u - u')^2 - \sigma v'^2 + 2\hat{\sigma}vv' - \check{\sigma}v^2. \quad (7.6)$$

- ii. *The $\check{\sigma}$ -length from the $\hat{\sigma}$ -focus between P and P' is*

$$l_{f_{\hat{\sigma}}}^2(\overrightarrow{PP'}) = (\hat{\sigma} - \check{\sigma})p^2 - 2vp, \quad (7.7)$$

where:

$$p = \hat{\sigma} \left(-(v' - v) \pm \sqrt{\hat{\sigma}(u' - u)^2 + (v' - v)^2 - \sigma\hat{\sigma}v'^2} \right), \quad \text{if } \hat{\sigma} \neq 0 \quad (7.8)$$

$$p = \frac{(u' - u)^2 - \sigma v'^2}{2(v' - v)}, \quad \text{if } \hat{\sigma} = 0. \quad (7.9)$$

Proof. Identity (7.6) is verified with CAS. For the second part, we observe that a cycle with the $\hat{\sigma}$ -focus (u, v) passing through $(u', v') \in \mathbb{A}$ has the parameters:

$$k = 1, \quad l = u, \quad n = p, \quad m = 2\hat{\sigma}pv' - u'^2 + 2uu' + \sigma v'^2.$$

Then, the formula (7.7) is verified by the CAS calculation. \square

Exercise 7.12. Check that:

- i. The value of p in (7.8) is the focal length of either of the two cycles, which are, in the parabolic case, upward or downward parabolas (corresponding to the plus or minus signs) with focus at (u, v) and passing (u', v') .
- ii. In the case $\sigma\check{\sigma} = 1$, the length from the centre (7.6) becomes the standard elliptic or hyperbolic distance $(u - u')^2 - \sigma(v - v')^2$ obtained in (7.2). Since these expressions appeared both as distances and lengths they are widely used.

On the other hand, in the parabolic point space, we obtain three additional lengths besides distance (7.3):

$$l_{c_{\hat{\sigma}}}^2(y, y') = (u - u')^2 + 2vv' - \check{\sigma}v^2$$

parametrised by three values $-1, 0$ or -1 of $\check{\sigma}$ (cf. Remark 3.11.i).

- iii. The parabolic distance (7.3) can be expressed in terms of the focal length p (7.8) as

$$d^2(y, y') = p^2 + 2(v - v')p,$$

an expression similar to (7.7).

7.3 Conformal Properties of Möbius Maps

All lengths $l(\overrightarrow{AB})$ in \mathbb{A} from Definition 7.9 are such that, for a fixed point A , every contour line $l(\overrightarrow{AB}) = c$ is a corresponding σ -cycle, which is a covariant object in the appropriate geometry. This is also true for distances if $\sigma = \check{\sigma}$. Thus, we can expect some covariant properties of distances and lengths.



Definition 7.13. We say that a distance or a length d is $\text{SL}_2(\mathbb{R})$ -conformal if, for fixed $y, y' \in \mathbb{A}$, the limit

$$\lim_{t \rightarrow 0} \frac{d(g \cdot y, g \cdot (y + ty'))}{d(y, y + ty')}, \quad \text{where } g \in \text{SL}_2(\mathbb{R}), \quad (7.10)$$

exists and its value depends only on y and g and is independent of y' .

Informally rephrasing this definition, we can say that a distance or length is $\text{SL}_2(\mathbb{R})$ -conformal if a Möbius map scales all small intervals originating at a point by the same factor. Also, since a scaling preserves the shape of cycles, we can restate the $\text{SL}_2(\mathbb{R})$ -conformality once more in familiar terms: small cycles are mapped to small cycles. To complete the analogy with conformality in the complex plane we note that preservation of angles (at least orthogonality) by Möbius transformations is automatic.

Exercise 7.14. Show $\text{SL}_2(\mathbb{R})$ -conformality in the following cases:

- i. The *distance* (7.2) is conformal if and only if the type of point and cycle spaces are the same, i.e. $\sigma\check{\sigma} = 1$. The parabolic distance (7.3) is conformal only in the parabolic point space. 
- ii. The lengths from centres (7.6) are conformal for any combination of values of $\sigma, \check{\sigma}$ and $\check{\check{\sigma}}$. 
- iii. The lengths from foci (7.7) are conformal for $\check{\sigma} \neq 0$ and any combination of values of σ and $\check{\sigma}$.

The conformal property of the distance (7.2) and (7.3) from Proposition 7.14.i is, of course, well known (see [22, 108]). However, the same property of non-symmetric lengths from Proposition 7.14.ii and 7.14.iii could

hardly be expected. As a possible reason, one remarks that the smaller group $\mathrm{SL}_2(\mathbb{R})$ (in comparison to all linear-fractional transforms of the whole \mathbb{R}^2) admits a larger number of conformal metrics, cf. Remark 5.3.

The exception of the case $\dot{\sigma} = 0$ from the conformality in 7.14.iii looks disappointing at first glance, especially in the light of the parabolic Cayley transform considered later in Section 10.3. However, a detailed study of algebraic structure invariant under parabolic rotations, see Chapter 11, will remove obscurity from this case. Indeed, our Definition 7.13 of conformality heavily depends on the underlying linear structure in \mathbb{A} – we measure a distance between points y and $y + ty'$ and intuitively expect that it is always small for small t . As explained in Section 11.4, the standard linear structure is incompatible with the parabolic rotations and thus should be replaced by a more relevant one. More precisely, instead of limits $y' \rightarrow y$ along the straight lines towards y , we need to consider limits along vertical lines, as illustrated in Fig. 10.1 and Definition 11.23.

We will return to the parabolic case of conformality in Proposition 11.24. An approach to the parabolic point space and a related conformality based on infinitesimal cycles will be considered in Section 7.6.

Remark 7.15. The expressions of lengths (7.6) and (7.7) are generally non-symmetric and this is a price one should pay for their non-triviality. All symmetric distances lead only to nine two-dimensional Cayley–Klein geometries, see [35; 39; 40; 90; 108, App. B]. In the parabolic case, a symmetric distance of a vector (u, v) is always a function of u alone, cf. Remark 7.21. For such a distance, a parabolic unit circle consists of two vertical lines (see dotted vertical lines in the second rows in Figs 6.3 and 6.5), which is not aesthetically attractive. On the other hand, the parabolic ‘unit cycles’ defined by lengths (7.6) and (7.7) are parabolas, which makes the parabolic Cayley transform (see Section 10.3) very natural.

We can also consider a distance between points in the upper half-plane which has a stronger property than $\mathrm{SL}_2(\mathbb{R})$ -conformality. Namely, the metric shall be preserved by $\mathrm{SL}_2(\mathbb{R})$ action or, in other words, Möbius transformations are isometries for it. We will study such a metric in Chapter 9.

7.4 Perpendicularity and Orthogonality

In a Euclidean space, the shortest distance from a point to a straight line is provided by the corresponding perpendicular. Since we have already

defined various distances and lengths, we may use them for a definition of the respective notions of perpendicularity.

Definition 7.16. Let l be a length or a distance. We say that a vector \overrightarrow{AB} is l -perpendicular to a vector \overrightarrow{CD} if function $l(\overrightarrow{AB} + \varepsilon \overrightarrow{CD})$ of a variable ε has a local extremum at $\varepsilon = 0$, cf. Fig. 1.10. This is denoted by $\overrightarrow{AB} \lambda_l \overrightarrow{CD}$ or, simply, $\overrightarrow{AB} \lambda \overrightarrow{CD}$ if the meaning of l is clear from the context.

Exercise 7.17. Check that:

- i. l -perpendicularity is not a symmetric notion (i.e. $\overrightarrow{AB} \lambda \overrightarrow{CD}$ does not imply $\overrightarrow{CD} \lambda \overrightarrow{AB}$), similar to f-orthogonality – see Section 6.6.
- ii. l -perpendicularity is linear in \overrightarrow{CD} , i.e. $\overrightarrow{AB} \lambda \overrightarrow{CD}$ implies $\overrightarrow{AB} \lambda r \overrightarrow{CD}$ for any real non-zero r . However, l -perpendicularity is not generally linear in \overrightarrow{AB} , i.e. $\overrightarrow{AB} \lambda \overrightarrow{CD}$ does not necessarily imply $r \overrightarrow{AB} \lambda \overrightarrow{CD}$.

There is a connection between l -perpendicularity and f-orthogonality.

Lemma 7.18. Let \overrightarrow{AB} be l_c -perpendicular (l_f -perpendicular) to a vector \overrightarrow{CD} for a length from the centre (from the focus) defined by the triple $(\sigma, \check{\sigma}, \hat{\sigma})$. Then, the flat cycle (straight line) AB is $\hat{\sigma}$ -(f-)orthogonal to the σ -cycle C_σ^s with $\hat{\sigma}$ -centre ($(-\hat{\sigma})$ -focus) at A passing through B . The vector \overrightarrow{CD} is tangent at B to the σ -implementation of C_σ^s .

Proof. Consider the cycle C_σ^s with its $\hat{\sigma}$ -centre at A and passing B in its σ -implementation. This cycle C_σ^s is a contour line for a function $l(X) = l_c(\overrightarrow{AX})$ with the triple $(\sigma, \check{\sigma}, \hat{\sigma})$. Therefore, the cycle separates regions where $l(X) < l_c(\overrightarrow{AB})$ and $l(X) > l_c(\overrightarrow{AB})$. The tangent line to C_σ^s at B (or, at least, its portion in the vicinity of B) belongs to one of these two regions, thus $l(X)$ has a local extremum at B . Therefore, \overrightarrow{AB} is l_c -perpendicular to the tangent line. The line AB is also $\hat{\sigma}$ -orthogonal to the cycle C_σ^s since it passes its $\hat{\sigma}$ -centre A , cf. Exercise 6.18.iv.

The second case of $l_f(\overrightarrow{AB})$ and f-orthogonality can be considered similarly with the obvious change of centre to focus, cf. Proposition 6.40.ii. \square

Obviously, perpendicularity turns out to be familiar in the elliptic case, cf. Lemma 7.20.e below. For the two other cases, the description is given as follows:

Exercise 7.19. Let $A = (u, v)$ and $B = (u', v')$. Then



- i. d -perpendicular (in the sense of (7.2)) to \overrightarrow{AB} in the *elliptic* or *hyperbolic* cases is a multiple of the vector

$$\begin{pmatrix} \sigma(v-v')^3 - (u-u')^2(v+v'(1-2\sigma\check{\sigma})) \\ \check{\sigma}(u-u')^3 - (u-u')(v-v')(-2v' + (v+v')\check{\sigma}\sigma) \end{pmatrix},$$

which, for $\sigma\check{\sigma} = 1$, reduces to the expected value $(v-v', \sigma(u-u'))$.

- ii. d -perpendicular (in the sense of (7.3)) to \overrightarrow{AB} in the *parabolic* case is $(0, t)$, $t \in \mathbb{R}$ which coincides with the *Galilean orthogonality* defined in [108, Sec. 3].
- iii. $l_{c_{\check{\sigma}}}$ -perpendicular (in the sense of (7.6)) to \overrightarrow{AB} is a multiple of $(\sigma v' - \check{\sigma}v, u-u')$.
- iv. $l_{f_{\check{\sigma}}}$ -perpendicular (in the sense of (7.7)) to \overrightarrow{AB} is a multiple of $(\sigma v' + p, u-u')$, where p is defined either by (7.8) or (7.9) for corresponding values of $\check{\sigma}$.

HINT: Contour lines for all distances and lengths are cycles. Use implicit derivation of (4.1) to determine the tangent vector to a cycle at a point. Then apply the formula to a cycle which passes (u', v') and is a contour line for a distance or length from (u, v) . \diamond

It is worth having an idea about different types of perpendicularity in terms of the standard Euclidean geometry. Here are some examples.

Exercise 7.20. Let $\overrightarrow{AB} = u + \iota v$ and $\overrightarrow{CD} = u' + \iota v'$. Then:

- e. In the elliptic case, d -perpendicularity for $\check{\sigma} = -1$ means that \overrightarrow{AB} and \overrightarrow{CD} form a right angle, or, analytically, $uu' + vv' = 0$.
- p. In the parabolic case, $l_{f_{\check{\sigma}}}$ -perpendicularity for $\check{\sigma} = 1$ means that \overrightarrow{AB} bisects the angle between \overrightarrow{CD} and the vertical direction, or, analytically,

$$u'u - v'p = u'u - v'(\sqrt{u^2 + v^2} - v) = 0, \quad (7.11)$$

where p is the focal length (7.8).

- h. In the hyperbolic case, d -perpendicularity for $\check{\sigma} = -1$ means that the angles between \overrightarrow{AB} and \overrightarrow{CD} are bisected by lines parallel to $u = \pm v$, or, analytically, $u'u - v'v = 0$. Compare with Exercise 6.3(A).

Remark 7.21. If one attempts to devise a parabolic length as a limit or an intermediate case for the elliptic $l_e = u^2 + v^2$ and hyperbolic $l_p = u^2 - v^2$ lengths, then the only possible guess is $l'_p = u^2$ (7.3), which is too trivial for an interesting geometry.

Similarly, the only orthogonality condition linking the elliptic $u_1u_2 + v_1v_2 = 0$ and the hyperbolic $u_1u_2 - v_1v_2 = 0$ cases from the above exercise seems to be $u_1u_2 = 0$ (see [108, Sec. 3] and 7.19.ii), which is again too trivial. This supports Remark 3.11.ii.

7.5 Infinitesimal-radius Cycles


Although parabolic zero-radius cycles defined in 5.13 do not satisfy our expectations for ‘smallness’, they are often technically suitable for the same purposes as elliptic and hyperbolic ones. However, we may want to find something which fits our intuition about ‘zero-sized’ objects better. Here, we present an approach based on non-Archimedean (non-standard) analysis – see, for example, [24, 104] for a detailed exposition.

Following Archimedes, a (positive) *infinitesimal number* x satisfies

$$0 < nx < 1, \quad \text{for any } n \in \mathbb{N}. \quad (7.12)$$

Apart from this inequality infinitesimals obey all other properties of real numbers. In particular, in our CAS computations, an infinitesimal will be represented by a positive real symbol and we replace some of its powers by zero if their order of infinitesimality will admit this. The existence of infinitesimals in the standard real analysis is explicitly excluded by the Archimedean axiom, therefore the theory operating with infinitesimals is known as non-standard or non-Archimedean analysis. We assume from now on that there exists an infinitesimal number ϵ .

Definition 7.22. A cycle C_σ^s , such that $\det C_\sigma^s$ is an infinitesimal number, is called an *infinitesimal radius cycle*.

Exercise 7.23. Let $\check{\sigma}$ and $\hat{\sigma}$ be two metric signs and let a point $(u_0, v_0) \in \mathbb{D}$ with $v_0 > 0$. Consider a cycle C_σ^s defined by 

$$C_\sigma^s = (1, u_0, n, u_0^2 - \hat{\sigma}n^2 + \epsilon^2), \quad (7.13)$$

where

$$n = \begin{cases} \frac{v_0 - \sqrt{v_0^2 - (\hat{\sigma} - \check{\sigma})\epsilon^2}}{\hat{\sigma} - \check{\sigma}}, & \text{if } \hat{\sigma} \neq \check{\sigma}, \\ \frac{\epsilon^2}{2v_0}, & \text{if } \hat{\sigma} = \check{\sigma}. \end{cases} \quad (7.14)$$

Then,

- i. The point (u_0, v_0) is $\hat{\sigma}$ -focus of the cycle.


- ii. The square of the $\check{\sigma}$ -radius is exactly $-\epsilon^2$, i.e. (7.13) defines an infinitesimal-radius cycle.
- iii. The focal length of the cycle is an infinitesimal number of order ϵ^2 .

HINT: Combining two quadratic equations (one defines the squared $\check{\sigma}$ -radius, another $-v$ -coordinate of the focus), we found that n satisfies the equation:

$$(\check{\sigma} - \check{\sigma})n^2 - 2v_0n + \epsilon^2 = 0.$$

Moreover, only the root from (7.14) of the quadratic case $\check{\sigma} - \check{\sigma} \neq 0$ gives an infinitesimal focal length. Then, we can find the m component of the cycle. The answer is also supported by CAS calculations. \diamond


The graph of cycle (7.13) in the parabolic space drawn at the scale of real numbers looks like a vertical ray starting at its focus, see Fig. 7.1(a), due to the following result.

Exercise 7.24. The infinitesimal cycle (7.13) consists of points which are infinitesimally close (in the sense of length from focus (7.7)) to its focus $F = (u_0, v_0)$: 

$$(u_0 + \epsilon u, v_0 + v_0 u^2 + ((\check{\sigma} - \check{\sigma})u^2 - \check{\sigma}) \frac{\epsilon^2}{4v_0} + O(\epsilon^3)). \quad (7.15)$$

Note that points below F (in the ordinary scale) are not infinitesimally close to F in the sense of length (7.7), but are in the sense of distance (7.3). Thus, having the set of points on the infinitesimal distance from an unknown point F we are not able to identify F . However, this is possible from the set of points on the infinitesimal length from F . Figure 7.1(a) shows elliptic, hyperbolic *concentric* and parabolic *confocal* cycles of decreasing radii which shrink to the corresponding infinitesimal-radius cycles.

It is easy to see that infinitesimal-radius cycles have properties similar to zero-radius ones, cf. Lemma 5.20.

Exercise 7.25. The image of $\mathrm{SL}_2(\mathbb{R})$ -action on an infinitesimal-radius cycle (7.13) by conjugation (4.7) is an infinitesimal-radius cycle of the same order. The image of an infinitesimal cycle under *cycle conjugation* is an infinitesimal cycle of the same or lesser order. 

Consideration of infinitesimal numbers in the elliptic and hyperbolic cases should not bring any advantages since the (leading) quadratic terms in these cases are non-zero. However, non-Archimedean numbers in the parabolic case provide a more intuitive and efficient presentation. For example, zero-radius cycles are not helpful for the parabolic Cayley transform (see

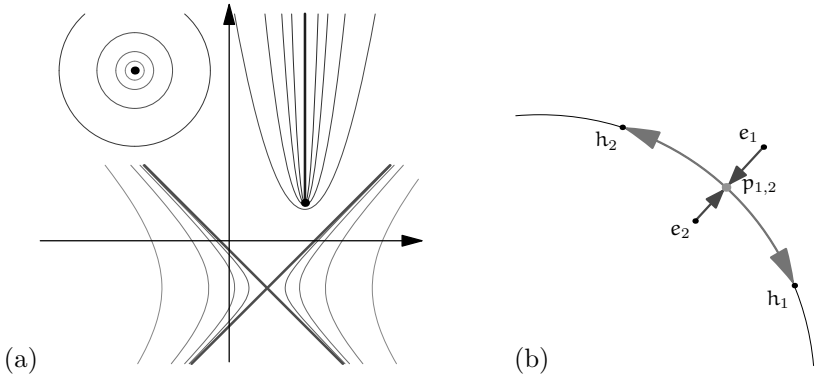



Figure 7.1 Zero-radius cycles and the ‘phase’ transition. (a) Zero-radius cycles in elliptic (black point) and hyperbolic (the red light cone) cases. The infinitesimal-radius parabolic cycle is the blue vertical ray starting at the focus. (b) Elliptic-parabolic-hyperbolic phase transition between fixed points of a subgroup. Two fixed points of an elliptic subgroup collide to a parabolic double point on the boundary and then decouple into two hyperbolic fixed points on the unit disk.

Section 10.3), but infinitesimal cycles are their successful replacements. Another illustration is the second part of the following result as a useful substitution for Exercise 6.6.iv.

Exercise 7.26. Let C_σ^s be the infinitesimal cycle (7.13) and $\check{C}_\sigma^s =$  (k, l, n, m) be a generic cycle. Then:

- i. Both the orthogonality condition $C_\sigma^s \perp \check{C}_\sigma^s$ (6.1) and the f-orthogonality $\check{C}_\sigma^s \dashv C_\sigma^s$ (6.15) are given by

$$ku_0^2 - 2lu_0 + m = O(\epsilon).$$

In other words, the cycle \check{C}_σ^s has the real root u_0 .

- ii. The f-orthogonality (6.15) $C_\sigma^s \dashv \check{C}_\sigma^s$ is given by

$$ku_0^2 - 2lu_0 - 2nv_0 + m = O(\epsilon). \quad (7.16)$$

In other words, the cycle \check{C}_σ^s passes the focus (u_0, v_0) of the infinitesimal cycle in the p-implementation.

It is interesting to note that the exotic f-orthogonality became a matching replacement for the usual one for infinitesimal cycles. Unfortunately, f-orthogonality is more fragile. For example, it is not invariant under a generic cycle conjugation (Exercise 6.38) and, consequently, we cannot use an infinitesimal-radius cycle to define a new parabolic inversion besides those shown in Fig. 6.4(c).

7.6 Infinitesimal Conformality


An intuitive idea of conformal maps, which is often provided in complex analysis textbooks for illustration purposes, is that they ‘send small circles into small circles with respective centres’. Using infinitesimal cycles, one can turn it into a precise definition.

Definition 7.27. A map of a region of \mathbb{A} to another region is *l -infinitesimally conformal* for a length l (in the sense of Definition 7.9) if, for any l -infinitesimal cycle,

- i. its image is an l -infinitesimal cycle of the same order and
- ii. the image of its centre or focus is displaced from the centre or focus of its image by an infinitesimal number of a greater order than its radius.


Remark 7.28. Note that, in comparison with Definition 7.13, we now work ‘in the opposite direction’. Formerly, we had the fixed group of motions and looked for corresponding conformal lengths and distances. Now, we take a distance or length (encoded in the infinitesimally-equidistant cycle) and check which motions respect it.

Natural conformalities for lengths from the centre in the elliptic and parabolic cases are already well studied. Thus, we are mostly interested here in conformality in the parabolic case, where lengths from the focus are more relevant. The image of an infinitesimal cycle (7.13) under $\mathrm{SL}_2(\mathbb{R})$ -action is a cycle. Moreover, it is again an infinitesimal cycle of the same order by Exercise 7.25. This provides the first condition of Definition 7.27. The second part fulfils as well.

Exercise 7.29. Let \check{C}_σ^s be the image under $g \in \mathrm{SL}_2(\mathbb{R})$ of an infinitesimal cycle C_σ^s from (7.13). Then, the $\check{\sigma}$ -focus of \check{C}_σ^s is displaced from $g(u_0, v_0)$ by infinitesimals of order ϵ^2 , while both cycles have $\check{\sigma}$ -radius of order ϵ . 

Consequently, $\mathrm{SL}_2(\mathbb{R})$ -action is infinitesimally-conformal in the sense of Definition 7.27 with respect to the length from the focus (Definition 7.9) for all combinations of σ , $\check{\sigma}$ and $\hat{\sigma}$.

Infinitesimal conformality seems to be intuitively close to Definition 7.13. Thus, it is desirable to understand a reason for the absence of exclusion clauses in Exercise 7.29 in comparison with Exercise 7.14.iii.

Exercise 7.30. Show that, for lengths from foci (7.7) and $\hat{\sigma} = 0$, the 

limit (7.10) at point $y_0 = u_0 + \iota v_0$ does exist but depends on the direction $y = u + \iota v$:

$$\lim_{t \rightarrow 0} \frac{d(g \cdot y_0, g \cdot (y_0 + ty))}{d(y_0, y_0 + ty)} = \frac{1}{(d + cu_0)^2 + \sigma c^2 v_0^2 - 2Kcv_0(d + cu_0)}, \quad (7.17)$$

where $K = \frac{u}{v}$ and $g = \begin{pmatrix} a & b \\ c & d \end{pmatrix}$. Thus, the length is not conformal.

However, if we consider points (7.15) of the infinitesimal cycle, then $K = \frac{\epsilon u}{v_0 u^2} = \frac{\epsilon}{v_0 u}$. Thus, the value of the limit (7.17) at the infinitesimal scale is independent of $y = u + \iota v$. It also coincides (up to an infinitesimal number) with the value in (11.26), which is defined through a different conformal condition.

Infinitesimal cycles are also a convenient tool for calculations of invariant measures, Jacobians, etc.

Remark 7.31. There are further connections between the infinitesimal number ϵ and the dual unit ε . Indeed, in non-standard analysis, ϵ^2 is a higher-order infinitesimal than ϵ and can effectively be treated as 0 at the infinitesimal scale of ϵ . Thus, it is simply a more relaxed version of the defining property of the dual unit $\varepsilon^2 = 0$. This explains why many results of differential calculus can be deduced naturally within a dual numbers framework [17], which naturally absorbs many proofs from non-standard analysis.

Using this analogy between ϵ and ε , we can think about the parabolic point space \mathbb{D} as a model for a subset of *hyperreal numbers* \mathbb{R}^* having the representation $x + \epsilon y$, with x and y being real. Then, a vertical line in \mathbb{D} (a special line, in Yaglom's terms [108]) represents a *monad*, that is, the equivalence class of hyperreals, which are different by an infinitesimal number. Then, a Möbius transformation of \mathbb{D} is an analytic extension of the Möbius map from the real line to the subset of hyperreals.

The graph of a parabola is a section, that is, a 'smooth' choice of a hyperreal representative from each monad. Geometric properties of parabolas studied in this work correspond to results about such choices of representatives and their invariants under Möbius transformations. It will be interesting to push this analogy further and look for a flow of ideas in the opposite direction: from non-standard analysis to parabolic geometry.

Chapter 8

Global Geometry of Upper Half-Planes

So far, we have been interested in the individual properties of cycles and (relatively) localised properties of the point space. We now describe some global properties which are related to the set of cycles as a whole.

8.1 Compactification of the Point Space

In giving Definitions 4.10 and 4.11 of the maps Q and M on the *cycle space*, we did not properly consider their domains and ranges. For example, the point $(0, 0, 0, 1) \in \mathbb{P}^3$ is transformed by Q to the equation $1 = 0$, which is not a valid equation of a conic section in any point space \mathbb{A} . We have also not yet accurately investigated singular points of the Möbius map (3.24). It turns out that both questions are connected.

One of the standard approaches [84, Sec. 1] for dealing with singularities of Möbius maps is to consider projective coordinates on the real line. More specifically, we assign, cf. Section 4.4.1, a point $x \in \mathbb{R}$ to a vector $(x, 1)$, then linear-fractional transformations of the real line correspond to linear transformations of two-dimensional vectors, cf. (1.1) and (4.9). All vectors with a non-zero second component can be mapped back to the real line. However, vectors $(x, 0)$ do not correspond to real numbers and represent the *ideal element*, see [95, Ch. 10] for a pedagogical introduction. The union of the real line with the ideal element produces the *compactified* real line. A similar construction is known for Möbius transformations of the complex plane and its compactification.

Since we already have a projective space of cycles, we may use it as a model for compactification of point spaces as well, as it turns out to be even more appropriate and uniform in all EPH cases. The identification of points with zero-radius cycles, cf. Exercise 5.18, plays an important rôle here.

Definition 8.1. The only irregular point $(0, 0, 0, 1) \in \mathbb{P}^3$ of the map Q is called the *zero-radius cycle at infinity* and is denoted by Z_∞ .

Exercise 8.2. Check the following:



- i. Z_∞ is the image of the zero-radius cycle $Z_{(0,0)} = (1, 0, 0, 0)$ at the origin under reflection (inversion) into the unit cycle $(1, 0, 0, -1)$ – see blue cycles in Fig. 6.4(b)–(d).
- ii. The following statements are equivalent:
 - (a) A point $(u, v) \in \mathbb{A}$ belongs to the *zero-radius cycle* $Z_{(0,0)}$ centred at the origin.
 - (b) The zero-radius cycle $Z_{(u,v)}$ is σ -orthogonal to the zero-radius cycle $Z_{(0,0)}$.
 - (c) The inversion $z \mapsto \frac{1}{z}$ in the unit cycle is singular in the point (u, v) .
 - (d) The image of $Z_{(u,v)}$ under inversion in the unit cycle is orthogonal to Z_∞ .

If any one of the above statements is true, we also say that the image of (u, v) under inversion in the unit cycle belongs to the zero-radius cycle at infinity.

HINT: These can be easily obtained by direct calculations, even without a CAS. \diamond

In the elliptic case, the compactification is done by adding to \mathbb{C} a single point ∞ (infinity), which is, of course, the elliptic zero-radius cycle. However, in the parabolic and hyperbolic cases, singularities of the inversion $z \mapsto \frac{1}{z}$ are not localised in a single point. Indeed, the denominator is a zero divisor for the whole zero-radius cycle. Thus, in each EPH case, the correct compactification is made by the union $\mathbb{A} \cup Z_\infty$.

It is common to identify the compactification $\dot{\mathbb{C}}$ of the space \mathbb{C} with a *Riemann sphere*. This model can be visualised by the *stereographic projection* (or polar projection) as follows – see Fig. 8.1(a) and [11, Sec. 18.1.4] for further details. Consider a unit sphere with a centre at the origin of \mathbb{R}^3 and the horizontal plane passing the centre. Any non-tangential line passing the north pole S will intersect the sphere at another point P and meet the plane at a point Q . This defines a one-to-one correspondence of the plane and the sphere within point S . If point Q moves far from the origin the point P shall approach S . Thus it is natural to associate S with infinity.

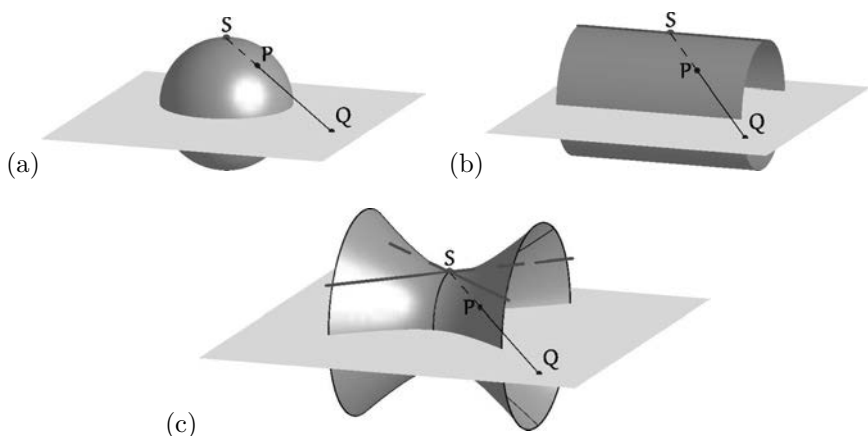


Figure 8.1 Compactification of \mathbb{A} and stereographic projections in (a) elliptic (b) parabolic and (c) hyperbolic point spaces. The stereographic projection from the point S defines the one-to-one map $P \leftrightarrow Q$ between points of the plane (point space) and the model—surfaces of constant curvature. The red point and lines correspond to the light cone at infinity—the ideal elements of the model.

A similar model can also be provided for the parabolic and hyperbolic spaces—see Fig. 8.1(b),(c) and further discussion in [39; 108, Sec. 10]. Indeed, the space \mathbb{A} can be identified with a corresponding surface of *constant curvature*: the sphere ($\sigma = -1$), the cylinder (Fig. 8.1(b), $\sigma = 0$), or the one-sheet hyperboloid (Fig. 8.1(c), $\sigma = 1$). The map of a surface to \mathbb{A} is given by the polar projection—see Fig. 8.1(a–c) as well as [39, Fig. 1; 108, Figs 129, 135, 179]. The ideal elements which do not correspond to any point of the plane are shown in red in Fig. 8.1. As we may observe, these correspond exactly to the zero-radius cycles in each case: the point (elliptic), the line (parabolic) and two lines, that is, the light cone (hyperbolic) at infinity. These surfaces provide ‘compact’ models of the corresponding \mathbb{A} in the sense that Möbius transformations which are lifted from \mathbb{A} to the constant curvature surface by the polar projection are not singular on these surfaces.

However, the hyperbolic case has its own caveats which may be easily overlooked as in [39], for example. A compactification of the hyperbolic space \mathbb{O} by a *light cone*—the hyperbolic zero-radius cycle—at infinity will, indeed, produce a closed Möbius-invariant object or a model of two-dimensional conformal *space-time*. However, it will not be satisfactory for reasons explained in the next section.

8.2 (Non)-Invariance of The Upper Half-Plane

There is an important difference between the hyperbolic case and the others.

Exercise 8.3. In the elliptic and parabolic cases, the upper half-plane in \mathbb{A} is preserved by Möbius transformations from $SL_2(\mathbb{R})$. However, in the hyperbolic case, any point (u, v) with $v > 0$ can be mapped to an arbitrary point (u', v') with $v' \neq 0$.

This is illustrated in Fig. 1.3. Any cone from the family (3.29) intersect both planes EE' and PP' over a connected curve (K -orbit—a circle and parabola, respectively) belonging to a half-plane. However, the intersection of a two-sided cone with the plane HH' is two branches of a hyperbola in different half-planes (only one of them is shown in Fig. 1.3). Thus, a rotation of the cone produces a transition of the intersection point from one half-plane to another and back again.

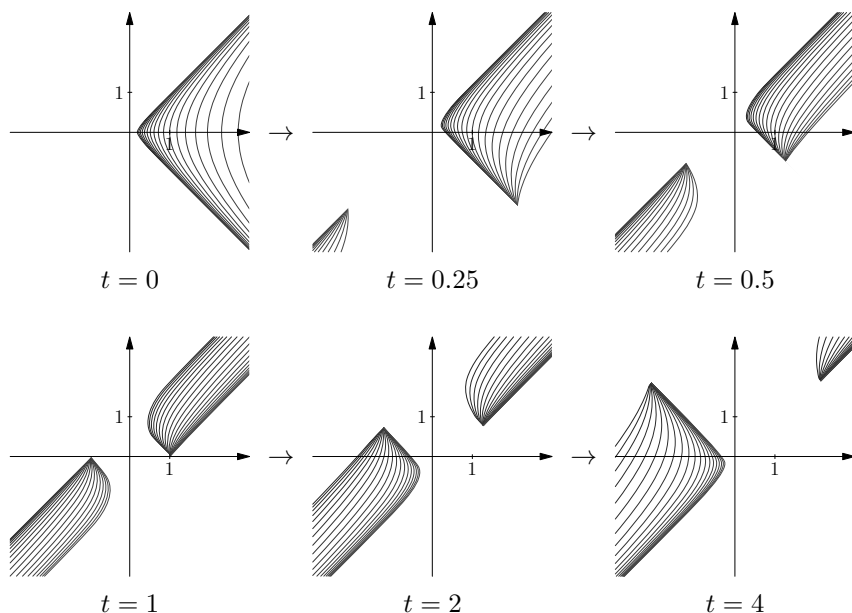


Figure 8.2 Six frames from a continuous transformation from the future to the past parts of the light cone. Animations as GIF and PDF (requires Adobe Reader) are provided on the accompanying DVD.

The lack of invariance of the half-planes in the hyperbolic case has many important consequences in seemingly different areas, for example:

Geometry: \mathbb{O} is not split by the real axis into two disjoint pieces: there are continuous paths (through the light cone at infinity) from the upper half-plane to the lower one which do not cross the real axis, cf. a sine-like curve consisting of two branches of a hyperbola in Fig. 8.3(a).

Physics: There is no Möbius-invariant way to separate the ‘past’ and ‘future’ parts of the light cone [96, Ch. II], i.e. there is a continuous family of Möbius transformations reversing the arrow of time and breaking causal orientation. For example, the family of matrices $\begin{pmatrix} 1 & -te_1 \\ te_1 & 1 \end{pmatrix}$, $t \in [0, \infty)$ provides such a transformation. Figure 8.2 illustrates this by the corresponding images for six subsequent values of t .

Analysis: There is no possibility of splitting the $L_2(\mathbb{R})$ space of functions into a direct sum of the Hardy-type space of functions having an analytic extension into the upper half-plane and its non-trivial complement, i.e. any function from $L_2(\mathbb{R})$ has an ‘analytic extension’ into the upper half-plane in the sense of hyperbolic function theory – see [58].

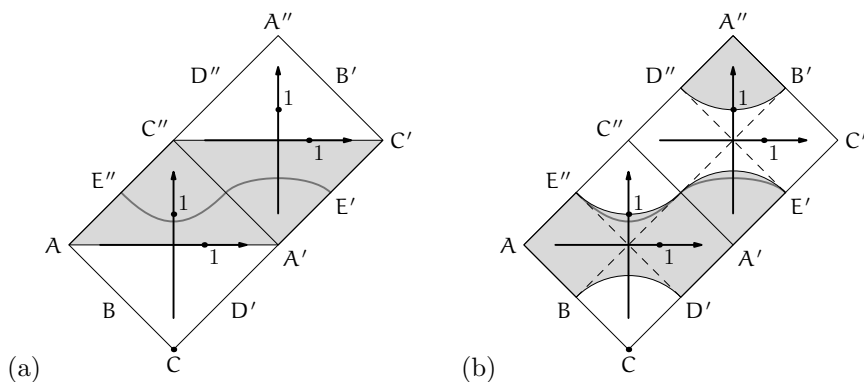


Figure 8.3 Hyperbolic objects in the double cover of \mathbb{O} . If we cross the light cone at infinity from one sheet, then we will appear on the other. The shaded region is the two-fold cover of the upper half-plane on (a) and the unit disk on (b). These regions are Möbius-invariant.

All of the above problems can be resolved in the following way – see [58, Sec. A.3; 96, Sec. III.4]. We take two copies \mathbb{O}^+ and \mathbb{O}^- of the hyperbolic point space \mathbb{O} , depicted by the squares $ACA'C'$ and $A'C'A'C'$ in Fig. 8.3, respectively. The boundaries of these squares are light cones at infinity and

we glue \mathbb{O}^+ and \mathbb{O}^- in such a way that the construction is invariant under the natural action of the Möbius transformation. This is achieved if the letters A, B, C, D, E in Fig. 8.3 are identified regardless of the number of primes attached to them.

This aggregate, denoted by $\tilde{\mathbb{O}}$, is a two-fold cover of \mathbb{O} . The *hyperbolic ‘upper’ half-plane* $\tilde{\mathbb{O}}^+$ in $\tilde{\mathbb{O}}$ consists of the upper half-plane in \mathbb{O}^+ and the lower one in \mathbb{O}^- , shown as a shaded region in Fig. 8.3(a). It is Möbius-invariant and has a matching complement in $\tilde{\mathbb{O}}$. More formally,

$$\tilde{\mathbb{O}}^+ = \{(u, v) \in \mathbb{O}^+ \mid u > 0\} \cup \{(u, v) \in \mathbb{O}^- \mid u < 0\}. \quad (8.1)$$

The hyperbolic ‘upper’ half-plane is bounded by two disjoint ‘real’ axes denoted by AA' and $C'C'$ in Fig. 8.3(a).

Remark 8.4. The hyperbolic orbit of the subgroup K in $\tilde{\mathbb{O}}$ consists of two branches of the hyperbola passing through $(0, v)$ in \mathbb{O}^+ and $(0, -v^{-1})$ in \mathbb{O}^- – see the sine-like curve in Fig. 8.3(a). If we watch the continuous rotation of a straight line generating a cone (3.29) then its intersection with the plane HH' in Fig. 1.3(b) will draw both branches. As mentioned in Remark 3.17.ii, they have the same focal length and form a single K -orbit.

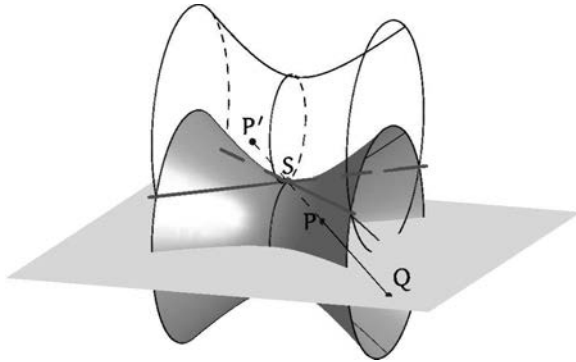


Figure 8.4 Double cover of the hyperbolic space, cf. Fig. 8.1(c). The second hyperboloid is shown as a blue skeleton. It is attached to the first one along the light cone at infinity, which is represented by two red lines. A crossing of the light cone implies a transition from one hyperboloid to another.

The corresponding model through a stereographic projection is presented in Fig. 8.4. In comparison with the single hyperboloid in Fig. 8.1(c), we add the second hyperboloid intersecting the first one over the light cone at

infinity. A crossing of the light cone in any direction implies a swap of hyperboloids, cf. the flat map in Fig. 8.3. A similar conformally-invariant two-fold cover of the Minkowski space-time was constructed in [96, Sec. III.4] in connection with the red shift problem in *extragalactic astronomy*—see Section 8.4 for further information.

8.3 Optics and Mechanics

We have already used many physical terms (light cone, space-time, etc.) to describe the hyperbolic point space. It will be useful to outline more physical connections for all EPH cases. Our list may not be exhaustive, but it illustrates that $\mathrm{SL}_2(\mathbb{R})$ not only presents some distinct areas but also links them in a useful way.

8.3.1 Optics

Consider an optical system consisting of centred lenses. The propagation of rays close to the symmetry axis through such a device is the subject of *paraxial optics*. See [30, Ch. 2] for a pedagogical presentation of matrix methods in this area—we give only a briefly outline here. A ray at a certain point can be described by a pair of numbers $P = (y, V)$ in respect to the symmetry axis A —see Fig. 8.5. Here, y is the height (positive or negative) of the ray above the axis A and $V = n \cos v$, where v is the angle of the ray with the axis and n is the *refractive index* of the medium.

The paraxial approximation to geometric optics provides a straightforward recipe for evaluating the output components from the given data:

$$\begin{pmatrix} y_2 \\ V_2 \end{pmatrix} = \begin{pmatrix} a & b \\ c & d \end{pmatrix} \begin{pmatrix} y_1 \\ V_1 \end{pmatrix}, \quad \text{for some } \begin{pmatrix} a & b \\ c & d \end{pmatrix} \in \mathrm{SL}_2(\mathbb{R}). \quad (8.2)$$

If two paraxial systems are aggregated one after another, then the composite is described by the product of the respective transfer matrices of the subsystems. In other words, we obtained an action of the group $\mathrm{SL}_2(\mathbb{R})$ on the space of rays. More complicated optical systems can be approximated locally by paraxial models.

There is a covariance of the theory generated by the conjugation automorphism $g : g' \mapsto gg'g^{-1}$ of $\mathrm{SL}_2(\mathbb{R})$. Indeed, we can simultaneously replace rays by gP and a system's matrices by gAg^{-1} for any fixed $g \in \mathrm{SL}_2(\mathbb{R})$. Another important invariant can be constructed as follows.

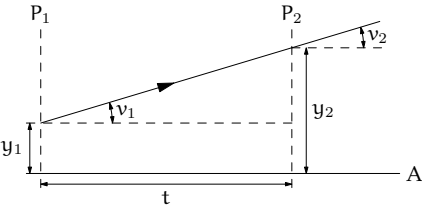
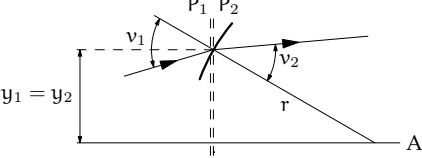
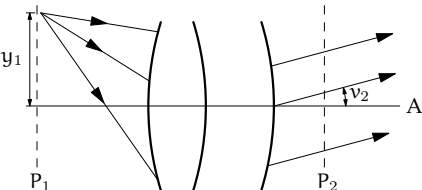
System	Transfer matrices
	Propagation in a homogeneous and isotropic medium with refractive index n : $\begin{pmatrix} y_2 \\ V_2 \end{pmatrix} = \begin{pmatrix} 1 & t/n \\ 0 & 1 \end{pmatrix} \begin{pmatrix} y_1 \\ V_1 \end{pmatrix}$
	A circular boundary between two regions with refractive indices n_1 and n_2 : $\begin{pmatrix} y_2 \\ V_2 \end{pmatrix} = \begin{pmatrix} 1 & 0 \\ \frac{n_1 - n_2}{r} & 1 \end{pmatrix} \begin{pmatrix} y_1 \\ V_1 \end{pmatrix}$
	A ray emitted from the focal plane. The output direction v_2 depends only on y_1 : $\begin{pmatrix} y_2 \\ V_2 \end{pmatrix} = \begin{pmatrix} a & b \\ c & 0 \end{pmatrix} \begin{pmatrix} y_1 \\ V_1 \end{pmatrix}$

Figure 8.5 Some elementary optical systems and their transfer matrices

For matrices from $\text{SL}_2(\mathbb{R})$, we note the remarkable relation

$$J^{-1}AJ = (A^{-1})^T, \quad \text{where } A \in \text{SL}_2(\mathbb{R}) \text{ and } J = \begin{pmatrix} 0 & -1 \\ 1 & 0 \end{pmatrix}. \quad (8.3)$$

Subsequently, we define a *symplectic form* on \mathbb{R}^2 using the matrix J :

$$y\tilde{V} - \tilde{y}V = \tilde{P}^T J P, \quad \text{where } P = \begin{pmatrix} y \\ V \end{pmatrix}, \quad \tilde{P} = \begin{pmatrix} \tilde{y} \\ \tilde{V} \end{pmatrix} \in \mathbb{R}^2. \quad (8.4)$$

Then, this form is invariant under the $\text{SL}_2(\mathbb{R})$ -action (8.2), due to (8.3):

$$\begin{aligned} \tilde{P}_1^T J P_1 &= (A\tilde{P})^T J A P = \tilde{P}^T A^T J A P = \tilde{P}^T J (J^{-1} A^T J) A P \\ &= \tilde{P}^T J A^{-1} A P = \tilde{P}^T J P, \end{aligned}$$

where $P_1 = A P$ and $\tilde{P}_1 = A \tilde{P}$. In other words, the symplectic form is an invariant of the covariant action of $\text{SL}_2(\mathbb{R})$ on the optical system, cf. Exercise 4.20.iii.

Example 8.5. The matrix J (8.3) belongs to the subgroup K . It is a transfer matrix between two focal planes of a system, cf. [30, Sec. II.8.2]. It swaps components of the vector (y, V) , therefore the ray height y_2 at the second focal plane depends only on the ray angle V_1 in the first, and *vice versa*.

8.3.2 Classical Mechanics

A Hamiltonian formalism in classical mechanics was motivated by an analogy between optics and mechanics – see [2, Sec. 46]. For a one-dimensional system, it replaces the description of rays through (y, V) by a point (q, p) in the *phase space* \mathbb{R}^2 . The component q gives the coordinate of a particle and p is its momentum.

Paraxial optics corresponds to transformations of the phase space over a fixed period of time t under quadratic Hamiltonians. They are also represented by linear transformations of \mathbb{R}^2 with matrices from $\mathrm{SL}_2(\mathbb{R})$, preserve the symplectic form (8.3) and are covariant under the linear changes of coordinates in the phase space with matrices from $\mathrm{SL}_2(\mathbb{R})$.

For a generic Hamiltonian, we can approximate it by a quadratic one at the infinitesimal scale of phase space and time interval t . Thus, the symplectic form becomes an invariant object in the tangent space of the phase space. There is a wide and important class of non-linear transformations of the phase space whose derived form preserves the symplectic form on the tangent space to every point. They are called *canonical transformations*. In particular, Hamiltonian dynamics is a one-parameter group of canonical transformations.

Example 8.6. The transformation of the phase space defined by the matrix J (8.3) is provided by the quadratic Hamiltonian $q^2 + p^2$ of the *harmonic oscillator*. Similarly to the optical Example 8.5, it swaps the coordinates and momenta of the system, rotating the phase space by 90 degrees.

8.3.3 Quantum Mechanics

Having a transformation ϕ of a set X we can always extend it to a linear transformation ϕ^* in a function space defined on X through the ‘change of variables’: $[\phi^*f](x) = f(\phi(x))$. Using this for transformations of the phase space, we obtain a language for working with statistical ensembles: functions on X can describe the probability distribution on the set.

However, there is an important development of this scheme for the case of a homogeneous space $X = G/H$. We use maps $p : G \rightarrow G/H$, $s : X \rightarrow G$ and $r : G \rightarrow H$ defined in Subsection 2.2.2. Let $\chi : H \rightarrow B(V)$ be a linear representation of H in a vector space V . Then, χ induces a linear representation of G in a space of V -valued functions on X given by the

formula (cf. [52, Sec. 13.2.(7)–(9)])

$$[\rho_\chi(g)f](x) = \chi(r(g^{-1} * s(x))) f(g^{-1} \cdot x), \quad (8.5)$$

where $g \in G$, $x \in X$ and $h \in H$. ‘ $*$ ’ denotes multiplication on G and ‘ \cdot ’ denotes the action (2.3) of G on X from the left.

One can build induced representations for the action $\mathrm{SL}_2(\mathbb{R})$ on the classical phase space and, as a result, quantum mechanics emerges from classical mechanics [68, 70]. The main distinction between the two mechanics is encoded in the factor $\chi(r(g^{-1} * s(x)))$ in (8.5). This term switches on self-interaction of functions in linear combinations. Such an effect is natural for *wave packets* rather than the classical statistical distributions.

Example 8.7. Let us return to the matrix J (8.3) and its action on the phase space from Example 8.6. In standard quantum mechanics, the representation (8.5) is induced by a complex-valued character of the subgroup K . Consequently, the action of J is $[\rho_\chi(J)f](p, q) = if(-p, q)$. There are eigenfunctions $w_n(q, p) = (q + ip)^n$ of this action and the respective eigenvalues compose the energy spectrum of a quantum harmonic oscillator. A similar discreteness is responsible for the appearance of spectral lines in the light emission by the atoms of chemical elements.

8.4 Relativity of Space-Time

Relativity describes an invariance of a kinematics with respect to a group of transformations, generated by transitions from one admissible reference system to another. Obviously, it is a counterpart of the Erlangen programme in physics and can be equivalently stated: a physical theory studies invariants under a group of transformations, acting transitively on the set of admissible observers. One will admit that group invariance is much more respected in physics than in mathematics.

We saw an example of $\mathrm{SL}_2(\mathbb{R})$ (symplectic) invariance in the previous section. The main distinction is that the transformations in kinematic relativity involve time components of space-time, while mechanical covariance was formulated for the phase space.

There are many good sources with a comprehensive discussion of relativity—see, for example, [13, 108]. We will briefly outline the main principles, only restricting ourselves to two-dimensional space-time with a one-dimensional spatial component. We also highlight the role of subgroups

N' and A' in the relativity formulation to make a closer connection to the origin of our development – cf. Section 3.3.

Example 8.8 (Galilean relativity of classical mechanics). Denote by (t, x) coordinates in \mathbb{R}^2 , which is identified with space-time. Specifically, t denotes time and x the spatial component. Then, the Galilean relativity principle tells us that the laws of mechanics will be invariant under the shifts of the reference point and the following linear transformations:

$$\begin{pmatrix} t' \\ x' \end{pmatrix} = \begin{pmatrix} t \\ x + vt \end{pmatrix} = G_v \begin{pmatrix} t \\ x \end{pmatrix}, \quad \text{where } G = \begin{pmatrix} 1 & 0 \\ v & 1 \end{pmatrix} \in \text{SL}_2(\mathbb{R}). \quad (8.6)$$

This map translates events to another reference system, which is moving with a constant speed v with respect to the first one. The matrix G_v in (8.6) belongs to the subgroup N' (3.11).

It is easy to see directly that parabolic cycles make an invariant family under the transformations (8.6). These parabolas are graphs of particles moving with a constant acceleration; the acceleration is the reciprocal of the focal length of this parabola (up to a factor). Thus, movements with a constant acceleration a form an invariant class in Galilean mechanics. A particular case is $a = 0$, that is, a uniform motion, which is represented by non-vertical straight lines. Each such line can be mapped to another by a Galilean transformation.

The class of vertical lines, representing sets of simultaneous events, is also invariant under Galilean transformations. In other words, Galilean mechanics possesses the absolute time which is independent from spatial coordinates and their transformations. See [108, Sec. 2] for a detailed examination of Galilean relativity.

A different type class of transformations, discovered by Lorentz and Poincare, is admitted in Minkowski space-time.

Example 8.9 (Lorentz–Poincare). We again take the space-time \mathbb{R}^2 with coordinates (t, x) , but consider linear transformations associated to elements of subgroup A' :

$$\begin{pmatrix} t' \\ x' \end{pmatrix} = \begin{pmatrix} \frac{t-vx}{\sqrt{1-v^2}} \\ \frac{-vt+x}{\sqrt{1-v^2}} \end{pmatrix} = L_v \begin{pmatrix} t \\ x \end{pmatrix} \quad \text{where } L_x = \frac{1}{\sqrt{1-v^2}} \begin{pmatrix} 1 & -v \\ -v & 1 \end{pmatrix}. \quad (8.7)$$

The physical meaning of the transformation is the same: they provide a transition from a given reference system to a new one moving with a velocity v with respect to the first. The relativity principle again requires the

laws of mechanics to be invariant under Lorentz–Poincaré transformations generated by (8.7) and shifts of the reference point.

The admissible values $v \in (-1, 1)$ for transformations (8.7) are bounded by 1, which serves as the *speed of light*. Velocities greater than the speed of light are not considered in this theory. The fundamental object preserved by (8.7) is the *light cone*:

$$C_0 = \{(t, x) \in \mathbb{R}^2 \mid t = \pm x\}. \quad (8.8)$$

More generally, the following quadratic form is also preserved:

$$d_h(t, x) = t^2 - x^2.$$

The light cone C_0 is obviously the collection of points $d_h(t, x) = 0$. For other values, we obtain hyperbolas with asymptotes formed by C_0 . The light cone separates areas of space-time where $d_h(t, x) > 0$ or $d_h(t, x) < 0$. The first consists of *time-like intervals* and the second of *space-like* ones. They can be transformed by (8.7) to pure time $(t, 0)$ or pure space $(0, x)$ intervals, respectively. However, no mixing between intervals of different kinds is admitted by Lorentz–Poincaré transformations.

Furthermore, for time-like intervals, there is a preferred direction which assigns the meaning of the future (also known as the arrow of time) to one half of the cone consisting of time-like intervals, e.g. if the t -component is positive. This *causal orientation* [96, Sec. II.1] is required by the real-world observation that we cannot remember the future states of a physical system but may affect them. Conversely, we may have a record of the system's past but cannot change it in the present.

Exercise 8.10. Check that such a separation of the time-like cone $d_h(t, x) > 0$ into future ($t > 0$) and past ($t < 0$) halves is compatible with the group of Lorentz–Poincaré transformations generated by the hyperbolic rotations (8.7).

However, the causal orientation is not preserved if the group of admissible transformations is extended to conformal maps by an addition of inversions—see Fig. 8.2. Such an extension is motivated by a study of the red shift in astronomy. Namely, spectral lines of chemical elements (cf. Example 8.7) observed from remote stars are shifted toward the red part of the spectrum in comparison to values known from laboratory measurements. Conformal (rather than Lorentz–Poincaré) invariance produces much better correlation to experimental data [96] than the school textbook explanation of a red shift based on the Doppler principle and an expanding universe.

Further discussion of relativity can be found in [13; 108, Sec. 11].

Chapter 9

Invariant Metric and Geodesics

The Euclidean metric is not preserved by automorphisms of the Lobachevsky half-plane. Instead, one has only a weaker property of conformality. However, it is possible to find such a metric on the Lobachevsky half-plane that Möbius transformations will be isometries. Similarly, in Chapter 7, we described a variety of distances and lengths and many of them had conformal properties with respect to $SL_2(\mathbb{R})$ action. However, it is worth finding a metric which is preserved by Möbius transformations. We will now proceed to do this, closely following [56].

Our consideration will be based on equidistant orbits, which physically correspond to wavefronts with a constant velocity. For example, if a stone is dropped into a pond, the resulting ripples are waves which travel the same distance from the drop point, assuming a constant wave velocity. An alternative description to wavefronts uses rays—the paths along which waves travel, i.e. the geodesics in the case of a constant velocity. The duality between wavefronts and rays is provided by Huygens' principle—see [2, Sec. 46].

Geodesics also play a central role in differential geometry, generalising the notion of a straight line. They are closely related to metrics: a geodesic is often defined as a curve between two points with an extremum of length. As a consequence, the metric is additive along geodesics.

9.1 Metrics, Curves' Lengths and Extrema

We start by recalling the standard definition—see [55, Sec. I.2].

Definition 9.1. A *metric* on a set X is a function $d : X \times X \rightarrow \mathbb{R}^+$ such that

- i. $d(x, y) \geq 0$ (positivity),
 - ii. $d(x, y) = 0$ if and only if $x = y$ (non-degeneracy),
 - iii. $d(x, y) = d(y, x)$ (symmetry) and
 - iv. $d(x, y) \leq d(x, z) + d(z, y)$ (the triangle inequality),
- for all $x, y, z \in X$.

Although adequate in many cases, the definition does not cover all metrics of interest. Examples include the non-symmetric lengths from Section 7.2 or distances (7.5) in the Minkowski space with the reverse triangle inequality $d(x, y) \geq d(x, z) + d(z, y)$.

Recall the established procedure of constructing geodesics in Riemannian geometry (two-dimensional case) from [107, Sec. 7]:

- i. Define the (pseudo-)Riemannian metric on the tangent space:

$$g(du, dv) = Edu^2 + Fdudv + Gdv^2. \quad (9.1)$$

- ii. Define the *length for a curve* Γ as:

$$\text{length}(\Gamma) = \int_{\Gamma} (Edu^2 + Fdudv + Gdv^2)^{\frac{1}{2}}. \quad (9.2)$$

- iii. Then, geodesics will be defined as the curves which give a stationary point for the length.
- iv. Lastly, the metric between two points is the length of a geodesic joining those two points.

Exercise 9.2. Let the quadratic form (9.1) be $\text{SL}_2(\mathbb{R})$ -invariant. Show that the above procedure leads to an $\text{SL}_2(\mathbb{R})$ -invariant metric.

We recall from Section 3.7 that an isotropy subgroup H fixing the hypercomplex unit ι under the action of (3.24) is K (3.8), N' (3.11) and A' (3.10) in the corresponding EPH cases. We will refer to H -action as *EPH rotation* around ι . For an $\text{SL}_2(\mathbb{R})$ invariant metric, the orbits of H will be equidistant points from ι , giving some indication what the metric should be. However, this does not determine the metric entirely since there is freedom in assigning values to the orbits.

Lemma 9.3. *The invariant infinitesimal metric in EPH cases is*

$$ds^2 = \frac{du^2 - \sigma dv^2}{v^2}, \quad (9.3)$$

where $\sigma = -1, 0, 1$ respectively.

In the proof below, we will follow the procedure from [16, Sec. 10].

Proof. In order to calculate the infinitesimal metric, consider the subgroups H of Möbius transformations which fix ι . Denote an element of these rotations by E_σ . We require an isometry, so

$$d(\iota, \iota + \delta v) = d(\iota, E_\sigma(\iota + \delta v)).$$

Using the Taylor series, we obtain

$$E_\sigma(\iota + \delta v) = \iota + J_\sigma(\iota)\delta v + o(\delta v),$$

where the Jacobian denoted J_σ is, respectively,

$$\begin{pmatrix} \cos 2\theta & -\sin 2\theta \\ \sin 2\theta & \cos 2\theta \end{pmatrix}, \quad \begin{pmatrix} 1 & 0 \\ 2t & 1 \end{pmatrix} \quad \text{or} \quad \begin{pmatrix} \cosh 2\alpha & \sinh 2\alpha \\ \sinh 2\alpha & \cosh 2\alpha \end{pmatrix}.$$

A metric is invariant under the above rotations if it is preserved under the linear transformation

$$\begin{pmatrix} dU \\ dV \end{pmatrix} = J_\sigma \begin{pmatrix} du \\ dv \end{pmatrix},$$

which turns out to be $du^2 - \sigma dv^2$ in the three cases.

To calculate the metric at an arbitrary point $w = u + iv$, we map w to ι by an affine Möbius transformation, which acts transitively on the upper half-plane

$$r^{-1} : w \rightarrow \frac{w - u}{v}. \quad (9.4)$$

Hence, there is a factor of $\frac{1}{v^2}$, so the resulting metric is $ds^2 = \frac{du^2 - \sigma dv^2}{v^2}$. \square

Corollary 9.4. *With the above notation, for an arbitrary curve Γ ,*

$$\text{length}(\Gamma) = \int_\Gamma \frac{(du^2 - \sigma dv^2)^{\frac{1}{2}}}{v}. \quad (9.5)$$

It is invariant under Möbius transformations of the upper half-plane.

The standard tools for finding geodesics for a given Riemannian metric are the Euler–Lagrange equations – see [107, Sec. 7.1]. For the metric (9.3), they take the form

$$\frac{d}{dt} \left(\frac{\dot{\gamma}_1}{y^2} \right) = 0 \quad \text{and} \quad \frac{d}{dt} \left(\frac{\sigma \dot{\gamma}_2}{y^2} \right) = \frac{\dot{\gamma}_1^2 - \sigma \dot{\gamma}_2^2}{y^3}, \quad (9.6)$$

where γ is a smooth curve $\gamma(t) = (\gamma_1(t), \gamma_2(t))$ and $t \in (a, b)$. This general approach can be used in the two non-degenerate cases (elliptic and hyperbolic) and produces curves with the minimum or maximum lengths,

respectively. However, the $\mathrm{SL}_2(\mathbb{R})$ -invariance of the metric allows us to use more elegant methods in this case. For example, in the Lobachevsky half-plane, the solutions are well known – semicircles orthogonal to the real axes or vertical lines, cf. Fig. 9.1(a) and [6, Ch. 15].

Exercise 9.5. For the elliptic space ($\sigma = -1$):

- i. Write a parametric equation of a circle orthogonal to the real line and check that the curve satisfies the Euler–Lagrange equations (9.6).
- ii. Geodesics passing the imaginary unit i are transverse circles to K -orbits from Fig. 1.2 and Exercise 4.16.iv with the equation, cf. Fig. 9.3(E)

$$(u^2 + v^2) - 2tu - 1 = 0, \quad \text{where } t \in \mathbb{R}. \quad (9.7)$$

- iii. The Möbius invariant metric is

$$m(z, w) = \sinh^{-1} \frac{|z - w|_e}{2\sqrt{\Im[z]\Im[w]}}, \quad (9.8)$$

where $\Im[z]$ is the imaginary part of a complex number z and $|z|_e^2 = u^2 + v^2$.

HINT: One can directly or, by using CAS, verify that this is a Möbius-invariant expression. Thus, we can transform z and w to i and a point on the imaginary axis by a suitable Möbius transformation without changing the metric. The shortest curve in the Riemannian metric (9.3) is the vertical line, that is, $du = 0$. For a segment of the vertical line, the expression (9.8) can easily be evaluated. See also [5, Thm. 7.2.1] for detailed proof and a number of alternative expressions. \diamond

Exercise 9.6. Show, similarly, that, in the hyperbolic case ($\sigma = 1$):

- i. There are two families of solutions passing the double unit j , one space-like (Fig. 9.3(H_S)) and one time-like (Fig. 9.3(H_T)), cf. Section 8.4:

$$(u^2 - v^2) - 2tu + 1 = 0, \quad \text{where } |t| > 1 \text{ or } |t| < 1. \quad (9.9)$$

The space-like solutions are obtained by A' rotation of the vertical axis and the time-like solution is the A' -image of the cycle $(1, 0, 0, 1)$ – cf. Fig. 3.1. They also consist of positive and negative cycles, respectively, which are orthogonal to the real axis.

- ii. The respective metric in these two cases is:

$$d(z, w) = \begin{cases} 2 \sin^{-1} \frac{|z - w|_h}{2\sqrt{\Im[z]\Im[w]}}, & \text{when } z - w \text{ is time-like} \\ 2 \sinh^{-1} \frac{|z - w|_h}{2\sqrt{\Im[z]\Im[w]}}, & \text{when } z - w \text{ is space-like,} \end{cases} \quad (9.10)$$

where $\Im[z]$ is the imaginary part of a double number z and $|z|_h^2 = u^2 - v^2$.
 HINT: The hint from the previous exercise can be used again here with some modification to space-/time-like curves and by replacing the minimum of the possible curves' lengths by the maximum. \diamond

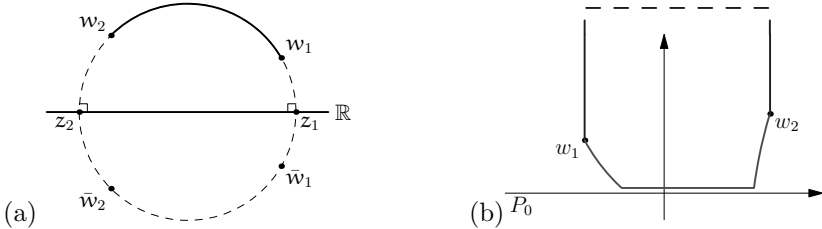


Figure 9.1 Lobachevsky geodesics and extrema of curves' lengths. (a) The geodesic between w_1 and w_2 in the Lobachevsky half-plane is the circle orthogonal to the real line. The invariant metric is expressed through the cross-ratios $[z_1, w_1, w_2, z_2] = [\bar{w}_1, w_1, w_2, \bar{w}_2]$. (b) Extrema of curves' lengths in the parabolic point space. The length of the blue curve (going up) can be arbitrarily close to 0 and can be arbitrarily large for the red one (going down).

The same geodesic equations can be obtained by Beltrami's method—see [13, Sec. 8.1]. However, the parabolic case presents yet another disappointment.

Exercise 9.7. Show that, for the parabolic case ($\sigma = 0$):

- i. The only solution of the Euler–Lagrange equations (9.6) are vertical lines, as in [108, Sec. 3], which are again orthogonal to the real axes.
- ii. Vertical lines minimise the curves' length between two points w_1 and w_2 . See Fig. 9.1(b) for an example of a blue curve with its length tending to zero value of the infimum. The respective 'geodesics' passing the dual unit ε are

$$u^2 - 2tu = 0. \quad (9.11)$$

Similarly, a length of the red curve can be arbitrarily large if the horizontal path is close enough to the real axis.

- iii. The only $\text{SL}_2(\mathbb{R})$ -invariant metric obtained from the above extremal consideration is either identically equal to 0 or infinity.

There is a similarity between all three cases. For example, we can uniformly write equations (9.7), (9.9) and (9.11) of geodesics through ι as

$$(u^2 - \sigma v^2) - 2tu + \sigma = 0, \quad \text{where } t \in \mathbb{R}.$$

However, the triviality of the parabolic invariant metric is awkward and we go on to study further the algebraic and geometric invariants to find a more adequate answer.

9.2 Invariant Metric

We seek all real-valued functions f of two points on the half-plane which are invariant under the Möbius action

$$f(g(z), g(w)) = f(z, w) \quad \text{for all } z, w \in \mathbb{A} \quad \text{and } g \in \text{SL}_2(\mathbb{R}).$$

We have already seen one like this in (9.8) and (9.10):

$$F(z, w) = \frac{|z - w|_\sigma}{\sqrt{\Im[z]\Im[w]}}, \quad (9.12)$$

which can be shown by a simple direct calculation (for CAS, see Exercise 9.5.iii). Recall that $|z|_\sigma^2 = u^2 - \sigma v^2$ by analogy with the distance $d_{\sigma, \sigma}$ (7.5) in EPH geometries and [108, App. C]. In order to describe other invariant functions we will need the following definition.

Definition 9.8. A function $f : X \times X \rightarrow \mathbb{R}^+$ is called a *monotonous* metric if $f(\Gamma(0), \Gamma(t))$ is a continuous monotonically-increasing function of t , where $\Gamma : [0, 1) \rightarrow X$ is a smooth curve with $\Gamma(0) = z_0$ that intersects all equidistant orbits of z_0 exactly once.

Exercise 9.9. Check the following:

- i. The function $F(z, w)$ (9.12) is monotonous.
- ii. If h is a monotonically-increasing, continuous, real function, then $f(z, w) = h \circ F(z, w)$ is a monotonous $\text{SL}_2(\mathbb{R})$ -invariant function.

In fact, the last example provides all such functions.

Theorem 9.10. A monotonous function $f(z, w)$ is invariant under $g \in \text{SL}_2(\mathbb{R})$ if and only if there exists a monotonically-increasing, continuous, real function h such that $f(z, w) = h \circ F(z, w)$.

Proof. Because of the Exercise 9.9.ii, we show the necessity only. Suppose there exists another function with such a property, say, $H(z, w)$. Due to invariance under $\text{SL}_2(\mathbb{R})$, this can be viewed as a function in one variable if we apply r^{-1} (cf. (9.4)) which sends z to ι and w to $r^{-1}(w)$. Now, by considering a fixed smooth curve Γ from Definition 9.8, we can completely

define $H(z, w)$ as a function of a single real variable $h(t) = H(i, \Gamma(t))$ and, similarly for $F(z, w)$,

$$H(z, w) = H(i, r^{-1}(w)) = h(t) \quad \text{and} \quad F(z, w) = F(i, r^{-1}(w)) = f(t),$$

where h and f are both continuous and monotonically-increasing since they represent metrics. Hence, the inverse f^{-1} exists everywhere by the inverse function theorem. So,

$$H(i, r^{-1}(w)) = h \circ f^{-1} \circ F(i, r^{-1}(w)).$$

Note that hf^{-1} is monotonic, since it is the composition of two monotonically-increasing functions, and this ends the proof. \square

Remark 9.11. The above proof carries over to a more general theorem which states: If there exist two monotonous functions $F(u, v)$ and $H(u, v)$ which are invariant under a transitive action of a group G , then there exists a monotonically-increasing real function h such that $H(z, w) = h \circ F(z, w)$.

As discussed in the previous section, in elliptic and hyperbolic geometries the function h from above is either $\sinh^{-1} t$ or $\sin^{-1} t$ (9.8) (9.10). Hence, it is reasonable to try inverse trigonometric and hyperbolic functions in the intermediate parabolic case as well.

Remark 9.12. The above result sheds light on the possibilities we have—we can either

- i. ‘label’ the equidistant orbits with numbers, i.e choose a function h which will then determine the geodesic, or
- ii. choose a geodesic which will then determine h .

These two approaches are reflected in the next two sections.

9.3 Geodesics: Additivity of Metric

As pointed out earlier, there might not be a metric function which satisfies all the traditional properties. However, we still need the key ones, and we therefore make the following definition:

Definition 9.13. *Geodesics* for a metric d are smooth curves along which d is additive, that is $d(x, y) + d(y, z) = d(x, z)$, for any three point, of the curve, such that y is between x and z .

This definition is almost identical to the Menger line—see [10, Sec. 2.3].

Remark 9.14. It is important that this definition is relevant in all EPH cases, i.e. in the elliptic and hyperbolic cases it would produce the well-known geodesics defined by the extremality condition.

Schematically, the proposed approach is:

$$\text{invariant metric} \xrightarrow{\text{additivity}} \text{invariant geodesic}. \quad (9.13)$$

Compare this with the Riemannian described in Section 9.1:

$$\text{local metric} \xrightarrow{\text{extrema}} \text{geodesic} \xrightarrow{\text{integration}} \text{metric}. \quad (9.14)$$

Let us now proceed with finding geodesics from a metric function.

Exercise 9.15. Let γ be a geodesic for a metric d . Write the differential equation for γ in term of d .

HINT: Consider $d(w, w')$ as a real function in four variables, say $f(u, v, u', v')$. Then write the infinitesimal version of the additivity condition and obtain the equation

$$\frac{\delta v}{\delta u} = \frac{-f'_3(u, v, u', v') + f'_3(u', v', u', v')}{f'_4(u, v, u', v') - f'_4(u', v', u', v')}, \quad (9.15)$$

where f'_n stands for the partial derivative of f with respect to the n -th variable. \diamond

A natural choice for a metric is, cf. Exercises 9.5.iii and 9.6.ii,

$$d_{\sigma, \mathring{\sigma}}(w, w') = \sin_{\mathring{\sigma}}^{-1} \frac{|w - w'|_{\sigma}}{2\sqrt{\Im[w]\Im[w']}}, \quad (9.16)$$

where the elliptic, parabolic and hyperbolic inverse sine functions are (see [38, 64])

$$\sin_{\mathring{\sigma}}^{-1} t = \begin{cases} \sinh^{-1} t, & \text{if } \mathring{\sigma} = -1, \\ 2t, & \text{if } \mathring{\sigma} = 0, \\ \sin^{-1} t, & \text{if } \mathring{\sigma} = 1. \end{cases} \quad (9.17)$$

Note that $\mathring{\sigma}$ is independent of σ although it takes the same three values, similar to the different signatures of point and cycle spaces introduced in Chapter 4. It is used to denote the possible sub-cases within the parabolic geometry alone.

Exercise 9.16. Check that:

- i. For $u = 0, v = 1$ and the metric $d_{p, \mathring{\sigma}}$ (9.16), Equation (9.15) is:

$$\frac{\delta v}{\delta u} = \frac{2v}{u} - \frac{\sqrt{|\mathring{\sigma}u^2 + 4v|}}{u}.$$

ii. The geodesics through ι for the metric $d_{p,\hat{\sigma}}$ (9.16) are parabolas:

$$(\hat{\sigma} + 4t^2)u^2 - 8tu - 4v + 4 = 0. \quad (9.18)$$

Let us verify which properties from Definition 9.1 are satisfied by the invariant metric derived from (9.16). Two of the four properties hold—it is clearly symmetric and positive for every two points. However, the metric of any point to a point on the same vertical line is zero, so $d(z, w) = 0$ does not imply $z = w$. This can be overcome by introducing a different metric function just for the points on the vertical lines—see [108, Sec. 3]. Note that we still have $d(z, z) = 0$ for all z .

The triangle inequality holds only in the elliptic point space, whereas, in the hyperbolic point space, we have the reverse situation: $d(w_1, w_2) \geq d(w_1, z) + d(z, w_2)$. There is an intermediate situation in the parabolic point space:

Lemma 9.17. *Take any $\text{SL}_2(\mathbb{R})$ -invariant metric function and take two points w_1, w_2 and the geodesic (in the sense of Definition 9.13) through the points. Consider the strip $\Re[w_1] < u < \Re[w_2]$ and take a point z in it. Then, the geodesic divides the strip into two regions where $d(w_1, w_2) \leq d(w_1, z) + d(z, w_2)$ and where $d(w_1, w_2) \geq d(w_1, z) + d(z, w_2)$.*

Proof. The only possible invariant metric function in parabolic geometry is of the form $d(z, w) = h \circ \frac{|\Re[z-w]|}{2\sqrt{\Im[z]\Im[w]}}$, where h is a monotonically-increasing, continuous, real function by Theorem 9.10. Fix two points w_1, w_2 and the geodesic through them. Now consider some point $z = a + ib$ in the strip. The metric function is additive along a geodesic, so $d(w_1, w_2) = d(w_1, w(a)) + d(w(a), w_2)$, where $w(a)$ is a point on the geodesic with real part equal to a . However, if $\Im[w(a)] < b$, then $d(w_1, w(a)) > d(w_1, z)$ and $d(w(a), w_2) > d(z, w_2)$, which implies $d(w_1, w_2) > d(w_1, z) + d(z, w_2)$. Similarly, if $\Im[w(a)] > b$, then $d(w_1, w_2) < d(w_1, z) + d(z, w_2)$. \square

Remark 9.18. The reason for the ease with which the result is obtained is the fact that the metric function is additive along the geodesics. This justifies the Definition 9.13 of geodesics, in terms of additivity.

To illustrate these ideas, look at the region where the converse of the triangular inequality holds for $d(z, w)_{\hat{\sigma}} = \sin_{\hat{\sigma}}^{-1} \frac{|\Re[z-w]|}{2\sqrt{\Im[z]\Im[w]}}$, shaded red in Fig. 9.2. It is enclosed by two parabolas both of the form $(\hat{\sigma} + 4t^2)u^2 - 8tu - 4v + 4 = 0$ (which is the general equation of geodesics) and both passing through the two fixed points. The parabolas arise from taking both signs of

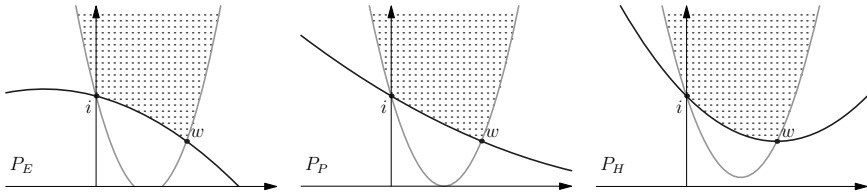


Figure 9.2 Showing the region where the triangular inequality fails (shaded red).

the root, when solving the quadratic equation to find t . Segments of these parabolas, which bound the red region, are of different types—one of them is between points w_1 and w_2 , the second joins these points with infinity.

9.4 Geometric Invariants

In the previous section, we defined an invariant metric and derived the respective geodesics. Now, we will proceed in the opposite direction. As we discussed in Exercise 9.7, the parabolic invariant metric obtained from the extremality condition is trivial. We work out an invariant metric from the Riemannian metric and predefined geodesics. It is schematically depicted, cf. (9.14), by

$$\text{Riemann metric} + \text{invariant geodesics} \xrightarrow{\text{integration}} \text{metric}. \quad (9.19)$$

A minimal requirement for the family of geodesics is that they should form an invariant subset of an invariant class of curves with no more than one curve joining every two points. Thus, if we are looking for $\text{SL}_2(\mathbb{R})$ -invariant metrics it is natural to ask whether geodesics are cycles. An invariant subset of cycles may be characterised by an invariant algebraic condition, e.g. orthogonality. However, the ordinary orthogonality is already fulfilled for the trivial geodesics from Exercise 9.7, so, instead, we will try f-orthogonality to the real axes, Definition 6.34. Recall that a cycle is f-orthogonal to the real axes if the real axes inverted in a cycle are orthogonal (in the usual sense) to the real axes.

Exercise 9.19. Check that a parabola $ku^2 - 2lu - 2nv + m = 0$ is $\hat{\sigma}$ -f-orthogonal to the real line if $l^2 + \hat{\sigma}n^2 - mk = 0$, i.e. it is a $(-\hat{\sigma})$ -zero radius cycle.

As a starting point, consider the cycles that pass through ι . It is enough to specify only one such f-orthogonal cycle—the rest will be obtained

by Möbius transformations fixing ι , i.e. parabolic rotations. Within these constraints there are three different families of parabolas determined by the value $\hat{\sigma}$.

Exercise 9.20. Check that the main parabolas passing ε



$$\hat{\sigma}u^2 - 4v + 4 = 0, \quad (9.20)$$

where $\hat{\sigma} = -1, 0, 1$, are f -orthogonal to the real line. Their rotations by an element of N' are parabolas (9.18).

Note that these are exactly the same geodesics obtained in (9.18). Hence, we already know what the metric function has to be. However, it is instructive to make the calculation from scratch since it does not involve anything from the previous section and is, in a way, more elementary and intuitive.

Exercise 9.21. Follow these steps to calculate the invariant metric:

- i. Calculate the metric from ε to a point on the main parabola (9.20).

HINT: Depending on whether the discriminant of the denominator in the integral (9.2) is positive, zero or negative, the results are trigonometric, rationals or hyperbolic, respectively:

$$\int_0^u \frac{dt}{\frac{1}{4}\hat{\sigma}t^2 + 1} = \begin{cases} 4 \log \frac{2+u}{2-u}, & \text{if } \hat{\sigma} = -1, \\ u, & \text{if } \hat{\sigma} = 0, \\ \tan^{-1} \frac{u}{2}, & \text{if } \hat{\sigma} = 1. \end{cases}$$

This is another example of EPH classification. \diamond

- ii. For a generic point (u, v) , find the N' rotation which puts the point on the main parabola (9.20).
- iii. For two given points w and w' , combine the Möbius transformation g such that $g : w \mapsto \varepsilon$ with the N' -rotation which puts $g(w')$ on the main parabola.
- iv. Deduce from the previous items the invariant metric from ε to (u, v) and check that it is a multiple of (9.16).
- v. The invariant parabolic metric for $\hat{\sigma} = 1$ is equal to the angle between the tangents to the geodesic at its endpoints.

We meet an example of the splitting of the parabolic geometry into three different sub-cases, this will followed by three types of Cayley transform in Section 10.3 and Fig. 10.3. The respective geodesics and equidistant orbits have been drawn in Fig. 9.3. There is one more gradual transformation

between the different geometries. We can see the transitions from the elliptic case to P_e , then to P_p , to P_h , to hyperbolic light-like and, finally, to space-like. To link it back, we observe a similarity between the final space-like case and the initial elliptic one.

Exercise 9.22. Show that all parabolic geodesics from ε for a given value of $\hat{\sigma}$ touch a certain parabola. This parabola can be called the *horizon* because geodesic rays will never reach points outside it. Note the similar effect for space-like and time-like geodesics in the hyperbolic case.

There is one more useful parallel between all the geometries. In Lobachevsky and Minkowski geometries, the *centres* of geodesics lie on the real axes. In parabolic geometry, the respective $\hat{\sigma}$ -*foci* (see Definition 5.2) of $\hat{\sigma}$ -geodesic parabolas lie on the real axes. This fact is due to the relations between f-orthogonality and foci, cf. Proposition 6.40.

9.5 Invariant Metric and Cross-Ratio

A very elegant presentation of the Möbius-invariant metric in the Lobachevsky half-plane is based on the cross-ratio (4.14)–see [6, Sec. 15.2].

Let w_1 and w_2 be two different points of the Lobachevsky half-plane. Draw a selfadjoint circle (i.e. orthogonal to the real line) which passes through w_1 and w_2 . Let z_1 and z_2 be the points of intersection of the circle and the real line, cf. Fig. 9.1(a). From Exercise 4.22.iii, a cross-ratio of four concyclic points is real, thus we define the function of two points

$$\rho(w_1, w_2) = \log[z_1, w_1, w_2, z_2].$$

Surprisingly, this simple formula produces the Lobachevsky metric.

Exercise 9.23. Show the following properties of ρ :

- i. It is Möbius-invariant, i.e. $\rho(w_1, w_2) = \rho(g \cdot w_1, g \cdot w_2)$ for any $g \in \text{SL}_2(\mathbb{R})$.
HINT: Use the fact that selfadjoint cycles form an invariant family and the Möbius-invariance of the cross-ratio, cf. Exercise 4.20.iv. \diamond
- ii. It is additive, that is, for any three different points w_1, w_2, w_3 on the arc of a selfadjoint circle we have $\rho(w_1, w_3) = \rho(w_1, w_2) + \rho(w_2, w_3)$.
HINT: Use the cancellation formula (4.18). \diamond
- iii. It coincides with the Lobachevsky metric (9.8).
HINT: Evaluate that $\rho(i, ia) = \log a$ for any real $a > 1$. Thus, $\rho(i, ia)$ is the Lobachevsky metric between i and ia . Then, apply the Möbius-invariance of ρ and the Lobachevsky metric to extend the identity for any pair of points. \diamond

This approach to the invariant metric cannot be transferred to the parabolic and hyperbolic cases in a straightforward manner for geometric reasons. As we can see from Fig. 9.3, there are certain types of geodesics which do not meet the real line. However, the case of e-geodesics in \mathbb{D} , which is the closest relative of the Lobachevsky half-plane, offers such a possibility.

Exercise 9.24. Check that:

- i. $[-2, \varepsilon, w, 2] = (u + 2)/(2 - u)$, where $w = u + \varepsilon(1 - u^2/4)$, $u > 0$ is the point of the e-geodesics (main parabola) (9.20) passing ε and 2.
- ii. Let z_1 and z_2 be the intersections of the real line and the e-geodesic (9.18) passing two different points w_1 and w_2 in the upper half-plane, then $\rho(w_1, w_2) = 4 \log[z_1, w_1, w_2, z_2]$ is the invariant metric.
HINT: Note that $\rho(\varepsilon, z) = 4 \log[-2, \varepsilon, z, 2]$ gives the metric calculated in Exercise 9.21.i and use the Möbius-invariance of the cross-ratio. \diamond
- iii. In the case of p-geodesics in \mathbb{D} , find a fixed parabola C in the upper half-plane which replaces the real line in the following sense. The cross-ratio of two points and two intersections of C with p-geodesics though the points produces an invariant metric. Find also the corresponding parabola for h-geodesics.

This is only a partial success in transferring of the elliptic theory to dual numbers. A more unified treatment for all EPH cases can be obtained from the projective cross-ratio [15]—see Section 4.5 for corresponding definitions and results. In addition, we define the map $P(x, y) = \frac{x}{y}$ on the subset of $\mathbb{P}^1(\mathbb{A})$ consisting of vectors $(x, y) \in \mathbb{A}^2$ such that y is not a zero divisor. It is a left inverse of the map $S(z) = (z, 1)$ from Section 4.5.

Exercise 9.25. [15] Let $w_1, w_2 \in \mathbb{P}^1(\mathbb{A})$ be two essentially distinct points.

- i. Let w_1 and \bar{w}_2 be essentially distinct, express a generic invariant metric in $\mathbb{P}^1(\mathbb{A})$ through $[w_1, \bar{w}_2, w_2, \bar{w}_1]$ using the Möbius-invariance of the projective cross-ratio and the method from Section 9.2.
- ii. For \mathbb{A} being complex or double numbers, let w_1 and w_2 be in the domain of P and $z_i = P(w_i)$, $i = 1, 2$. Show that, cf. Fig. 9.1(a),

$$[w_1, \bar{w}_1, w_2, \bar{w}_2] = S \left(\frac{|z_1 - z_2|_\sigma^2}{4\Im[z_1]\Im[z_2]} \right). \quad (9.21)$$

Deduce a generic Möbius-invariant metric on \mathbb{A} based on (9.12).

To obtain the respective notion of geodesics in $\mathbb{P}^1(\mathbb{A})$ from the above Möbius-invariant metric we can again use the route from Section 9.3.

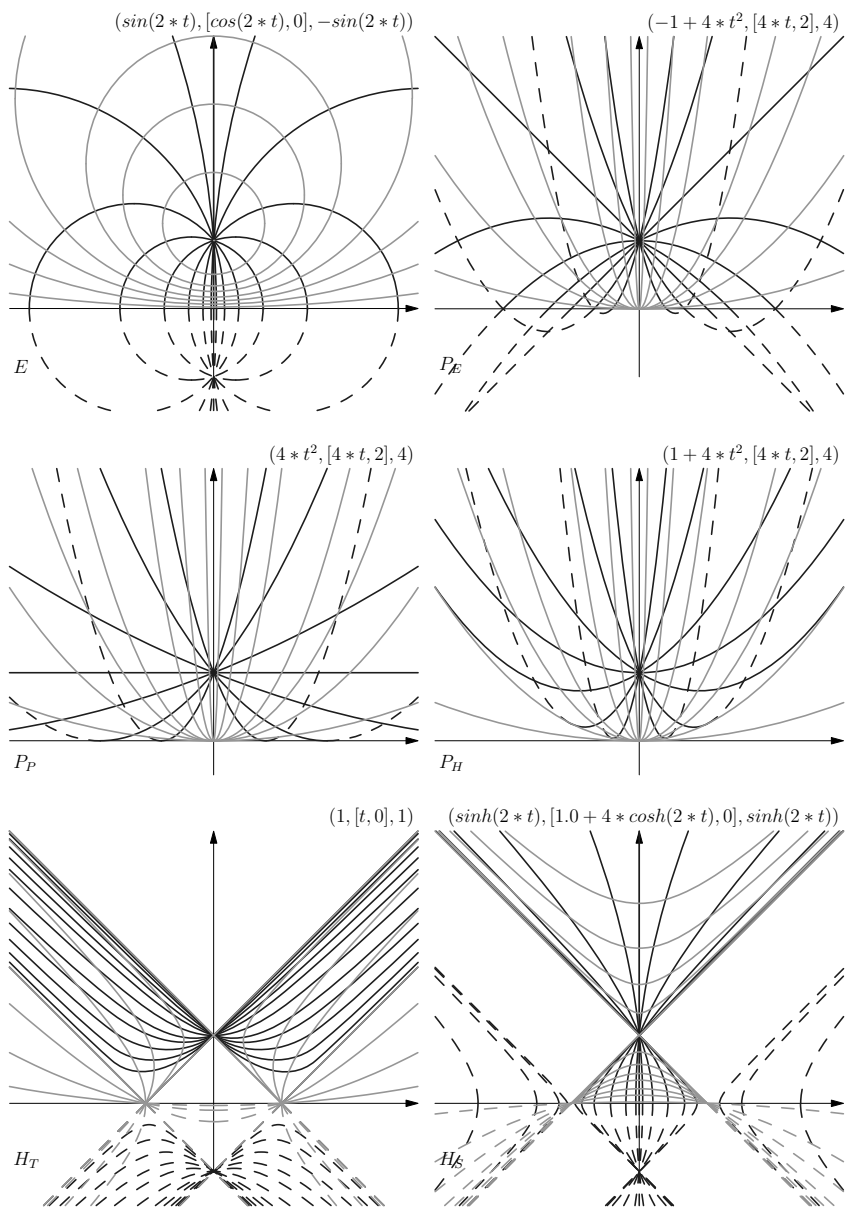


Figure 9.3 Showing geodesics (blue) and equidistant orbits (green) in EPH geometries. Above are written $(k, [l, n], m)$ in $ku^2 - 2lu - 2nv + m = 0$, giving the equation of geodesics.

Chapter 10

Conformal Unit Disk

The upper half-plane is a universal object for all three EPH cases, which was obtained in a uniform fashion considering two-dimensional homogeneous spaces of $\mathrm{SL}_2(\mathbb{R})$. However, universal models are rarely well-suited to all circumstances. For example, it is more convenient, for many reasons, to consider the compact *unit disk* in \mathbb{C} rather than the unbounded upper half-plane:

... the reader must become adept at frequently changing from one model to the other as each has its own particular advantage. [5, Sec. 7.1]

Of course, both models are conformally-isomorphic through the *Cayley transform*.

We derive similar constructions for parabolic and hyperbolic cases in this chapter. However, we shall see that there is not a ‘universal unit disk’. Instead, we obtain something specific in each EPH case from the same upper half-plane. As has already happened on several occasions, the elliptic and hyperbolic cases are rather similar and, thus, it is the parabolic case which requires special treatment.

10.1 Elliptic Cayley Transforms

In the elliptic and hyperbolic cases, the Cayley transform is given by the matrix $Y_\sigma = \begin{pmatrix} 1 & -\iota \\ \sigma\iota & 1 \end{pmatrix}$, where $\sigma = \iota^2$ and $\det Y_\sigma = 2$. The matrix Y_σ produces the respective Möbius transform $\mathbb{A} \rightarrow \mathbb{A}$:

$$\begin{pmatrix} 1 & -\iota \\ \sigma\iota & 1 \end{pmatrix} : w = (u + \iota v) \mapsto Y_\sigma w = \frac{(u + \iota v) - \iota}{\sigma\iota(u + \iota v) + 1}. \quad (10.1)$$

The same matrix Y_σ acts by conjugation $g_Y = \frac{1}{2}Y_\sigma g Y_\sigma^{-1}$ on an element $g \in \text{SL}_2(\mathbb{R})$:

$$g_Y = \frac{1}{2} \begin{pmatrix} 1 & -\iota \\ \sigma\iota & 1 \end{pmatrix} \begin{pmatrix} a & b \\ c & d \end{pmatrix} \begin{pmatrix} 1 & \iota \\ -\sigma\iota & 1 \end{pmatrix}. \quad (10.2)$$

The connection between the two forms (10.1) and (10.2) of the Cayley transform is $g_Y Y_\sigma w = Y_\sigma(gw)$, i.e. Y_σ intertwines the actions of g and g_Y .

The Cayley transform in the elliptic case is very important [77, Sec. IX.3; 101, Ch. 8, (1.12)], both for complex analysis and representation theory of $\text{SL}_2(\mathbb{R})$. The transformation $g \mapsto g_Y$ (10.2) is an isomorphism of the groups $\text{SL}_2(\mathbb{R})$ and $\text{SU}(1, 1)$. Namely, in complex numbers, we have

$$g_Y = \frac{1}{2} \begin{pmatrix} \alpha & \beta \\ \bar{\beta} & \bar{\alpha} \end{pmatrix}, \text{ with } \alpha = (a+d) + (b-c)i \text{ and } \beta = (b+c) + (a-d)i. \quad (10.3)$$

The group $\text{SU}(1, 1)$ acts transitively on the *elliptic unit disk*. The images of the elliptic actions of subgroups A , N , K are given in Fig. 10.3(E). Any other subgroup is conjugated to one of them and its class can be easily distinguished in this model by the number of *fixed points on the boundary* – two, one and zero, respectively. A closer inspection demonstrates that there are always *two* fixed points on the whole plane. They are either

- one strictly inside and one strictly outside of the unit circle,
- one *double* fixed point on the unit circle, or
- two different fixed points exactly on the circle.

Consideration of Fig. 7.1(b) shows that the parabolic subgroup N is like a phase transition between the elliptic subgroup K and hyperbolic A , cf. (1.2). Indeed, if a fixed point of a subgroup conjugated to K approaches a place on the boundary, then the other fixed point moves to the same place on the unit disk from the opposite side. After they collide to a parabolic double point on the boundary, they may decouple into two distinct fixed points on the unit disk representing a subgroup conjugated to A .

In some sense the elliptic Cayley transform swaps complexities. In contrast to the upper half-plane, the K -action is now simple but A and N are not. The simplicity of K orbits is explained by diagonalisation of the corresponding matrices:

$$\frac{1}{2} \begin{pmatrix} 1 & -i \\ -i & 1 \end{pmatrix} \begin{pmatrix} \cos \phi & \sin \phi \\ -\sin \phi & \cos \phi \end{pmatrix} \begin{pmatrix} 1 & i \\ i & 1 \end{pmatrix} = \begin{pmatrix} e^{i\phi} & 0 \\ 0 & e^{-i\phi} \end{pmatrix}. \quad (10.4)$$

These diagonal matrices generate Möbius transformations which correspond to multiplication by the unimodular scalar $e^{2i\phi}$. Geometrically, they are isometric rotations, i.e. they preserve distances $d_{e,e}$ (7.2) and length l_{c_e} .

Exercise 10.1. Check, in the elliptic case, that the real axis is transformed to the *unit circle* and the upper half-plane is mapped to the *elliptic unit disk*

$$\mathbb{R} = \{(u, v) \mid v = 0\} \rightarrow \mathbb{T}_e = \{(u, v) \mid l_{c_e}^2(u, v) = u^2 + v^2 = 1\}, \quad (10.5)$$

$$\mathbb{R}_+^e = \{(u, v) \mid v > 0\} \rightarrow \mathbb{D}_e = \{(u, v) \mid l_{c_e}^2(u, v) = u^2 + v^2 < 1\}, \quad (10.6)$$

where the length from centre $l_{c_e}^2$ is given by (7.6) for $\sigma = \check{\sigma} = -1$ and coincides with the distance $d_{e,e}$ (7.2).

$\mathrm{SL}_2(\mathbb{R})$ acts transitively on both sets and the unit circle is generated, for example, by the point $(0, 1)$, and the unit disk by $(0, 0)$.

10.2 Hyperbolic Cayley Transform

A hyperbolic version of the Cayley transform was used in [58]. The above formula (10.2) in \mathbb{O} becomes

$$g_Y = \frac{1}{2} \begin{pmatrix} \alpha & \beta \\ -\bar{\beta} & \bar{\alpha} \end{pmatrix}, \text{ with } \alpha = a + d - (b + c)\mathbf{j} \text{ and } h = (a - d)\mathbf{j} + (b - c), \quad (10.7)$$

with some subtle differences in comparison to (10.3). The corresponding A , N and K orbits are given in Fig. 10.3(H). However, there is an important distinction between the elliptic and hyperbolic cases similar to the one discussed in Section 8.2.

Exercise 10.2. Check, in the hyperbolic case, that the real axis is transformed to the cycle

$$\mathbb{R} = \{(u, v) \mid v = 0\} \rightarrow \mathbb{T}_h = \{(u, v) \mid l_{c_h}^2(u, v) = u^2 - v^2 = -1\}, \quad (10.8)$$

where the length from the centre $l_{c_h}^2$ is given by (7.6) for $\sigma = \check{\sigma} = 1$ and coincides with the distance $d_{h,h}$ (7.2). On the hyperbolic unit circle, $\mathrm{SL}_2(\mathbb{R})$ acts transitively and it is generated, for example, by point $(0, 1)$.

$\mathrm{SL}_2(\mathbb{R})$ acts also *transitively on the whole complement*

$$\{(u, v) \mid l_{c_h}^2(u, v) \neq -1\}$$

to the unit circle, i.e. on its ‘inner’ and ‘outer’ parts together.

Recall from Section 8.2 that we defined $\tilde{\mathbb{O}}$ to be the two-fold cover of the hyperbolic point space \mathbb{O} consisting of two isomorphic copies \mathbb{O}^+ and \mathbb{O}^- glued together, cf. Fig. 8.3. The conformal version of the *hyperbolic unit disk* in $\tilde{\mathbb{O}}$ is, cf. the upper half-plane from (8.1),

$$\tilde{\mathbb{D}}_h = \{(u, v) \in \mathbb{O}^+ \mid u^2 - v^2 > -1\} \cup \{(u, v) \in \mathbb{O}^- \mid u^2 - v^2 < -1\}. \quad (10.9)$$

Exercise 10.3. Verify that:

- i. $\tilde{\mathbb{D}}_h$ is conformally-invariant and has a boundary $\tilde{\mathbb{T}}_h$ – two copies of the unit hyperbolas in \mathbb{O}^+ and \mathbb{O}^- .
- ii. The hyperbolic Cayley transform is a one-to-one map between the hyperbolic upper half-plane $\tilde{\mathbb{O}}^+$ and hyperbolic unit disk $\tilde{\mathbb{D}}_h$.

We call $\tilde{\mathbb{T}}_h$ the *hyperbolic unit cycle* in \mathbb{O} . Figure 8.3(b) illustrates the geometry of the hyperbolic unit disk in $\tilde{\mathbb{O}}$ compared to the upper half-plane. We can also say, rather informally, that the hyperbolic Cayley transform maps the ‘upper’ half-plane onto the ‘inner’ part of the unit disk.

One may wish that the hyperbolic Cayley transform diagonalises the action of subgroup A , or some conjugate of it, in a fashion similar to the elliptic case (10.4) for K . Geometrically, it corresponds to hyperbolic rotations of the hyperbolic unit disk around the origin. Since the origin is the image of the point ι in the upper half-plane under the Cayley transform, we will use the isotropy subgroup A' . Under the Cayley map (10.7), an element of the subgroup A' becomes

$$\frac{1}{2} \begin{pmatrix} 1 & -j \\ j & 1 \end{pmatrix} \begin{pmatrix} \cosh t & -\sinh t \\ -\sinh t & \cosh t \end{pmatrix} \begin{pmatrix} 1 & j \\ -j & 1 \end{pmatrix} = \begin{pmatrix} e^{jt} & 0 \\ 0 & e^{-jt} \end{pmatrix}, \quad (10.10)$$

where $e^{jt} = \cosh t + j \sinh t$. The corresponding Möbius transformation is a multiplication by e^{2jt} , which obviously corresponds to isometric hyperbolic rotations of \mathbb{O} for distance $d_{h,h}$ and length l_{c_h} . This is illustrated in Fig. 10.1(H:A').

10.3 Parabolic Cayley Transforms

The parabolic case benefits from a larger variety of choices. The first, natural, attempt is to define a Cayley transform from the same formula (10.1) with the parabolic value $\sigma = 0$. The corresponding transformation is defined by the matrix $\begin{pmatrix} 1 & -\varepsilon \\ 0 & 1 \end{pmatrix}$ and, geometrically, produces a shift one unit down.

However, within the extended FSCc, a more general version of the parabolic Cayley transform is also possible. It is given by the matrix

$$Y_{\check{\sigma}} = \begin{pmatrix} 1 & -\varepsilon \\ \check{\sigma}\varepsilon & 1 \end{pmatrix}, \quad \text{where } \check{\sigma} = -1, 0, 1 \text{ and } \det Y_{\check{\sigma}} = 1 \text{ for all } \check{\sigma}. \quad (10.11)$$

Here, $\check{\sigma} = -1$ corresponds to the parabolic Cayley transform P_e with an elliptic flavour, and $\check{\sigma} = 1$ to the parabolic Cayley transform P_h with a hyperbolic flavour. Finally, the parabolic-parabolic transform P_p is given by the upper-triangular matrix mentioned at the beginning of this section.

Figure 10.3 presents these transforms in rows P_e , P_p and P_h , respectively. The row P_p almost coincides with Fig. 1.1 and the parabolic case in Fig. 1.2. Consideration of Fig. 10.3 by following the columns from top to bottom gives an impressive mixture of many common properties (e.g. the number of fixed points on the boundary for each subgroup) with several gradual mutations.

The description of the parabolic unit disk admits several different interpretations in terms of lengths from Definition 7.9.

Exercise 10.4. The parabolic Cayley transform $P_{\check{\sigma}}$, as defined by the matrix $Y_{\check{\sigma}}$ (10.11), always acts on the V -axis as a shift one unit down.

If $\check{\sigma} \neq 0$, then $P_{\check{\sigma}}$ transforms the real axis to the *parabolic unit cycle* such that

$$\mathbb{T}^{p\check{\sigma}} = \{(u, v) \in \mathbb{D} \mid l^2(B, (u, v)) \cdot (-\check{\sigma}) = 1\}, \quad (10.12)$$

and the image of upper half-plane is

$$\mathbb{D}^{p\check{\sigma}} = \{(u, v) \in \mathbb{D} \mid l^2(B, (u, v)) \cdot (-\check{\sigma}) < 1\}, \quad (10.13)$$

where the length l and the point B can be any of the following:

- i. $l^2 = l_{c_e}^2(B, (u, v)) = u^2 + \check{\sigma}v$ is the (p,p,e)-length (7.6) from the e-centre $B_e = (0, -\frac{\check{\sigma}}{2})$.
- ii. $l^2 = l_{f_h}^2(B, (u, v))$ is the (p,p,h)-length (7.8) from the h-focus $B = (0, -1 - \frac{\check{\sigma}}{4})$.
- iii. $l^2 = l_{f_p}^2(B, (u, v)) = \frac{u^2}{v+1}$ is the (p,p,p)-length (7.9) from the p-focus $B = (0, -1)$.

HINT: The statements are slightly tautological, since, by definition, p-cycles are the loci of points with certain defined lengths from their respective centres or foci. \diamond

Remark 10.5. Note that both the elliptic (10.5) and hyperbolic (10.8) unit cycles can be also presented in the form similar to (10.12),

$$\mathbb{D}_{\sigma} = \{(u', v') \mid l_{c_{\sigma}}^2(B, (u, v)) \cdot (-\sigma) = 1\},$$

in terms of the (σ, σ) -length from the σ -centre $B = (0, 0)$ as in Exercise 10.4.i.

The above descriptions (10.4.i and 10.4.iii) are attractive for reasons given in the following two exercises. Firstly, we note that K -orbits in the elliptic case (Fig. 10.1(E:K)) and A' -orbits in the hyperbolic case (Fig. 10.1(H:A')) of the Cayley transform are concentric.

Exercise 10.6. N -orbits in the parabolic cases (Fig. 10.3($P_e : N$, $P_p : N$, $P_h : N$)) are *concentric parabolas* (or straight lines) in the sense of Definition 4.3 with e-centres at $(0, \frac{1}{2})$, $(0, \infty)$ and $(0, -\frac{1}{2})$, respectively. Consequently, the N -orbits are loci of equidistant points in terms of the (p,p,e)-length from the respective centres.

Secondly, we observe that Cayley images of the isotropy subgroups' orbits in elliptic and hyperbolic spaces in Fig. 10.1(E:K) and (H:A) are equidistant from the origin in the corresponding metrics.

Exercise 10.7. The Cayley transform of orbits of the parabolic isotropy subgroup in Fig. 10.1($P_e : N'$) comprises confocal parabolas consisting of points on the same l_{f_p} -length (7.7) from the point $(0, -1)$ – cf. 10.4.iii.

We will introduce linear structures preserved by actions of the subgroups N and N' on the parabolic unit disk in Chapter 11.

Remark 10.8. We see that the variety of possible Cayley transforms in the parabolic case is larger than in the other two cases. It is interesting that this variety is a consequence of the parabolic degeneracy of the generator $\varepsilon^2 = 0$. Indeed, for both the elliptic and the hyperbolic signs in $\iota^2 = \pm 1$, only one matrix (10.1) out of two possible $\begin{pmatrix} 1 & \iota \\ \pm\sigma\iota & 1 \end{pmatrix}$ has a non-zero determinant. Also, all these matrices are non-singular only for the degenerate parabolic value $\iota^2 = 0$.

Orbits of the isotropy subgroups A' , N' and K from Exercise 3.20 under the Cayley transform are shown in Fig. 10.1, which should be compared with the action of the same subgroup on the upper half-plane in Fig. 3.1.

10.4 Cayley Transforms of Cycles

The next natural step within the FSCc is to expand the Cayley transform to the space of cycles.

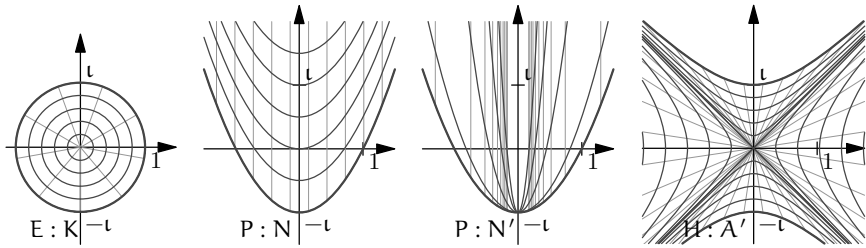


Figure 10.1 Action of the isotropy subgroups of l under the Cayley transform – subgroup K in the elliptic case, N' in the parabolic and A' in the hyperbolic. Orbits of K and A' are concentric while orbits of N' are confocal. We also provide orbits of N which are concentric in the parabolic case. The action of K , N' and A' on the upper half-plane are presented in Fig. 3.1.

10.4.1 Cayley Transform and FSSc

The effect of the Cayley transform on cycles turns out to be a cycle similarity in the elliptic and hyperbolic cases only, the degeneracy of the parabolic case requires a special treatment.

Exercise 10.9. Let C_a^s be a cycle in \mathbb{A} . Check that:

- (e, h) In the elliptic or hyperbolic cases, the Cayley transform of the cycle C_σ is $R_\sigma \hat{C}_\sigma C_\sigma \hat{C}_\sigma R_\sigma$, i.e. the composition of the similarity (6.10) by the cycle $\hat{C}_\sigma = (\sigma, 0, 1, 1)$ and the similarity by the real line (see the first and last drawings in Fig. 10.2).
- (p) In the parabolic case, the Cayley transform maps a cycle (k, l, n, m) to the cycle $(k - 2\sigma n, l, n, m - 2n)$.

HINT: We can follow a similar path to the proof of Theorem 4.13. Alternatively, for the first part, we notice that the matrix Y_σ of the Cayley transform and the FSCc matrix of the cycle \hat{C}_σ^s are different by a constant factor. The reflection in the real line compensates the effect of complex conjugation in the similarity (6.10). \diamond

Exercise 10.10. Investigate what are images under the Cayley transform of zero-radius cycles, selfadjoint cycles, orthogonal cycles and f-orthogonal cycles.

The above extension of the Cayley transform to the cycle space is linear, but in the parabolic case it is not expressed as a similarity of matrices (*reflections in a cycle*). This can be seen, for example, from the

fact that the parabolic Cayley transform does not preserve the zero-radius cycles represented by matrices with zero p-determinant. Since orbits of all

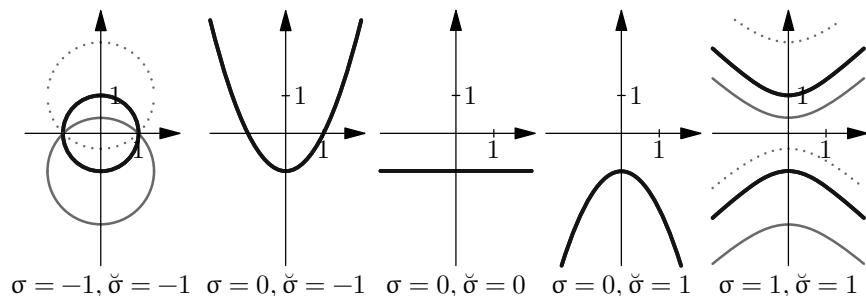


Figure 10.2 Cayley transforms in elliptic ($\sigma = -1$), parabolic ($\sigma = 0$) and hyperbolic ($\sigma = 1$) spaces. In each picture, the reflection of the real line in the green cycles (drawn continuously or dotted) is the blue ‘unit cycle’. Reflections in the solidly-drawn cycles send the upper half-plane to the unit disk and reflections in the dashed cycles send it to its complement. Three Cayley transforms in the parabolic space ($\sigma = 0$) are themselves elliptic ($\check{\sigma} = -1$), parabolic ($\check{\sigma} = 0$) and hyperbolic ($\check{\sigma} = 1$), giving a gradual transition between proper elliptic and hyperbolic cases.

subgroups in $\mathrm{SL}_2(\mathbb{R})$, as well as their Cayley images, are cycles in the corresponding metrics, we may use Exercises 10.9(p) and 4.16.ii to prove the following statements (in addition to Exercise 10.6).


Exercise 10.11. Verify that:

- i. A -orbits in transforms P_e and P_h are segments of parabolas with focal length $\frac{1}{4}$ and passing through $(0, -1)$. Their p-foci (i.e. vertices) belong to two parabolas $v = (-u^2 - 1)$ and $v = (u^2 - 1)$ respectively, which are the boundaries of parabolic circles in P_h and P_e (note the swap!).
- ii. K -orbits in transform P_e are parabolas with focal length less than $\frac{1}{4}$. In transform P_h , they are parabolas where the reciprocal of the focal length is larger than -4 .

Since the action of the parabolic Cayley transform on cycles does not preserve zero-radius cycles, one would be better using infinitesimal-radius cycles from Section 7.5 instead. Indeed, the Cayley transform preserves infinitesimality.


Exercise 10.12. Show that images of infinitesimal cycles under the parabolic Cayley transform are, themselves, infinitesimal cycles.

We recall a useful expression of concurrence with an infinitesimal cycle's focus through f-orthogonality from Exercise 7.26.ii. Some caution is required since f-orthogonality of generic cycles is not preserved by the parabolic Cayley transform, just like it is not preserved by cycle similarity in Exercise 10.9(p). A remarkable exclusion happens for infinitesimal cycles.

Exercise 10.13. An infinitesimal cycle C_σ^a (7.13) is f-orthogonal (in the sense of Exercise 7.26.ii) to a cycle \tilde{C}_σ^a if and only if the Cayley transform 10.9(p) of C_σ^a is f-orthogonal to the Cayley transform of \tilde{C}_σ^a . 

10.4.2 Geodesics on the Disks

We apply the advice quoted at the beginning of this chapter to the invariant distance discussed in Chapter 9. The equidistant curves and respective geodesics in \mathbb{A} are cycles, they correspond to certain cycles on the unit disks. As on many previous occasions we need to distinguish the elliptic and hyperbolic cases from the parabolic one.

Exercise 10.14. [56] Check that: 

(e,h) Elliptic and hyperbolic Cayley transforms (10.1) send the respective geodesics (9.7) and (9.9) passing ι to the straight line passing the origin. Consequently, any geodesics is a cycle orthogonal to the boundary of the unit disk. The respective invariant metrics on the unit disks are, cf. [108, Table VI],

$$\sin_{\tilde{\sigma}}^{-1} \frac{|w - w'|_{\sigma}}{2\sqrt{(1 + \sigma w\bar{w})(1 + \sigma w'\bar{w}')}}, \quad (10.14)$$

where $\tilde{\sigma} = 1$ in the elliptic case and has a value depending on the degree of space- or light-likeness in the hyperbolic case.

(p) The $\tilde{\sigma}$ -parabolic Cayley transform (10.11) maps the $\tilde{\sigma}$ -geodesics (9.18) passing ε to the parabolas passing the origin:

$$(\tilde{\sigma} - 4\check{\sigma} + 4t^2)u^2 - 8tu - 4v = 0.$$

The invariant $\tilde{\sigma}$ -metric on the $\tilde{\sigma}$ -parabolic unit circle is

$$\sin_{\tilde{\sigma}}^{-1} \frac{|u - u'|}{\sqrt{(1 + v + \tilde{\sigma}u^2)(1 + v' + \tilde{\sigma}u'^2)}}. \quad (10.15)$$

The appearance of straight lines as geodesics in the elliptic and hyperbolic disks is an illustration of its 'own particular advantage' mentioned in the opening quote to this chapter.

We will look closer on isometric transformations the unit disks in the next chapter.

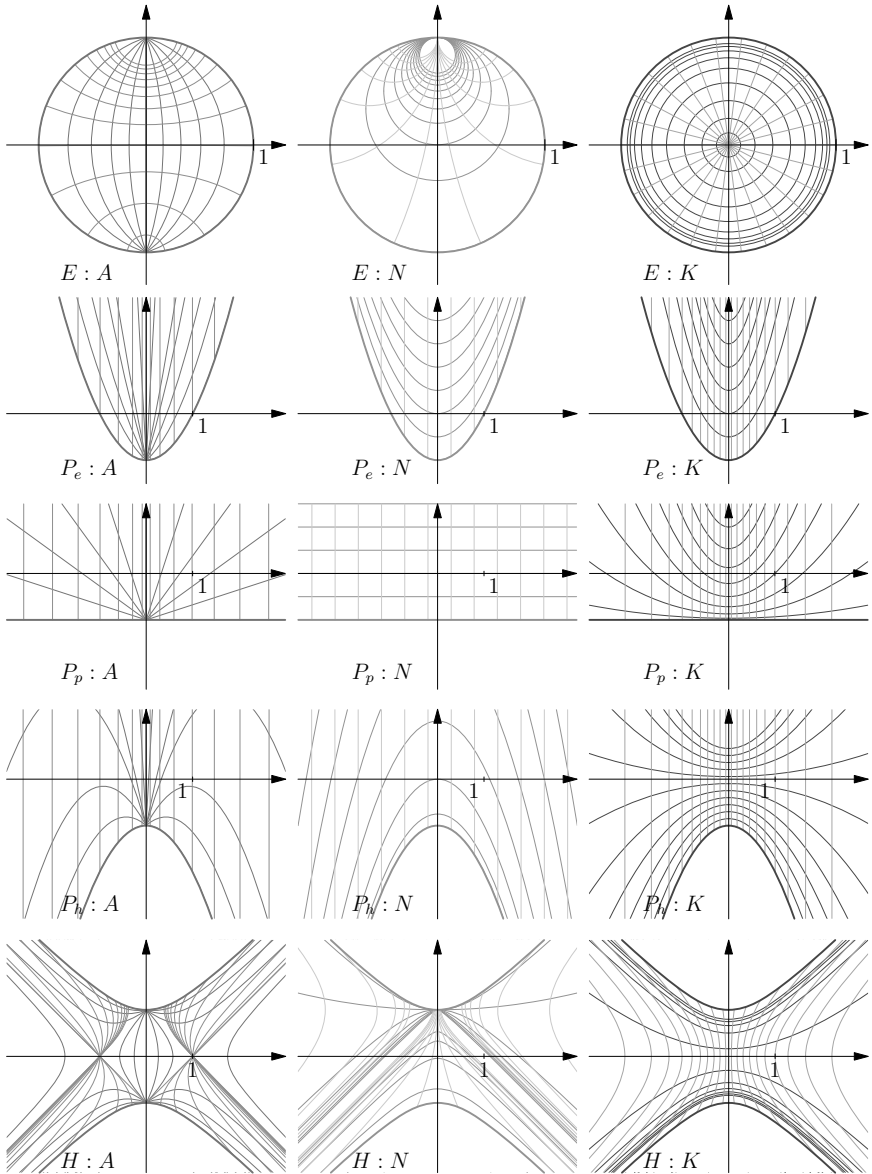


Figure 10.3 EPH unit disks and actions of one-parameter subgroups A , N and K .

(E): The elliptic unit disk.

(P_e), (P_p), (P_h): The elliptic, parabolic and hyperbolic flavours of the parabolic unit disk.

(H): The hyperbolic unit disk.

Chapter 11

Unitary Rotations

One of the important advantages of the elliptic and hyperbolic unit disks introduced in Sections 10.1–10.2 is a simplification of isotropy subgroup actions. Indeed, images of the subgroups K and A' , which fix the origin in the elliptic and hyperbolic disks, respectively, consist of diagonal matrices—see (10.4) and (10.10). These diagonal matrices produce Möbius transformations, which are multiplications by hypercomplex unimodular numbers and, thus, are linear. In this chapter, we discuss the possibility of similar results in the parabolic unit disks from Section 10.3.

11.1 Unitary Rotations—An Algebraic Approach

Consider the elliptic unit disk $z\bar{z} < 1$ (10.6) with the Möbius transformations transferred by the Cayley transform (10.1) from the upper half-plane. The isotropy subgroup of the origin is conjugated to K and consists of the diagonal matrices $\begin{pmatrix} e^{i\phi} & 0 \\ 0 & e^{-i\phi} \end{pmatrix}$ (10.4). The corresponding Möbius transformations are linear and are represented geometrically by rotation of \mathbb{R}^2 by the angle 2ϕ . After making the identification $\mathbb{R}^2 = \mathbb{C}$, this action is given by the multiplication $e^{2i\phi}$. The rotation preserves the (elliptic) distance (7.5) given by

$$x^2 + y^2 = (x + iy)(x - iy). \quad (11.1)$$

Therefore, the orbits of rotations are circles and any line passing the origin (a ‘spoke’) is rotated by an angle 2ϕ —see Fig. 11.1(E). We can also see that those rotations are isometries for the conformally-invariant metric (10.14) on the elliptic unit disk. Moreover, the rotated ‘spokes’—the straight lines through the origin—are geodesics for this invariant metric.

A natural attempt is to employ the algebraic aspect of this construction and translate to two other cases (parabolic and hyperbolic) through the respective hypercomplex numbers.

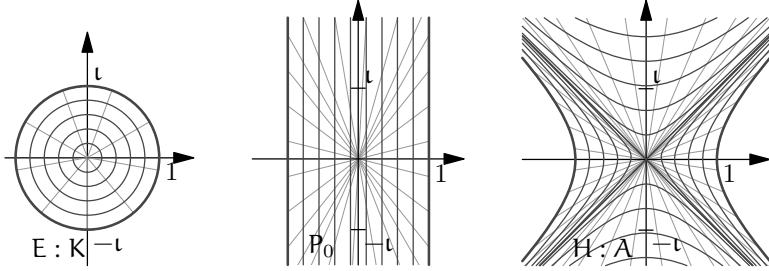


Figure 11.1 Rotations of algebraic wheels, i.e. multiplication by e^{lt} : elliptic (E), trivial parabolic (P_0) and hyperbolic (H). All blue orbits are defined by the identity $x^2 - l^2 y^2 = r^2$. Green ‘spokes’ (straight lines from the origin to a point on the orbit) are ‘rotated’ from the real axis.

Exercise 11.1. Use the algebraic similarity between the three number systems from Fig. A.2 and its geometric depiction from Fig. 11.1 to check the following for each EPH case:

- i. The algebraic EPH disks are defined by the condition $d_{\sigma,\sigma}(0, z) < 1$, where $d_{\sigma,\sigma}^2(0, z) = z\bar{z}$.
- ii. There is the one-parameter group of automorphisms provided by multiplication by e^{lt} , $t \in \mathbb{R}$. Orbits of these transformations are ‘rims’ $d_{\sigma,\sigma}(0, z) = r$, where $r < 1$.
- iii. The ‘spokes’, that is, the straight lines through the origin, are rotated. In other words, the image of one spoke is another spoke.

The value of e^{lt} can be defined, e.g. from the Taylor expansion of the exponent. In particular, for the parabolic case, $\varepsilon^k = 0$ for all $k \geq 2$, so $e^{\varepsilon t} = 1 + \varepsilon t$. Then, the parabolic rotations explicitly act on dual numbers as follows:

$$e^{\varepsilon x} : a + \varepsilon b \mapsto a + \varepsilon(ax + b). \quad (11.2)$$

In other words, the value of the imaginary part does not affect transformation of the real one, but not *vice versa*. This links the parabolic rotations with the Galilean group [108] of symmetries of classical mechanics, with the absolute time disconnected from space, cf. Section 8.4.

The obvious algebraic similarity from Exercise 11.1 and the connection to classical kinematics is a widespread justification for the following viewpoint on the parabolic case, cf. [38, 108]:

- The parabolic trigonometric functions cosp and sinp are trivial:

$$\text{cosp } t = \pm 1, \quad \text{sinp } t = t. \quad (11.3)$$

- The parabolic distance is independent from v if $u \neq 0$:

$$u^2 = (u + \varepsilon v)(u - \varepsilon v). \quad (11.4)$$

- The polar decomposition of a dual number is defined by, cf. [108, App. C(30')]:

$$u + \varepsilon v = u(1 + \varepsilon \frac{v}{u}), \quad \text{thus} \quad |u + \varepsilon v| = u, \quad \arg(u + \varepsilon v) = \frac{v}{u}. \quad (11.5)$$

- The parabolic wheel looks rectangular, see Fig. 11.1(P_0).

These algebraic analogies are quite explicit and are widely accepted as an ultimate source for parabolic trigonometry [38, 78, 108]. However, we will see shortly that there exist geometric motivation and a connection with the parabolic equation of mathematical physics.

11.2 Unitary Rotations – A Geometrical Viewpoint

We make another attempt at describing parabolic rotations. The algebraic attempt exploited the representation of rotation by hypercomplex multiplication. However, in the case of dual numbers this leads to a degenerate picture. If multiplication (a linear transformation) is not sophisticated enough for this, we can advance to the next level of complexity: linear-fractional.

In brief, we change our viewpoint from algebraic to geometric. Elliptic and hypercomplex rotations of the respective unit disks are also Möbius transformations from the one-parameter subgroups K and A' in the respective Cayley transform. Therefore, the parabolic counterpart corresponds to Möbius transformations from the subgroup N' .

For the sake of brevity, we will only treat the elliptic version P_e of the parabolic Cayley transform from Section 10.3. We use the Cayley transform defined by the matrix

$$C_\varepsilon = \begin{pmatrix} 1 & -\varepsilon \\ -\varepsilon & 1 \end{pmatrix}.$$

The Cayley transform of matrices (3.7) from the subgroup N is

$$\begin{pmatrix} 1 & -\varepsilon \\ -\varepsilon & 1 \end{pmatrix} \begin{pmatrix} 1 & t \\ 0 & 1 \end{pmatrix} \begin{pmatrix} 1 & \varepsilon \\ \varepsilon & 1 \end{pmatrix} = \begin{pmatrix} 1 + \varepsilon t & t \\ 0 & 1 - \varepsilon t \end{pmatrix} = \begin{pmatrix} e^{\varepsilon t} & t \\ 0 & e^{-\varepsilon t} \end{pmatrix}. \quad (11.6)$$

This is not too different from the diagonal forms in the elliptic (10.4) and hyperbolic (10.10). However, the off-diagonal $(1, 2)$ -term destroys harmony. Nevertheless, we will continue defining a unitary parabolic rotation to be the Möbius transformation with the matrix (11.6), which is no longer multiplication by a scalar. For the subgroup N' , the matrix is obtained by transposition of (11.6).

In the elliptic and hyperbolic cases, the image of reference point $(-\iota)$ is:

$$\begin{pmatrix} e^{it} & 0 \\ 0 & e^{-it} \end{pmatrix} : -i \mapsto \sin 2t - i \cos 2t, \quad (11.7)$$

$$\begin{pmatrix} e^{jt} & 0 \\ 0 & e^{-jt} \end{pmatrix} : -j \mapsto -\sinh 2t - j \cosh 2t, \quad (11.8)$$

Exercise 11.2. Check that parabolic rotations with the upper-triangular matrices from the subgroup N become:

$$\begin{pmatrix} e^{\varepsilon t} & t \\ 0 & e^{-\varepsilon t} \end{pmatrix} : -\varepsilon \mapsto t - \varepsilon(1 - t^2). \quad (11.9)$$

This coincides with the *cyclic rotations* defined in [108, Sec. 8]. A comparison with the Euler formula seemingly confirms that $\sin p t = t$, but suggests a new expression for $\csc p t$:

$$\csc p t = 1 - t^2, \quad \sin p t = t.$$

Therefore, the parabolic Pythagoras' identity would be

$$\sin^2 t + \csc^2 t = 1, \quad (11.10)$$

which fits well between the elliptic and hyperbolic versions:

$$\sin^2 t + \csc^2 t = 1, \quad \sinh^2 t - \cosh^2 t = -1.$$

The identity (11.10) is also less trivial than the version $\csc^2 t = 1$ from (11.3)–(11.4)–see also [38]. The possible ranges of the cosine and sine functions are given by the table:

	elliptic	parabolic	hyperbolic
cosine	$[-1, 1]$	$(-\infty, 1]$	$[1, \infty)$
sine	$[-1, 1]$	$(-\infty, \infty)$	$(-\infty, \infty)$

There is a second option for defining parabolic rotations for the lower-triangular matrices from the subgroup N' . The important difference is now that the reference point cannot be $-\varepsilon$ since it is a fixed point (as well as any point on the vertical axis). Instead, we take ε^{-1} , which is an ideal element (a point at infinity), since ε is a divisor of zero. The proper treatment is based on the projective coordinates, where point ε^{-1} is represented by a vector $(1, \varepsilon)$ —see Section 8.1.

Exercise 11.3. Check the map of reference point ε^{-1} for the subgroup N' :

$$\begin{pmatrix} e^{-\varepsilon t} & 0 \\ t & e^{\varepsilon t} \end{pmatrix} : \frac{1}{\varepsilon} \mapsto \frac{1}{t} + \varepsilon \left(1 - \frac{1}{t^2}\right). \quad (11.11)$$

A comparison with (11.9) shows that this form is obtained by the substitution $t \mapsto t^{-1}$. The same transformation gives new expressions for parabolic trigonometric functions. The parabolic ‘unit cycle’ is defined by the equation $u^2 - v = 1$ for both subgroups—see Fig. 10.1(P) and (P') and Exercise 10.4. However, other orbits are different and we will give their description in the next section. Figure 10.1 illustrates Möbius actions of matrices (11.7), (11.8) and (11.6) on the respective ‘unit disks’, which are images of the upper half-planes under the respective Cayley transforms from Sections 10.1 and 10.3.

At this point, the reader may suspect that the structural analogy mentioned at the beginning of the section is insufficient motivation to call transformations (11.9) and (11.11) ‘parabolic rotation’ and the rest of the chapter is a kind of post-modern deconstruction. To dispel any doubts, we present the following example:

Example 11.4 (The heat equation and kernel).

The dynamics of heat distribution $f(x, t)$ over a one-dimensional infinite string is modelled by the partial differential equation

$$(\partial_t - k\partial_x^2)f(x, t) = 0, \quad \text{where } x \in \mathbb{R}, \ t \in \mathbb{R}_+. \quad (11.12)$$

For the initial-value problem with the data $f(x, 0) = g(x)$, the solution is given by the convolution

$$u(x, t) = \frac{1}{\sqrt{4\pi kt}} \int_{-\infty}^{\infty} \exp\left(-\frac{(x-y)^2}{4kt}\right) g(y) dy,$$

with the function $\exp(-\frac{x^2}{4kt})$, which is called the *heat kernel*.

Exercise 11.5. Check that the Möbius transformations

$$\begin{pmatrix} 1 & 0 \\ c & 1 \end{pmatrix} : x + \varepsilon t \mapsto \frac{x + \varepsilon t}{c(x + \varepsilon t) + 1}$$

from the subgroup N' do not change the heat kernel.

HINT: N' -orbits from Fig. 3.1 are contour lines of the function $\exp(-\frac{u^2}{t})$. \diamond

The last example hints at further works linking the parabolic geometry with parabolic partial differential equations.

11.3 Rebuilding Algebraic Structures from Geometry

Rotations in elliptic and hyperbolic cases are given by products of complex or double numbers, respectively, and, thus, are linear. However, non-trivial parabolic rotations (11.9) and (11.11) (Fig. 10.1(P) and (P')) are not linear.

Can we find algebraic operations for dual numbers which linearise these Möbius transformations? To this end, we will ‘revert a theorem into a definition’ and use this systematically to recover a compatible algebraic structure.

11.3.1 Modulus and Argument

In the elliptic and hyperbolic cases, orbits of rotations are points with a constant norm (modulus), either $x^2 + y^2$ or $x^2 - y^2$. In the parabolic case, we already employed this point of view in Chapter 9 to treat orbits of the subgroup N' as equidistant points for certain Möbius-invariant metrics, and we will do this again.

Definition 11.6. Orbits of actions (11.9) and (11.11) are contour lines for the following functions which we call the respective moduli (norms):

$$\text{for } N : |u + \varepsilon v| = u^2 - v, \quad \text{for } N' : |u + \varepsilon v|' = \frac{u^2}{v + 1}. \quad (11.13)$$

Remark 11.7. The definitions are supported by the following observations:

- i. The expression $|(u, v)| = u^2 - v$ represents a parabolic distance from $(0, \frac{1}{2})$ to (u, v) —see Exercise 10.6—which is in line with the parabolic Pythagoras’ identity (11.10).
- ii. The modulus for N' expresses the parabolic focal length from $(0, -1)$ to (u, v) as described in Exercise 10.7.

The only straight lines preserved by both parabolic rotations N and N' are vertical lines, so we will treat them as ‘spokes’ for parabolic ‘wheels’. Elliptic spokes, in mathematical terms, are ‘points on the complex plane with the same argument’. Therefore we again use this for the parabolic definition.

Definition 11.8. Parabolic arguments are defined as follows:

$$\text{for } N : \arg(u + \varepsilon v) = u, \quad \text{for } N' : \arg'(u + \varepsilon v) = \frac{1}{u}. \quad (11.14)$$

Both Definitions 11.6 and 11.8 possess natural properties with respect to parabolic rotations.

Exercise 11.9. Let w_t be a parabolic rotation of w by an angle t in (11.9) or in (11.11). Then

$$|w_t|^{(\prime)} = |w|^{(\prime)}, \quad \arg^{(\prime)} w_t = \arg^{(\prime)} w + t,$$

where the primed versions are used for subgroup N' .

Remark 11.10. Note that, in the commonly-accepted approach, cf. [108, App. C(30')], the parabolic modulus and argument are given by expressions (11.5), which are, in a sense, opposite to our present agreements.

11.3.2 Rotation as Multiplication

We revert again theorems into definitions to assign multiplication. In fact, we consider parabolic rotations as multiplications by unimodular numbers, thus we define multiplication through an extension of properties from Exercise 11.9:

Definition 11.11. The product of vectors w_1 and w_2 is defined by the following two conditions:

- i. $\arg^{(\prime)}(w_1 w_2) = \arg^{(\prime)} w_1 + \arg^{(\prime)} w_2$ and
- ii. $|w_1 w_2|^{(\prime)} = |w_1|^{(\prime)} \cdot |w_2|^{(\prime)}$.

Hereafter, primed versions of formulae correspond to the case of subgroup N' and unprimed to the subgroup N .

We also need a special form of parabolic conjugation which coincides with sign reversion of the argument:

Definition 11.12. Parabolic conjugation is given by

$$\overline{u + \varepsilon v} = -u + \varepsilon v. \quad (11.15)$$

Obviously, we have the properties $|\overline{w}|^{(\prime)} = |w|^{(\prime)}$ and $\arg^{(\prime)} \overline{w} = -\arg^{(\prime)} w$. A combination of Definitions 11.6, 11.8 and 11.11 uniquely determines expressions for products.

Exercise 11.13. Check the explicit expressions for the parabolic products:

$$\text{For } N : \quad (u, v) * (u', v') = (u + u', (u + u')^2 - (u^2 - v)(u'^2 - v')). \quad (11.16)$$

$$\text{For } N' : \quad (u, v) * (u', v') = \left(\frac{uu'}{u + u'}, \frac{(v + 1)(v' + 1)}{(u + u')^2} - 1 \right). \quad (11.17)$$

Although both the above expressions look unusual, they have many familiar properties, which are easier to demonstrate from the implicit definition rather than the explicit formulae.

Exercise 11.14. Check that both the products (11.16) and (11.17) satisfy the following conditions:

- i. They are commutative and associative.
- ii. The respective rotations (11.9) and (11.11) are given by multiplications of a dual number with the unit norm.
- iii. The product $w_1 \bar{w}_2$ is invariant under the respective rotations (11.9) and (11.11).
- iv. For any dual number w , the following identity holds:

$$|w\bar{w}| = |w|^2.$$

In particular, the property (11.14.iii) will be crucial below for an inner product.

We defined multiplication through the modulus and argument described in the previous subsection. Our notion of the norm is rotational-invariant and unique up to composition with a monotonic function of a real argument—see the discussion in Section 9.2. However, the argument can be defined with greater freedom—see Section 11.6.2.

11.4 Invariant Linear Algebra

Now, we wish to define a linear structure on \mathbb{R}^2 which is invariant under point multiplication from the previous subsection (and, thus, under the parabolic rotations, cf. Exercise 11.14.ii). Multiplication by a real scalar is straightforward (at least for a positive scalar)—it should preserve the

argument and scale the norm of a vector. Thus, we have formulae, for $a > 0$,

$$a \cdot (u, v) = (u, av + u^2(1 - a)) \quad \text{for } N \text{ and} \quad (11.18)$$

$$a \cdot (u, v) = \left(u, \frac{v+1}{a} - 1 \right) \quad \text{for } N'. \quad (11.19)$$

On the other hand, the addition of vectors can be done in several different ways. We present two possibilities—one is tropical and the other, exotic.

11.4.1 Tropical form

Exercise 11.15 (Tropical mathematics). Consider the so-called max-plus algebra \mathbb{R}_{\max} , namely the field of real numbers together with minus infinity: $\mathbb{R}_{\max} = \mathbb{R} \cup \{-\infty\}$. Define operations $x \oplus y = \max(x, y)$ and $x \odot y = x + y$. Check that:

- i. The addition \oplus and the multiplication \odot are associative.
- ii. The addition \oplus is commutative.
- iii. The multiplication \odot is distributive with respect to the addition \oplus ;
- iv. $-\infty$ is the neutral element for \oplus .

Similarly, define $\mathbb{R}_{\min} = \mathbb{R} \cup \{+\infty\}$ with the operations $x \oplus y = \min(x, y)$, $x \odot y = x + y$ and verify the above properties.

The above example is fundamental in the broad area of *tropical mathematics* or idempotent mathematics, also known as Maslov dequantisation algebras—see [79] for a comprehensive survey.

Let us introduce the lexicographic order on \mathbb{R}^2 :

$$(u, v) < (u', v') \quad \text{if and only if} \quad \begin{cases} \text{either } u < u', \\ \text{or } u = u', v < v'. \end{cases}$$

Exercise 11.16. Check that the above relation is transitive.

One can define functions \min and \max of a pair of points on \mathbb{R}^2 , respectively. Then, an addition of two vectors can be defined either as their minimum or maximum.

Exercise 11.17. Check that such an addition is commutative, associative and distributive with respect to scalar multiplications (11.18) and (11.19) and, consequently, is invariant under parabolic rotations.

Although an investigation of this framework looks promising, we do not study it further for now.

11.4.2 Exotic form

Addition of vectors for both subgroups N and N' can be defined by the following common rules, where subtle differences are hidden within the corresponding Definitions 11.6 (norms) and 11.8 (arguments).

Definition 11.18. Parabolic addition of vectors is defined by the formulae:

$$\arg^{(n)}(w_1 + w_2) = \frac{\arg^{(n)} w_1 \cdot |w_1|^{(n)} + \arg^{(n)} w_2 \cdot |w_2|^{(n)}}{|w_1 + w_2|^{(n)}} \text{ and } \quad (11.20)$$

$$|w_1 + w_2|^{(n)} = |w_1|^{(n)} \pm |w_2|^{(n)}, \quad (11.21)$$

where primed versions are used for the subgroup N' .

The rule for the norm of sum (11.21) may look too trivial at first glance. We should say, in its defence, that it fits well between the elliptic $|w + w'| \leq |w| + |w'|$ and hyperbolic $|w + w'| \geq |w| + |w'|$ triangle inequalities for norms – see Section 9.3 for their discussion.

The rule (11.20) for the argument of the sum is also not arbitrary. From the law of sines in Euclidean geometry, we can deduce that

$$\sin(\phi - \psi') = \frac{|w| \cdot \sin(\psi - \psi')}{|w + w'|} \text{ and } \sin(\psi' - \phi) = \frac{|w'| \cdot \sin(\psi - \psi')}{|w + w'|},$$

where $\psi^{(n)} = \arg w^{(n)}$ and $\phi = \arg(w + w^{(n)})$. Using parabolic expression (11.3) for the sine, $\sin \theta = \theta$, we obtain the arguments addition formula (11.20).

A proper treatment of zeros in the denominator of (11.20) can be achieved through a representation of a dual number $w = u + \varepsilon v$ as a pair of homogeneous polar (projective) coordinates $[a, r] = [|w|^{(n)} \cdot \arg^{(n)} w, |w|^{(n)}]$ (primed version for the subgroup N'). Then, the above addition is defined component-wise in the homogeneous coordinates

$$w_1 + w_2 = [a_1 + a_2, r_1 + r_2], \quad \text{where } w_i = [a_i, r_i].$$

The multiplication from Definition 11.11 is given in the homogeneous polar coordinates by

$$w_1 \cdot w_2 = [a_1 r_2 + a_2 r_1, r_1 r_2], \quad \text{where } w_i = [a_i, r_i].$$

Thus, homogeneous coordinates linearise the addition (11.20) and (11.21) and multiplication by a scalar (11.18).

Both formulae (11.20) and (11.21) together uniquely define explicit expressions for the addition of vectors. However, these expressions are rather cumbersome and not really much needed. Instead, we list the properties of these operations.

Exercise 11.19. Verify that the vector additions for subgroups N and N' defined by (11.20) and (11.21) satisfy the following conditions:

- i. they are commutative and associative;
- ii. they are distributive for multiplications (11.16) and (11.17). Consequently:
- iii. they are parabolic rotationally-invariant;
- iv. they are distributive in both ways for the scalar multiplications (11.18) and (11.19), respectively:

$$a \cdot (w_1 + w_2) = a \cdot w_1 + a \cdot w_2, \quad (a + b) \cdot w = a \cdot w + b \cdot w.$$

To complete the construction, we need to define the zero vector and the inverse. The inverse of w has the same argument as w and the opposite norm.

Exercise 11.20. Check that, for corresponding subgroups, we have:

- (N) The zero vector is $(0, 0)$ and, consequently, the inverse of (u, v) is $(u, 2u^2 - v)$.
- (N') The zero vector is $(\infty, -1)$ and, consequently, the inverse of (u, v) is $(u, -v - 2)$.

Thereafter, we can check that scalar multiplications by negative reals are given by the same identities (11.18) and (11.19) as for positive ones.

11.5 Linearisation of the Exotic Form

Some useful information can be obtained from the transformation between the parabolic unit disk and its linearised model. In such linearised coordinates (a, b) , the addition (11.20) and (11.21) is done in the usual coordinate-wise manner: $(a, b) + (a', b') = (a + a', b + b')$.

Exercise 11.21. Calculate values of a and b in the linear combination $(u, v) = a \cdot (1, 0) + b \cdot (-1, 0)$ and check the following:

i. For the subgroup N , the relations are:

$$u = \frac{a-b}{a+b}, \quad v = \frac{(a-b)^2}{(a+b)^2} - (a+b), \quad (11.22)$$

$$a = \frac{u^2-v}{2}(1+u), \quad b = \frac{u^2-v}{2}(1-u). \quad (11.23)$$

ii. For the subgroup N' , the relations are:

$$u = \frac{a+b}{a-b}, \quad v = \frac{(a+b)}{(a-b)^2} - 1, \quad a = \frac{u(u+1)}{2(v+1)}, \quad b = \frac{u(u-1)}{2(v+1)}.$$

We also note that both norms (11.13) have exactly the same value $a+b$ in the respective (a, b) -coordinates. It is not difficult to transfer parabolic rotations from the (u, v) -plane to (a, b) -coordinates.

Exercise 11.22. Show that:

i. The expression for N action (11.9) in (a, b) coordinates is:

$$\begin{pmatrix} e^{\varepsilon t} & t \\ 0 & e^{-\varepsilon t} \end{pmatrix} : (a, b) \mapsto \left(a + \frac{t}{2}(a+b), b - \frac{t}{2}(a+b) \right). \quad (11.24)$$

HINT: Use identities (11.22). \diamond

ii. After (Euclidean) rotation by 45° given by

$$(a, b) \mapsto (a+b, a-b), \quad (11.25)$$

formula (11.24) coincides with the initial parabolic rotation (11.2) shown in Fig. 11.1(P_0).

iii. The composition of transformations (11.22) and (11.25) maps algebraic operations from Definitions 11.11 and 11.18 to the corresponding operations on dual numbers.

This should not be surprising, since any associative and commutative two-dimensional algebra is formed either by complex, dual or double numbers [78]. However, it does not trivialise our construction, since the above transition is essentially singular and shall be treated within the birational geometry framework [73]. Similar singular transformations of time variable in the hyperbolic setup allow us to linearise many non-linear problems of mechanics [88, 89].

Another application of the exotic linear algebra is the construction of linear representations of $\text{SL}_2(\mathbb{R})$ induced by characters of subgroup N' which are realised as parabolic rotations [67].

11.6 Conformality and Geodesics

We conclude our consideration of the parabolic rotations with a couple of links to other notions considered earlier.


11.6.1 *Retrospective: Parabolic Conformality*

The irrelevance of the standard linear structure for parabolic rotations manifests itself in many different ways, e.g. in an apparent ‘non-conformality’ of lengths from parabolic foci, that is, with the parameter $\check{\sigma} = 0$ in Proposition 7.14.iii. Adapting our notions to the proper framework restores a clear picture.

The initial Definition 7.13 of conformality considers the usual limit $y' \rightarrow y$ along a straight line, i.e. a ‘spoke’ in terms of Fig. 11.1. This is justified in the elliptic and hyperbolic cases. However, in the parabolic setting the proper ‘spokes’ are vertical lines—see Definition 11.8 of the argument and the illustration in Fig. 10.1(P) and (P'). Therefore, the parabolic limit should be taken along the vertical lines.

Definition 11.23. We say that a length l is *p-conformal* if, for any given $P = u + \nu v$ and another point $P' = u' + \nu v'$, the following limit exists and is independent from u' :

$$\lim_{v' \rightarrow \infty} \frac{l(\overrightarrow{QQ'})}{l(\overrightarrow{PP'})}, \quad \text{where } g \in \text{SL}_2(\mathbb{R}), \quad Q = g \cdot P, \quad Q' = g \cdot P'.$$

Exercise 11.24. Let the focal length be given by the identity (7.7) with $\sigma = \check{\sigma} = 0$: 

$$l_{f_{\check{\sigma}}}^2(\overrightarrow{PP'}) = -\check{\sigma}p^2 - 2vp, \quad \text{where } p = \frac{(u' - u)^2}{2(v' - v)}.$$

Check that $l_{f_{\check{\sigma}}}$ is p-conformal and, moreover,

$$\lim_{v' \rightarrow \infty} \frac{l_{f_{\check{\sigma}}}(\overrightarrow{QQ'})}{l_{f_{\check{\sigma}}}(\overrightarrow{PP'})} = \frac{1}{(cu + d)^2}, \quad \text{where } g = \begin{pmatrix} a & b \\ c & d \end{pmatrix} \quad (11.26)$$

and $Q = g \cdot P, Q' = g \cdot P'$.

11.6.2 *Perspective: Parabolic Geodesics*

We illustrated unitary rotations of the unit disk by an analogy with a wheel. Unitarity of rotations is reflected in the rigid structure of transverse

‘rims’ and ‘spokes’. The shape of ‘rims’ is always predefined—they are orbits of rotations. They also define the loci of points with the constant norm. However, there is some flexibility in our choice of parabolic ‘spokes’, i.e. points with the same value of argument. This is not determined even under the strict guidance of the elliptic and hyperbolic cases.

In this chapter, we take the simplest possible assumption: elliptic and hyperbolic ‘spokes’ are straight lines passing through the origin. Consequently, we have looked for parabolic ‘spokes’ which are straight lines as well. The only family of straight lines invariant under the parabolic rotations (11.9) and (11.11) are vertical lines, thus we obtained the situation depicted in Fig. 10.1.

However, the above path is not the only possibility. We can view straight lines in the elliptic and hyperbolic cases as geodesics for the invariant distance on the respective unit disks, see Exercise 10.14(e,p). This is perfectly consistent with unitary rotations and suggests that parabolic ‘rims’ for rotations (11.11) shall be respective parabolic geodesics on the parabolic unit disk, see Fig. 11.2.

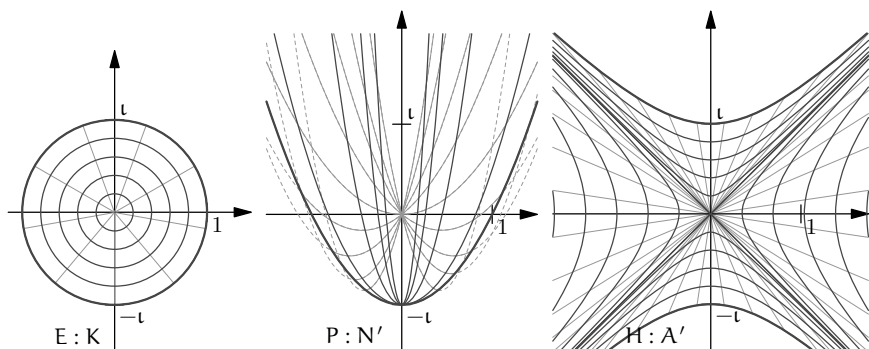


Figure 11.2 Geodesics as spokes. In each case ‘rims’ are points equidistant from the origin, ‘spokes’ are geodesics between the origin and any point on the rims.

There are three flavours of parabolic geodesics, cf. Fig. 9.3(P_E – P_H) and Exercise 10.14(p). All of them can be used as ‘spokes’ of parabolic unit disk, but we show only the elliptic flavour in Fig. 11.2.

Exercise 11.25. Define the parabolic argument to be constant along geodesics from Exercise 10.14(p) drawn by blue lines in Fig. 9.3. What is the respective multiplication formula? Is there a rotation-invariant linear algebra?

Epilogue: About the Cover

The cover of this book depicts the painting ‘A Vityaz at the Crossroads’ (1882) by V.M. Vasnetsov. It is based on the archetypal situation from Russian epics: a *vityaz* (knight) on a mission arrives at a crossroads with a telling stone. The scripture on the stone gives directions:

Continue straight and death will greet you, with no way to pass, drive or fly. Turn to the left and you will become rich. Turn to the right and you will be married.

Despite this advice, the vityaz goes forward and, after some adventures, accomplishes his mission, becoming both rich and happily married.

Now we shall compare the stone’s directions with the following variant of the EPH classification, cf. (1.2):



The left direction corresponds to the elliptic case with all its richness of complex analysis and its applications. The right turn to hyperbolic theory leads to the marriage of the relativity of Minkowski space-time and non-linear dynamics. The usual perception of continuing straight on to the parabolic case enters a desert of degenerate cases and trivial results. There is no chance to do solid research, to write a decent PhD thesis or to obtain a substantial grant.

I hope that the tale of this book dispels fears. The parabolic case can be fruitful and deliver many features of both elliptic and hyperbolic cases. In particular, parabolic geometry has useful relations to mathematical physics.

Our treatment of three EPH cases was uniformly based on the structural properties of the group $SL_2(\mathbb{R})$. In the spirit of the Erlangen programme, we investigated invariants of its actions on the homogeneous spaces produced

by the subgroups K , N and A . It turned out that each subgroup is associated with the respective type of hypercomplex numbers: complex, dual and double. Our present findings and their further development in [67–69] support the following general principle:

Principle (Similarity and Correspondence.)

- i. Subgroups K , N and A play a similar rôle in the structure of the group $\mathrm{SL}_2(\mathbb{R})$ and its associated geometries.*
- ii. The subgroups can be swapped simultaneously with the respective replacement of the hypercomplex unit ι .*

Here, the two parts are interrelated – without a swap of imaginary units there can be no similarity between different subgroups and their respective types of geometries. Further work will reveal more supporting evidence from representation theory, analytic functions and operator theory.

Acknowledgements: I am very grateful to Tasha D’Cruz and Lindsay Robert Wilson for their help in the preparation of this book.

Appendix A

Supplementary Material

A.1 Dual and Double Numbers

Complex numbers form a two-dimensional commutative associative algebra with an identity. Up to a suitable choice of a basis there are exactly three different types of such algebras—see [78]. They are spanned by a basis consisting of 1 and a hypercomplex unit ι . The square of ι is -1 for complex numbers, 0 for dual numbers and 1 for double numbers. In these cases, we write the hypercomplex unit ι as i , ε and j , respectively.

The arithmetic of hypercomplex numbers is defined by associative, commutative and distributive laws. For example, the product is

$$(u + \iota v)(u' + \iota v') = (uu' + \iota^2 vv') + \iota(uv' + u'v), \quad \text{where } \iota^2 = -1, 0, \text{ or } 1.$$

Further comparison of hypercomplex numbers is presented in Fig. A.2.

Despite significant similarities, only complex numbers belong to mainstream mathematics. Among their obvious advantages is the following:

- i. A product of complex numbers is equal to zero if and only if at least one factor is zero. This property is called the absence of *zero divisors*. Dual and double numbers both have large set of zero divisors.
- ii. Complex numbers are *algebraically closed*, that is, any polynomial with one variable with complex coefficients has a complex root. It is easy to see that dual and double numbers are not algebraically closed for the same reason as real numbers.

The first property is not very crucial, since zero divisors can be treated through appropriate techniques, e.g. projective coordinates, cf. Section 8.1. The property of being algebraically-closed was not used in the present work. Thus, the absence of these properties is not an insuperable obstacle in the study of hypercomplex numbers. On the other hand, hypercomplex

numbers naturally appeared in Section 3.3 from $\mathrm{SL}_2(\mathbb{R})$ action on the three different types of homogeneous spaces.

A.2 Classical Properties of Conic Sections

We call cycles three types of curves: circles, parabolas and equilateral hyperbolas. They belong to a large class of conic sections, i.e. they are the intersection of a cone with a plane, see Fig. 1.3. Algebraically, cycles are defined by a quadratic equation (4.1) and are a subset of *quadrics*.

The beauty of conic sections has attracted mathematicians for several thousand years. There is an extensive literature—see [36, Sec. 6] for an entry-level introduction and [11, Ch. 17] for a comprehensive coverage. We list below the basic definitions only in order to clarify the distinction between the classical foci, the centres of conic sections and our usage.

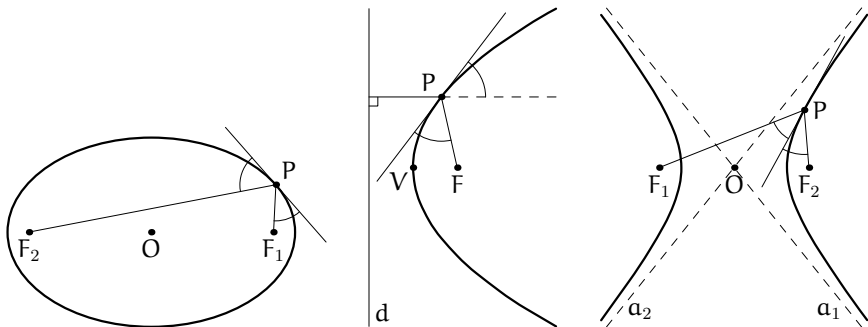


Figure A.1 Classical definitions of conic sections through the distances from foci. Equality of some angles can be derived and results in corresponding ray reflection.

We use the notation $|P_1P_2|$ and $|Pl|$ for the Euclidean distance between points P_1 , P_2 and between a point P and a line l .

Ellipse – a set of points P such that $|PF_1| + |PF_2| = \text{const}$ for two fixed points F_1 and F_2 , called the *foci* of the ellipse—see Fig. A.1. The midpoint O of the interval F_1F_2 is the ellipse’s *centre*. A *circle* is a particular case of an ellipse with $F_1 = F_2 = O$.

Parabola – a set of points P such that $|PF| = |Pd|$ for a fixed point F and a line d . They are called the *focus* and *directrix*, respectively. The point of the parabola nearest to the directrix is its *vertex*. The centre of a parabola is not usually defined.

Hyperbola – a set of points P such that $|PF_1| - |PF_2| = \pm \text{const}$ for two fixed points F_1 and F_2 called the *foci* of the hyperbola. A hyperbola has two disjoint branches which tend to their *asymptotes* – see lines a_1 and a_2 in Fig. A.1. The midpoint O of the interval F_1F_2 , which is also the intersection of the asymptotes, is the hyperbola’s *centre*.

The above definition in terms of distances allows us to deduce the equality of the respective angles in each case – see Fig. A.1 and [36, Sec. 6]. This implies reflection of the respective rays. For example, any ray perpendicular to the directrix is reflected by the parabola to pass its focus – the ‘burning point’. There are many applications of this, from the legendary burning of the Roman fleet by Archimedes to practical (parabolic) satellite dishes.

A.3 Comparison with Yaglom’s Book

The profound book by Yaglom [108] is already a golden classic appreciated by several generations of mathematicians and physicists. To avoid confusion, we provide a comparison of our notions and results with Yaglom’s.

Firstly, there is a methodological difference. Yaglom started from notions of length and angles and then derived objects (notably parabolas) which carry them out in an invariant way. We worked in the opposite direction by taking invariant objects (FSCc matrices) and deriving the respective notions and properties, which were also invariant. This leads to significant distinctions in our results which are collected in Fig. A.3.

In short, we tried to avoid an overlap with Yaglom’s book [108] – our results are either new or obtained in a different manner.

A.4 Other Approaches and Results

The development of parabolic and hyperbolic analogues of complex analysis has a long but sporadic history. In the absence of continuity, there are many examples when a researcher started from a scratch without any knowledge of previous works. There may be even more forgotten papers on the subject. To improve the situation, we list here some papers without trying to be comprehensive or even representative.

The survey and history of Cayley–Klein geometries is presented in Yaglom’s book [108] and this will be completed by the work [90] which provides the full axiomatic classification of EPH cases. A search for hyperbolic func-

tion theory was attempted several times starting from the 1930s—see, for example, [78, 80, 83, 91, 105]. Despite some important advances, the obtained hyperbolic theory is not yet as natural and complete as complex analysis is. Parabolic geometry was considered in [108] with rather trivial ‘parabolic calculus’ described in [17]. There is also interest in this topic from different areas: differential geometry [8, 17, 18, 28, 74, 75, 99, 109], quantum mechanics [1, 41, 46–51, 102, 103], group representations [34, 35], space-time geometry [13, 39, 40, 45, 82], hypercomplex analysis [19, 25, 26, 58] and non-linear dynamics [88, 89].

A.5 FSCc with Clifford Algebras

FSCc can also be expressed through Clifford algebras [65] and this is used in our CAS. Although, in this case, we need to take care on the non-commutativity of numbers, many matrix expressions have a simpler form. Clifford algebras also admit straightforward generalisation to higher dimensions.

We use four-dimensional Clifford algebra $\mathcal{C}(\sigma)$ with unit 1, two generators e_0 and e_1 , and the fourth element of the basis, their product e_0e_1 . The multiplication table is $e_0^2 = -1$, $e_1^2 = \sigma$ and $e_0e_1 = -e_1e_0$. Here, $\sigma = -1, 0$ and 1 in the respective EPH cases. The point space \mathbb{A} consists of vectors $ue_0 + ve_1$. An isomorphic realisation of $\mathrm{SL}_2(\mathbb{R})$ is obtained if we replace a matrix $\begin{pmatrix} a & b \\ c & d \end{pmatrix}$ by $\begin{pmatrix} a & be_0 \\ -ce_0 & d \end{pmatrix}$ for any σ . The Möbius transformation of $\mathbb{A} \rightarrow \mathbb{A}$ for all three algebras $\mathcal{C}(\sigma)$ by the same expression, cf. (3.24), is

$$\begin{pmatrix} a & be_0 \\ -ce_0 & d \end{pmatrix} : ue_0 + ve_1 \mapsto \frac{a(ue_0 + ve_1) + be_0}{-ce_0(ue_0 + ve_1) + d}, \quad (\text{A.1})$$

where the expression $\frac{a}{b}$ in a non-commutative algebra is understood as ab^{-1} .

In Clifford algebras, the FSCc matrix of a cycle (k, l, n, m) is, cf. (4.5),

$$C_{\check{\sigma}}^s = \begin{pmatrix} l\check{e}_0 + sn\check{e}_1 & m \\ k & -l\check{e}_0 - sn\check{e}_1 \end{pmatrix}, \quad \text{with } \check{e}_0^2 = -1, \check{e}_1^2 = \check{\sigma}, \quad (\text{A.2})$$

where the EPH type of $\mathcal{C}(\check{\sigma})$ may be different from the type of $\mathcal{C}(\sigma)$. In terms of matrices (A.1) and (A.2) the $\mathrm{SL}_2(\mathbb{R})$ -similarity (4.7) has exactly the same form $\tilde{C}_{\check{\sigma}}^s = gC_{\sigma}^s g^{-1}$. However, the cycle similarity (6.10) becomes simpler, e.g. there is no need in conjugation:

$$C_{\check{\sigma}}^s : \tilde{C}_{\check{\sigma}}^s \mapsto C_{\check{\sigma}}^s \tilde{C}_{\check{\sigma}}^s C_{\check{\sigma}}^s. \quad (\text{A.3})$$

The cycle product is $\Re \operatorname{tr}(C_{\check{\sigma}}^s \tilde{C}_{\check{\sigma}}^s)$ [65]. Its ‘imaginary’ part (vanishing for hypercomplex numbers) is equal to the symplectic form of cycles’ centres.

	Elliptic	Parabolic	Hyperbolic
Unit	$\mathbf{i}^2 = -1$	$\varepsilon^2 = 0$	$\mathbf{j}^2 = 1$
Number	$w = x + \mathbf{i}y$	$w = x + \varepsilon y$	$w = x + \mathbf{j}y$
Conjugation	$\bar{w} = x - \mathbf{i}y$	$\bar{w} = x - \varepsilon y$	$\bar{w} = x - \mathbf{j}y$
Euler formula	$e^{\mathbf{i}t} = \cos t + \mathbf{i} \sin t$	$e^{\varepsilon t} = 1 + \varepsilon t$	$e^{\mathbf{j}t} = \cosh t + \mathbf{j} \sinh t$
Modulus	$ w _e^2 = w\bar{w} = x^2 + y^2$	$ w _p^2 = w\bar{w} = x^2$	$ w _h^2 = w\bar{w} = x^2 - y^2$
Argument	$\arg w = \tan^{-1} \frac{y}{x}$	$\arg w = \frac{y}{x}$	$\arg w = \tanh^{-1} \frac{y}{x}$
Zero divisors	0	$x = 0$	$x = \pm y$
Inverse	$\bar{w}/ w _e^2$	$\bar{w}/ w _p^2$	$\bar{w}/ w _h^2$
Unit cycle	circle $ w _e^2 = 1$	unit strip $x = \pm 1$	unit hyperbola $ w _h^2 = 1$

Figure A.2 The correspondence between complex, dual and double numbers.

Notion	Yaglom’s usage	This work
Circle	Defined as a locus of equidistant points in metric $d(u, v; u', v') = u - u' $. Effectively is a pair of vertical lines.	A limiting case of p-cycles with $n = 0$. Forms a Möbius-invariant subfamily of self-adjoint p-cycles (Definition 6.12). In this case, all three centres coincide. We use the term ‘circle’ only to describe a drawing of a cycle in the elliptic point space \mathbb{C} .
Cycle	Defined as a locus of points having fixed angle view to a segment. Effectively is a non-degenerate parabola with a vertical axis.	We use this word for a point of the projective cycle space \mathbb{P}^3 . Its drawing in various point spaces can be a circle, parabola, hyperbola, single or pair of lines, single point or an empty set.
Centre	Absent, Yaglom’s cycles are ‘centreless’.	A cycle has three EPH centres.
Diameter	A quarter of the parabola’s focal length.	The distance between real roots.
Special lines	Vertical lines, special role reflects absolute time in Galilean mechanics.	The intersection of invariant sets of self-adjoint and zero radius p-cycles, i.e. having the form $(1, l, 0, l^2)$.
Orthogonal, perpendicular	The relation between two lines, if one of them is special. Delivers the shortest distance.	We have a variety of different orthogonality and perpendicularity relations, which are not necessary local and symmetric.
Inversion in circles.	Defined through the degenerated p-metric	Conjugation with a degenerate parabola ($n = 0$).
Reflection in cycles	Defined as a reflection in the parabola along the special lines.	Composition of conjugation with three parabolas – see Exercise 6.33.

Figure A.3 Comparison with the Yaglom book.

Appendix B

How to Use the Software

The enclosed DVD with software is derived from several open-source projects, notably Debian GNU–Linux [100], GiNaC library of symbolic calculations [4], *Asymptote* [37] and many others. Thus, our work is distributed under the *GNU General Public License (GPL) 3.0* [32].

You can download an ISO image of a Live GNU–Linux DVD with our CAS from the [arXiv.org](https://arxiv.org) page of paper [63] through the link to Data Conservancy Project. Updated versions of the ISO image may be uploaded there in future.

In this Appendix, we only briefly outline how to start using the enclosed DVD. As soon as it is running, further help may be obtained on the computer screen. We also describe how to run most of the software on the disk on computers without a DVD drive at the end of Sections B.1, B.2.1 and B.2.2.

B.1 Viewing Colour Graphics

The easiest part is to view colour illustrations on your computer. There are not many hardware and software demands for this task – your computer should have a DVD drive and be able to render HTML pages. The last task can be done by any web browser. If these requirements are satisfied, perform the following steps:

1. Insert the DVD disk into the drive of your computer.
2. Mount the disk, if required by your OS.
3. Open the contents of the DVD in a file browser.
4. Open the file `index.html` from the top-level folder of the DVD in a web browser, which may be done simply by clicking on its icon.

5. Click in the browser on the link **View book illustrations**.

If your computer does not have a DVD drive (e.g. is a netbook), but you can gain brief access to a computer with a drive, then you can copy the top-level folder `doc` from the enclosed DVD to a portable medium, say a memory stick. Illustrations (and other documentation) can be accessed by opening the `index.html` file from this folder.

In a similar way, the reader can access ISO images of bootable disks, software sources and other supplementary information described below.

B.2 Installation of CAS

There are three major possibilities of using the enclosed CAS:

- A. To boot your computer from the DVD itself.
- B. To run it in a Linux emulator.
- C. *Advanced*: recompile it from the enclosed sources for your platform.

Method A is straightforward and can bring some performance enhancement. However, it requires hardware compatibility; in particular, you must have the so-called i386 architecture. Method B will run on a much wider set of hardware and you can use CAS from the comfort of your standard desktop. However, this may require an additional third-party programme to be installed.

B.2.1 Booting from the DVD Disk

WARNING: it is a general principle, that running a software within an emulator is more secure than to boot your computer in another OS. Thus we recommend using the method described in Section B.2.2.

It is difficult to give an exact list of hardware requirements for DVD booting, but your computer must be based on the i386 architecture. If you are ready to have a try, follow these steps:

1. Insert the DVD disk into the drive of your computer.
2. Switch off or reboot the computer.
3. Depending on your configuration, the computer may itself attempt to boot from the DVD instead of its hard drive. In this case you can proceed to step 5.
4. If booting from the DVD does not happen, then you need to reboot again

and bring up the ‘boot menu’, which allows you to chose the boot device manually. This menu is usually prompted by a ‘magic key’ pressed just after the computer is powered on – see your computer documentation. In the boot menu, chose the CD/DVD drive.

5. You will be presented with the screen shown on the left in Fig. B.1. Simply press Enter to chose the ‘Live (486)’ or ‘Live (686-pae)’ (for more advanced processors) to boot. To run 686-pae kernel in an emulator, e.g. VirtualBox, you may need to allow ‘PAE option’ in settings.
6. If the DVD booted well on your computer you will be presented with the GUI screen shown on the right in Fig. B.1. Congratulations, you can proceed to Section B.3.

If the DVD boots but the graphic X server did not start for any reason and you have the text command prompt only, you can still use most of the CAS. This is described in the last paragraph of Section B.3.



Figure B.1 Initial screens of software start up. Left, DVD boot menu; right, initial screen after the booting.

If your computer does not have a DVD drive you may still boot the CAS on your computer from a spare USB stick of at least 1Gb capacity. For this, use **UNetbootin** [3] or a similar tool to put an ISO image of a boot disk on the memory stick. The ISO image(s) is located at the top-level folder **iso-images** of the DVD and the file **README** in this folder describes them. You can access this folder as described in Section B.1.

B.2.2 Running a Linux Emulator

You can also use the enclosed CAS on a wide range of hardware running various operating systems, e.g. Linux, Windows, Mac OS, etc. To this

end you need to install a so-called *virtual machine*, which can emulate i386 architecture. I would recommend VirtualBox [85] – a free, open-source program which works well on many existing platforms. There are many alternatives (including open-source), for example: Qemu [9], Open Virtual Machine [86] and some others.

Here, we outline the procedure for VirtualBox – for other emulators you may need to make some adjustments. To use VirtualBox, follow these steps:

1. Insert the DVD disk in your computer.
2. Open the `index.html` file from the top directory of the DVD disk and follow the link ‘Installing VirtualBox’. This is a detailed guide with screenshots. Below we list only the principal steps from this guide.
3. Go to the web site of VirtualBox [85] and proceed to the download page for your platform.
4. Install VirtualBox on your computer and launch it.
5. Create a new virtual machine. Use either the entire DVD or the enclosed ISO images for the virtual DVD drive. If you are using the ISO images, you may wish to copy them first to your hard drive for better performance and silence. See the file `README` in the top-level folder `iso-images` for a description of the image(s).
6. Since a computer emulation is rather resource-demanding, it is better to close all other applications on slower computers (e.g. with a RAM less than 1Gb).
7. Start the newly-created machine. You will need to proceed through steps 5–6 from the previous subsections, as if the DVD is booting on your real computer. As soon as the machine presents the GUI, shown on the right in Fig. B.1, you are ready to use the software.

If you succeeded in this you may proceed to Section B.3. Some tips to improve your experience with emulations are described in the detailed electronic manual.

B.2.3 *Recompiling the CAS on Your OS*

The core of our software is a C++ library which is based on GiNaC [4] – see its web page for up-to-date information. The latter can be compiled and installed on both Linux and Windows. Subsequently, our library can also be compiled on these computers from the provided sources. Then, the library can be used in your C++ programmes. See the top-level folder `src` on the DVD and the documentation therein.

Our interactive tool is based on `pyGiNaC` [14]—a `Python` binding for `GiNaC`. This may work on many flavours of Linux as well. Please note that, in order to use `pyGiNaC` with the recent `GiNaC`, you need to apply my patches to the official version. The DVD contains the whole `pyGiNaC` source tree which is already patched and is ready to use.

There is also a possibility to use our library interactively with `swiGiNaC` [98], which is another `Python` binding for `GiNaC` and is included in many Linux distributions. The complete sources for binding our library to `swiGiNaC` are in the corresponding folder of the enclosed DVD. However, `swiGiNaC` does not implement full functionality of our library.

B.3 Using the CAS and Computer Exercises

Once you have booted to the GUI with the open CAS window as described in Subsections B.2.1 or B.2.2, you may need to configure your keyboard (if it is not a US layout). To install, for example, a Portuguese keyboard, you may type the following command at the prompt of the open window:

```
In [2]: !change-xkbd pt
```

The keyboard will be switched and the corresponding national flag displayed at the bottom-left corner of the window. For another keyboard you need to use the international two-letter country code instead of `pt` in the above command. The first exclamation mark tells that the interpreter needs to pass this command to the shell.

B.3.1 *Warming Up*

The first few lines at the top of the CAS windows suggest several commands to receive a quick introduction or some help on the `IPython` interpreter. Our CAS was loaded with many predefined objects—see Section B.5. Let us see what `C` is, for example:

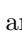
```
In [3]: print C
-----> print(C)
[cycle2D object]
```

```
In [4]: print C.string()
-----> print(C.string())
(k, [L,n],m)
```

Thus, \mathbf{C} is a two-dimensional cycle defined with the quadruple (k, l, n, m) . Its determinant is:

```
In [5]: print C.hdet()
-----> print(C.hdet())
k*m-L**2+si*n**2
```

Here, \mathbf{si} stands for σ – the signature of the point space metric. Thus, the answer reads $km - l^2 + \sigma n^2$ – the determinant of the FSCc matrix of \mathbf{C} .

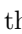
As an exercise, the reader may now follow the proof of Theorem 4.13, remembering that the point \mathbf{P} and cycle \mathbf{C} are already defined. In fact, all statements and exercises marked by the symbol  on the margins are already present on the DVD. For example, to access the proof of Theorem 4.13, type the following at the prompt:

```
In [6]: %ed ex.4.13.py
```

Here, the *special* `%ed` instructs the external editor `jed` to visit the file `ex.4.13.py`. This file is a `Python` script containing the same lines as the proof of Theorem 4.13 in the book. The editor `jed` may be manipulated from its menu and has command keystrokes compatible with GNU Emacs. For example, to exit the editor, press `Ctrl-X Ctrl-C`. After that, the interactive shell executes the visited file and outputs:

```
In [6]: %ed ex.4.13.py
Editing... done. Executing edited code...
Conjugated cycle passes the Moebius image of P: True
```

Thus, our statement is proven.

For any other CAS-assisted statement or exercise you can also visit the corresponding solution using its number next to the symbol  in the margin. For example, for Exercise 6.22, open file `ex.6.22.py`. However, the next mouse sign marks the item 6.24.i, thus you need to visit file `ex.6.24.i.py` in this case. These files are located on a read-only file system, so to modify them you need to save them first with a new name (`Ctrl-X Ctrl-W`), exit the editor, and then use `%ed special` to edit the freshly-saved file.

B.3.2 Drawing Cycles

You can visualise cycles instantly. First, we open an `Asymptote` instance and define a picture size:

```
In [7]: A=asy()
Asymptote session is open.  Available methods are:
      help(), size(int), draw(str), fill(str), clip(str), ...
```

```
In [8]: A.size(100)
```

Then, we define a cycle with centre $(0,1)$ and σ -radius 2:

```
In [9]: Cn=cycle2D([0,1],e,2)
```

```
In [10]: print Cn.string()
-----> print(Cn.string())
(1, [0,1],-2-si)
```

This cycle depends on a variable **sign** and it must be substituted with a numeric value before a visualisation becomes possible:

```
In [11]: A.send(cycle2D(Cn.subs(sign==1)).asy_string())
```

```
In [12]: A.send(cycle2D(Cn.subs(sign==0)).asy_string())
```

```
In [13]: A.send(cycle2D(Cn.subs(sign==1)).asy_string())
```

By now, a separate window will have opened with cycle **Cn** drawn triply as a circle, parabola and hyperbola. Note that you do not need to retype inputs 12 and 13 from scratch. Up/down arrows scroll the input history, so you can simply edit the value of **sign** in the input line 10. Also, since you are in Linux, the **Tab** key will do a completion for you whenever possible.

The interactive shell evaluates and remember all expressions, so it may sometime be useful to restart it. It can be closed by **Ctrl-D** and started from the Main Menu (the bottom-left corner of the screen) using Accessories → CAS pycyle. In the same menu folder, there are two items which open documentation about the library in PDF and HTML formats.

B.3.3 *Further Usage*

There are several batch checks which can be performed with CAS. Open a terminal window from Main Menu → Accessories → LXTerminal. Type at the command prompt:

```
$ cd CAS/pycycle/
$ ./run-pyGiNaC.sh test_pycycle.py
```


A comprehensive test of the library will be performed and the end of the output will look like this:

```
True: sl2_clifford_list: (0)
True: sl2_clifford_matrix: (0)
True: jump_fnct (-1)
```

Finished. The total number of errors is 0

Under normal circumstances, the reported total number of errors will, of course, be zero. You can also run all exercises from this book in a batch. From a new terminal window, type:

```
$ cd CAS/pycycle/Examples/
$ ./check_all_exercises.sh
```

Exercises will be performed one by one with their numbers reported. Numerous graphical windows will be opened to show pencils of cycles. These windows can be closed by pressing the **q** key for each of them. This batch file suppresses all output from the exercises, except those containing the **False** string. Under normal circumstances, these are only Exercises 7.14.i and 7.14.ii.

You may also access the CAS from a command line. This may be required if the graphic X server failed to start for any reason. From the command prompt, type the following:

```
$ cd CAS/pycycle/Examples/
$ ./run-pyGiNaC.sh
```

The full capacity of the CAS is also accessible from the command prompt, except for the preview of drawn cycles in a graphical window. However, EPS files can still be created with **Asymptote**—see **shipout()** method.

B.4 Library for Cycles

Our **C++** library defines the class **cycle** to manipulate cycles of arbitrary dimension in a symbolic manner. The derived class **cycle2D** is tailored to manipulate two-dimensional cycles. For the purpose of the book, we briefly list here some methods for **cycle2D** in the **pyGiNaC** binding form only.

constructors There are two main forms of **cycle2D** constructors:

```
C=cycle2D(k,[l,n],m,e) # Cycle defined by a quadruple
Cr=([u,v],e,r) # Cycle with center at [u,v] and radius r2
```

In both cases, we use a metric defined by a Clifford unit e .

operations Cycles can be added (+), subtracted (-) or multiplied by a scalar (method `exmul()`). A simplification is done by `normal()` and substitution by `subs()`. Coefficients of cycles can be normalised by the methods `normalize()` (k -normalisation) and `normalize_det()`.

evaluations For a given cycle, we can make the following evaluations: `hdet()` – determinant of its FSCc matrix, `radius_sq()` – square of the radius, `val()` – value of a cycle at a point, which is the power of the point to the cycle.

similarities There are the following methods for building cycle similarities: `sl2_similarity()`, `matrix_similarity()` and `cycle_similarity()` with an element of $SL_2(\mathbb{R})$, a matrix or another cycle, respectively.

checks There are several checks for cycles, which return GiNaC relations. The latter may be converted to Boolean values if no variables are presented within them. The checks for a single cycle are: `is_linear()`, `is_normalized()` and `passing()`, the latter requires a parameter (point). For two cycles, they are `is_orthogonal()` and `is_f_orthogonal()`.

specialisation Having a cycle defined through several variables, we may try to specialise it to satisfy some further conditions. If these conditions are *linear* with respect to the cycle's variables, this can be achieved through the very useful method `subject_to()`. For example, for the above defined cycle C , we can find

```
C2=C.subject_to([C.passing([u,v]), C.is_orthogonal(C1)])
```

where $C2$ will be a generic cycle passing the point $[u,v]$ and orthogonal to $C1$. See the proof of Theorem 4.13 for an application.

specific There are the following methods specific to two dimensions: `focus()`, `focal_length()` – evaluation of a cycle's focus and focal length and `roots()` – finding intersection points with a vertical or horizontal line. For a generic line, use method `line_intersect()` instead.

drawing For visualisation through `Asymptote`, you can use various methods: `asy_draw()`, `asy_path()` and `asy_string()`. They allow you to define the bounding box, colour and style of the cycle's drawing. See the examples or full documentation for details of usage.

Further information can be obtained from electronic documentation on the enclosed DVD, an inspection of the test file `CAS/pycycle/test.pycycle.py` and solutions of the exercises.

B.5 Predefined Objects at Initialisation

For convenience, we predefine many GiNaC objects which may be helpful. Here is a brief indication of the most-used:

`realsymbol`. `a`, `b`, `c`, `d`: elements of $SL_2(\mathbb{R})$ matrix.

`u`, `v`, `u1`, `v1`, `u2`, `v2`: coordinates of points.

`r`, `r1`, `r2`: radii.

`k`, `l`, `n`, `m`, `k1`, `l1`, `n1`, `m1`: components of cycles.

`sign`, `sign1`, `sign2`, `sign3`, `sign4`: signatures of various metrics.

`s`, `s1`, `s2`, `s3`: s parameters of FSCc matrices.

`x`, `y`, `t`: spare to use.

`varidx`. `mu`, `nu`, `rho`, `tau`: two-dimensional indexes for Clifford units.

`matrix`. `M`, `M1`, `M2`, `M3`: diagonal 2×2 matrices with entries -1 and i -th `sign` on their diagonal.

`sign_mat`, `sign_mat1`, `sign_mat2`: similar matrices with i -th `s` instead of `sign`.

`clifford_unit`. `e`, `es`, `er`, `et`: Clifford units with metrics derived from matrices `M`, `M1`, `M2`, `M3`, respectively.

`cycle2D`. The following cycles are predefined:

```
C=cycle2D(k,[l,n],m,e)      # A generic cycle
```

```
C1=cycle2D(k1,[l1,n1],m1,e)# Another generic cycle
```

```
Cr=([u,v],e,r2) # Cycle with centre at [u,v] and radius r2
```

```
Cu=cycle2D(1,[0,0],1,e)     # Unit cycle
```

```
real_line=cycle2D(0,[0,1],0,e)
```

```
Z=cycle2D([u,v], e)         # Zero radius cycles at [u,v]
```

```
Z1=cycle2D([u1,v1], e)      # Zero radius cycles at [u1,v1]
```

```
Zinf=cycle2D(0,[0,0],1,e)   # Zero radius cycles at infinity
```

The solutions of the exercises make heavy use of these objects. Their exact definition can be found in the file `CAS/pycycle/init_cycle.py` from the home directory.

Bibliography

- [1] F. Antonuccio. Hyperbolic numbers and the Dirac spinor. In V. V. Dvoeglazov, (editor). *The Photon and Poincare Group*, Nova Science Publisher, Inc., Commack, 1999. E-print: [arXiv:hep-th/9812036](https://arxiv.org/abs/hep-th/9812036) (Last accessed 31.12.2011). ↑160
- [2] V. I. Arnol'd. *Mathematical Methods of Classical Mechanics*. Graduate Texts in Mathematics, vol. 60. Springer-Verlag, New York, 1991. Translated from the 1974 Russian original by K. Vogtmann and A. Weinstein, corrected reprint of the 1989 second edition. ↑53, 113, 117
- [3] A. Kovacs and G. Kovacs. *UNetbootin—Create Bootable Live USB drives for Linux*, 2011. URL: <http://unetbootin.sourceforge.net/> (Last accessed 31.12.2011). ↑165
- [4] C. Bauer, A. Frink, R. Kreckel, and J. Vollinga. *GiNaC is Not a CAS*, 2001. URL: <http://www.ginac.de/> (Last accessed 31.12.2011). ↑163, 166
- [5] A. F. Beardon. *The Geometry of Discrete Groups*. Graduate Texts in Mathematics, vol. 91. Springer-Verlag, New York, 1995. Corrected reprint of the 1983 original. ↑66, 120, 131
- [6] A. F. Beardon. *Algebra and Geometry*. Cambridge University Press, Cambridge, 2005. ↑1, 33, 53, 120, 128
- [7] A. F. Beardon and I. Short. Conformal symmetries of regions. *Irish Math. Soc. Bull.* 59:49–60, 2007. ↑66
- [8] E. Bekkara, C. Frances, and A. Zeghib. On lightlike geometry: isometric actions, and rigidity aspects. *C. R. Math. Acad. Sci. Paris* 343(5):317–321, 2006. ↑160
- [9] F. Bellard. *QEMU—A Generic and Open Source Machine Emulator and Virtualizer*, 2011. URL: <http://qemu.org/> (Last accessed 31.12.2011). ↑166
- [10] W. Benz. *Classical Geometries in Modern Contexts. Geometry of Real Inner Product spaces*. Birkhäuser Verlag, Basel, 2007. ↑124
- [11] M. Berger. *Geometry. II*. Universitext. Springer-Verlag, Berlin, 1987. Translated from the 1977 French original by M. Cole and S. Levy. ↑106, 158
- [12] M. Berger. *Geometry. I*. Universitext. Springer-Verlag, Berlin, 1994. Translated from the 1977 French original by M. Cole and S. Levy, corrected reprint of the 1987 translation. ↑59, 74

- [13] D. Boccaletti, F. Catoni, R. Cannata, V. Catoni, E. Nichelatti, and P. Zampetti. *The Mathematics of Minkowski Space-time and an Introduction to Commutative Hypercomplex Numbers*. Birkhäuser Verlag, Basel, 2008. ↑114, 116, 121, 160
- [14] J. Brandmeyer. *PyGiNaC—A Python Interface to the C++ Symbolic Math Library GiNaC*, 2004. URL: <http://sourceforge.net/projects/pyginac/> (Last accessed 31.12.2011). ↑167
- [15] S. Brewer. Projective cross-ratio on hypercomplex numbers. *Adv. Appl. Clifford Algebras*, 2012. (to appear). E-print: [arXiv:1203.2554](https://arxiv.org/abs/1203.2554) (Last accessed 31.12.2011). ↑53, 54, 129
- [16] T. K. Carne. *Geometry and Groups*, 2006. URL: <http://www.dpmms.cam.ac.uk/~tkc/GeometryandGroups> (Last accessed 31.12.2011). ↑119
- [17] F. Catoni, R. Cannata, and E. Nichelatti. The parabolic analytic functions and the derivative of real functions. *Adv. Appl. Clifford Algebras* 14(2):185–190, 2004. ↑104, 160
- [18] F. Catoni, R. Cannata, V. Catoni, and P. Zampetti. N -dimensional geometries generated by hypercomplex numbers. *Adv. Appl. Clifford Algebras* 15(1), 2005. ↑160
- [19] P. Cerejeiras, U. Kähler, and F. Sommen. Parabolic Dirac operators and the Navier-Stokes equations over time-varying domains. *Math. Methods Appl. Sci.* 28(14):1715–1724, 2005. ↑160
- [20] S.-S. Chern. Finsler geometry is just Riemannian geometry without the quadratic restriction. *Notices Amer. Math. Soc.* 43(9):959–963, 1996. ↑88
- [21] J. Cnops, *Hurwitz pairs and applications of Möbius transformations*. Habilitation Dissertation, Universiteit Gent, Faculteit van de Wetenschappen, 1994. See also [22]. ↑50
- [22] J. Cnops. *An Introduction to Dirac Operators on Manifolds*. Progress in Mathematical Physics, vol. 24. Birkhäuser Boston Inc., Boston, MA, 2002. ↑6, 47, 49, 50, 51, 55, 73, 87, 96, 174
- [23] H. S. M. Coxeter and S. L. Greitzer. *Geometry Revisited*. Random House, New York, 1967. ↑viii, 40, 45, 59, 60, 66, 74, 86, 94
- [24] M. Davis. *Applied Nonstandard Analysis*. Wiley-Interscience, New York, 1977. ↑100
- [25] D. Eelbode and F. Sommen. Taylor series on the hyperbolic unit ball. *Bull. Belg. Math. Soc. Simon Stevin* 11(5):719–737, 2004. ↑160
- [26] D. Eelbode and F. Sommen. The fundamental solution of the hyperbolic Dirac operator on $\mathbb{R}^{1,m}$: a new approach. *Bull. Belg. Math. Soc. Simon Stevin* 12(1):23–37, 2005. ↑160
- [27] J. P. Fillmore and A. Springer. Möbius groups over general fields using Clifford algebras associated with spheres. *Internat. J. Theoret. Phys.* 29(3):225–246, 1990. ↑50, 81, 87
- [28] P. Fjelstad and S. G. Gal. Two-dimensional geometries, topologies, trigonometries and physics generated by complex-type numbers. *Adv. Appl. Clifford Algebras* 11(1):81–107 (2002), 2001. ↑160
- [29] G. I. Garas'ko. *Начала финслеровой геометрии для физиков. [Elements of Finsler Geometry for Physicists]*. TETRU, Moscow, 2009. 268 pp. URL: <http://hypercomplex.xpsweb.com/articles/487/ru/pdf/00-gbook.pdf> (Last accessed 31.12.2011). ↑88

- [30] A. Gerrard and J. M. Burch. *Introduction to Matrix Methods in Optics*. Dover Publications Inc., New York, 1994. Corrected reprint of the 1975 original. ↑111, 112
- [31] I. M. Glazman and Ju. I. Ljubič. *Finite-dimensional Linear Analysis*. Dover Publications Inc., Mineola, NY, 2006. Translated from the Russian and edited by G. P. Barker and G. Kuerti, reprint of the 1974 edition. ↑viii
- [32] GNU. *General Public License (GPL)*. Free Software Foundation, Inc., Boston, USA, version 3, 2007. URL: <http://www.gnu.org/licenses/gpl.html> (Last accessed 31.12.2011). ↑163
- [33] I. Gohberg, P. Lancaster, and L. Rodman. *Indefinite Linear Algebra and Applications*. Birkhäuser Verlag, Basel, 2005. ↑61, 74, 76
- [34] N. A. Gromov. *Контракции и аналитические продолжения классических групп. Единый подход. (Russian) [Contractions and Analytic Extensions of Classical Groups. Unified Approach]*. Akad. Nauk SSSR Ural. Otdel. Komi Nauchn. Tsentr, Syktyvkar, 1990. ↑160
- [35] N. A. Gromov. Transitions: Contractions and analytical continuations of the Cayley–Klein groups. *Int. J. Theor. Phys.* 29:607–620, 1990. ↑97, 160
- [36] V. Gutenmacher and N. B. Vasilyev. *Lines and Curves. A Practical Geometry HandBook*. Birkhäuser Verlag, Basel, 2004. Based on an English translation of the original Russian edition by A. Kundu. ↑158, 159
- [37] A. Hammerlindl, J. Bowman, and T. Prince. *Asymptote—powerful descriptive vector graphics language for technical drawing, inspired by MetaPost*, 2004. URL: <http://asymptote.sourceforge.net/> (Last accessed 31.12.2011). ↑163
- [38] F. J. Herranz, R. Ortega, and M. Santander. Trigonometry of spacetimes: a new self-dual approach to a curvature/signature (in)dependent trigonometry. *J. Phys. A* 33(24):4525–4551, 2000. E-print: [arXiv:math-ph/9910041](https://arxiv.org/abs/math-ph/9910041) (Last accessed 31.12.2011). ↑124, 143, 144
- [39] F. J. Herranz and M. Santander. Conformal compactification of spacetimes. *J. Phys. A* 35(31):6619–6629, 2002. E-print: [arXiv:math-ph/0110019](https://arxiv.org/abs/math-ph/0110019) (Last accessed 31.12.2011). ↑97, 107, 160
- [40] F. J. Herranz and M. Santander. Conformal symmetries of spacetimes. *J. Phys. A* 35(31):6601–6618, 2002. E-print: [arXiv:math-ph/0110019](https://arxiv.org/abs/math-ph/0110019) (Last accessed 31.12.2011). ↑97, 160
- [41] D. Hestenes and G. Sobczyk. *Clifford Algebra to Geometric Calculus. A Unified Language for Mathematics and Physics*. Fundamental Theories of Physics. D. Reidel Publishing Co., Dordrecht, 1984. ↑160
- [42] L. Hörmander. *The Analysis of Linear Partial Differential Operators III: Pseudo-differential Operators*. Springer-Verlag, Berlin, 1985. ↑25
- [43] R. Howe. On the role of the Heisenberg group in harmonic analysis. *Bull. Amer. Math. Soc. (N.S.)* 3(2):821–843, 1980. ↑1, 19, 20
- [44] R. Howe and E.-C. Tan. *Nonabelian harmonic analysis. Applications of $SL(2, \mathbf{R})$* . Springer-Verlag, New York, 1992. ↑19, 20
- [45] J. Hucks. Hyperbolic complex structures in physics. *J. Math. Phys.* 34(12):5986–6008, 1993. ↑160

- [46] R. Hudson, *Generalised translation-invariant mechanics*. D. Phil. thesis, Bodleian Library, Oxford, 1966. ↑160
- [47] R. Hudson. Translation invariant phase space mechanics. In A. Khrennikov, (editor). *Quantum Theory: Reconsideration of Foundations—2*, Växjö Univ. Press, Växjö, 2004, pp. 301–314. ↑160
- [48] A. Yu. Khrennikov. Hyperbolic quantum mechanics. *Dokl. Akad. Nauk* 402(2):170–172, 2005. ↑160
- [49] A. Khrennikov. Hyperbolic Quantum Mechanics. *Adv. Appl. Clifford Algebras* 13(1):1–9, 2003. E-print: [arXiv:quant-ph/0101002](https://arxiv.org/abs/quant-ph/0101002) (Last accessed 31.12.2011). ↑160
- [50] A. Khrennikov. Hyperbolic quantization. *Adv. Appl. Clifford Algebr.* 18(3–4):843–852, 2008. ↑160
- [51] A. Khrennikov and G. Segre. Hyperbolic quantization. In L. Accardi, W. Freudenberger, and M. Schürman, (editors). *Quantum Probability and Infinite Dimensional Analysis*, World Scientific Publishing, Singapore, 2007, pp. 282–287. ↑160
- [52] A. A. Kirillov. *Elements of the Theory of Representations*. Springer-Verlag, Berlin, 1976. Translated from the Russian by E. Hewitt, Grundlehren der Mathematischen Wissenschaften, Band 220. ↑17, 19, 22, 23, 52, 114
- [53] A. A. Kirillov. Merits and demerits of the orbit method. *Bull. Amer. Math. Soc. (N.S.)* 36(4):433–488, 1999. ↑52
- [54] A. A. Kirillov. *A Tale on two Fractals*, MCCME, Moscow, 2010. URL: <http://www.math.upenn.edu/~kirillov/MATH480-F07/tf.pdf>, in publication. ↑8, 47, 50, 51, 52, 58, 68
- [55] A. A. Kirillov and A. D. Gvishiani. *Theorems and Problems in Functional Analysis*. Problem Books in Mathematics. Springer-Verlag, New York, 1982. ↑viii, 67, 91, 117
- [56] A. V. Kisil. Isometric action of $SL_2(\mathbb{R})$ on homogeneous spaces. *Adv. App. Clifford Algebras* 20(2):299–312, 2010. E-print: [arXiv:0810.0368](https://arxiv.org/abs/0810.0368) (Last accessed 31.12.2011). ↑117, 139
- [57] V. V. Kisil. Möbius transformations and monogenic functional calculus. *Electron. Res. Announc. Amer. Math. Soc.* 2(1):26–33, 1996. On-line (Last accessed 31.12.2011). ↑16
- [58] V. V. Kisil. Analysis in $\mathbf{R}^{1,1}$ or the principal function theory. *Complex Variables Theory Appl.* 40(2):93–118, 1999. E-print: [arXiv:funct-an/9712003](https://arxiv.org/abs/funct-an/9712003) (Last accessed 31.12.2011). ↑15, 32, 109, 133, 160
- [59] V. V. Kisil. Two approaches to non-commutative geometry. In H. Begehr, O. Celebi, and W. Tutschke, (editors). *Complex Methods for Partial Differential Equations*, Kluwer Academic Publishing, Dordrecht, 1999, pp. 215–244. E-print: [arXiv:funct-an/9703001](https://arxiv.org/abs/funct-an/9703001) (Last accessed 31.12.2011). ↑vii
- [60] V. V. Kisil. Meeting Descartes and Klein Somewhere in a Noncommutative Space. In A. Fokas, J. Halliwell, T. Kibble, and B. Zegarlinski, (editors). *Highlights of Mathematical Physics*, American Mathematical Society, Providence, RI, 2002, pp. 165–189. E-print: [arXiv:math-ph/0112059](https://arxiv.org/abs/math-ph/0112059) (Last accessed 31.12.2011). ↑vii, viii, 15, 16
- [61] V. V. Kisil. Spectrum as the support of functional calculus. *Functional Analysis and its Applications*, Elsevier, Amsterdam, 2004, pp. 133–141. E-print: [arXiv:math.FA/0208249](https://arxiv.org/abs/math.FA/0208249) (Last accessed 31.12.2011). ↑16

- [62] V. V. Kisil. Erlangen program at large-0: Starting with the group $SL_2(\mathbf{R})$. *Notices Amer. Math. Soc.* 54(11):1458–1465, 2007. E-print: [arXiv:math/0607387](#) (Last accessed 31.12.2011). ↑20, 35
- [63] V. V. Kisil. Fillmore–Springer–Cnops construction implemented in GiNaC. *Adv. Appl. Clifford Algebr.* 17(1):59–70, 2007. Updated full text and source files: E-print: [arXiv:cs.MS/0512073](#) (Last accessed 31.12.2011). ↑49, 163
- [64] V. V. Kisil. Erlangen program at large—2: Inventing a wheel. The parabolic one. *Trans. Inst. Math. of the NAS of Ukraine* 7:89–98, 2010. E-print: [arXiv:0707.4024](#) (Last accessed 31.12.2011). ↑35, 124
- [65] V. V. Kisil. Erlangen program at large–1: Geometry of invariants. *SIGMA, Symmetry Integrability Geom. Methods Appl.* 6(076):45, 2010. E-print: [arXiv:math.CV/0512416](#) (Last accessed 31.12.2011). ↑14, 48, 49, 160
- [66] V. V. Kisil. Covariant transform. *Journal of Physics: Conference Series* 284(1):012038, 2011. E-print: [arXiv:1011.3947](#) (Last accessed 31.12.2011). ↑15
- [67] V. V. Kisil. Erlangen program at large—2 1/2: Induced representations and hypercomplex numbers. *Известия Коми научного центра УрО РАН [Izvestiya Komi nauchnogo centra UrO RAN]* 5(1):4–10, 2011. E-print: [arXiv:0909.4464](#) (Last accessed 31.12.2011). ↑15, 152, 156
- [68] V. V. Kisil. Erlangen Programme at Large 3.2: Ladder operators in hypercomplex mechanics. *Acta Polytechnica* 51(4):44–53, 2011. E-print: [arXiv:1103.1120](#) (Last accessed 31.12.2011). ↑16, 114, 156
- [69] V. V. Kisil. Erlangen programme at large: an Overview. In S. V. Rogosin and A. A. Koroleva, (editors). *Advances in Applied Analysis*, Birkhäuser Verlag, Basel, 2012, pp. 1–78. E-print: [arXiv:1106.1686](#) (Last accessed 31.12.2011). ↑vii, 156
- [70] V. V. Kisil. Hypercomplex representations of the Heisenberg group and mechanics. *Internat. J. Theoret. Phys.* 51(3):964–984, 2012. E-print: [arXiv:1005.5057](#) (Last accessed 31.12.2011). ↑16, 114
- [71] F. Klein. *Elementary Mathematics from an Advanced Standpoint. Arithmetic, Algebra, Analysis*. Dover Publications Inc., Mineola, NY, 2004. Translated from the third German edition by E. R. Hedrick and C. A. Noble, reprint of the 1932 translation. ↑viii
- [72] F. Klein. *Elementary Mathematics from an Advanced Standpoint. Geometry*. Dover Publications Inc., Mineola, NY, 2004. Translated from the third German edition and with a preface by E. R. Hendrik and C. A. Noble, reprint of the 1949 translation. ↑viii
- [73] J. Kollár and S. Mori. *Birational Geometry of Algebraic Varieties*. Cambridge Tracts in Mathematics, vol. 134. Cambridge University Press, Cambridge, 2008. Paperback reprint of the hardback 1998 edition. ↑152
- [74] N. G. Konovenko. Algebras of differential invariants for geometrical quantities on affine line. *Visn., Ser. Fiz.-Mat. Nauky, Kyiv. Univ. Im. Tarasa Shevchenka* 2008(2):9–15, 2008. ↑160
- [75] N. G. Konovenko and V. V. Lychagin. Differential invariants of nonstandard projective structures. *Dopov. Nats. Akad. Nauk Ukr., Mat. Pryr. Tekh. Nauky* 2008(11):10–13, 2008. ↑160
- [76] S. Lang. *Algebra*. Addison-Wesley, New York, 1969. ↑21

- [77] S. Lang. $SL_2(\mathbf{R})$. Graduate Texts in Mathematics, vol. 105. Springer-Verlag, New York, 1985. Reprint of the 1975 edition. ↑1, 2, 15, 19, 20, 31, 132
- [78] M. A. Lavrent'ev and B. V. Shabat. *Проблемы гидродинамики и их математические модели. [Problems of hydrodynamics and their mathematical models]*. Izdat. "Nauka", Moscow, Second, 1977. ↑36, 143, 152, 157, 160
- [79] G. L. Litvinov. The Maslov dequantization, and idempotent and tropical mathematics: a brief introduction. *Zap. Nauchn. Sem. S.-Peterburg. Otdel. Mat. Inst. Steklov. (POMI)* 326(Teor. Predst. Din. Sist. Komb. i Algoritm. Metody. 13):145–182, 282, 2005. E-print: [arXiv:math/0507014](https://arxiv.org/abs/math/0507014) (Last accessed 31.12.2011). ↑149
- [80] I. P. Mel'nichenko and S. A. Plaksa. *Коммутативные алгебры и пространственные потенциальные поля [Commutative Algebras and Spatial Potential Fields]*. Inst. Math. NAS Ukraine, Kiev, 2008. ↑160
- [81] W. Miller Jr. *Lie Theory and Special Functions*. Mathematics in Science and Engineering, vol. 43. Academic Press, New York, 1968. ↑15
- [82] R. Mirman. *Quantum Field Theory, Conformal Group Theory, Conformal Field Theory. Mathematical and Conceptual Foundations, Physical and Geometrical Applications*. Nova Science Publishers Inc., Huntington, NY, 2001. ↑160
- [83] A. E. Motter and M. A. F. Rosa. Hyperbolic calculus. *Adv. Appl. Clifford Algebras* 8(1):109–128, 1998. ↑160
- [84] P. J. Olver. *Classical Invariant Theory*. London Mathematical Society Student Texts, vol. 44. Cambridge University Press, Cambridge, 1999. ↑50, 105
- [85] Oracle. *VirtualBox—Powerful x86 and AMD64/Intel64 Virtualization Product*, 2011. URL: <http://www.virtualbox.org> (Last accessed 31.12.2011). ↑166
- [86] OVMTP. *Open Virtual Machine—the Open Source Implementation of VMware Tools*, 2011. URL: <http://open-vm-tools.sourceforge.net/> (Last accessed 31.12.2011). ↑166
- [87] J. R. Parker. *Hyperbolic Spaces*. University of Durham, 2007. URL: <http://maths.dur.ac.uk/~dma0jrp/img/HSjyvaskyla.pdf> (Last accessed 31.12.2011). ↑14
- [88] V. N. Pilipchuk. *Nonlinear Dynamics. Between Linear and Impact Limits*. Lecture Notes in Applied and Computational Mechanics, vol. 52. Springer, Berlin, 2010. ↑152, 160
- [89] V. N. Pilipchuk. *Non-smooth Spatio-temporal Coordinates in Nonlinear Dynamics*, January 2011. E-print: [arXiv:1101.4597](https://arxiv.org/abs/1101.4597) (Last accessed 31.12.2011). ↑152, 160
- [90] R. I. Pimenov. Unified axiomatics of spaces with maximal movement group. *Litov. Mat. Sb.* 5:457–486, 1965. ↑97, 159
- [91] S. Plaksa. Commutative algebras of hypercomplex monogenic functions and solutions of elliptic type equations degenerating on an axis. In H. G. W. Begehr, (editor). *Further Progress in Analysis. Proceedings of the 6th international ISAAC congress, Catania, Italy, July 25–30, 2005*, World Scientific, Singapore, 2009, pp. 977–986. ↑160
- [92] G. Pólya and G. Szegő. *Problems and Theorems in Analysis. I Series, Integral Calculus, Theory of Functions*. Classics in Mathematics. Springer-Verlag, Berlin, 1998. Translated from the German by Dorothee Aepli, reprint of the 1978 English translation. ↑viii

- [93] L. S. Pontryagin. *Обобщения чисел [Generalisations of numbers]*. Библиотечка “Квант” [Library “Kvant”], vol. 54. “Nauka”, Moscow, 1986. ↑35
- [94] I. R. Porteous. *Clifford Algebras and the Classical Groups*. Cambridge Studies in Advanced Mathematics, vol. 50. Cambridge University Press, Cambridge, 1995. ↑50, 87
- [95] W. W. Sawyer. *Prelude to Mathematics*. Popular Science Series. Dover Publications, New York, 1982. ↑46, 105
- [96] I. E. Segal. *Mathematical Cosmology and Extragalactic Astronomy*. Pure and Applied Mathematics, vol. 68. Academic Press, New York, 1976. ↑109, 111, 116
- [97] M. A. Shubin. *Pseudodifferential Operators and Spectral Theory*. Springer-Verlag, Berlin, Second, 2001. Translated from the 1978 Russian original by S. I. Andersson. ↑25
- [98] O. Skavhaug and O. Certik. *swiGiNaC—A Python Interface to GiNaC, Built With SWIG*, 2010. URL: <http://swiginac.berlios.de/> (Last accessed 31.12.2011). ↑167
- [99] G. Sobczyk. The hyperbolic number plane. *College Math Journal* 26(4):268–280, 1995. ↑160
- [100] *Debian—the universal operating system*. Software in the Public Interest, Inc., 1997. URL: <http://www.debian.org/> (Last accessed 31.12.2011). ↑163
- [101] M. E. Taylor. *Noncommutative Harmonic Analysis*. Mathematical Surveys and Monographs, vol. 22. American Mathematical Society, Providence, RI, 1986. ↑19, 132
- [102] S. Ulrych. Relativistic quantum physics with hyperbolic numbers. *Phys. Lett. B* 625(3–4):313–323, 2005. ↑160
- [103] S. Ulrych. Considerations on the hyperbolic complex Klein–Gordon equation. *J. Math. Phys.* 51(6):063510, 8, 2010. ↑160
- [104] V. A. Uspenskii. *Что такое нестандартный анализ? [What is non-standard analysis?]*. “Nauka”, Moscow, 1987. With an appendix by V. G. Kanovei. ↑100
- [105] J. C. Vignaux and A. Durañona y Vedia. Sobre la teoría de las funciones de una variable compleja hiperbólica [On the theory of functions of a complex hyperbolic variable]. *Univ. nac. La Plata. Publ. Fac. Ci. fis. mat.* 104:139–183, 1935. ↑160
- [106] N. Ja. Vilenkin. *Special Functions and the Theory of Group Representations*. Translations of Mathematical Monographs, vol. 22. American Mathematical Society, Providence, RI, 1968. Translated from the Russian by V. N. Singh. ↑15
- [107] P. M. H. Wilson. *Curved Spaces. From Classical Geometries to Elementary Differential Geometry*. Cambridge University Press, Cambridge, 2008. ↑118, 119
- [108] I. M. Yaglom. *A Simple Non-Euclidean Geometry and its Physical Basis*. Heidelberg Science Library. Springer-Verlag, New York, 1979. Translated from the Russian by Abe Shenitzer. ↑2, 4, 13, 40, 43, 45, 76, 87, 92, 94, 96, 97, 99, 100, 104, 107, 114, 115, 116, 121, 122, 125, 139, 142, 143, 144, 147, 159, 160
- [109] D. N. Zejliger. *Комплексная линейчатая геометрия. Поверхности и конгруэнции. [Complex Lined Geometry. Surfaces and Congruency]*. GTTI, Leningrad, 1934. ↑160

This page intentionally left blank

Index

- \mathbb{A} (point space), 36
- A subgroup, 2, 30, 156
- A -orbit, 3, 37, 139
- A' subgroup, 31, 41, 42, 118, 134
- A' -orbit, 42
- \mathbb{C} (complex numbers), 36
- $\check{C}_{\check{\sigma}}$ (ghost cycle), 79
- \mathbb{D} (dual numbers), 36
- \mathbb{D}_{σ} (unit disk), 133
- \mathbb{H}^1 (Heisenberg group), 19
- K subgroup, 2, 15, 30, 118, 156
- K -orbit, 3, 37, 37–40, 42, 57, 108, 110, 139
- M map, 47, 105
- N subgroup, 2, 30, 156
- N -orbit, 3, 37, 139
- N' subgroup, 31, 41, 118
- N' -orbit, 42
- \mathbb{O} (double numbers), 36
- $\tilde{\mathbb{O}}$ (two-fold cover of double numbers), 110
- $\tilde{\mathbb{O}}^+$ (hyperbolic upper half-plane), 110
- P (projection from the projective space), 129
- $\mathbb{P}^1(\mathbb{A})$ (projective space), 53
- \mathbb{P}^3 (projective space), 46
- Q map, 46, 73, 105
- $R_{\check{\sigma}}^s$ (cycle representing the real line), 85
- \mathbb{R}^* (hyperreals), 104
- S (section to the projective space), 54
- $\mathrm{SL}_2(\mathbb{R})$ group, 1, 19
- $\mathrm{SU}(1, 1)$ group, 132
- \mathbb{T}_{σ} (unit cycle), 133
- $Z_{\check{\sigma}}^s(y)$ ($\check{\sigma}$ -zero-radius cycle), 64
- Z_{∞} (zero-radius cycle at infinity), 106
- $[z_1, z_2, z_3, z_4]$ (cross-ratio), 53
- ∞ (point at infinity), 106
- \perp (perpendicularity), 98
- \overrightarrow{AB} (directed interval), 94
- \dashv (f-orthogonality), 88
- $ax + b$ group, 1, 19, 37
- ε (parabolic unit), 2
- ϵ (infinitesimal), 100
- i (imaginary unit), 2
- ι (hypercomplex unit), 2, 35, 157
- $\check{\iota}$ (hypercomplex unit in cycle space), 6, 47
- j (hyperbolic unit), 2
- k -normalised cycle, 13, 58, 64, 65, 91, 93, 171
- $l_c(\overrightarrow{AB})$ (length from centre), 94
- $l_f(\overrightarrow{AB})$ (length from focus), 94
- p map, 22, 113
- r map, 22, 113
- s map, 22, 113
- σ ($\sigma := \iota^2$), 2, 35
- $\check{\sigma}$ ($\check{\sigma} := \check{\iota}^2$), 47
- $\check{\sigma}$ -focus, 56, 128
- \mathfrak{sl}_2 (Lie algebra), 27
- χ (Heaviside function), 78
- \curlyboxplus , *see* CAS exercise

- abelian
 - group, *see* commutative group
- absolute
 - time, 115, 142, 162
- abstract group, 18, 20
- acceleration, 115
- action
 - derived, 4, 27, 30, 37
 - transitive, 1, 21, 23, 37
- adjoint
 - representation, 52
- affine group, *see* $ax + b$ group
- algebra
 - associative, 157
 - Clifford, 14, 49, 50, 81, 160
 - matrix similarity, 160
 - Möbius map, 160
 - commutative, 157
 - Lie, 23–27, 52
- algebraically-closed, 157
- analysis
 - complex, 15
 - functional, 45
 - harmonic, 15
 - non-Archimedean, *see*
 - non-standard
 - non-standard, 100, 104
- Archimedes, 100, 159
- arrow
 - time, of, 109, 116
- associative
 - algebra, 157
- associativity, 18
- astronomy
 - extragalactic, 111, 116
- Asymptote**, 163, 168
- asymptote
 - hyperbola, of, 38, 159
- Bergman
 - integral, 15
 - space, 15
- birational
 - geometry, 152
- boundary effect on the upper
 - half-plane, 8, 57, 65, 71, 80, 88
- cancellation
 - formula for cross-ratios, 54, 128
- canonical
 - transformation, 113
- CAS, viii, 48, 100, 160, 163–172
 - exercise, 33, 37–39, 41, 48, 49, 54, 60, 61, 64–68, 70, 71, 79–83, 85–87, 89, 92, 94–96, 98, 100–103, 106, 120, 127, 137–139, 153
 - pyGiNaC, 167
 - swiGiNaC, 167
- case
 - elliptic, 2, 35
 - hyperbolic, 2, 35
 - parabolic, 2, 35
- category theory, 9
- Cauchy
 - integral, 15
- Cauchy–Riemann
 - operator, 15
- Cauchy–Schwarz inequality, 67–68, 72
- causal
 - orientation, 109, 116
- Cayley transform, 131, 139
 - cycle, of, 136
 - elliptic, 131
 - hyperbolic, 131
 - parabolic, 134
- centre
 - cycle, of, 7, 36, 44, 56, 58, 93, 94, 128, 135, 158, 162
 - ellipse, of, 158
 - hyperbola, of, 159
 - length from, 14, 94, 95, 96, 132–135
- circle, 44, 158
 - imaginary, 44, 56, 60, 63
 - parabolic (Yaglom term), 76, 162
 - unit, *see* elliptic unit cycle
- classical
 - mechanics, 113
- Clifford
 - algebra, 14, 49, 50, 81, 160
 - matrix similarity, 160
 - Möbius map, 160

- coaxial
 - cycles, 40, 60
- commutation relation
 - Heisenberg, 26
- commutative
 - algebra, 157
 - group, 18
- commutator, 26
- compactification, 105
- complex
 - analysis, 15
 - numbers, 33, 157
- computer algebra system, *see* CAS
- concentric, 7, 44, 60, 101, 136
 - parabolas, 56, 136
- conccyclic, 54
- condition
 - Vahlen, 81, 87
- cone, 4, 158
 - light, 41, 65, 82, 102, 109, 116
 - infinity, at, 107, 109
- confocal, 101
 - parabolas, 136
- conformal
 - infinitesimally, 103
 - space-time, 107
- conformality, 14, 96
 - parabolic, 153
- congruence
 - matrix, of, 52
- conic
 - section, 2, 4, 39, 158
- conjugated subgroups, 21
- conjugation, 21, 52
 - cycles, of, 11, 101
- constant
 - curvature, 107
- construction
 - Fillmore–Springer–Cnops, 6, 47, 134
 - Gelfand–Naimark–Segal, 9, 61
- continuous group, 19
- contour line, 38, 96, 98, 99, 146
- correspondence
 - Kirillov, 52
 - principle of similarity and correspondence, 156
- coset space, 22
- cover
 - two-fold
 - hyperbolic plane, 110, 133
- cross-ratio, 53, 128
 - cancellation formula, 54, 128
 - projective, 53, 53–54, 129
- curvature, 38
 - constant, 107
- curve
 - length, 118
- cycle, 4, 43, 46, 158
 - $\check{\sigma}$ -product, 61, 69, 93
 - Cayley transform, 136
- centre, 7, 36, 44, 56, 58, 93, 94, 128, 135, 158, 162
- concentric, 101
- confocal, 101
- conjugation, 11, 101
- diameter, 91, 162
- equation, 6, 43, 46
- f-ghost, 89
- flat, 44
- focal length, 56, 92
- focus, 7, 36, 56, 92, 128, 135, 158
- ghost, 79, 85
- infinitesimal radius, of, 100, 100–104, 138
- inversion, 84, 84–87, 89
- isotropic, 11, 72
- matrix, 6, 46
 - Clifford algebra, 160
- normalised, 8, 58
 - det-, 58, 64, 66, 87, 92, 171
 - k -, 13, 58, 64, 65, 91, 93, 171
- orthogonality, 49, 102
- parabolic (Yaglom term), 162
- positive, 62, 120
- radius, 13, 58, 91, 171
 - infinitesimal, of, 100, 100–104
 - zero, 101
- reflection, 11, 84, 84–87, 137
- selfadjoint, 75, 88, 128, 162
- similarity, 80, 137, 171

- Clifford algebra, 160
- space, 6, 46, 105, 162
- unit
 - elliptic, 133
 - hyperbolic, 134
 - parabolic, 135
- zero-radius, 8, 11, 51, 62, 64–66, 68, 72–74, 92, 101, 106, 126, 162
 - elliptic, 65
 - hyperbolic, 65
 - infinity, at, 106
 - parabolic, 65
- cycles
 - coaxial, 40, 60
 - disjoint, 67, 72, 74
 - f-orthogonal, 11, 14, 88, 98, 139, 171
 - intersecting, 67, 72, 74
 - orthogonal, 6, 9, 44, 69, 69–80, 84–85, 120, 139, 171
 - pencil, viii, 59, 68, 72, 74, 170
 - orthogonal, 74, 82, 86
 - radical axis, 40, 60
 - tangent, 58, 67, 74
 - Descartes–Kirillov condition, 68
- decomposition
 - Iwasawa, 2, 31, 37
- degeneracy
 - parabolic, 78, 136
- dequantisation
 - Maslov, 149
- derived action, 4, 27, 30, 37
- Descartes–Kirillov
 - condition for tangent circles, 68
- det-normalised cycle, 58, 64, 66, 87, 92, 171
- determinant, 8
- diameter
 - cycle, of, 91, 162
- directrix, 7, 38
 - parabola, of, 56, 158
- discriminant, 62
- disjoint
 - cycles, 67, 72, 74
- disk
 - unit, 131
 - elliptic, 132, 133
 - hyperbolic, 133
 - metric, 139, 141
 - parabolic, 135
- distance, 13, 92, 92, 96, 132–134, 141
 - conformal, 96
 - inversive between cycles, 66
- distinct, essentially, 53, 129
- divisor
 - zero, 2, 34, 35, 41, 53, 106, 145, 157
- double
 - numbers, 2, 156, 157
- dual
 - numbers, 2, 34, 156, 157
- dynamics
 - non-linear, 152, 155, 160
- e-centre, 44
- e-focus, 56
- element
 - ideal, 105
- ellipse, 158
 - centre, 158
 - focus, 158
- elliptic
 - case, 2, 35
 - Cayley transform, 131
 - rotation, 132
 - unit
 - cycle, 133
 - disk, 132, 133
 - upper half-plane, 33, 41
 - zero-radius cycle, 65
- EPAL, *see* Erlangen programme at large, 15
- EPH classification, 2, 36, 127
- equation
 - heat, 145
 - quadratic, 158
- Erlangen programme, vii, 1, 155
 - at large, vii, 15
- essentially distinct, 53, 129
- Euclidean

- geometry, viii, 99
 - space, 97
- Euler
 - formula, 144, 161
 - operator, 37
- exponential map, 24, 31
- extragalactic astronomy, 111, 116
- f-ghost cycle, 89
- f-orthogonality, 11, 14, 88, 98, 102, 126, 139, 171
- Fillmore–Springer–Cnops
 - construction, 6, 47, 134
- flat cycles, 44
- focal
 - length, 40, 92, 101, 115
 - cycle, of, 56
 - parabola, of, 56
 - orthogonality, *see* f-orthogonality
- focus, 62, 92
 - cycle, of, 7, 36, 56, 128, 135, 158
 - ellipse, of, 158
 - elliptic, 56
 - hyperbola, of, 38, 159
 - hyperbolic, 56
 - length from, 14, 94, 95, 96, 103, 135
 - p-conformality, 153
 - parabola, of, 7, 38, 56, 158
 - parabolic, 56
- form
 - symplectic, 53, 54, 112–113, 160
- formula
 - cancellation for cross-ratios, 54, 128
 - Euler, 144, 161
- FSCc, *see* Fillmore–Springer–Cnops construction
- function
 - Heaviside, 10, 78
 - norm of, 46
 - orthogonality of, 46
 - special, 15
- functional
 - analysis, 45
- Galilean
 - orthogonality, 99
 - space-time, 115, 142
 - transformation, 115
- Gelfand–Naimark–Segal construction, 9, 61
- geodesics, 123, 117–129, 139, 141, 154
- geometry
 - birational, 152
 - commutative, vii
 - Euclidean, viii, 99
 - hyperbolic, 36
 - Lobachevsky, viii, 36
 - non-commutative, vii, 16
 - Riemann, 36, 118
- ghost cycle, 79, 85
- GiNaC, *see* CAS, 166
- GNS construction, *see* Gelfand–Naimark–Segal construction
- GNU, 163
 - General Public License (GPL), 163
 - Linux, 163
 - emulator, 164, 165
- GPL, *see* GNU General Public License
- group, 1, 18
 - $SL_2(\mathbb{R})$, 1, 19, 21
 - Lie algebra, 27
 - one-dimensional subgroup, 24
 - $ax + b$, 1, 19, 29, 37
 - Lie algebra, 24–26
 - one-dimensional subgroup, 23
- abelian, *see* commutative group
- abstract, 18, 20
- affine, *see* $ax + b$ group
- commutative, 18
- continuous, 19
- Heisenberg, 1, 16, 19
 - Lie algebra, 26
 - one-dimensional subgroup, 24
- law, *see* group multiplication
- Lie, 19, 23
- locally compact, 19
- multiplication, 18
- non-commutative, 18
- representation

- linear, 15
 - transformation, 17, 20
- h-centre, 44
- h-focus, 56
- half-plane
 - boundary effect, 8, 57, 65, 71, 80, 88
 - invariance, 33, 34, 108, 110
 - lower, 21, 40, 42
 - non-invariance, 34, 108, 110
 - upper, 21, 40, 42, 131
 - elliptic, 33, 41
 - hyperbolic, 34, 110
 - parabolic, 34, 41
- Hamiltonian, 113
 - quadratic, 113
- Hardy
 - space, 15
- harmonic
 - analysis, 15
 - oscillator, 113
 - quantum, 114
- heat
 - equation, 145
 - kernel, 145
- Heaviside
 - function, 10, 78
- Heisenberg
 - commutation relation, 26
 - group, 1, 16, 19
 - Lie algebra, 26
 - one-dimensional subgroup, 24
- Hilbert
 - space, 46, 61
- homogeneous space, 21, 21–23
- horizon, 128
- Huygens
 - principle, 117
- hyperbola, 44, 159
 - asymptote, 38, 159
 - centre, 159
 - focal length, 40, 115
 - focus, 38, 159
- hyperbolic
 - case, 2, 35
 - Cayley transform, 131
 - geometry, 36
 - plane
 - two-fold cover, 110, 133
 - rotation, 134
 - unit
 - cycle, 134
 - disk, 133
 - unit (j), 2
 - upper half-plane, 34, 110
 - zero-radius cycle, 65
- hyperboloid, 107
- hypercomplex
 - unit (ι), 2, 157
- hyperreal
 - number, 104
- ideal
 - element, 105
- idempotent
 - mathematics, 149
- identity, 18
 - Jacobi, 26
 - Pythagoras'
 - parabolic, 144, 146
- imaginary
 - circle, 44, 56, 60, 63
 - unit (i), 2
- indefinite
 - product, 62
- index
 - refractive, 111
- induced
 - representation, 52, 113, 152
- inequality
 - Cauchy–Schwarz, 67–68, 72
 - triangle, 118, 125, 150
- infinitesimal
 - number, 100, 104
 - radius cycle, 100, 100–104, 138
- infinitesimally conformal, 103
- inner
 - product, 46
 - norm of vector, 91
- integral
 - Bergman, 15

- Cauchy, 15
- intersecting
 - cycles, 67, 72, 74
- intertwining map, 48
- interval
 - space-like, 116, 120
 - time-like, 116, 120
- invariant
 - metric, 117–129, 146
 - subset, 20
 - vector fields, 24
- inverse, 18
- inversion
 - circles, in (Yaglom term), 162
 - first kind, of the (Yaglom term), 87
 - in a cycle, 84, 84–87, 89, 106
 - second kind, of the (Yaglom term), 87, 162
- inversive distance between cycles, 66
- isotropic cycles, 11, 72
- isotropy subgroup, 21, 40–42, 134, 136
 - orbit, 42, 66
- Iwasawa decomposition, 2, 31, 37
- Jacobi identity, 26
- kernel
 - heat, 145
- Kirillov
 - correspondence, 52
 - Descartes–Kirillov condition for
 - tangent circles, 68
 - orbit method, 52
- Krein
 - space, 61
- Laplace
 - operator, 15
- left shift, 21, 22, 24
- length, 14, 94
 - conformal, 96
 - curve, of, 118
 - focal, of a cycle, 56, 92
 - focal, of a hyperbola, 40, 115
 - focal, of a parabola, 56
 - from centre, 14, 94, 95, 96, 132–135
 - from focus, 14, 94, 95, 96, 101, 103, 135
 - p-conformality, 153
- Lie
 - algebra, 23–27, 52
 - commutator, 26
 - groups, 19, 23
- light
 - cone, 41, 65, 82, 102, 107, 109, 116
 - infinity, at, 107, 109
 - speed, of, 116
- line
 - contour, 38, 96, 98, 99, 146
 - Menger, 124
 - special (Yaglom term), 162
 - spectral, 114, 116
- linear
 - space, 45
- linear-fractional transformations, *see* Möbius map
- Lobachevsky
 - geometry, viii, 36
- locally compact group, 19
- loop, 23
- Lorentz–Poincare
 - transformation, 115
- lower half-plane, 21, 40, 42
- map
 - M , 47, 105
 - Q , 46, 73, 105
 - p , 22, 113
 - r , 22, 113
 - s , 22, 113
 - exponential, 24, 31
 - intertwining, 48
 - Möbius, 1, 17, 21
 - Clifford algebra, 160
 - on cycles, 6, 48
 - on the real line, 30
 - preserving orthogonality, 73
- Maslov
 - dequantisation, 149
- mathematics
 - idempotent, 149

- tropical, 149
- matrix
 - congruence, 52
 - cycle, of, 6, 46
 - Clifford algebra, 160
 - similarity, 48, 171
 - Clifford algebra, 160
 - transfer, 112
- mechanics
 - classical, 113
 - quantum, 16, 113
- Menger line, 124
- metric, 117
 - invariant, 117–129, 146
 - monotonous, 122
 - unit disk, 139, 141
- Minkowski
 - space-time, 51, 111, 115, 155
- Möbius map, 1, 17, 21
 - Clifford algebra, 160
 - on cycles, 6, 48
 - on the real line, 30
- modulus
 - parabolic, 146
- monad, 104
- monotonous
 - metric, 122
- mother wavelet, 15
- netbook, 164
- nilpotent unit, *see* parabolic unit
- non-Archimedean analysis, *see*
 - non-standard analysis
- non-commutative
 - geometry, vii, 16
 - group, 18
 - space, vii
- non-linear dynamics, 152, 155, 160
- non-locality, 10, 12, 71, 78
- non-standard
 - analysis, 100, 104
 - monad, 104
- norm
 - function, of, 46
 - inner product, from, 91
 - parabolic, 146
 - normalised cycle, 8, 58
 - det-, 58, 64, 66, 87, 92, 171
 - k -, 13, 58, 64, 65, 91, 93, 171
- number
 - infinitesimal, 100, 104
 - system, 35
 - signature, 44
- numbers
 - complex, 33, 157
 - double, 2, 34, 156, 157
 - dual, 2, 34, 156, 157
 - split-complex, *see* dual numbers
- one-dimensional subgroup, 23
 - $ax + b$ group, of, 23
 - group $SL_2(\mathbb{R})$, of, 24
 - Heisenberg group, of, 24
- open
 - source, 163
- operator
 - Cauchy–Riemann, 15
 - Euler, 37
 - Laplace, 15
 - pseudo-differential, 25
- optics
 - illusion, 82
 - paraxial, 111
- orbit, 21
 - isotropy subgroup, 42, 66
 - method of Kirillov, 52
 - subgroup A' , of, 42
 - subgroup A , of, 3, 37, 139
 - subgroup K , of, 3, 37, 37–40, 42, 57, 108, 110, 139
 - subgroup N , of, 3, 37, 139
 - subgroup N' , of, 42
- orientation
 - causal, 109, 116
- orthogonal
 - pencil of cycles, 74, 82, 86
- orthogonality
 - cycles, of, 6, 9, 44, 49, 69, 69–80, 84–85, 102, 120, 139, 171
 - focal, *see* f-orthogonality
 - function, of, 46
 - Galilean, 99

- preserving map, 73
- second kind, of the, *see*
 - f-orthogonality
- oscillator
 - harmonic, 113
 - quantum, 114
- p-centre, 44
- p-focus, 56
- packet
 - wave, 114
- parabola, 44, 158
 - directrix, 7, 38, 56, 158
 - focal length, 56
 - focus, 7, 38, 56, 158
 - vertex, 7, 56, 158
- parabolas
 - concentric, 136
 - confocal, 136
- parabolic
 - case, 2, 35
 - Cayley transform, 134
 - circle (Yaglom term), 76, 162
 - cycle (Yaglom term), 162
 - degeneracy, 78, 136
 - modulus, 146
 - norm, 146
 - Pythagoras' identity, 144, 146
 - trigonometric functions, 143
 - unit
 - cycle, 135
 - disk, 135
 - unit (ε), 2
 - upper half-plane, 34, 41
 - zero-radius cycle, 65
- paraxial
 - optics, 111
- PDO, *see* pseudo-differential operator
- pencil
 - cycles, of, viii, 59, 68, 72, 74, 170
 - orthogonal, 74, 82, 86
- periodic table, 35
- perpendicular, 14, 98
- phase
 - space, 113
 - tangent space of, 113
- plane
 - hyperbolic
 - two-fold cover, 110, 133
- Plato's cave, 6
- point
 - cycle, of, 66, 94
 - infinity, at, 106
 - power, of, viii, 40, 45, 65, 93, 94, 171
 - space, 6, 46, 162
- polar
 - projection, *see* stereographic projection
- Pontryagin
 - space, 61
- positive
 - cycle, 62, 120
- power
 - cycle, of, 66, 94
 - point, of, viii, 40, 45, 65, 93, 94, 171
- principle
 - Huygens, 117
 - similarity and correspondence, 156
- product
 - cycle, 61, 69, 93
 - indefinite, 62
 - inner, 46
 - norm of vector, 91
- projection
 - polar, *see* stereographic
 - stereographic, 106
- projective
 - cross-ratio, 53, 53–54, 129
- projective space, 6, 46, 50, 53, 150, 157
- pseudo-differential operator, 25
- pyGiNaC, 167
- Pythagoras'
 - identity
 - parabolic, 144, 146
- Python, 167, 168
- quadratic
 - equation, 158
 - discriminant, 62

- Hamiltonian, 113
- quadric, 158
- quantum
 - harmonic oscillator, 114
 - mechanics, 16, 113
- radical axis
 - cycles, of, 40, 60
- radius
 - cycle, of, 13, 58, 91, 171
- ray, 111, 117
 - reflection, 159
- real line
 - $ax + b$ map, 22, 27
 - Möbius map, 30
- red shift, 111, 116
- reference
 - system, 114
- reflection
 - in a cycle, 11, 84, 84–87, 106, 137
 - ray, of, 159
- refractive
 - index, 111
- relativity, 114, 155
- representation
 - adjoint, 52
 - group
 - linear, 15
 - induced, 52, 113, 152
- Riemann
 - geometry, 36, 118
 - sphere, 106
- right shift, 21, 24
- rotation, 41, 118
 - elliptic, 132
 - hyperbolic, 134
 - parabolic
 - tropical, 149
 - right, 21, 24
- signature
 - number systems, of, 44
- similarity
 - cycles, of, 80, 137, 171
 - Clifford algebra, 160
 - matrix, of, 48, 171
 - Clifford algebra, 160
 - principle of similarity and correspondence, 156
- source
 - open, 163
- space
 - Bergman, 15
 - commutative, vii
 - cycles, of, 6, 46, 105, 162
 - Euclidean, 97
 - Hardy, 15
 - Hilbert, 46, 61
 - Krein, 61
 - linear, 45
 - non-commutative, vii
 - phase, 113
 - tangent space of, 113
 - point, 6, 46, 162
 - Pontryagin, 61
 - projective, 6, 46, 50, 53, 150, 157
 - tangent, 24, 52, 88, 118
 - phase space, of, 113
- space-like interval, 116, 120
- space-time, 107, 114
 - Galilean, 115, 142
 - Minkowski, 51, 111, 115, 155
- special
 - function, 15
 - line (Yaglom term), 162
- spectral
 - line, 114, 116
- speed
 - light, of, 116
- sphere
 - Riemann, 106
- split-complex numbers, *see* dual numbers
- stereographic
 - projection, 106
- section
 - conic, 2, 4, 39, 158
- selfadjoint cycle, 75, 88, 128, 162
- shift
 - left, 21, 22, 24
 - red (astronomy), 111, 116

- subgroup, *20*
 - A , *2, 30, 156*
 - orbit, *3, 37, 139*
 - A' , *31, 41, 42, 115, 118, 134, 143*
 - orbit, *42*
 - K , *2, 15, 30, 118, 143, 156*
 - orbit, *3, 37, 37–40, 42, 57, 108, 110, 139*
 - N , *2, 30, 156*
 - orbit, *3, 37, 139*
 - N' , *31, 41, 115, 118, 143*
 - orbit, *42*
 - conjugated, *21*
 - isotropy, *21, 40–42, 134, 136*
 - orbit, *42, 66*
 - one-dimensional, *23*
- subset
 - invariant, *20*
- swiGiNaC**, *167*
- symplectic
 - form, *53, 54, 112–113, 160*
- system
 - reference, *114*
- tangent, *9, 57, 70–72, 76–79, 98, 127*
 - cycles, *58, 67, 74*
 - Descartes–Kirillov condition, *68*
 - space, *24, 52, 88, 118*
 - phase space, of, *113*
- Taylor
 - series, *15*
- time
 - absolute, *115, 142, 162*
 - arrow, *109, 116*
- time-like interval, *116, 120*
- trace, *8*
- transfer
 - matrix, *112*
- transform
 - Cayley, *131, 139*
 - cycle, of, *136*
 - elliptic, *131*
 - hyperbolic, *131*
 - parabolic, *134*
 - wavelet, *15*
- transformation
 - canonical, *113*
 - Galilean, *115*
 - group, *17, 20*
 - linear-fractional, *see Möbius map*
 - Lorentz–Poincare, *115*
 - Möbius, *see Möbius map*
- transitive, *1, 21, 23, 37*
- triangle
 - inequality, *118, 125, 150*
- tropical
 - mathematics, *149*
 - parabolic rotation, *149*
- unit
 - circle, *see elliptic unit cycle*
 - cycle
 - elliptic, *133*
 - hyperbolic, *134*
 - parabolic, *135*
 - disk, *131*
 - elliptic, *132, 133*
 - hyperbolic, *133*
 - metric, *139, 141*
 - parabolic, *135*
 - hyperbolic (j), *2*
 - hypercomplex (ι), *2, 157*
 - imaginary (i), *2*
 - nilpotent, *see parabolic unit*
 - parabolic (ε), *2*
- upper half-plane, *21, 40, 42, 131*
 - boundary effect, *8, 57, 65, 71, 80, 88*
 - elliptic, *33, 41*
 - hyperbolic, *34, 110*
 - parabolic, *34, 41*
- Vahlen condition, *81, 87*
- vector fields
 - invariant, *24*
- vertex
 - parabola, of, *7, 56, 158*
- wave, *117*
 - packet, *114*
- wavelet, *1*

- mother, 15
 - transform, 15
- Yaglom term
 - inversion
 - circles, in, 162
 - second kind, of , 162
 - parabolic
 - circle, 162
- cycle, 162
 - special line, 162
- zero
 - divisor, 2, 34, 35, 41, 53, 106, 145, 157
- zero-radius cycle, 8, 11, 51, 62, 64–66, 68, 72–74, 92, 101, 106, 126, 162
- infinity, at, 106